

DISSERTATION

CROSSING THE BLOOD-BRAIN BARRIER: SIRNA TREATMENT FOR PRION DISEASES

Submitted by

Heather Rose Bender

Department of Microbiology, Immunology, Pathology

In partial fulfillment of the requirements

For the Degree of Doctor of Philosophy

Colorado State University

Fort Collins, Colorado

Fall 2017

Doctoral Committee:

Advisor: Mark Zabel

Glenn Telling  
Daniel Gustafson  
James Bamburg  
Steve Dow

Copyright by Heather Rose Bender 2017

All Rights Reserved

## ABSTRACT

### CROSSING THE BLOOD-BRAIN BARRIER: SIRNA TREATMENT FOR PRION DISEASES

Protein misfolding diseases such as prion diseases, Alzheimer's disease, and Parkinson's disease, are fatal neurodegenerative diseases caused by a misfolded protein. There are no known therapeutics that extend survival times of afflicted individuals with these diseases. An attractive therapeutic option for protein misfolding disorder is RNA interference, which uses either short hairpin RNA or small interfering RNA (siRNA) to target a specific mRNA for degradation that results in a reduction of protein levels. The reduction of a target mRNA/protein can result in a decrease of misfolded protein in the central nervous system (CNS). However, crossing the blood-brain barrier remains the main challenge for developing RNA interference therapeutics to the CNS. Liposomes are commonly utilized to deliver siRNA to peripheral sites and are being investigated for their ability to deliver siRNA to the brain. We have previously reported on a new liposome delivery system that delivered siRNA targeted towards the cellular prion protein, PrP<sup>C</sup>, to mouse neuroblastoma cells. PrP<sup>C</sup> is a normal host cellular protein that misfolds into a protease resistant isomer, PrP<sup>Res</sup>, which leads to the development of prion diseases. We call these siRNA delivery vehicles: liposome-siRNA-peptide complexes (LSPCs). LSPCs are targeted towards the CNS using a small peptide from the rabies virus glycoprotein, called RVG-9r. In the second chapter of this dissertation, we show that an intravenous injection of LSPCs results in a 40-50% reduction of neuronal PrP<sup>C</sup>. Upon injection of LSPCs, we observed that half of all treated mice had PrP<sup>C</sup> siRNA targeted towards the area of the brain several hours after injection. However, we also observed a clearance of PrP<sup>C</sup> siRNA by the kidneys in the other half of LSPCs-treated mice. Therefore, we designed two other liposomal delivery vehicles that would allow us to encapsulate the siRNA in the liposome and covalently link RVG-9r to the outside of the liposome. We also added PEG lipids to these new delivery vehicles to extend the circulation half-life of the liposomes. We call these additional delivery vehicles peptide-addressed liposome-encapsulated therapeutic siRNA (PALETS). The two PALETS formulations include one cationic (DOTAP [1,2-dioleoyl-3-trimethylammonium-propane]) PALETS and one anionic (DSPE [1,2-Distearoyl-sn-glycero-3-phosphoethanolamine]) PALETS. We have utilized the cation protamine sulfate to encapsulate the siRNA within the anionic PALETS. The addition of protamine sulfate to the siRNA resulted in an encapsulation efficiency of 80-90% in DSPE PALETS. Four days after treatment with LSPCs and PALETS, LSPCs

have the biggest decrease in neuronal PrP<sup>C</sup> on the cellular surface, while DOTAP PALETS have the greatest reduction of PrP<sup>C</sup>-positive cells. DSPE PALETS showed no statistical difference between the treated and untreated mice at this time point; however, two of the three treated mice did have a decrease in their neuronal PrP<sup>C</sup>, indicating that this delivery vehicle is able to deliver PrP<sup>C</sup> siRNA to the brain. There was no reduction in mRNA levels of any of the treated mice in the brain but the DOTAP LSPCs and DOTAP PALETS resulted in a 2-fold decrease of PrP<sup>C</sup> mRNA levels in the kidney, while DSPE PALETS resulted in a 2-fold increase of PrP<sup>C</sup> mRNA levels in the same organ.

The first therapeutics for prion diseases targeted the mechanism of conversion between PrP<sup>C</sup> and PrP<sup>Res</sup>. These therapeutics were successful in decreasing the amount of PrP<sup>Res</sup> *in vitro* but they had limited success *in vivo*. Challenges of these therapeutics included toxicity, inability to cross the blood-brain barrier, strain specificity, and/or failure to affect survival times. PrP<sup>C</sup> became an attractive therapeutic option when it was shown that PrP-null mice did not develop any outward phenotypic differences from the removal of PrP<sup>C</sup>. Our LSPCs, with PrP<sup>C</sup> siRNA, reduced the amount of PrP<sup>C</sup> protein and PrP<sup>C</sup> mRNA levels in mouse neuroblastoma cells. This reduction in PrP<sup>C</sup> resulted in a concomitant decrease of PrP<sup>Res</sup> and a ‘curing’ of the prion-infected cells. In the third chapter of this dissertation, we have treated two different mouse models with our LSPCs at different time points to assess the pharmacodynamics of the treatment. *In vivo* live imaging followed by flow cytometry revealed delivery of PrP<sup>C</sup> siRNA to the brain one hour after intravenous injection. The LSPCs resulted in a decrease of neuronal PrP<sup>C</sup> in a C57Bl/6 mouse model at 24, 48 hours, and 4 days after treatment. A decrease in neuronal PrP<sup>C</sup> was also observed in a CD1 mouse model at 4 and 15 days after treatment. Surprisingly, mRNA levels did not always concur with the protein level data. At certain time points, the mice with the biggest decline in PrP<sup>C</sup> protein had the greatest increase of PrP<sup>C</sup> mRNA. Off-target effects were observed in the kidney, which might have been caused non-specifically by LSPCs treatment and not by the PrP<sup>C</sup> siRNA. We also show that PrP<sup>C</sup> protein levels decrease by 70% in prion-infected mice after three consecutive LSPCs treatments spaced two weeks apart. Analysis of mRNA levels of these mice after three treatments revealed a simultaneous reduction in PrP<sup>C</sup> mRNA levels.

Several researchers have shown a reversal in prion neuropathology that results after decreasing the amount of PrP<sup>C</sup>, either by a Cre/*loxP* system or short hairpin RNA. Therefore, we treated prion-infected mice with our LSPCs treatment targeting PrP<sup>C</sup>. Two treatment studies were conducted to determine the optimal dosing regimen of LSPCs treatment. The first study treated prion-infected mice with LSPCs every two weeks starting at 120 days post

inoculation and the second study treated mice with LSPCs every 3-5 weeks starting at 120 days post inoculation. The mice were intraperitoneally inoculated with a low dose of RML-5 prions to simulate a more natural prion infection. Unfortunately, in the fourth chapter of this dissertation we show that neither of the dosing regimens resulted in an increase in survival times of prion-infected mice. The mice in these two dosing studies were also subjected to burrowing and nesting behavioral tests to determine if LSPCs treatment improves behavioral outcomes. We show that LSPCs treatment every two weeks improves behavior scores at 141 and 169 days post inoculation in some treated groups. This improvement in behavior indicates that, while the LSPCs treatment are not affecting survival times, they are improving behavioral outcomes of prion-infected mice. Surprisingly, three of the uninfected, treated controls died immediately after LSPCs treatment of an apparent Type III hypersensitivity. Therefore, we performed ELISAs to measure the immune response towards the RVG-9r peptide. Several groups of treated mice in the terminal dosing studies had increased levels of IgG against RVG-9r compared to the infected, untreated control. In another study, it was revealed that three total IgG levels against RVG-9r increased after three subsequent LSPCs treatments spaced two weeks apart. We also assessed the amount of PrP<sup>Res</sup> in the brains and spleens of LSPCs-treated mice. Using the protein misfolding cyclic amplification assay, we determined that LSPCs treatment causes an increase in PrP<sup>Res</sup> levels in the brain after one to six LSPCs treatments. No trends can be seen in the spleen.

Taken together these results indicate that the current LSPCs formulation using RVG-9r and PrP<sup>C</sup> siRNA result in an immune response that may interfere with any benefits of the treatment. Another explanation for these results is that PrP<sup>C</sup> may be tightly regulated at the transcriptional level, so the cell may try to return the mRNA/protein levels to normal by increasing PrP<sup>C</sup> mRNA when it detects a decrease in PrP<sup>C</sup> mRNA or protein levels. The increase in PrP<sup>C</sup> may be the cause of the increase of PrP<sup>Res</sup> observed in these studies. Therefore, transiently decreasing PrP<sup>C</sup> via siRNA may not be the best therapeutic option available. It is recommended that more studies are undertaken to further elucidate the transcriptional regulation and immune response towards the LSPCs treatment. LSPCs will need to be further modified to become a viable therapeutic option for prion diseases.

## ACKNOWLEDGEMENTS

I would like to express my sincere gratitude and utmost appreciation for my advisor Dr. Mark Zabel. He inspires everyone around him with his love of science, research, and teaching. Mark created an awesome laboratory environment with his creative thinking and adventurous nature. I will always remember our numerous Z lab outings, which fostered an incredible sense of camaraderie within the laboratory. I thank him for his continuous support of my studies and research, and for his patience, motivation, and immense knowledge. I could not have imagined a better advisor and mentor for my Ph.D. study.

Besides my advisor, I would like to thank the rest of my committee: Dr. Glenn Telling, Dr. Dan Gustafson, Dr. Jim Bamburg, and Dr. Steve Dow for their insightful comments and encouragement that allowed me to further develop my research skills.

I thank my fellow labmates for the stimulating discussions and all the fun we have had over the last five years. I especially thank Sarah Kane, who is trudging through this dissertation process with me, and who has been an incredible friend and lab mate. It was an honor to work with Sarah who embodies everything a great scientist should be, from her excellent creative thinking skills to her unyielding pursuit of scientific progress. I want to thank Aimee Ortega and Kaitlyn Miedema, my two office mates, for their never-ending laughter and smiles.

The research in this dissertation would not have been possible without the help from my undergraduate and master's students: Kendra Jones, Amanda Hitpas, Jessica Annis, and Luke Mollnow. I am grateful to all the assistance these students provided and I will greatly miss their enthusiasm for science.

I am grateful to my family and friends who have provided me moral and emotional support throughout my educational pursuits. I would especially like to acknowledge my mother, Rose, who has always been a pillar of support throughout my life. Without her unending encouragement, I probably would have never gone to college. I thank her for all the sacrifices she has made to not only provide for our family but to ensure that I received an education. I honestly cannot express how appreciative I am of everything that she has done and continues to do, and all the encouragement and advice I have received from her.

Lastly, I thank my pets who have had no choice but to live with me for the past five years. They have been extremely tolerant of my scientific rants, bursts of anger, and excitement at Eureka! moments. The love and cuddles that I received from them have honestly helped me get through some of the most difficult days of my life. I look

forward to many more years of trying to explain my science to an indifferent cat who only wants his food. (At this very moment, the dominant cat is bemoaning his existence because he has to be locked in a room due to his radioactive body, such is life.)

## DEDICATION

*To my beautiful and loving mother, may you always find happiness*

*And to my grandparents, Raymond and Carol Wyatt*

*Your life was a blessing*

*Your memory a treasure...*

*You are loved beyond words*

*And missed beyond measure*

*-Renee Wood*

## TABLE OF CONTENTS

ABSTRACT.....	ii
ACKNOWLEDGEMENTS.....	v
DEDICATION.....	vii
LIST OF TABLES.....	x
LIST OF FIGURES.....	xi
Chapter 1: Introduction.....	1
Prions.....	1
<i>History: A new but old disease.....</i>	<i>1</i>
<i>Discovering Prions: Characteristics of the scrapie agent.....</i>	<i>3</i>
<i>Beyond the Discovery of Prions: The cellular prion protein (PrP<sup>C</sup>).....</i>	<i>6</i>
History of the cellular prion protein.....	6
Structure, Regulation, and Trafficking of PrP <sup>C</sup> .....	7
Function or lack thereof of PrP <sup>C</sup> .....	10
<i>Prion and Protein Misfolding Diseases.....</i>	<i>17</i>
<i>Prion Therapeutics.....</i>	<i>22</i>
The ‘Anti’ Therapeutic Group.....	22
Polycationic Compounds.....	24
Polyanionic Compounds.....	25
Immunotherapeutics/Immunomodulation.....	26
Targeting PrP <sup>C</sup> .....	28
Other Therapeutic Approaches.....	29
siRNA and Liposomes.....	30
<i>From RNA Interference Discovery to Mechanism.....</i>	<i>30</i>
<i>Challenges of RNAi Based Therapeutics.....</i>	<i>32</i>
Expression of RNAi.....	32
Delivery of siRNA in vivo: Considerations of stability and targeting.....	33
Off-Target Effects and the Immune System.....	39
The Blood-Brain Barrier.....	40
Introduction to Work in this Dissertation.....	43
References.....	46
Chapter 2: Delivery of therapeutic siRNA to the CNS using cationic and anionic liposomes.....	60
Summary.....	60
Introduction.....	60
Materials and Methods.....	62
Results.....	67
Discussion.....	75
References.....	80
Chapter 3: Intravenous injection of LSPCs delivers PrP <sup>C</sup> siRNA to the brain <i>in vivo</i> and reduce neuronal PrP <sup>C</sup> .....	83
Summary.....	83
Introduction.....	83
Materials and Methods.....	86
Results.....	89
Discussion.....	110
References.....	118
Chapter 4: LSPCs do not increase the survival periods of prion-infected mice, but do improve behavioral outcomes at specific time points.....	122
Summary.....	122
Introduction.....	123
Materials and Methods.....	125
Results.....	129
Discussion.....	145
References.....	151

Overall Conclusions.....	154
Future Directions .....	157
Appendix A – Additional Figures.....	160
Appendix B – List of Abbreviations.....	163

## LIST OF TABLES

Table 4.1. Treatment groups of the 1st terminal study .....	130
Table 4.2. Number of treatments and DPI treated in 1st terminal study .....	130
Table 4.3. Treatment groups of the 2nd terminal study .....	130
Table 4.4. Number of treatments and DPI treated in 2nd terminal study .....	130
Table 4.5. Repetitive LSPCs treatments of early time point mice indicating the dpi that mice were treated and euthanized .....	142

## LIST OF FIGURES

Figure 1.1. Artistic representation of PrP <sup>C</sup> .....	8
Figure 1.2. Mechanisms of prion therapeutics that have shown promise in animal models. ....	23
Figure 1.3. RNAi pathway in humans for long dsRNA, siRNA, and shRNA.....	31
Figure 2.1. Experimental setup of LSPCs and PALETS experiments.....	67
Figure 2.2. Schematic representation of LSPCs and PALETS.....	68
Figure 2.3. Protocol of the thin lipid film hydration method.....	68
Figure 2.4. Encapsulation of siRNA within DSPE PALETS using the cation protamine sulfate. ....	70
Figure 2.5. Protein analysis and biodistribution of LSPCs treatment in vivo.....	71
Figure 2.6. Comparison of PrP <sup>C</sup> protein levels between LSPCs and PALETS treated mice. ....	72
Figure 2.7. mRNA analysis of LSPCs and PALETS treated four days after treatment. ....	74
Figure 3.1. LSPCs injected intravascularly deliver PrP <sup>C</sup> siRNA to the brain.....	91
Figure 3.2. Scrambled LSPCs and control peptide LSPCs cause an increase in PrP <sup>C</sup> mRNA levels.....	92
Figure 3.3. RVG-9r binds to the majority of neuronal and kidney cells. ....	93
Figure 3.4. Study design of pharmacodynamics experiments of CR1/2 hemi and CD1 mice. ....	94
Figure 3.5. Western blot analysis of PrP <sup>C</sup> levels in the brains of CR1/2 treated mice. ....	96
Figure 3.6. Western blot analysis of PrP <sup>C</sup> levels in the brains of CD1 treated mice. ....	97
Figure 3.7. Flow cytometric and ddPCR analysis of CR1/2 hemi mice 24 hours after LSPCs treatment.....	99
Figure 3.8. Flow cytometric and ddPCR analysis of CR1/2 hemi mice 48 hours after LSPCs treatment.....	100
Figure 3.9. Flow cytometric and ddPCR analysis of CR1/2 hemi mice four days after LSPCs treatment. ....	101
Figure 3.10. Flow cytometric and ddPCR analysis of CD1 mice 48 hours after LSPCs treatment. ....	103
Figure 3.11. Flow cytometric and ddPCR analysis of CD1 mice 4 days after LSPCs treatment. ....	105
Figure 3.12. Flow cytometric and ddPCR analysis of CD1 mice 15 days after LSPCs treatment. ....	106
Figure 3.13. Flow cytometric and ddPCR analysis of CD1 mice 21 days after LSPCs treatment. ....	107
Figure 3.14. Flow cytometric and ddPCR analysis of a repeating two-week dosing regimen in FVB mice. ....	109
Figure 4.1. Survival curves of LSPCs-treated FVB mice in 1 <sup>st</sup> terminal study.....	131
Figure 4.2. Survival curves of LSPCs-treated CD1 mice in 2 <sup>nd</sup> terminal study. ....	132
Figure 4.3. Analyzing PrP <sup>Res</sup> deposition in prion-infected mice of the LSPCs terminal studies using western blot. ....	133
Figure 4.4. Analysis of PrP <sup>Res</sup> deposition in the brains of mice from the 1 <sup>st</sup> LSPCs treatment terminal study. ....	134
Figure 4.5. Analysis of activated astrocytes using GFAP immunostain in the brains of mice from the 1 <sup>st</sup> LSPCs treatment terminal study.....	135
Figure 4.6. Burrowing rates of LSPCs-treated mice from the 1 <sup>st</sup> terminal study. ....	136
Figure 4.7. Nesting scores of LSPCs-treated mice from the 1 <sup>st</sup> terminal study.....	137
Figure 4.8. Burrowing rates of LSPCs-treated mice from the 2 <sup>nd</sup> terminal study. ....	139
Figure 4.9. Nesting scores of LSPCs-treated mice from the 2 <sup>nd</sup> terminal study.....	140
Figure 4.10. Total IgG levels against RVG-9r in LSPCs-treated terminal mice. ....	141
Figure 4.11. PMCA amplification of PrP <sup>Res</sup> in LSPCs-treated early time point mice.....	143
Figure 4.12. Total IgG levels against RVG-9r in the brains of early time point mice repeatedly treated with LSPCs. .....	144
Figure A.1. In vivo live imaging of LSPCs-treated mice 24 hours after treatment.....	160
Figure A.2. Percent of PrP <sup>C</sup> -positive cells using scrambled siRNA and RVM peptide. ....	161
Figure A.3. Comparison of PrP <sup>C</sup> levels in C57Bl/6 and CR1/2 hemi mice.....	162

# Chapter 1:

## Introduction

### Prions

#### *History: A new but old disease*

In Europe and England in the mid-18<sup>th</sup> century, sheep farmers changed their breeding protocols to select for more desirable traits related to wool production and quality. This breeding protocol resulted in a massive increase of inbreeding among the sheep flocks. Shortly after the increase in inbreeding, sheep farmers started to notice that their flocks succumbed to a disease that the farmers had never seen before. The first reports of this disease were in 1732 in Spain and England under the name 'rickets,' which would later be known as scrapie<sup>1-3</sup>. It is unclear if the inbreeding caused the scrapie epidemic, but some have speculated that while the farmers were selecting for wool production, they may inadvertently have selected for a genetic element that led to scrapie susceptibility<sup>1</sup>.

An excerpt published in 1811 in the General View of the Agriculture of the County of Cambridge describes the clinical signs of rickets (scrapie) as seen by a sheep farmer of an affected flock during the 18<sup>th</sup>-century epidemic:

At this time the animal appears extremely uneasy, constantly rubbing its head against the hurdles and fences, and scratching its back and sides with its horns, starting suddenly, running a few steps, then falling down, where it will remain a short time and then rise and begin feeding as in perfect health. The skin is perfectly free from eruption and other appearances of disease, nor are there any traces of the disorder discoverable by examination of the entrails, the body, or the head of the animal...<sup>2</sup>

Clinical signs of scrapie during this epidemic included emaciation, paresis of hind limbs, trembling, ataxia, and excessive drinking. The clinical signs appeared in animals between 2-4 years of age and lasted between 10-12 weeks after the initial onset. As mentioned in the excerpt, necropsies of affected animals showed no anatomical abnormalities<sup>1,2</sup>. No defining pathological features of scrapie disease would be found until 1898 when Besnoit and colleagues discovered neuronal vacuolation in all affected sheep<sup>4,5</sup>. In 1936, scrapie was classified under a new disease group known as transmissible spongiform encephalopathies (TSE)<sup>1-3,6,7</sup>.

The epidemic ended when farmers started breeding rams from scrapie-resistant breeds to ewes from susceptible breeds. At this time, researchers believed scrapie was hereditary since the altered breeding protocol resulted in sheep breeds that were resistant to scrapie. However, investigations in the 1930s revealed that the scrapie agent, while probably having a hereditary component, was also infectious. The Cuillé and Chelle experiments and a

louping-ill-vaccine-related scrapie outbreak, both occurring in the 1930s, revealed the infectious nature of the scrapie agent<sup>3,6,8,9</sup>. Cuillé and Chelle inoculated seventeen sheep through various routes with central nervous system (CNS) material from scrapie-infected sheep. Eight of the inoculated animals later developed scrapie. In a similar experiment, these same two researchers discovered that the scrapie agent could pass through a porcelain filter<sup>8,9</sup>. At the same time, a new scrapie outbreak, associated with vaccination of louping-ill vaccine, was affecting flocks in England and Scotland. Louping-ill vaccine is prepared using brain, spinal cord, and spleen from animals affected by the louping-ill virus, and formalin-fixed to inactivate the virus<sup>3,6,8</sup>. Researchers discovered that brain tissue used to generate a batch of the louping-ill vaccine in 1935 was contaminated with scrapie. Several important conclusions came from these studies: the scrapie agent is transmissible, it passes through a membrane that catches bacteria and larger microorganisms, and it is present in the brain, spinal cord, and/or spleen of infected animals<sup>8</sup>. Even with these breakthroughs, the scientific investigation into the cause of the scrapie epidemic/outbreaks did not intensify until after two human TSEs were discovered: Creutzfeldt-Jakob disease (CJD) and kuru.

In 1920, Hans-Gerard Creutzfeldt described a 23-year-old female patient as having ataxia, dementia, tremors, and spasticity. The patient had several symptoms related to other neurodegenerative disorders, but she also had symptoms that did not fit these previously described diseases. Therefore, Creutzfeldt proposed that he had discovered a new disease<sup>10</sup>. A year later, Alfons Jakob described nearly identical symptoms in three additional patients. Autopsy findings of these three patients revealed astrocyte proliferation and severe neuronal degeneration in the cerebral cortex and basal ganglia. Jakob proposed that both his and Creutzfeldt's patients were suffering from the same neurodegenerative disease<sup>11</sup>. This disease would later be referred to as Creutzfeldt-Jakob disease or CJD<sup>12</sup>.

In a remote region of the Eastern Highlands of New Guinea, Carleton Gajdusek and Vincent Zigas discovered a new disease called kuru. Early symptoms of kuru included ataxia and tremors, and later symptoms included cerebellar ataxia, tremors, dysarthria, paralysis, dementia, and eventually death. Kuru affected children of all ages/gender and adult females but rarely affected adult males. There were no gross pathological findings upon autopsy of any affected individual<sup>1,13-16</sup>. However, microscopic examination of the CNS revealed neuronal degeneration, plaques, and astroglia proliferation in all patients<sup>15</sup>.

Later it was discovered that kuru was transmitted through the cannibalistic consumption of nervous system material during death rituals. The Fore people commonly performed rituals of respect for their dead relatives by consuming the flesh and organs of the individual. The women performed the dismemberment of the bodies during

the ritual and often had children crowding around them. Women and children also ate the nervous tissue of the dead individual more often than the males of the tribe. This gender task difference revealed why women and children had a higher incidence of kuru than men. The incidence of kuru dropped dramatically when cannibalism within the tribe stopped<sup>1,16</sup>.

In 1959, kuru, scrapie, and CJD were all proposed to be similar diseases based on epizootiological, etiological, and pathological characteristics. Hadlow suggested a link between scrapie and kuru. He noted that both diseases have a long incubation period, affect restricted populations, and have a similar clinical disease course. Kuru and scrapie also have the same neuropathological characteristics such as activated astrocytes and widespread neuronal degeneration<sup>6,17</sup>. Klatzo performed a pathological study on the brains of twelve kuru patients and noted that there were striking similarities between the pathological characteristics of kuru and CJD<sup>6,18</sup>. Experimental transmission of kuru and CJD into chimpanzees proved that these diseases not only share common neuropathological features, but they also share the infectious nature that characterizes scrapie<sup>17,19,20</sup>. These theories about relatedness would one day lead to the discovery that the same etiological agent causes all three diseases, and to the classification of all three diseases as TSEs.

### ***Discovering Prions: Characteristics of the scrapie agent***

Scrapie research did not intensify until the 1960s-70s due to the lack of laboratory animal models for the disease. In the 1960s, R.L. Chandler successfully transmitted scrapie disease to laboratory mice inoculated intracerebrally with scrapie from a goat<sup>21</sup>. The results from these studies showed that the mice developed similar clinical signs and neuropathological characteristics of scrapie disease in goats and sheep<sup>21,22</sup>. Early research of scrapie in mice provided details about how the agent spread throughout the bodily organs. Peripheral exposure of scrapie demonstrated that the scrapie agent replicates in lymphocytic organs such as the spleen, then moves to the spinal cord where it can infiltrate the brain<sup>23-25</sup>. These early studies led to many hypotheses about the identity of the scrapie agent, which resulted in many discoveries on the characteristics of the scrapie agent.

During the scrapie epidemic in the 17<sup>th</sup> and 18<sup>th</sup> centuries, researchers noticed that most of the scrapie-afflicted sheep were also affected by sarcosporidiosis caused by the parasite *Sarcosporidia*. These researchers proposed that a heavy infection of *Sarcosporidia* was likely the cause of scrapie, and was the scrapie agent. However, not all sheep infested with *Sarcosporidia* also contracted scrapie<sup>2</sup>. Then in the 1930s, Cuillé and Chelle proved that the activity of the scrapie agent did not decrease when filtered through porcelain filters. They suggested

that the scrapie agent is a virus and cannot be a bacterium or a parasite due to its small size<sup>8,9</sup>. This result was confirmed when scrapie activity remained intact after filtration through 50 nm filters. Activity was significantly reduced when passed through 25 nm filters suggesting that the operational size of scrapie is around 50-30 nm in diameter<sup>26</sup>. The virus hypothesis was the most prevalent theory of the identity of the scrapie agent<sup>27,28</sup>, but the identity was far from solved.

The virus hypothesis was an attractive theory at the time but it could not explain many of the unusual biochemical characteristics of the scrapie agent. Experiments involving ultraviolet (UV) and ionizing irradiation<sup>29-33</sup>, and nucleic acid enzymes<sup>29,34-37</sup> provided some of the most compelling pieces of evidence that scrapie is not a virus. Viruses store their genetic information within DNA/RNA and do not replicate without these molecules<sup>27</sup>. Nucleic acids are destroyed under UV and ionizing irradiation and using RNase and DNase treatment. Unlike viruses, the activity of the scrapie agent does not diminish under high concentrations of UV and ionizing irradiation, RNases, and DNases, suggesting that the main component of scrapie is not a nucleic acid<sup>29-37</sup>. Also, Alper et al. found the molecular weight of the scrapie agent to be  $1.5-2 \times 10^5$  Daltons, which indicates an impossibly small DNA/RNA genome of around 800 nucleotides. A genome of this size would be too small to encode anything useful<sup>30</sup>. Therefore, it was proposed that scrapie must not be a virus since it replicates without the use of a nucleic acid.

Other hypotheses of the identity of the scrapie agent included: infectious carbohydrate molecule<sup>29</sup>, self-replicating membrane<sup>29</sup>, viroid<sup>38,39</sup>, and replicating protein<sup>29,40-42</sup> among others. Since there was such a wide range of hypotheses to describe the scrapie agent, researchers performed many biochemical experiments to try and deduce the identity of the scrapie agent. The agent does not have reduced activity when boiled. The activity of scrapie decreased only when temperatures of 100°C are reached<sup>29,35</sup>. The agent is resistant to formalin inactivation, which usually inactivates viruses<sup>37</sup>. Several chemicals that inactivate other infectious agents have little to no effect on the scrapie agent, including most organic solvents<sup>29,43</sup>, some detergents<sup>29,35,43</sup>, and treatment with fluorocarbons<sup>29,35,44</sup>. Some chemicals that did affect the titer of the scrapie agent include urea<sup>29,44</sup>, sodium dodecyl sulfate detergent<sup>43</sup>, phenol<sup>29,44</sup>, proteolytic enzymes after fluorocarbon treatment<sup>29,35,44</sup>, and periodate<sup>44</sup>. These characteristics excluded most of the hypotheses about the agent but also resulted in much confusion on the actual identity.

The intracellular location of the scrapie agent was of great interest to early scrapie researchers. It became immediately apparent, with the advent of the mouse scrapie model, that the scrapie agent associates with membranes<sup>29,45-49</sup>. Differential centrifugation of scrapie-infected brain homogenate showed scrapie agent activity

located in every cellular fraction, with the crude mitochondrial fraction showing the greatest activity<sup>45,46</sup>. Techniques using ultrasonic vibrations and filtration revealed scrapie activity was highest in crude mitochondrial sub-fractions containing plasma membrane and endoplasmic reticulum<sup>48</sup>. Several years later, the advent of two techniques resulted in the discovery of the precise location of the scrapie agent. The two techniques were: a mouse scrapie cell line, SMB cells, was developed using brain homogenate from a mouse infected with the Chandler scrapie strain<sup>50</sup>, and the Bingham and Burke method of separating plasma membrane from endoplasmic reticulum<sup>49</sup>. Scrapie activity was isolated to the plasma membrane by separating it from the mitochondrial fraction using these two techniques<sup>49</sup>.

This discovery led to the membrane hypothesis, which stated that the scrapie agent does not contain nucleic acids but instead is a membrane-bound complex of macromolecules. The membrane hypothesis explains some of the unusual physicochemical properties of the scrapie agent, including that the agent is partially resistant to proteolytic enzymes and heat, and that all cellular fractions contain some scrapie activity<sup>29,47</sup>. However, questions remained whether the scrapie agent was a self-replicating membrane, or if the agent only associated with membranes.

In the late 1970s, Stanley Prusiner performed purification experiments on the scrapie agent that ultimately led to the identity of the agent. He used differential centrifugation, detergent treatment, and a sucrose gradient to purify the scrapie agent from cell constituents. Using the purified scrapie agent, he determined that, while the scrapie agent associated with membranes, its infectious nature remained intact when isolated away from membranes<sup>51-53</sup>. The scrapie agent was also found to aggregate and be of a hydrophobic nature<sup>52,54,55</sup>. The agent was also inactivated and reactivated using carbethoxylation and hydroxylamine<sup>56</sup>. Prusiner postulated the scrapie agent was a protein because of the above conclusions, and because chemicals that disrupt/denature proteins inactivate the scrapie agent. He defined the agent as a proteinaceous infectious particle, aka prions<sup>53,55</sup>.

The prion hypothesis remained highly controversial for some time but the discovery of a protein that was purified from scrapie brains helped cement the hypothesis in the scientific field. A highly protease-resistant protein, PrP (aka the prion protein), was found upon proteinase K (PK) digestion of hamster brains infected with scrapie. This PK-resistant fragment has a molecular weight of 27,000-30,000 Daltons. PrP27-30 is only found in infected brains and is the only major protein found in these samples<sup>57-59</sup>. PrP27-30 is also found in patients with kuru, CJD, and another human TSE disease Gerstmann-Sträussler-Scheinker syndrome (GSS)<sup>57,58,60</sup>. Further analysis of PrP27-30 revealed that it has 245 amino acids, and is highly enriched with glycine residues<sup>61</sup>. Electron microscopy images of PrP27-30 showed aggregation of the fragment into rod-shaped particles that were 100-200 nm in length. The rod-

shaped aggregates stained with Congo red and showed a green birefringence, which along with glycine residues, indicates that PrP27-30 is an amyloid protein. The authors of this study speculate PrP27-30 contains  $\beta$ -pleated sheets as this is another characteristic of amyloid protein<sup>62</sup>. PrP27-30 was also discovered to be a glycoprotein with multiple carbohydrate residues<sup>63</sup>. With the discovery of a short sequence of PrP27-30 in prion-infected samples, the next question became what biological process leads to the creation of this protein.

### ***Beyond the Discovery of Prions: The cellular prion protein (PrP<sup>C</sup>)***

#### *History of the cellular prion protein*

For many years, it was postulated that scrapie, kuru, and CJD were hereditary and possessed a genetic element of transmissibility. This hypothesis existed because some sheep were known to be resistant to scrapie infection, and Gajdusek had initially postulated a genetic basis of kuru transmissibility due to more women and children being afflicted with the disease<sup>15,16</sup>. However, this genetic element, much like the prion, was highly elusive. Scrapie mouse models provided an ideal model to study the genetic control of the scrapie agent quantitatively. Inbred strains of mice that were bred with half-inbred strains of mice revealed that an autosomal dominant gene with a single pair of alleles controlled the incubation period of the ME7 scrapie strain. The authors coined this gene *sinc*, with the *s7* allele for short incubation periods and the *p7* allele for long incubation periods<sup>64,65</sup>. Interestingly, even though the alleles correlated with short and long incubation times, the titer of the scrapie agent remained at the same concentration upon terminal disease in both the brains and spleens of scrapie-infected mice. These data indicated that the *sinc* alleles only determine the delay or time to initial replication of the scrapie agent, and not either the rate of replication or endpoint concentration of the agent<sup>66,67</sup>. Incubation periods influenced by different alleles of *sinc* also change depending on the scrapie strain utilized. Infections with the ME7 strain resulted in long incubation periods in mice expressing the *p7* allele and short incubation periods in mice with the *s7* allele. However, infections with the 22A strain in mice expressing the *s7* allele resulted in long incubation times and short ones in mice expressing the *p7* allele. This strain dichotomy implies that the interaction between the scrapie strain and the product of the *sinc* gene determines incubation periods<sup>68,69</sup>.

A gene that controls incubation time in sheep, *sip*, was found at the same time as *sinc* was found in mice. Using the SSBP/1 strain of sheep scrapie, the *sip<sup>sA</sup>* allele in either homozygote or heterozygote form results in short incubation times, and the *sip<sup>pA</sup>* homozygote results in extremely long incubation periods that extend beyond the animal's lifetime<sup>69,70</sup>. However, just like *sinc*, the incubation periods are reversed when CH1641 scrapie strain is

used. Since both *sinc* and *sip* have this characteristic, it was assumed that they were homologs and that the same gene controlled incubation time in both sheep and mice<sup>69</sup>.

The sequencing of the NH<sub>2</sub>-terminal of PrP27-30 provided a template from which tissues could be screened for the scrapie agent. Two different laboratories found that PrP27-30 is part of a larger, PK-sensitive protein called PrP33-35. Uninfected tissues from mice and hamsters contain PrP33-35, which indicates that a host gene encodes the infectious form of scrapie<sup>71-74</sup>. Various tissues including brain, spleen, heart, lung, and kidney express this host gene, *prnp*, and its concomitant protein<sup>71,75</sup>. *Prnp* encodes two different alleles A and B for long and short incubation times, respectively<sup>76</sup>. PrP33-35 resembles PrP27-30 in that it has a hydrophobic NH<sub>2</sub>-terminus, and two N-glycosylation sites<sup>71,73</sup>. To differentiate the uninfected from the infectious form of PrP33-35, the notations PrP<sup>C</sup>, for the cellular form, and PrP<sup>Sc</sup> or PrP<sup>Res</sup>, for the scrapie form/PK-resistant form, are utilized<sup>75</sup>.

Questions arose as to whether *prnp* was the only gene involved in scrapie infection or whether it was part of a complex. Along with *sinc* and *sip*, another gene, *prn-i*, was found to control incubation times. *Prn-i* was mapped close to the location of *prnp* on chromosome 2 in mice and was found to have two alleles *N* and *I* that controlled short and long incubation times, respectively<sup>77,78</sup>. It was proposed that *prnp*, *prn-i*, and *sinc* are congruent, instead of being separate genes acting in a prion protein complex, due to multiple shared characteristics<sup>79,80</sup>. To determine this, gene-targeted mice, with *prnp*<sup>A</sup> and *sinc*<sup>s7</sup> alleles, which gives long incubation times, had shortened incubation times with mouse scrapie when the A allele was changed to a B allele. These results indicate that the *prnp* gene and its alleles is the sole determinant of incubation times<sup>80</sup>.

#### *Structure, Regulation, and Trafficking of PrP<sup>C</sup>*

5'-untranslated regions, non-coding exons (humans), introns (murine and bovine), and/or 3'-untranslated regions control gene expression of *prnp*. The *prnp* promoter doesn't contain a traditional TATA box. Instead, the promoter is highly G/C rich and contains binding sites for several transcription factors including Sp1. The promoter also contains CpG islands near the transcription start sites. These characteristics of the promoter indicate that *prnp* is a housekeeping gene, and the protein may be involved in housekeeping functions<sup>75,81-85</sup>.

Most adult tissues express PrP<sup>C</sup> mRNA and protein, with the highest levels being in neurons within the CNS. Specifically, PrP<sup>C</sup> is highly expressed in anterior brain regions, synaptic layers of the hippocampus and dentate gyrus, and the molecular cell layer in the cerebellum<sup>86</sup>. Expression of PrP<sup>C</sup> protein is lower in all other adult tissues compared to the brain. During embryogenesis, PrP<sup>C</sup> mRNA and protein expression begins at E8.5-9 when the

embryo switches from an anaerobic to an aerobic state. Some researchers believe that this suggests PrP<sup>C</sup> functions in the defense against antioxidants<sup>87,88</sup>. It is not known whether the embryonic expression continues until birth, or whether it stops during embryogenesis and then commences again after birth. After birth, there is a 4-fold increase in PrP<sup>C</sup> protein levels in the brain until day 35<sup>89</sup>.

After day 35 in the postnatal mouse, PrP<sup>C</sup> expression is steady throughout the lifetime of the animal<sup>89</sup>. Also, PrP<sup>C</sup> mRNA expression remains stable during scrapie infection<sup>75,90,91</sup>. However, several scenarios lead to an increase in PrP<sup>C</sup> expression. Activation of T lymphocytes by immune complexes or vesicular stomatitis virus increased PrP<sup>C</sup> protein expression<sup>92</sup>. The activation of dendritic cells by lipopolysaccharide and CpG oligodeoxynucleotides also upregulated the expression of PrP<sup>C93</sup>. The increase in PrP<sup>C</sup> in lymphocytes led to an increase in susceptibility to prion infection, indicating that more PrP<sup>C</sup> leads to more PrP<sup>Res94</sup>. PrP<sup>C</sup> mRNA and protein are also upregulated during heat shock response<sup>95</sup>. These results imply that PrP<sup>C</sup> may modulate immune responses or provide a cell signaling/defense mechanism during cellular stress<sup>92,93,95</sup>. No instances of natural downregulation of PrP<sup>C</sup> have been reported.

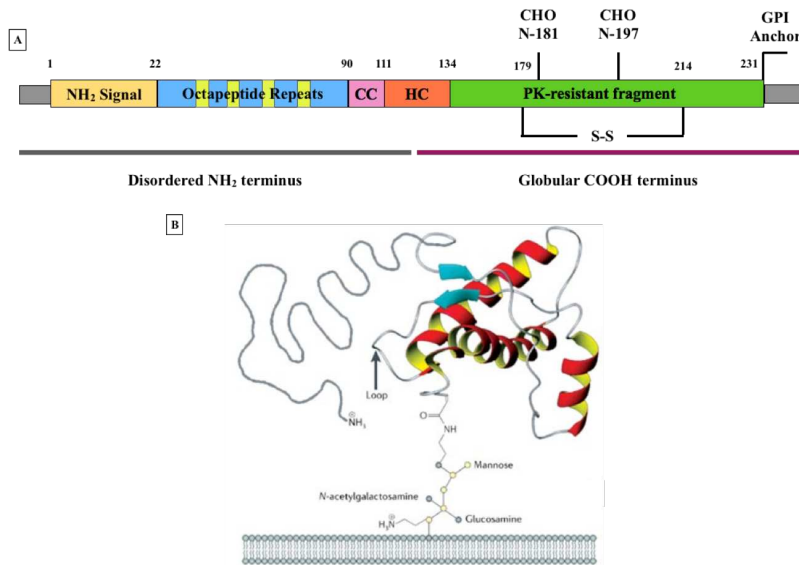


**Figure 1.1. Artistic representation of PrP<sup>C</sup>.**

A) Diagram of *prnp* gene structure. Nucleotide number locations are shown for the gene components. CC=Charged Clusters. HC=Hydrophobic Core. S-S=Disulfide bridge. B) Secondary structure of the PrP<sup>C</sup> protein. *Nature Reviews Microbiology*. 2006. 4:765-775. DOI: 10.1038/nrmicro1492

Unlike PrP<sup>Res</sup>, PrP<sup>C</sup> is a soluble protein and is highly sensitive to PK digestion. The *prnp* gene encodes for an immature 250-amino acid protein. A signal peptide on the NH<sub>2</sub>-terminus, encompassing residues 1-22, targets the immature protein to the endoplasmic reticulum (ER) for further posttranslational processing. This NH<sub>2</sub>-terminal signal peptide is eventually cleaved off. The hydrophobic peptide of the COOH-terminus is replaced with a glycosylphosphatidylinositol (GPI) anchor<sup>96</sup>. In mice, the mature protein is 208-amino acids, encompassing residues 23-231<sup>97</sup>. The mRNA molecule encoding PrP<sup>C</sup> is 2.1kb long<sup>72</sup> and has an open reading frame that is contained within exon 2 (sheep and humans) or 3 (mice), depending on the species. The *prnp* gene is located on chromosome 2 in mice and chromosome 20 in humans and is part of the *PRN* locus<sup>96</sup>.

PrP<sup>C</sup> contains a structured globular domain from residues 125-228, three  $\alpha$ -helices and two  $\beta$ -sheets, and a disordered flexible NH<sub>2</sub>-terminus tail from residues 23-124 that contains four or five octapeptide repeat units<sup>97-99</sup>. While the cellular form of PrP<sup>C</sup> contains mostly  $\alpha$ -helices, the infectious form contains mostly  $\beta$ -pleated sheets. It is this conversion of secondary structure that allows PrP<sup>C</sup> to become infectious and pathologic<sup>100,101</sup>. The COOH-terminus globular domain of PrP<sup>C</sup> also includes a disulfide bridge at Cysteine residues 179 and 214.

Post-translational modification of PrP<sup>C</sup> occurs in the form of glycosylation in the Golgi apparatus. The *N*-glycosylation sites take the form Asn-X-Thr. In human PrP<sup>C</sup>, the glycosylation sites are Asn-181-Ile-Thr and Asn-197-Phe-Thr, and in the mouse asparagine residues 180 and 196 are glycosylated. These glycosylation sites can be deglycosylated using PNGase F digestion, which produces a 27 kDa PrP<sup>C</sup> molecule<sup>102,103</sup>. PrP<sup>C</sup> can exist as three separate isoforms due to the glycosylation: un-, mono-, or diglycosylated. At any one given time, all three forms are present in specific brain regions, but the primary form expressed in most brain regions is the diglycosylated form. The existence of these three isoforms suggests that each isoform may have a physiological role or may determine the efficiency of prion strain replication. For example, different glycoform ratios have been used to identify strains of PrP<sup>Res</sup>, such as variant CJD from bovine spongiform encephalopathy (BSE)<sup>103,104</sup>.

As discussed above, PrP<sup>C</sup> enters the ER, via a NH<sub>2</sub>-terminus signal, where cleavage of the signal peptide and transfer of the GPI anchor occurs. PrP<sup>C</sup> then migrates through the ER where it acquires its folded structure before moving on to the Golgi to be glycosylated<sup>105</sup>. Studies have shown that there are three different topologies of PrP<sup>C</sup> that exist within the ER. The usual form of the protein, <sup>Sec</sup>PrP, translocates to the plasma membrane. The other two topologies are transmembrane forms that span the ER membrane at residues 110-135: <sup>Ctm</sup>PrP, which has its COOH-terminus in the ER lumen, and <sup>Ntm</sup>PrP, which has its NH<sub>2</sub>-terminus in the ER lumen<sup>106-108</sup>. While the exact

function/relevance of these two transmembrane forms is unclear, <sup>C<sup>tm</sup></sup>PrP does cause a prion-like disease without PrP<sup>Res</sup>, indicating that more than one topology of PrP<sup>C</sup> can be involved in prion infection<sup>106,108</sup>. The ER-Golgi network is of particular importance for prion disease because if PrP<sup>C</sup> exit from this network is blocked then no disease is apparent<sup>109</sup>. Also, in some inherited forms of prion disease, immature PrP<sup>C</sup> misfolds in the ER and subsequently leads to disease<sup>105</sup>. PrP<sup>C</sup> is shown to associate with lipid components before its exit from the Golgi and is rapidly transported to the plasma membrane (<1 hour after synthesis)<sup>109</sup>.

PrP<sup>C</sup> is found on the surface of the cell membrane after translocation from the ER-Golgi network<sup>29,47</sup>. In a seminal paper, Brown and Rose showed that GPI anchored proteins localize in specialized locations on the cell surface called lipid rafts<sup>110</sup>. These lipid rafts are highly-ordered lipid structures enriched in sphingolipids and cholesterol<sup>111-114</sup>. The saturated acyl chains of the GPI-anchored protein target it to lipid rafts because the acyl chains are highly attracted to the sphingolipids<sup>113</sup>. The importance of the lipid composition of lipid rafts was demonstrated when the lipid rafts became disorganized upon depletion of either cholesterol or sphingolipid<sup>112</sup>. Reduction of cholesterol also results in a decrease in PrP<sup>Res</sup> formation<sup>115</sup>. This conclusion has led to the argument that PrP<sup>C</sup> is converted to PrP<sup>Res</sup> on the cell surface in lipid rafts. However, there is also evidence that conversion takes place in clathrin-coated endosomes during PrP<sup>C</sup> recycling<sup>112,115,116</sup>.

PrP<sup>C</sup> is translocated out of the plasma membrane and endocytosed in less than one hour<sup>117</sup>. Studies revealed that PrP<sup>C</sup> moves out of lipid rafts into a non-lipid raft membrane region before being endocytosed<sup>118</sup>. This movement occurs due to the polybasic residues in the NH<sub>2</sub>-terminus. It is unknown whether the NH<sub>2</sub>-terminus sends a signal or if it interacts with transmembrane proteins with internalization regions<sup>112,118,119</sup>. After PrP<sup>C</sup> moves out of the lipid raft domain, it becomes internalized into clathrin-coated pits<sup>117,118,120</sup>. The binding of Cu<sup>2+</sup> ions to the octapeptide repeats mediates the internalization but Cu<sup>2+</sup> is not required. Binding of other ligands also causes increased endocytosis; however, again it is not known if the endocytic pathway is physiologically dependent on these ligands<sup>117,121</sup>. During endocytosis, PrP<sup>C</sup> moves from early to late endosomes and eventually to lysosomes<sup>122</sup>. The half-life of PrP<sup>C</sup> varies from 3-6 hours in established cultured cells to 1.5-2 hours in primary cell culture<sup>119,123,124</sup>.

#### *Function or lack thereof of PrP<sup>C</sup>*

The first attempts to discover the function of PrP<sup>C</sup> came from the generation of PrP-null mice. The Zürich I strain of mice replaced a small section of exon 3 of the *prnp* gene with a neo cassette, and the Edinburgh (Npu) strain of mice inserted a neo cassette into exon 3 after residue 93. The Zürich I and Edinburgh mice were on

C57Bl/6J x 129/Sv or 129/Sv only backgrounds, respectively. The mice in both PrP-null strains show no physical/gross abnormalities nor do they have any detectable outward behavioral differences<sup>125,126</sup>. The PrP-null strains do not have any PrP<sup>Res</sup> accumulation upon prion infection and do not display any neuropathology related to prion disease<sup>127,128</sup>. The function of PrP<sup>C</sup> remains elusive since these PrP-null mice showed no outward phenotypic difference compared to the wild-type.

Subtle differences in circadian rhythms, behavior, memory, and neuronal organization do exist within these PrP-null mice. Zürich I and Edinburgh PrP-null mice have elevated circadian motor activity during the constant darkness cycle. Also, these mice are more sensitive to sleep fragmentation and deprivation compared to wild-type mice. The circadian differences return to normal after reintroduction of PrP<sup>C</sup>, indicating that the alterations are due to PrP<sup>C</sup> depletion. These data implicate a possible loss-of-function role of PrP<sup>C</sup> depletion in a human prion disease with altered circadian patterns (FFI, discussed below)<sup>129</sup>. There is also mossy fiber reorganization in the hippocampus, which might contribute to changes in locomotor activity observed in PrP-null mice<sup>130-132</sup>. There are other hippocampal alterations noted within PrP-null mice including deficits in short- and long-term memory. The altered hippocampal synapses and neural circuits point to a function of PrP<sup>C</sup> within the hippocampus, but none of these lines of evidence point to what that function is<sup>133,134</sup>. One hypothesis to explain the results of the PrP-null mice is that PrP<sup>C</sup> interacts with a ligand for its normal function. Therefore, depletion of PrP<sup>C</sup> might then either cause no signaling or an altered signaling through this ligand producing the small effects seen in PrP-null mice. However, since these mice display no overt phenotype, it is also suggested that the ligand interacts with another protein to abrogate the loss of PrP<sup>C</sup><sup>125,126</sup>.

Many papers examining the function of PrP<sup>C</sup>, and of its conversion to PrP<sup>Res</sup>, have alluded to an accessory protein that either helps with the function of PrP<sup>C</sup> or helps in the conversion of PrP<sup>C</sup> to PrP<sup>Res</sup>. Therefore, some researchers focused their attention on ligands or receptors of PrP<sup>C</sup> to elucidate if this 'protein X' exists. There are numerous ligands/receptors of PrP<sup>C</sup> that bind to it or that it binds to, including Synapsin Ib, Bcl-2, GFAP, Nrf2, NCAM, and Hsp60 among others. Perhaps the biggest contenders for the identity of protein X include the 37kDa/67kDa laminin receptor, stress-inducible protein 1 (STI1), and copper (Cu<sup>2+</sup>).

Laminin is the major glycoprotein found in the extracellular matrix of the basement membrane. It is made up of three different subunits  $\alpha$ ,  $\beta$ , and  $\gamma$ . Laminin functions in cell differentiation, proliferation, migration, and neurite outgrowth, and the 37 kDa/67 kDa laminin receptor (LRP) functions in cell signaling. PrP<sup>C</sup> binds to the LRP

at residues 161-179. The LRP binding site on PrP<sup>C</sup> encompasses residues 144-179. There is a secondary LRP binding site on PrP<sup>C</sup> at residues 53-93 that requires co-binding of heparan sulfate<sup>135</sup>. Binding of PrP<sup>C</sup> to LRP results in increased internalization of PrP<sup>C</sup> into endosomes<sup>136</sup>. PrP<sup>C</sup> binds to laminin in a saturable manner with a dissociation constant ( $K_d$ ) of  $2 \times 10^{-8}$  M. In primary rat hippocampal slices and PC12 cells, the interaction between PrP<sup>C</sup> and laminin resulted in neurite outgrowth. Also, treatment with anti-PrP antibodies reduced but did not eliminate neurite outgrowth, indicating that there is a redundant protein to compensate for the loss of PrP<sup>C</sup><sup>137</sup>. Treatment of rats with either anti-PrP antibodies or anti-laminin antibodies decreased the retention of fear memory in the animals. The authors speculate that the reduced memory retention is due to an inhibition of ERK1/2 and PKA signaling since PrP<sup>C</sup> and laminin are known to bind to these signaling molecules<sup>138</sup>. Protein X is believed to aid in the conversion of PrP<sup>C</sup> to PrP<sup>Res</sup>. The conversion is not optimal when residues 167, 171, and 218 are removed from PrP<sup>C</sup>, indicating that these sites might be the protein X binding sites. Since LRP binds to PrP<sup>C</sup> at two of these residues, the authors conjecture that LRP could be the putative protein X<sup>135,139,140</sup>.

Stress-inducible protein 1 (STI1) helps PrP<sup>C</sup> enter the endocytic pathway into early endosomes<sup>141</sup>. The main role of STI1 is to help regulate the heat shock response initiated by Hsp70, and it is a 66 kDa protein that colocalizes with PrP<sup>C</sup> on the cell surface. STI1 colocalizes with PrP<sup>C</sup> specifically in hippocampal neurons where it initiates both neuritogenesis and neuroprotective functions with PrP<sup>C</sup> through the MAPK and PKA signaling pathways<sup>142</sup>. Another study found that STI1 and PrP<sup>C</sup> provided protection from oxidative stress by modulating the activity of superoxide dismutase (SOD). STI1 and PrP<sup>C</sup> also protected retinal neurons from apoptosis using the cAMP/PKA signaling pathway<sup>143</sup>.

The octapeptide repeat region in the NH<sub>2</sub>-terminus of PrP<sup>C</sup> contains four Histidine residues, which bind Cu<sup>2+</sup> ions with a  $K_d$  of 5  $\mu$ M<sup>144,146</sup>. There is a fifth Cu<sup>2+</sup> binding site either located at His 96 or His 111 with a  $K_d$  in the nanomolar to femtomolar range<sup>147</sup>. Cu<sup>2+</sup> binding to PrP<sup>C</sup> in wild-type mice showed that Cu<sup>2+</sup> aids in the endocytosis of PrP<sup>C</sup> by aiding movement of PrP<sup>C</sup> to a non-lipid raft part of the membrane before it becomes endocytosed. Cu<sup>2+</sup> might work in conjunction with either laminin or STI1 to aid in endocytosis of PrP<sup>C</sup><sup>117,118,148</sup>. PrP-null mice have excess free Cu<sup>2+</sup> because of the inability to bind it at the cell surface due to the lack of PrP<sup>C</sup>. PrP-null mice also have a lower cellular membrane Cu<sup>2+</sup> content in synaptosomal fractions due to a lack of PrP<sup>C</sup> at synapses, which increases the susceptibility of these mouse lines to oxidative stress<sup>146,148</sup>. It is possible the increased susceptibility to oxidative stress is either caused by a decrease in Cu<sup>2+</sup> metabolism or a decrease in SOD activity.

SOD facilitates the response to oxidative stress thru the reduction of  $\text{Cu}^{2+}$ , which partitions a superoxide radical into  $\text{O}_2$  or  $\text{H}_2\text{O}_2$ . In PrP-null mice, lower cellular membrane concentrations of  $\text{Cu}^{2+}$  results in lower SOD activity and an increase in oxidative stress damage. Some studies have shown that PrP<sup>C</sup> has its own SOD activity in primary and secondary cultures, which might aid in resistance to oxidative stress<sup>149,150</sup>. However, this putative function of PrP<sup>C</sup> remains highly controversial because it does not explain some of the other functional features of PrP<sup>C</sup>. Instead, it is thought that perhaps the SOD activity of PrP<sup>C</sup> acts as a buffer system for excess  $\text{Cu}^{2+}$  at the synapse<sup>148</sup>.

The anti-oxidative stress function of PrP<sup>C</sup> remains highly contentious because some groups reported adverse cellular effects due to the binding of  $\text{Cu}^{2+}$ <sup>145,147</sup>. Binding of  $\text{Cu}^{2+}$  to the fifth binding site causes a conformational change in the secondary structure from  $\alpha$ -helices to  $\beta$ -sheets. It is not known if this structural change results in infectious isomers<sup>147</sup>, but the conversion of cellular PrP<sup>C</sup> to infectious PrP<sup>Res</sup> is mediated by a transformation of  $\alpha$ -helices into  $\beta$ -sheets. Also, duplication of more than one octapeptide repeat results in two human prion diseases, fCJD and GSS (discussed below)<sup>147,151</sup>. During oxidative stress, PrP<sup>C</sup> is cleaved into a 28.5 kDa NH<sub>2</sub>-terminal peptide. It is unclear what, if any, function this peptide might have, including if it retains any PrP<sup>C</sup> function (known or otherwise) after cleavage<sup>151</sup>. There is more evidence pointing to a neuroprotective role against oxidative stress, but it is hard to reconcile some of these negative findings. Therefore, the exact reason of  $\text{Cu}^{2+}$  binding remains questionable.

The observation that PrP<sup>C</sup> can bind to the anti-apoptotic protein Bcl-2 is evidence that supports an anti-apoptotic role for PrP<sup>C</sup>. Bcl-2 associates with the Bax protein, and suppresses cell death in a homodimeric complex. When Bcl-2 no longer binds to Bax, and Bax forms homodimers, a pro-apoptotic signal is initiated. It was shown that PrP<sup>C</sup> bound to the 37 amino acids of the COOH-terminus of Bcl-2<sup>152,153</sup>. The interaction between PrP<sup>C</sup> and Bcl-2 rescued serum-deprived PrP-null primary hippocampal neurons from apoptosis<sup>154</sup>. Analysis of the PrP-null serum-deprived cells revealed DNA fragmentation consistent with apoptosis, suggesting that under certain conditions apoptosis is upregulated in these cells versus wild-type. Transfection of a PrP-expressing vector into PrP-null serum-deprived cells rescued the pro-apoptotic phenotype of the cells<sup>154</sup>. Similar results were seen in hypoxic or ischemic mouse and cell line models. PrP-null cells or mice with hypoxic or ischemic damage had larger and more extensive lesions than wild-type counterparts. Again, suggesting that PrP-null tissues are more susceptible to injury caused by both oxidative stress and/or apoptosis<sup>155-157</sup>. Deletion of the octapeptide repeats abolishes the phenotype of rescuing primary human neurons from Bax-induced apoptosis<sup>158</sup>. The octapeptide repeats on PrP<sup>C</sup> share homology with the

anti-apoptotic BH2 domain on Bcl-2, indicating that the octapeptide repeats might mediate the anti-apoptotic function of PrP<sup>C</sup>. By binding to Bcl-2, PrP<sup>C</sup> indirectly inhibits the Bax conformational change to a pro-apoptotic state<sup>159</sup>.

There is also evidence that PrP<sup>C</sup> either migrates to sites of damage or is upregulated in response to oxidative or apoptotic lesions. Studies have reported a 35% increase in PrP<sup>C</sup> protein expression in the injured hemisphere eight hours after injury in a cerebral ischemia mouse model, whereas the uninjured hemisphere showed no increase<sup>156</sup>. In a perinatal case of hypoxic-ischemic injury, PrP<sup>C</sup> mRNA increased and accumulated in damaged axons and neuronal somata. The authors note that the accumulation could be due to altered trafficking of neuronal proteins after injury, but it could also be due to an upregulation of PrP<sup>C</sup> in response to the injury, perhaps to activate a neuroprotective function<sup>155</sup>.

There are some conflicting reports on both the proposed antioxidant and anti-apoptotic functions of PrP<sup>C</sup> despite these conclusions on the possible neuroprotective function of the protein. If PrP<sup>C</sup> does indeed have a neuroprotective effect either as an antioxidant or anti-apoptotic role, one would think that the more PrP<sup>C</sup> expression, the better or, the less, the worse. However, overexpression of PrP<sup>C</sup> in either cultured cells, primary cells, or mouse lines results in deleterious effects. Overexpression in cells results in a pro-apoptotic phenotype mediated by caspase 3 activation. The overexpressing cells also displayed an increased sensitivity to a pro-apoptotic chemical called staurosporine<sup>160</sup>. Transgenic mice that overexpress PrP<sup>C</sup> have a spontaneous neurologic disease characterized by spongiform degeneration and skeletal myopathy reminiscent of scrapie infection<sup>161</sup>. On the other hand, in PrP-null mice, either before or after birth, there are no significant deleterious effects due to the loss of PrP<sup>C</sup>. If PrP<sup>C</sup> does have a neuroprotective function, PrP-null neurons should either be in oxidative stress or apoptosis, unless there is a compensatory mechanism<sup>162,163</sup>. Due to these studies, the role of PrP<sup>C</sup> as an anti-apoptotic protein is still questionable. Some argue that overexpressing PrP<sup>C</sup> does not mimic the physiological nature of PrP<sup>C</sup>, and the damage caused by overexpression might be due to an overexpression of the protein. Another theory is that PrP<sup>C</sup> may have slightly different functions in different cell lines. Some cell lines may display a pro-apoptotic role and some an anti-apoptotic role. These differing responses might be due to available ligands/receptors for PrP<sup>C</sup>. If a ligand is not available, such as STII, then perhaps PrP<sup>C</sup> becomes pro-apoptotic. If it is available, then the function becomes anti-apoptotic<sup>164</sup>.

The role of PrP<sup>C</sup> as a signaling molecule is much less debated than its antioxidant or neuroprotective functions. Besides the MAPK/ERK, PKA, and STAT1 cascades, PrP<sup>C</sup> has also been implicated in Ca<sup>2+</sup> signaling/homeostasis, the tyrosine kinase pathway, and the PI3K pathway. Organotypic retinal explants showed an increase in neuroprotection due to PrP<sup>C</sup> activating the MAPK/ERK and PKA pathways, and antibody clustering of PrP<sup>C</sup> also activates these pathways<sup>165-167</sup>. However, antibody clustering was also shown to cause severe neuronal apoptosis in the brains of mice. One explanation for this dichotomy is that as a single molecule, PrP<sup>C</sup> might signal through neuroprotective pathways, but as a dimer, it might signal through these pathways and result in neuronal damage<sup>168</sup>. The MAPK/ERK pathway is activated by the non-receptor Src-related family kinases, such as Fyn, during antibody clustering of PrP<sup>C</sup><sup>169</sup>. The Src kinase family also interacted independently of MAPK/ERK using the PI3K/Akt pathway, resulting in neurite outgrowth and survival<sup>166</sup>. It is hypothesized that PrP<sup>C</sup> activates the PKA and other signaling pathways through the binding of Cu<sup>2+</sup> or by the regulation of intracellular levels of Ca<sup>2+</sup> (mainly in the ER and mitochondria)<sup>170-172</sup>. Therefore, PrP<sup>C</sup> could be said to be a master regulator of multiple signaling pathways using a wide array of ligands/signaling molecules. Lastly, the PI3K/Akt pathway was shown to be activated for neurite outgrowth/survival and in response to reactive oxygen species. PrP<sup>C</sup> overexpression leads to activation of this pathway, whereas PrP-null cells are more sensitive to reactive oxygen species due to a decrease in PI3K/Akt activity<sup>166,173</sup>. These discoveries were made using an array of either primary or cultured cells from a neuronal or non-neuronal origin, suggesting that the interaction between signaling pathways and PrP<sup>C</sup> is universal.

PrP<sup>C</sup> also directs signaling pathways within the immune system. PrP<sup>C</sup> modulates the phosphorylation of PKC during mitogen activation, which results in activation of the MAPK pathway<sup>174</sup>. PrP<sup>C</sup> also associated with Fyn and Src tyrosine kinases upon antibody clustering. The interaction with Fyn was dependent on PrP<sup>C</sup> interaction with ZAP-70 after CD8 and CD3 signaling. This process was found to be caveolin independent and led to the amplification and diversification of T cells<sup>175</sup>. Another study reported that, instead of Fyn, PrP<sup>C</sup> interacted with Src tyrosine kinase for T cell activation<sup>176</sup>. The difference in results could be due to different cell lines or to different antibodies/methods used for antibody clustering of PrP<sup>C</sup>, as this approach does not mimic the real physiological state.

While neuronal cells are researchers' primary focus for the function of PrP<sup>C</sup>, PrP<sup>C</sup> is also widely expressed on non-neuronal cells, such as cells of the immune system. PrP<sup>C</sup> is found on hematopoietic stem cells (HSCs), which gives rise to all lymphoid cells, and functions to either protect HSCs from apoptosis or helps sustain a self-renewal

process<sup>177-179</sup>. The expression of PrP<sup>C</sup> on differentiated leukocytes is highly regulated and depends on the maturation and activation state of the cells. The protein is expressed on lymphocytes, monocytes, dendritic cells (DCs) and platelets, but not erythrocytes or granulocytes<sup>178,180,181</sup>. T and B lymphocytes and DCs have the highest expression of PrP<sup>C</sup> within the immune system, with DCs having the highest expression in the body besides neurons. Within DCs, CD8<sup>+</sup> conventional DCs express the highest amount of PrP<sup>C</sup>, indicating that PrP<sup>C</sup> is involved in Th1 immune responses<sup>93,182</sup>. Germinal centers of the spleen contain most of the PrP<sup>C</sup> expression observed on lymphocytes<sup>183</sup>, which suggests a potential role of PrP<sup>C</sup> in antigen activation of lymphocytes.

Indeed, PrP<sup>C</sup> expression increases 4-fold after activation of lymphocytes with mitogens, such as lipopolysaccharide, concanavalin A, or CpG oligodeoxynucleotides<sup>181,184</sup>. A lack of PrP<sup>C</sup> either in mice or on primary splenocytes results in a decrease in the proliferation of T lymphocytes in response to antigen presenting cells<sup>174,182</sup>. On the cell membrane, PrP<sup>C</sup> colocalizes with MHC class II and the TCR/CD3 complex<sup>93,183</sup>. The assemblage of PrP<sup>C</sup> with these complexes occurs due to clustering of PrP<sup>C</sup> by localization of flotillin 1 and 2 and the rearrangement of PrP<sup>C</sup> to the cellular 'cap', which results in recruitment of Fyn, Lck, and the TCR/CD3 complex. These activities lead to the activation of T cells<sup>185</sup>. PrP<sup>C</sup> also plays a significant role in the synapse between DCs and T cells, which could involve the flotillin activation of capping. When T cells are deficient in PrP<sup>C</sup>, proliferation in response to antigen presenting cells is not affected. However, dendritic cells deficient in PrP<sup>C</sup> lead to a reduction in the proliferation of T cells by antigen presenting cells. Thus, PrP<sup>C</sup> has an important function not only at the neurological synapse but also the immunological synapse<sup>182</sup>.

It is well understood that the conversion of PrP<sup>C</sup> to PrP<sup>Res</sup> involves a change of the secondary structure from  $\alpha$ -helices into  $\beta$ -sheets. This pathological conformer accumulates within the spleen, lymph nodes, Peyer's patches, and tonsils upon initial peripheral infection. It does not cause any pathology within these tissues, only within the CNS. This pathology includes spongiform degeneration, activation of glial cells, neuronal loss, and accumulation of amyloid plaques<sup>186,187</sup>. It is unclear whether the accumulation of PrP<sup>Res</sup> results in the pathology (gain-of-function hypothesis) or whether a loss-of-function of PrP<sup>C</sup> caused by the accumulation of PrP<sup>Res</sup> results in the pathology of prion diseases. An early study using prion-infected tissue grafted into the brains of PrP-null mice showed no clinical disease and no prion-related pathology, even though PrP<sup>Res</sup> had moved into the surrounding tissues. This was the first study to indicate that perhaps PrP<sup>Res</sup> was not neurotoxic, or at the very least did not fully contribute to the pathology of prion infection<sup>188,189</sup>. Another study by Mallucci's group removed PrP<sup>C</sup> using a *Cre/loxP* system after

establishing prion infection. They noted that the spongiform degeneration reversed upon removal of PrP<sup>C</sup> even though deposits of PrP<sup>Res</sup> remained in the brain tissue<sup>190,191</sup>. In two different human prion diseases (FFI and CJD), neuronal apoptosis does not correlate with deposition of PrP<sup>Res</sup><sup>192,193</sup>. These conclusions have led to the highly controversial loss-of-function hypothesis, which states that the pathology observed in prion infection is due to the loss of the physiological function of PrP<sup>C</sup>. This would make sense if the physiological function were truly an antioxidant or anti-apoptotic role. Reducing neuroprotection in the CNS along with the deposition of PrP<sup>Res</sup> could lead to the morphological characteristics seen in brain tissue of prion-infected individuals. However, since the function of PrP<sup>C</sup> is not known, this explanation is mere speculation. Other causes of the neuropathology could include withdrawal of activation signaling mechanisms, selective vulnerability of neurons to PrP<sup>Res</sup>, or early axonal changes due to PrP<sup>Res</sup> deposition<sup>194</sup>.

### ***Prion and Protein Misfolding Diseases***

#### ***Scrapie***

Natural scrapie disease is found in sheep and goats. It is usually characterized by weight loss, ataxia, and pruritus. Clinical signs in goats mimic that seen in sheep, but may also include hyperesthesia, bruxism, and regurgitation. There are two forms of scrapie: typical and atypical. The clinical signs described above indicate typical scrapie. Clinical signs of atypical scrapie include ataxia, weight loss, and behavioral changes, such as irritability and anxiety. Animals with atypical scrapie usually do not show pruritus<sup>195</sup>. The average age of onset of atypical scrapie is 6.5 years of age, whereas typical scrapie usually presents between 2-5 years with 3.5 years being the average. Both sexes are equally affected by both forms. Transmission of atypical scrapie is not well understood. Some suggest it is a spontaneous disease rather than an infectious disease. Transmission of typical scrapie usually occurs through the oral route, and frequently involves the eating of the placenta (one of the most infectious tissues for scrapie prions). Exposure to scrapie also occurs through contaminated milk (horizontal transmission), feces, and the environment where prions like to bind to the soil. After exposure, prions spread to the gut-associated lymphoid tissues (GALT), and then ascend to the CNS 10-12 months after exposure. A breeding protocol to select for sheep that carry the resistant genotype is still in effect in Europe to reduce the number of sheep affected by scrapie<sup>196</sup>.

Three different codons determine a sheep's susceptibility to scrapie: A136V, R154H, and Q171R/H. These codons lead to five alleles and fifteen different genotypes of resistance/susceptibility. Sheep fall into Risk Groups 1-5 based on their genotypes at these positions. The most resistant genotype (Risk Group 1) is ARR/ARR. The most

susceptible (Risk Group 5) genotypes are VRQ/VRQ, VRQ/ARQ, VRQ/ARH, and VRQ/AHQ. All the other genotypes fall in the intermediate susceptibility range<sup>196</sup>.

#### *Bovine Spongiform Encephalopathy (BSE)*

BSE, or mad cow disease, was first diagnosed in a cow in 1986 in the United Kingdom and thereupon revealed a BSE epidemic that devastated cattle herds. Clinical signs of BSE include aggression, tremors, gait abnormalities, and hyperreactivity to stimuli. An E211K polymorphism, a 12 base pair insertion/deletion in the 1<sup>st</sup> intron, and a 23 base pair insertion/deletion in the *prnp* promoter confer susceptibility of cattle to BSE. Like scrapie, there is an atypical form of BSE that is thought to occur spontaneously. Unlike scrapie, BSE does not spread from animal to animal. Tissues (with the exception of the CNS) and excreta, such as milk, feces, and urine, are not infectious<sup>195</sup>. The leading theory as to the origin of BSE is that scrapie was naturally passaged through cattle enough times to break the species barrier<sup>197</sup>. The species barrier of prion disease occurs because one type of prion from one species usually does not transmit to another species. Thus, most prion diseases are confined to the species' that they naturally infect. However, it is thought that cattle were fed meat and bone meal (MBM) that was contaminated with tissues from scrapie-infected sheep, and accumulated enough scrapie prions that the species barrier threshold was lowered<sup>195</sup>. In the early 1980s, the process of rendering carcasses in MBM production changed such that scrapie prions were not inactivated and were allowed to contaminate the MBM stock. It could have been possible that scrapie was able to pass the species barrier in the United Kingdom sooner/easier than other locations due to the higher prevalence of scrapie compared to other locations<sup>198</sup>. Alternative theories do exist as to the origin of BSE, such as cattle developing a genetic mutation that led to a spontaneous generation of prions or that BSE was already endemic in the UK just not recognized. However, these theories cannot explain how BSE emerged in one general location at one particular time and why it was never observed before. The most unusual aspect of the BSE epidemic is that it resulted in a unique prion with such an altered host range that not only does it infect cattle, but it also spread and infected humans (vCJD) and zoo animals (FSE) (discussed more below)<sup>198,199</sup>.

#### *Chronic Wasting Disease (CWD)*

CWD was first recognized in 1967 at a Colorado research facility and was characterized as a TSE in 1978<sup>200</sup>. The prevailing theory on the origin of CWD is that it is an altered form of scrapie (much like BSE). However, some have argued that it could have also been a spontaneous conversion of PrP<sup>C</sup> to PrP<sup>Res</sup>

<sup>201,202</sup>. CWD has been detected in almost half the states in the United States, two Canadian provinces, South Korea, and Norway. It affects both free-ranging and captive populations of the cervid family, such as mule deer, white- and black-tailed deer, Rocky Mountain Elk, Shira's moose, and Norwegian reindeer<sup>195,203</sup>. Prevalence of CWD in these herds ranges from <0.1% to 100%. Clinical signs of prion disease include loss of body condition, ataxia, excessive salivation, and behavioral changes. In nature, CWD only affects animals from the *Cervidae* family; however, it can be transmitted experimentally to a wide range of animal models suggesting that perhaps it can cross several species' barriers<sup>195</sup>. Several polymorphisms confer susceptibility to the disease: S96G, where S confers a delay of disease, M132L, where MM confers susceptibility, and S225F, where SS confers susceptibility<sup>204</sup>. Transmission of CWD can occur horizontally and environmentally, where it is known to persist in the soil for years. In oral exposure, it spreads to the GALT and lymphoreticular system (LRS) and ascends to the CNS with an incubation period of 16 months to 5 years. Infectious CWD prions are detected in a wide range of tissues, including CNS, LRS, blood, muscle, pancreas, fat, urine and feces, and antler velvet<sup>195</sup>.

#### *Transmissible Mink Encephalopathy (TME) and Feline Spongiform Encephalopathy (FSE)*

Two other prion diseases that were caused by consumption of prion-contaminated food products are TME and FSE. In 1947, TME was discovered in captive-farmed mink, while FSE developed in parallel with the BSE epidemic in the 1980s and affected wild and captive felines. It is well established that FSE developed from feeding felines BSE-contaminated products, while TME may derive from either scrapie or BSE contamination. Both diseases have similar clinical signs, such as aggression, depression, ataxia, and tremors. The incubation period for TME is 6-12 months, and 2-8 years for FSE<sup>195</sup>.

#### *Creutzfeldt-Jakob Disease (CJD)*

CJD comes in a few forms: sporadic CJD (sCJD), familial or genetic CJD (f/gCJD), iatrogenic CJD (iCJD), and variant CJD (vCJD). Sporadic CJD and f/gCJD occur in middle to late age, while iCJD and vCJD occur in a variety of ages. For sCJD and f/gCJD, clinical signs include dementia and cerebellar dysfunction. Sporadic CJD accounts for 85% of all CJD cases, and f/gCJD accounts for most other cases. Iatrogenic CJD and vCJD have been on the decline since their identification, so they account for 1-2% of CJD cases. The V129M polymorphism increases the risk of developing any form of CJD and determines the specific clinicopathological phenotype seen in CJD patients. In f/gCJD, other polymorphisms, such as E200K, I210V, D178N, and V180I, contribute to susceptibility to disease. There does not need to be a familial connection in f/gCJD, which is why some refer to it

only as gCJD. Also, f/gCJD results with the insertion or deletion of octapeptide repeats. Sporadic CJD is a spontaneous disease, whereas iCJD results from the injection/implantation of contaminated tissues. Sources of tissue contamination include corneal and dura mater grafts, EEG needles, and injection of human growth hormone or gonadotropin hormone<sup>205</sup>.

There was a concern that if BSE did indeed come from scrapie, then it might have the potential to cross the species barrier again, potentially into humans. Therefore, to ensure identification of a new variant, surveillance of CJD increased during the BSE outbreak. In May to October of 1995, three cases of a new variant of CJD were identified, later called vCJD. These patients had early onset of disease symptoms (<50 years of age) with psychiatric indications and ataxia<sup>198,199</sup>. It was later found that the molecular and biological characteristics of vCJD matched those of BSE. Researchers believe that vCJD arose from the consumption of BSE tainted meat products<sup>104,206</sup>. In BSE, only nervous tissue has a high amount of prions, with muscle and milk containing none. However, the process of slaughter could lead to the contamination of muscle and milk products with CNS tissue contaminated with BSE. The V129M polymorphism is associated with an increased risk of vCJD, with nearly all cases being 129MM homozygotes. While vCJD is declining along with BSE, concern remains about 'silent' carriers and whether these carriers will lead to a second outbreak of vCJD<sup>198,199</sup>.

### *Kuru*

The origin of kuru is still somewhat of a mystery. Theories include a new or existing neurotropic virus that evolved through the serial passage of brain material<sup>16</sup>, ingestion of scrapie or BSE that transmitted to humans<sup>16</sup>, or ingestion of an individual affected by CJD<sup>16,207,208</sup>. The most likely theory is that an individual from the Fore tribe was affected with a sporadic case of CJD, and the remains of that person were consumed upon death, which led to the evolution of the CJD agent into the kuru agent. Evidence to support this claim includes similarity of plaques from CJD and kuru cases<sup>207</sup>, comparable neuronal degeneration<sup>207,208</sup>, analogous transmission patterns, and similar strain characteristics between kuru and classical CJD<sup>208</sup>.

As previously stated, the kuru epidemic waned after cannibalism declined among the Fore people. The last noted death was in 2005, and there are no known current cases of the disease<sup>209</sup>. A secondary cause of the decline of kuru was established upon examination of the *prnp* gene at codon 129 in susceptible and non-susceptible individuals. Susceptible individuals that contracted the disease early in the epidemic were almost always homozygous for Met at position 129. These individuals also displayed the shortest incubation time of the disease.

Following the deaths of the most susceptible population, the disease started to affect heterozygotes (Val/Met) at position 129, and very rarely Val homozygotes. Patients with the Val homozygote genotype had incubation periods of 20 years or greater, and most never showed clinical symptoms of the disease even after being exposed. The decrease in the exposure and depletion of susceptible individuals within the population resulted in the end of kuru<sup>210,211</sup>.

#### *Fatal Familial Insomnia (FFI) and Gerstmann-Sträussler-Scheinker syndrome (GSS)*

There are two other autosomal dominant human prion diseases: FFI and GSS. Insomnia, or lack of sleep, characterizes FFI, with ataxia, myoclonus, and seizures also common. Neurodegeneration within the CNS is predominantly within the thalamic nuclei with minimal PrP<sup>Res</sup> deposition. The incubation period of FFI is 20-72 years. FFI is linked to two polymorphisms D178N and 129MM. Early onset dementia around 30-60 years of age with a slow disease progression that includes ataxia, dysarthria, and Parkinsonian signs characterizes GSS. GSS is also associated with two polymorphisms of the *prnp* gene: 129MM and P102L<sup>205</sup>.

#### *Alzheimer's and Other Protein Misfolding Diseases*

In recent years, a controversy surrounding prion diseases and other protein misfolding diseases has emerged. Some say that prion diseases should be classified with other protein misfolding diseases and others claim that the protein misfolding diseases might all be prion diseases (albeit caused by different proteins). Protein misfolding diseases, such as Alzheimer's disease (AD), Parkinson's disease (PD), and Huntington's disease (HD), are diseases caused by a misfolded cellular protein. This misfolded protein is either infectious, like prion diseases, or the accumulation of the misfolded protein results in neuronal degeneration. Protein misfolding diseases usually cause neurodegeneration but can cause damage to other organ systems as well, such as Type II diabetes. Some proteins that are involved in these diseases include amyloid precursor protein (APP) in AD,  $\alpha$ -synuclein in PD and other synucleopathies, and huntingtin in HD. These misfolded proteins share common characteristics with PrP<sup>Res</sup>, such as insolubility and adaptation of highly ordered fibrillary aggregates. Specifically, AD not only shares characteristics with PrP<sup>Res</sup> but also has a connection with PrP<sup>C212,213</sup>.

Amyloid- $\beta$  (A $\beta$ ) and tau are the two proteins in AD that misfold and accumulate within neurons. A $\beta$  is derived from APP through cleavage by  $\beta$ - and  $\gamma$ -secretase. This cleavage results in the generation of two toxic peptides: A $\beta$ <sub>1-40</sub> and A $\beta$ <sub>1-42</sub>. In the search for PrP<sup>C</sup> ligands, amyloid-like precursor protein 1 (APLP1) was found to precipitate with PrP<sup>C</sup>, indicating that it may be a PrP<sup>C</sup> ligand. APLP1 is a member of the APP family and is thought

to concentrate with PrP<sup>C</sup> on the cell surface. The function or reason for the interaction between APLP1 and PrP<sup>C</sup> is unknown<sup>214</sup>. PrP<sup>C</sup> was also found to be a receptor for the Aβ<sub>1-42</sub> peptide. The direct interaction between PrP<sup>C</sup> and Aβ<sub>1-42</sub> mediates a decrease in long-term potentiation observed in AD neurons. The decrease in long-term potentiation of Aβ<sub>1-42</sub> infected cells is abrogated when PrP<sup>C</sup> is not present or when anti-PrP antibodies are used<sup>215</sup>. Two independent studies have shown that PrP<sup>C</sup> is also upregulated in Aβ plaques of AD. Whether the upregulation is due to a functional role of PrP<sup>C</sup> or just abnormal protein turnover is unclear, but these conclusions indicate perhaps PrP<sup>C</sup> has either a functional role in AD or a functional role with APP/Aβ<sup>216,217</sup>. Evidence for a functional role of PrP<sup>C</sup> with APP/Aβ was confirmed when PrP<sup>C</sup> was found to regulate Aβ levels through β-secretase activity. PrP-null mice showed an increase in Aβ, suggesting that the amount of Aβ is dependent upon the presence/absence of PrP<sup>C</sup>. Mice infected with scrapie also had increased levels of Aβ. The authors found that the regulation of Aβ by PrP<sup>C</sup> occurred during the β-secretase processing step. This study indicates that it may not be wise to decrease cellular levels of PrP<sup>C</sup>, as it may lead to an increase in AD cases<sup>218</sup>.

### ***Prion Therapeutics***

#### *The 'Anti' Therapeutic Group*

The first therapeutics investigated for anti-prion activity were antivirals since the scrapie agent was thought to be a slow virus. Some antivirals tested for their anti-prion activity include β-propiolactone, adenine arabinoside, amantadine, rifampicin, and cytosine arabinoside. These antivirals were tested in mice inoculated with the Chandler scrapie<sup>219,220</sup> or CJD mouse strains<sup>221</sup>. None of the antivirals had any effect on survival time of prion-infected mice. These results helped solidify the conclusion that the scrapie agent does not contain nucleic acid<sup>219-221</sup>. Despite the lack of a benefit of antiviral therapy, several clinical studies of human prion disease with antiviral therapies were published. Acyclovir, amantadine, and vidarabine were all tested for their effectiveness in treating clinical stage human prion disease. A few patients presented with transient improvements in their clinical state. However, there was no benefit in survival times or permanent improvement in clinical state<sup>222</sup>. The polyene antibiotic amphotericin B (AmB) was evaluated for anti-prion activity due to its membrane association and low toxicity in animal models. Polyene antibiotics are used for the treatment of fungal infections. The antibiotic binds to ergosterol in the membrane of fungi and disrupts the membrane. AmB delayed the onset of clinical signs and prolonged survival times in hamsters and mice inoculated with the 263K strain of scrapie in both early and late treatment regimens<sup>223-</sup>

<sup>227</sup>. Early treatment (2.5 mg/kg) of AmB resulted in a 40-day increase in survival time in both intracerebral and intraperitoneal prion-inoculated hamsters and mice. Higher doses of AmB (25 mg/kg) with an intraperitoneal

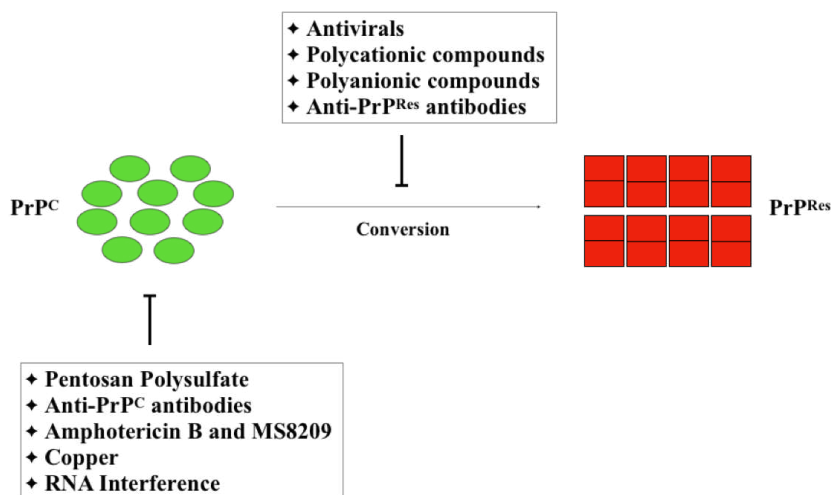


**Figure 1.2. Mechanisms of prion therapeutics that have shown promise in animal models.**

A graphic depiction of the mechanisms of some of the compounds that have shown promise as anti-prion compounds

inoculation of prions resulted in a 60-day increase in survival time<sup>224,225</sup>. Hamsters inoculated with the TME strain Drowsy had no effect on survival times with AmB treatment<sup>226</sup>. An AmB derivative, MS-8209, also showed an increase in survival time with a decrease in toxicity compared to AmB<sup>225</sup>. Treatment of SCID mice with AmB further emphasized that these polyene antibiotics do not act directly on PrP<sup>Res</sup>, but instead interfere with the mechanism between PrP<sup>C</sup> conversion to PrP<sup>Res</sup><sup>228</sup>. Treatment of scrapie-infected cell cultures with polyene AmB or MS-8209 revealed an increase in PrP<sup>C</sup> accumulation on the cell surface and an alteration of lipid content in lipid rafts. The alteration of lipid content suggests that the antibiotics are binding to cholesterol in lipid rafts and altering its composition, thereby providing a blockade for PrP<sup>Res</sup> conversion. The treatment could also be altering trafficking of PrP<sup>C</sup> to the cell surface<sup>229,230</sup>. One clinical study reported that 0.25-1 mg/day treatment of AmB to CJD patients did not affect symptoms or disease progression<sup>222</sup>. Polyene antibiotics are used safely in humans but can cause toxicity, have limited bioavailability in the brain, and are prion strain specific. Therefore, use of these compounds as therapeutics for prion diseases is limited.

During a cell culture screening for anti-prion drugs in scrapie-infected N2a cells, the antimalarial drug quinacrine was found to reduce PrP<sup>Res</sup> levels *in vitro*. Quinacrine showed some cellular toxicity but did not affect protein biosynthesis in these cells. At this point, quinacrine had been used for decades for the treatment of malaria, so it was approved for human use and was found to cross the BBB<sup>231,232</sup>. Therefore, quinacrine became the poster child for prion therapeutics. Multiple human clinical trials were started to evaluate its effectiveness in human prion disease. However, shortly after quinacrine's *in vitro* anti-prion activity was reported, several discouraging reports about quinacrine's activity were also published. Quinacrine did not prolong survival times in mice infected with scrapie either through an intraperitoneal drug regimen or an intraventricular drug infusion regimen<sup>233,234</sup>. Mefloquine, another antimalarial drug, was also found to reduce PrP<sup>Res</sup> levels *in vitro* but had no effect *in vivo*<sup>235</sup>. Several human clinical trials reported transient clinical benefits with the treatment of both quinacrine and chlorpromazine at 300-600 mg/day, but there were no permanent improvements in clinical stage or elongation of survival times<sup>236-238</sup>. These studies have noted that the bioavailability of quinacrine in the brain is minimal, which could explain the results. However, one study that blocked the efflux of quinacrine, which resulted in much higher amounts of the drug in the brain, reported no prolonging of survival times in scrapie-infected mice. They did observe quinacrine-resistant conformers of PrP<sup>Res</sup>, indicating that prions can establish drug resistance<sup>239</sup>. Another study hypothesized that quinacrine may work in a strain dependent manner, and may be effective against mouse prions but not human prions<sup>240</sup>. Long term exposure and high doses of quinacrine cause liver toxicity, cardiomyopathy, and toxic psychosis. Therefore, quinacrine might be effective at treating early stage disease, but its efficacy at late clinical stage and its toxic properties make it an unsuitable candidate for prion therapeutics.

#### *Polycationic Compounds*

Polycationic compounds contain multiple positively-charged groups on their terminal ends. A significant number of these compounds are used in gene transfection for the delivery of nucleic acids to cells. Polyamines are polycationic compounds that contain amine groups as the cationic groups. Some polyamines include polyethyleneimine (PEI), polypropyleneimine (PPI), and polyamidoamine. Polyamines are usually used in transfection reagents because they are hydrophilic and they contain some hydrophobic groups that associate with

cell membranes. Multiple generations of polyamines result in more primary amine groups being added to the compound (generation 1 has 4 primary amines, and generation 4 has 32 primary amines)<sup>241-243</sup>.

Supattapone's group accidentally stumbled upon the anti-prion activity of polyamine compounds during their transfection studies. They found that the polyamine compounds in Superfect reduced the amount of existing PrP<sup>Res</sup> within mouse neuroblastoma (N2a) cells. The polyamines PEI and PPI were the most effective when they had the most primary amines (generation 4.0)<sup>241</sup>. Further work of this group concluded that PPI had no effect on PrP<sup>C</sup> levels and that it rendered PrP<sup>Res</sup> more sensitive to proteolytic digestion. Supattapone hypothesizes that the amines on the compounds rip apart oligomers of PrP<sup>Res</sup>, making them more susceptible to normal cellular protein degradation. One limitation observed using these polyamine compounds is that they are strain specific, so some strains are more resistant to the effects of these compounds than others. The strain specificity indicates that a drug-resistant phenotype develops with some strains of prions. Also, these compounds do not readily cross the blood-brain barrier (BBB)<sup>242</sup>.

#### *Polyanionic Compounds*

Polyanionic compounds contain at least one negatively-charged terminal moiety that is typically either a sulfate or a carboxylate group. Sulfated glycosaminoglycans (GAGs), which are also polyanionic, are present in amyloid plaques of prion diseases. Whether they function to impair or benefit polymerization is unknown. Multiple different polyanionic compounds have been investigated for their effect on prion disease after GAGs were found to bind to PrP<sup>Res</sup> aggregates. The polyanion HPA-23 (ammonium 5-tungsto-2-antimoniate) is effective at increasing survival periods in mice inoculated with the 139A strain of scrapie. The effect was only produced when mice were treated four hours after inoculation. While the exact mechanism is unknown, it is thought that HPA-23 acts on the LRS to prevent peripheral accumulation of prions<sup>244,245</sup>. Similarly, dextran sulfate with a molecular weight of 500 kDa (DS-500) was effective at decreasing PrP<sup>Res</sup> levels in N2a cells, and in a scrapie mouse model. Unlike HPA-23, DS-500 increases survival time when administered either several weeks before or after inoculation due to its longer half-life<sup>245-247</sup>. DS-500 is known to decrease PrP<sup>Res</sup> levels in the spleen early in infection, possibly by activating splenic immune cells. However, DS-500 is quite toxic *in vivo*. Another polyanion that is less toxic than DS-500 is pentosan polysulphate (PS), which results in complete protection of scrapie-infected mice when given at a 1 mg dose seven hours after inoculation<sup>247,248</sup>. In clinical trials, PS is well tolerated at high doses and leads to cognitive improvements with slow disease progression in a majority of patients<sup>222</sup>. Treatment with the above polyanions

results in increased endocytosis of PrP<sup>C</sup> *in vitro*. While the polyanions don't alter PrP<sup>C</sup> synthesis, they seem to shift more PrP<sup>C</sup> into late endosomes and lysosomes. It is not known whether this action is a result of direct or indirect contact with PrP<sup>C</sup>, but the decrease in PrP<sup>C</sup> would lead to less substrate available for PrP<sup>Res</sup> conversion<sup>249</sup>. Other less toxic polyanions include heparan sulfate (HS) and HS mimetics. Two HS-like compounds, HM2602 and HM5004, block prion replication both *in vitro* and *in vivo* in mice and hamsters infected with either 263K or a BSE prion strain<sup>250</sup>.

The histopathological stain congo red (CR) stains amyloid fibrils. Its ability to bind to amyloid, including PrP<sup>Res</sup> deposits in the brain, made it an attractive therapeutic option. CR decreases levels of PrP<sup>Res</sup> in mouse neuroblastoma cells<sup>247</sup>. It is also effective at prolonging survival times in hamsters intracerebrally or intraperitoneally inoculated with either 263K or 139H prion strains. In intracerebrally inoculated hamsters, pretreatment of 10 mg of CR one week before inoculation and 5 mg weekly afterward produced the largest benefit on survival times. Pretreatment of CR did not have any impact on intraperitoneally inoculated hamsters, but the treatment of CR and intraperitoneal inoculation on the same day produced a modest effect in elongation of survival times<sup>251</sup>. However, mice treated with CR had increased levels of splenic prions and did not have an increase in survival periods of scrapie-infected mice, suggesting that CR may be strain/animal dependent<sup>252</sup>. Multiple mechanisms for the activity of CR include increasing endocytosis of PrP<sup>C</sup><sup>249</sup>, binding to PrP<sup>C</sup> to cause competitive inhibition with endogenous GAGs<sup>253</sup>, and stabilizing the structure of PrP<sup>Res</sup><sup>252,254</sup>. The stabilization of PrP<sup>Res</sup> by CR may lead to either inhibition of denaturation that hinders conversion<sup>254</sup> or an increase in proteolysis that results in more PrP<sup>Res</sup> being generated<sup>252</sup>. Whatever the mechanism might be, CR does not make a good therapeutic as it cannot cross the BBB and it is toxic, possibly even carcinogenic/mutagenic.

#### *Immunotherapeutics/Immunomodulation*

Prions do not elicit an immune response because they are derived from a normal host cellular protein. However, therapeutic strategies toward eliciting an immune response against prions have increased over the last decade. Antibodies against PrP<sup>C</sup> and PrP<sup>Res</sup>, active and passive immunizations, and immunostimulation/immunosuppression therapeutic strategies have all shown promise. The purification of PrP 27-30 and the generation of PrP-null mouse models enabled the production of antibodies targeted against PrP<sup>C</sup> or PrP<sup>Res</sup><sup>59,128,255</sup>. Both polyclonal and monoclonal antibodies raised against PrP<sup>C</sup> were shown to decrease levels of PrP<sup>Res</sup> in N2a scrapie-infected cells. Mechanisms of action include interfering with epitope binding of PrP<sup>Res</sup>, steric

hindrance to prevent conversion, or interference of binding of other proteins (protein X). Antibodies with epitopes in both the COOH- and NH<sub>2</sub>-terminus of PrP<sup>C</sup> are effective at reducing PrP<sup>Res</sup> levels<sup>255-259</sup>. The 6H4 antibody operates like phosphoinositide phospholipase C cleavage of PrP<sup>C</sup>, which cleaves the GPI anchor from the cell membrane, indicating that this antibody directly occludes PrP<sup>C</sup> and may increase turnover of the protein<sup>260</sup>. SAF34 and SAF61 antibodies were shown to increase the clearance of PrP<sup>C</sup> from the cell surface making it unavailable for PrP<sup>Res</sup> conversion<sup>261</sup>. Most of the antibodies that have shown anti-prion activity can reduce PrP<sup>Res</sup> levels to undetectable amounts. These studies indicate that the cells are ‘cured’. However, a few studies report that there is a hidden cellular reservoir of PrP<sup>Res</sup> that allows its replication after treatment is suspended. These results suggest that PrP<sup>Res</sup> is cleared through normal cellular degradation pathways, and antibody therapeutics may need to be given continuously throughout the animal’s/individual’s life. Several *in vivo* studies have shown efficacy of the 6H4 antibody and the ICSM18 and ICSM35 antibodies to increase survival periods. There was no sign of autoimmunity in any of the animals. The *in vivo* antibodies were efficacious against peripheral prion infections in the early stage of disease<sup>262</sup>.

The biggest challenge for the use of immunotherapies in prion diseases is overcoming tolerance to PrP<sup>C</sup>. Both active and passive immunization studies have been employed to overcome this problem. Passive immunization with ICSM18 or ICSM35, with no adjuvant, resulted in a 153% extension in survival time<sup>263</sup>. Active immunization with recombinant PrP<sup>C</sup> and complete Freund’s adjuvant (CFA) also resulted in an increase in survival time by two weeks but was not effective in preventing disease<sup>264</sup>. Mucosal vaccination of a *Salmonella* PrP<sup>C</sup> vector in an oral inoculation mouse model resulted in a 200-day increase of survival times, with no PrP<sup>Res</sup> detected in the brain after 500 days post-inoculation<sup>265</sup>. These studies led to an activation of Th2 immune responses and no activation of Th1 immunity, which is important because vaccination of AD patients with an Aβ peptide resulted in a massive Th1 immune response, resulting in cessation of the trial<sup>261,262,264,265</sup>. Thus, there is a need for careful characterization of vaccination strategies towards prion diseases in mouse models before being used in human clinical trials.

Other immune system exploitations for prion disease include immunostimulation and immunosuppression. Immunostimulation with several adjuvants, namely CpG oligodeoxynucleotides and CFA, increased survival times of prion-infected mice. Use of CFA in both intracerebral and intraperitoneal prion inoculation proved effective at elongating survival times. The authors speculate since it is effective with both types of inoculation routes it must have a local effect on the CNS, perhaps by activating microglia for increased phagocytosis of PrP<sup>Res</sup><sup>262,266</sup>. On the other hand, immunosuppression using anti-inflammatory drugs, such as prednisone and dapsone, have been proven

effective at increasing survival times. These two compounds were also shown to produce long-term survivors that showed no clinical signs of prion disease 200 days after non-treated controls died. It is thought that prednisone and dapsone cross the BBB and modulate neuronal inflammation during prion disease<sup>267,268</sup>. The exact mechanisms of how these techniques work to improve survival are not known but may provide insight into which cells/mechanisms to target with therapeutics.

### *Targeting PrP<sup>C</sup>*

As discussed above, PrP-null mice are phenotypically normal<sup>126,162</sup>. They have some minor phenotypes associated with the knockout of PrP<sup>C</sup>, but they otherwise live healthy lives<sup>129,132-134</sup>. The loss of PrP<sup>C</sup> in these mice allows them to be resistant to prion infection, while having no detrimental effects with the ablation of PrP<sup>C</sup><sup>127,190</sup>. Some have suggested that there must be a compensatory mechanism during embryogenesis that counteracts the loss of PrP<sup>C</sup>. However, post-natal knockout of PrP<sup>C</sup> in a *Cre/loxP* mouse also produced mice that were mostly phenotypically normal. PrP<sup>C</sup> was eliminated in these mice by Cre recombinase at twelve weeks of age, which resulted in a decline of both medium and slow afterhyperpolarizations in hippocampal CA1 cells, indicating that there were some synaptic changes within these mice<sup>163</sup>. Also, when PrP<sup>C</sup> was eliminated in the *Cre/loxP* mice after established prion infection, there was a reversal of the spongiosis and neuronal loss seen in prion infection even though PrP<sup>Res</sup> continued to accumulate. The depletion of PrP<sup>C</sup> in these mice after prion infection leads to an increase in survival time compared to the PrP-expressing counterparts<sup>190</sup>. These conclusions suggest that 1) reduction or elimination of PrP<sup>C</sup> has no detrimental effects, 2) animals with no PrP<sup>C</sup> are resistant to prion infection, and 3) removal of PrP<sup>C</sup> during prion infection results in reversal of disease pathology. Therefore, PrP<sup>C</sup> has become an attractive therapeutic target for the treatment of prion diseases.

Therapeutic targeting of PrP<sup>C</sup> has occurred through the use of RNA interference (RNAi) technology, such as short hairpin RNA (shRNA) and small interfering RNA (siRNA) (mechanism of technology discussed later). Expression of shRNA in lentiviral vectors and treatment with siRNA in primary or cultured cells results in a substantial decrease in expression levels of PrP<sup>C</sup> mRNA and protein. shRNA and siRNA are effective in multiple different types of cell lines with different expression levels of PrP<sup>C</sup>, suggesting that these therapeutics could be used to not only affect PrP<sup>C</sup> and PrP<sup>Res</sup> concentrations in the CNS but also in peripheral areas. Treatment of prion-infected cells with either shRNA or siRNA reduces the levels of PrP<sup>Res</sup> dependent on the level of reduction of PrP<sup>C</sup>. The decrease in PrP<sup>Res</sup> levels could be due to proteases that attack the prion aggregates or the elimination of PrP<sup>Res</sup>

through normal protein processing mechanisms, such as the proteasome<sup>269-274</sup>. Some of these studies report that the levels of PrP<sup>Res</sup> drop so substantially that the cells become ‘cured’ of prion infection. However, one study noted that even though PrP<sup>Res</sup> levels were reduced to nearly non-detectable levels, de novo generation of PrP<sup>Res</sup> was still occurring<sup>271</sup>. This study insinuates that perhaps the cell lines are not completely cured, and designation of such should be given carefully.

Stereotactic injection of shRNA or siRNA is standard practice when treating mice with these molecules. A single stereotactic injection of shRNA within the hippocampus of prion-infected mice resulted in a decrease of PrP<sup>C</sup> and PrP<sup>Res</sup> levels and reversed the early neuronal pathology of prion infection. This single treatment resulted in a 24% increase in lifespan of these mice<sup>275</sup>. Generation of chimeric mice that express shRNA in 50% of their cells results in prolonged survival when infected with prions<sup>276,277</sup>. These results have led to attempts to generate livestock with reduced or eliminated levels of PrP<sup>C</sup>. The hypothesis being that cattle or goats with decreased levels of PrP<sup>C</sup> could be resistant to either BSE or scrapie, and could be bred to generate herds that withstand prion outbreaks<sup>273,278</sup>.

A limitation of the stereotactic technique in mammalian models is that the injections cause damage to CNS tissue and only deliver the shRNA/siRNA to local areas around the injection. A recent study employed the use of liposomal technology (discussed later) to package siRNA with a neuronal targeting peptide so that the siRNA was delivered to the BBB with an intravenous injection. The authors reported a 70% reduction in PrP<sup>C</sup> levels in N2a cells, and a concomitant reduction in PrP<sup>Res</sup> of prion-infected cells. The liposomes protected the siRNA from serum degradation for transport through the bloodstream, and the peptide was specific to receptors commonly found on neurons. These liposome-siRNA-peptide complexes (LSPCs) crossed the BBB and selectively targeted neuronal cells *in vivo*. This delivery method has the potential to overcome the complications of previous delivery methods<sup>272</sup>. The success of RNAi technology in prion disease needs to be further addressed in mouse models. Limitations that need to be overcome include delivery methods, toxicity of double-stranded RNA or vectors, and some leakage of PrP<sup>C</sup> expression that results in de novo PrP<sup>Res</sup> propagation after treatment.

#### *Other Therapeutic Approaches*

Another RNA therapeutic option for prion diseases, besides shRNA and siRNA, are RNA molecules known as aptamers. Aptamers are oligonucleotides (RNA or DNA) that bind to a particular target molecule and originate from a larger pool of random oligonucleotide sequences. Using both PrP<sup>C</sup> and PrP<sup>Res</sup> as target molecules, two RNA aptamers have been described to influence PrP<sup>Res</sup> levels. DP7 is a 2'-aminopyrimidine-RNA aptamer that

binds specifically to the  $\alpha$ -helix-rich PrP<sup>C</sup> protein. It was generated from human PrP<sup>C</sup> residues 90-141 and binds human, mouse, and hamster PrP<sup>C</sup>. PrP<sup>Res</sup> levels decreased by 53% upon treatment with DP7 in scrapie-infected N2a cells. The authors speculate that the inhibitory effect is due to the aptamer blocking or interfering with polymerization of PrP<sup>Res</sup>, thereby making it more PK-sensitive<sup>279</sup>. SAF-93 is a 2'-fluoro-RNA aptamer that binds specifically to the  $\beta$ -sheet conformation of PrP<sup>Res</sup>. SAF-93, when bound to PrP<sup>Res</sup>, is PK-resistant, indicating that it binds to the infectious form in the PK-resistant core. As with DP7, there was inhibition of PrP<sup>Res</sup> conversion with the treatment of SAF-93 in infected cells. The mechanism is not known, but the authors conjecture that the binding to PrP<sup>Res</sup> occludes binding of PrP<sup>C</sup> for conversion<sup>280</sup>. *In vivo* efficacy is unknown for the above aptamers.

Other compounds discovered to have anti-prion activity include curcumin (a major component of the spice turmeric), statins such as lovastatin and squalastatin, inhibitors of cell signaling pathways, 2-aminothiazoles (IND24 and IND81), and dimethyl sulfoxide. These compounds decreased levels of PrP<sup>Res</sup>, or inhibited the conversion of PrP<sup>Res</sup> *in vitro*, but were unable to produce any meaningful effects *in vivo* or selected for drug-resistant prion strains. Some of the data is contradictory with some studies reporting benefits of these compounds while others report no benefits<sup>281-285</sup>.

## siRNA and Liposomes

### *From RNA Interference Discovery to Mechanism*

In the 1980s and early 1990s, experiments with plants revealed a mechanism that silenced exogenous and endogenous genes. Introduction of a purple gene for flowers into petunias resulted in white flowers produced from the gene silencing of both the exogenous and endogenous gene. This process became known as post-transcriptional gene silencing. The mechanism was unknown but it was accepted that both sense and anti-sense RNA silenced target gene expression, as observed in other models. In 1998, Fire and Mello discovered that the introduction of double-stranded RNA (dsRNA) into the nematode *Caenorhabditis elegans* (*C. elegans*) resulted in specific gene silencing. This silencing was more potent than using either sense or anti-sense single-stranded RNA (ssRNA). This phenomenon became known as RNA interference (RNAi)<sup>286</sup>. Gene silencing through RNAi is mediated by dsRNA molecules 21-23 nucleotides long<sup>288,289</sup>. The anti-sense strand, or guide strand of the dsRNA, is complementary to

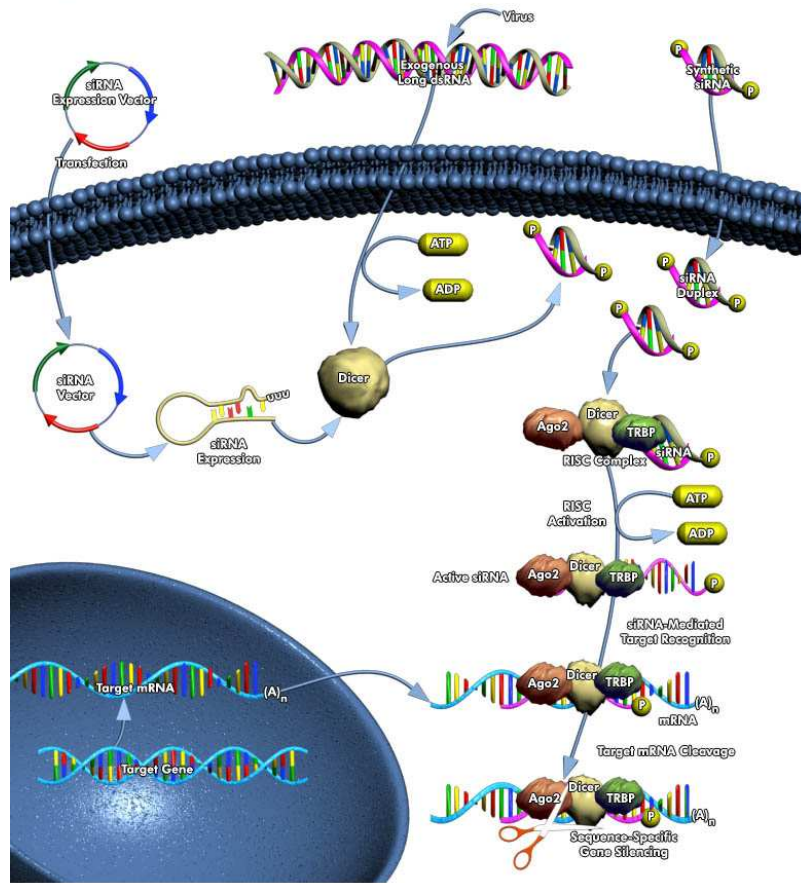


**Figure 1.3. RNAi pathway in humans for long dsRNA, siRNA, and shRNA.** Qiagen

and will bind the target gene. The sense strand, or passenger strand, eventually becomes degraded. When the guide strand associates with its target mRNA and an endonuclease, the result is cleavage of the mRNA, which causes a decrease in protein expression. Many organisms possess RNAi, from *Drosophila melanogaster* (fruit flies), plants, *C. elegans*, fungi, to mammals including mice and humans. RNAi evolved as an immune response towards any dsRNA, including endogenous (transposons) and exogenous (viruses) sources<sup>287</sup>.

The mechanism to induce RNAi starts with the introduction of a long dsRNA, short hairpin RNA (shRNA) or a small interfering RNA (siRNA) of 21-23 nucleotides into the cell. The long dsRNA is cleaved into smaller 21-23 nucleotide fragments, which is accomplished through the action of the Dicer RNase III (Dcr) protein. In *D. melanogaster*, Dcr works in concert with another protein, R2D2, to cleave the long dsRNA into 21-23 fragments through ATP hydrolysis<sup>288-291</sup>. After Dcr processing, the siRNA fragments load into the RNA induced silencing complex (RISC) by association with an Argonaute (Ago) protein. The main Ago protein utilized in siRNA gene

silencing is Ago2. siRNA molecules are designed with 2-3 nucleotide 3' overhangs so that the PAZ domain in Ago2 can bind to the siRNA. In humans, Ago2 binds to the Tar RNA binding protein to complete the RISC complex. RISC remains inactive until the passenger strand has been removed<sup>290,292-297</sup>. The passenger strand is either removed when Dcr hands the siRNA to Ago2<sup>296</sup> or by an ATP-dependent helicase<sup>287,289</sup> that unwinds the siRNA when loaded into Ago2. RISC is activated when Ago2 has exposed the guide strand and can bind to its target mRNA. The target mRNA is cleaved by the PIWI domain of the Ago2 protein, which contains an endonuclease catalytic site. The mRNA is cleaved at a single site, which attracts endo- and exonucleases to digest the rest of the mRNA and results in reduced levels of protein translation<sup>290,294,297</sup>.

Several factors are important to produce the optimal amount of gene silencing. Two modifications are required to load the siRNA in the correct orientation in Ago2. Synthetic or natural siRNAs need to possess a 5' phosphate group. If synthetic siRNA does not already have the 5' phosphate group, then the cellular kinase Clp1 will immediately phosphorylate the RNA upon cell entry<sup>289,297,298</sup>. The 5' phosphate along with a divalent cation enables the RNA molecule to bind to the PIWI domain of Ago2<sup>297</sup>. Second, a 2-3 nucleotide 3' overhang is needed for the RNA molecule to bind to the PAZ domain of Ago2<sup>290,299</sup>. Also, mRNA cleavage is more robust when the siRNA has a low internal stability on the 5' end of the anti-sense strand, and a reduced thermodynamic stability in the 10-14 nucleotide region of the siRNA. Thermodynamic instability is achieved with the addition of more A/U base pairs at the 5' end. These characteristics are referred as the asymmetry rule of siRNA<sup>289,300</sup>.

### ***Challenges of RNAi Based Therapeutics***

RNAi technology represents a novel gene therapy that can target any gene for downregulation. The use of this technology, not only in the research lab but also as a therapeutic, became extremely appealing. Therapeutic RNAi technology soon exploded leading to new developments in siRNA synthesis and expression, stability and efficacy, and delivery systems.

#### ***Expression of RNAi***

Expression of siRNA in mammalian cells can occur in multiple ways. A direct injection of long dsRNA leads to the formation of siRNA molecules. This practice is common in plants and nematodes but in mammals, long dsRNA activates the interferon response. Therefore, synthetic siRNA molecules are produced for the use of mammalian studies. Injection of siRNA into mammalian cells allows the siRNA to bypass the Dcr cleavage step of the RNAi pathway and proceed directly to Ago2 in the RISC complex. One disadvantage to the chemical synthesis

method is the problem of delivering the siRNA both systemically and across the plasma membrane because siRNA molecules are easily digested by serum nucleases and have a short half-life. They also do not cross the negatively-charged plasma membrane due to the negatively-charged backbone of the siRNA<sup>301</sup>. Other popular expression methods include utilization of either a viral or non-viral vector. Viral and non-viral vectors offer an advantage over chemically synthesized siRNAs in that the vectors provide a more stable expression of siRNA, whereas the chemically synthesized siRNA is only transiently present and effective. Lentiviral and adeno-associated viral vectors are the most commonly used because they can be introduced into non-dividing cells. The siRNA is typically processed from a shRNA expressed from either a U6 or H1 promoter. These vectors integrate into the chromosome, which allows for stable expression of siRNA. However, this is also a drawback in utilizing this technology for human therapeutic use as chromosomal mutations are probably not the best therapeutic strategy<sup>302-304</sup>. Non-viral vectors include the use of plasmids that express shRNA from RNA polymerase II or III promoters. Non-viral vectors are not easily introduced into non-dividing cells, unlike their viral counterparts<sup>305,306</sup>. The choice of expression system is dependent upon the application of the siRNA therapeutic, such as cell type, expression duration, and delivery method.

#### *Delivery of siRNA in vivo: Considerations of stability and targeting*

The *in vitro* use of siRNA has shown that it is capable of downregulating genes in a wide range of situations. Once the siRNA is intracellular, it decreases expression of any targeted mRNA. However, the challenge of getting it to the cell remains the biggest blockade for siRNA *in vivo* applications. The seminal studies that used synthetic siRNA *in vivo* used the hydrodynamic method of injection into mice. These studies injected close to one milliliter of naked siRNA into the tail veins of mice, which creates a high-pressure system to push the siRNA into cells. This method is extremely effective for the transfection of siRNA into hepatocytes. Naked siRNA in hepatocytes can reduce viral titers of hepatitis C virus<sup>307</sup> and Fas protein<sup>308</sup> to inhibit damage generated by hepatitis C infection and fulminant hepatitis, respectively. Also, siRNA targeted towards either caspase 3 or 8 within hepatocytes can reverse damage caused by hepatic ischemia<sup>309</sup>. SiRNA is found in the liver and kidney several minutes after hydrodynamic injection with lower concentrations found in the lung, spleen, and heart<sup>310</sup>. While this method is effective in delivering siRNA to the liver, hydrodynamic injection in humans results in tissue damage, so is it not an ideal method for clinical use. Other methods of delivery include non-hydrodynamic intravenous injection or site-specific injection.

Non-hydrodynamic intravenous injection is an attractive alternative for systemic administration of siRNA as this administration can be used in a clinical setting. The major drawbacks of this method include siRNA degradation and lack of targeting. The half-life of siRNA depends on the thermodynamic stability of the 5' end. Due to the asymmetry rule, the 5' end is already thermodynamically unstable to allow RISC loading. This instability also allows attack from serum exonucleases. The half-life of any particular siRNA molecule can range from 15 minutes to several hours in 100% serum conditions<sup>311-314</sup>. Endonucleases also participate in siRNA degradation by attacking the 2'OH on the ribose sugar of the RNA. Nonetheless, nuclease stability can be achieved using modifications on the termini or the backbone of the siRNA.

Typical modifications include phosphorothioate (PS), 2'-O-methyl, 2'-fluoro, locked nucleic acids (LNAs), and cholesterol. The addition of PS to the siRNA backbone results in an increase of half-life to 24 hours in 50% human serum. The addition of more PS groups confers more stability but too many groups causes toxic effects<sup>309,312,315</sup>. Maximal siRNA activity is retained when 2'-O-methyl modifications are incorporated on every third nucleotide and 2'-fluoro modifications are incorporated into the pyrimidine bases. 2'-O-methyl and 2'-fluoro also increased half-life to 24 hours in 50-100% serum. Neither of these modifications generates toxicity, but too many modifications on the backbone can abolish siRNA activity<sup>309,312-314,316</sup>. LNAs incorporate a methylene bridge into the siRNA to increase the stability of the backbone, which also increases nuclease stability. LNAs at the terminal ends retain maximal activity compared to incorporation into the core region of the siRNA<sup>316</sup>. Terminal cholesterol siRNA modification not only increases nuclease stability but also increases transfection efficiency of siRNA into hepatocytes. In the absence of hydrodynamic injection and any transfection reagent, cholesterol-siRNA was delivered to hepatocytes, where it decreased apoB protein levels<sup>317,318</sup>. This was one of the first studies that indicated siRNA could be targeted to specific cell types using a targeting peptide. Due to the importance of the 5' phosphate on the anti-sense strand, any terminal modifications should be located on the 3' end of the anti-sense strand or the 5' and 3' ends of the sense strand to retain maximal RNAi activity.

Several types of peptides are used for cell-specific delivery of siRNA: cell-penetrating peptides (CPPs), membrane-penetrating peptides (MPPs), and cell targeting peptides. MPPs are peptides that can readily cross membranes, from plasma membranes to endosomal membranes. Various viruses can cross membranes quickly due to membrane targeting peptide domains. Several groups have tried to use peptides from influenza virus<sup>319</sup>, adenovirus, and rhinovirus<sup>320</sup> to destabilize both plasma and endosomal membranes and deliver oligonucleotides to

the cytoplasm. Several polycations can also be used as MPPs, such as polylysine, the cationic polymer PEI, and the neutral lipid DOPE (1,2-dioleoyl-sn-glycero-3-phosphoethanolamine)<sup>321</sup>. The MPPs penetratin and transportin also decreased GFP expression in COS-7, C166-GFP, and EOMA-GFP cell lines, which are resistant to siRNA transfection via liposomes<sup>322</sup>. CPPs, such as the TAT peptide from HIV-1, are more commonly used than MPPs for siRNA research, and result in more tissue-specific RNAi activity. The Tat peptide from HIV-1 was fused to a double-stranded RNA binding domain to aid in delivery of siRNA. SiRNA complexed to the TAT/RNA binding domain was directed towards multiple different cell types *in vivo* and had reduced off-target effects compared to lipid transfection of the same siRNA<sup>316</sup>.

Common cell targeting peptides include cholesterol, aptamers, CpG oligodeoxynucleotides for Toll-like receptor (TLRs) expressing cells,  $\alpha$ -tocopherol (Vitamin E), and some viral peptides such as TAT from HIV-1<sup>316,323</sup>. Aptamers are selected for their ability to bind to a cellular receptor on specific cell types. A 2'-fluoro modified aptamer for the PSMA cell surface receptor delivered siRNA directly to prostate cancer cells. The siRNA was targeted towards several anti-apoptotic mRNAs and resulted in tumor regression in a xenograft mouse model<sup>324</sup>. Another 2'-fluoro modified aptamer conjugated to anti-HIV siRNA showed a dual inhibition of HIV infection. The aptamer was targeted towards the gp120 cell surface receptor on HIV-infected T cells, and the siRNA was targeted towards the Tat/Rev mRNA. The aptamer-siRNA conjugate delivered the siRNA to HIV-infected cells only. It resulted in a decrease of Tat/Rev mRNA, and a reduction in HIV-infected T cells due to the blockade of gp120 binding to CD4 due to the aptamer<sup>325</sup>. The CNS is especially difficult to deliver siRNA to due to the BBB. Several CPPs have managed to traverse the BBB and deliver siRNA to neuronal cells within the CNS. An intravascular injection of  $\alpha$ -tocopherol conjugated siRNA resulted in receptor-mediated uptake in the brain. The siRNA was targeted toward beta-secretase 1, which led to a reduction of A $\beta$  peptides in a mouse model of AD. The  $\alpha$ -tocopherol-conjugated siRNA was also attached to serum high-density lipoprotein to mediate BBB crossing<sup>326</sup>. A small peptide of the rabies virus glycoprotein (RVG), which binds to nicotinic acetylcholine receptors, was shown to deliver siRNA to neuronal cells within the CNS. A nine-arginine residue stretch (RVG-9r) enabled RVG to bind to the anionic backbone of the siRNA for *in vivo* delivery. The siRNA decreased SOD1 mRNA in the brain, and protected neurons from Japanese encephalitis virus by reducing viral proteins. RVG-9r also increased serum stability up to 8 hours<sup>327</sup>.

Another way to protect siRNA from serum degradation is to use a vehicle delivery system. Vehicle delivery systems include polymers, dendrimers, and liposomes. Liposomes have become the most widely used siRNA vehicle since cationic liposomes were found to efficiently deliver plasmid DNA and other gene therapy products to cells. Liposome formulations include cationic, anionic, neutral, and ionizable lipids. Cationic lipids are the most widely used lipid for liposomes as they easily complex with siRNA through the negative charge of the phosphate backbone and the positive charge of the lipid<sup>328-333</sup>. However, other lipid formulations other than cationic lipids efficiently transfect different cell types. The application of the therapeutic determines which liposome formulation performs better. For example, it is extremely difficult to load some drugs into conventional cationic liposomes. Therefore, stable nucleic acid lipid particles (SNALP) were generated to possess a positive charge in acidic pH, to facilitate pH gradient loading, and a neutral charge at physiological pH to ensure drug retention. The charge difference of SNALPs is due to the mixture of cationic, neutral, and ionizable lipids within the liposome<sup>334,335</sup>. Cationic lipids (DOTAP [1,2-dioleoyl-3-trimethylammonium-propane (chloride salt)], DOTMA [1,2-di-octadecenyl-3-trimethylammonium propane (chloride salt)]) used for RNAi purposes are often synthetically engineered. Anionic liposomes come from more natural sources as cell membranes are composed of anionic lipids. Therefore, anionic liposomes can evade the immune system more efficiently than cationic liposome. A positively-charged molecule should be employed to condense the siRNA before loading into anionic liposomes if anionic lipids are used for RNAi purposes<sup>336</sup>. A helper lipid is usually included in liposome formulations, such as cholesterol or DOPE, to aid in liposome fluidity and to create a more rigid structure, so therapeutic drugs are retained within the liposome<sup>337</sup>. Liposomes, with either cationic or anionic lipids, are cleared by the mononuclear phagocyte system of the liver and spleen. Thus, they tend to have short half-lives in circulation. The incorporation of either PEG groups or G<sub>M1</sub> ganglioside generates stealth liposomes with longer half-lives. Clearance kinetics with either of these moieties is dose independent<sup>338</sup>. CPPs can target liposomes towards a particular cell type. Targeting ligands are either attached via covalent bonds or electrostatic interactions. Thus, generating a targeted siRNA delivery vehicle that is resistant to nucleases.

There is much speculation about how liposomes deliver siRNA into the cytoplasm of cells. Early experiments with fluorescent liposomes indicated that they fused to the plasma membrane and deposited their contents into the cytoplasm. However, any siRNA that is electrostatically attached to the outside of the liposome cannot enter the cell through this mechanism. This may not be a problem since it was shown that the addition of

DNA to liposomes resulted in destabilization of the liposomes, such that the DNA ended up on the inside of the lipid bilayer<sup>339</sup>. The same mechanism could occur with siRNA, leaving minimal amounts attached on the outside. Another mechanism of siRNA cytoplasmic entry is through endosomes. After transfection, liposomes are concentrated within cytoplasmic vesicles. It is believed that liposomes undergo endocytosis after interacting with the plasma membrane<sup>340</sup>. The mechanism of endosomal escape is still a little unclear. Some have speculated that the interaction between the negatively-charged endosomal membrane and the positively-charged liposome creates a destabilization effect of the membrane so siRNA can escape. However, this would imply that liposomes are no longer intact after endosomal escape, which seems not to be the case in some cell types<sup>330,339</sup>. Others have postulated that the bilayer phase properties contribute to endosomal escape such that a hexagonal bilayer more efficiently escapes the endosome than a lamellar bilayer<sup>341</sup>. Polymer vehicle delivery systems are not able to escape the endosome unless a membrane-disrupting peptide is used<sup>330</sup>. The exact cell entry mechanism, whether plasma membrane fusion or endosomal escape, may depend on cell type and liposome formulation.

Liposomes as siRNA delivery systems are extremely efficient in delivering siRNA to cells; however, toxicity issues have arisen with their use. Cationic formulations become immunogenic when they interact with negatively-charged serum proteins, which leads to an increase in cytokines and complement production. Also, since cationic liposomes are exceptionally effective at delivering siRNA to cells, they may inadvertently deliver siRNA to immune cells allowing for more immune activation<sup>342</sup>. Cationic lipids can also lead to an increase in reactive oxygen intermediates leading to toxicity of cells. There is some debate as to whether the liposome or the whole liposome/siRNA complex leads to immune activation. Some studies have shown that empty liposome or naked siRNA do not induce immune activation<sup>342,343</sup>, while other studies have demonstrated that they do<sup>324,344,345</sup>. Immune activation may depend on the concentration of liposome, formulation of the liposome, concentration of siRNA, and cell type. Anionic lipids are less immunogenic since they are derived from naturally-occurring lipids and do not readily associate with serum proteins<sup>336</sup>. However, a complete toxicity profile for anionic liposomes is lacking due to little research on anionic lipids.

Besides intravenous injection, intraperitoneal injections also deliver siRNA systemically. The exact mechanism of systemic delivery via intraperitoneal injection is not known but is thought to occur via diffusion directly into cells, uptake by vasculature and dissemination, or uptake by the lymphatic system. This injection method has shown promise in delivering siRNA to organs within the intraperitoneal cavity. In a mouse model of

septic shock, siRNA targeted towards TNF $\alpha$  resulted in protection against sepsis induced by lipopolysaccharide<sup>346</sup>. Intraperitoneal injections are efficient in delivering siRNA to abdominal tumors, specifically tumors caused by ovarian cancer. SiRNA directed towards either the tyrosine kinase receptor EphA2 or the integral membrane protein claudin 3 resulted in a decrease in tumor growth when the siRNA was injected intraperitoneally. Maximal delivery of the siRNAs was achieved through the complexation of lipid particles, either DOPC (1,2-dioleoyl-sn-glycero-3-phosphocholine) lipids or a lipid-like particle (98N<sub>12-5</sub>). This route of systemic delivery is important because it is less evasive and less technically challenging than an intravenous injection, and it is a clinically relevant route as some chemotherapeutic drugs are already administered this way<sup>346-348</sup>.

While systemic delivery shows promise in delivering siRNA to highly vascularized parts of the body, it does have a few limitations. Therefore, local delivery of siRNA has been investigated as an alternative. Nuclease stability of siRNA and cell-specific distribution is not as problematic in local administration as it is in systemic delivery. Also, local delivery decreases the risk of triggering an interferon response (discussed below) caused by the siRNA. Local delivery is attractive for delivering siRNA to tumors, or to privileged sites such as the eye and the brain. Intratumoral injections of siRNA have reduced tumor growth and angiogenesis in mouse xenograft models of melanoma, breast cancer, and cervical cancer. An increase in apoptosis and cytotoxicity in malignant cells developed by targeting various proteins (CSF1, Raf1, E6/E7) that have enhanced function in cancer cells, which resulted in reduction of tumors<sup>349-352</sup>.

Pump infusion into the third ventricle or stereotactic injections has been employed for local delivery to the CNS. Stereotactic injections have been used for both prion diseases and HD. The prion disease RNAi therapeutics were discussed above, but, briefly, they resulted in reversal of neuropathology by targeting PrP<sup>C</sup>. A Huntington's disease study, involving siRNA, targeted exogenous mutant huntingtin in an HD mouse model. The cholesterol-modified siRNA using an intrastriatal injection resulted in a reversal of HD neuropathology and motor deficits<sup>353</sup>. Studies using siRNA against  $\alpha$ -synuclein revealed that a one-month infusion into the substantia nigra of squirrel monkeys decreased  $\alpha$ -synuclein without reducing the number of dopaminergic neurons or activating microglia<sup>354</sup>. A functional study to determine the physiological role of APP revealed that siRNA reduction of APP results in a reduction of spontaneous alternation, suggesting that APP may be involved in short-term spatial working memory<sup>355</sup>.

Lastly, local delivery to the eye is so efficient that many RNAi ocular drugs are currently in Phase II/III clinical trials. Local delivery to the retina through an intravitreal injection was achieved using the transfection reagent TransitTKO. The retina is especially hard to deliver drugs to given the inner limiting membrane of the retina<sup>356</sup>. The delivery of VEGF siRNA by either subretinal<sup>357</sup> or subconjunctival<sup>358</sup> injection results in a reduction in choroidal neovascularization. Neovascularization is particularly damaging in age-related macular degeneration as it leads to blindness. However, in other reports the activation of TLR3 by RNAi was shown to decrease neovascularization in a siRNA sequence independent manner, indicating that RNAi within the ocular region results in an immune response. Nevertheless, RNAi drugs aimed at ocular targets are being developed<sup>309,356</sup>.

#### *Off-Target Effects and the Immune System*

In the first years of RNAi technology, researchers were extremely excited that no off-target effects were observed. Most siRNA molecules were selected based on homology screens, such that any homology with an endogenous gene was excluded. Therefore, many publications reported that the expression of the few control genes that were monitored for off-target effects (OTEs) were not disrupted because there was no homology with the siRNA. However, a microarray analysis of hundreds of expression profiles revealed a dozen to several hundred genes are regulated by any one siRNA molecule<sup>359</sup>. This finding was a major setback for the field, and research into the exact cause of the OTEs intensified. It was found that the seed region of a siRNA or shRNA, which corresponds to the 2-7 or 2-8 bases in the core region, determines the OTEs of a specific RNAi molecule. One nucleotide change in this seed region results in a different set of OTEs. Specifically, complementarity between the seed region of the RNAi molecule and the 3' untranslated region of mRNA determines which genes' expression is affected. This mechanism is remarkably similar to how micro RNAs (miRNAs) function by repressing translation through the binding of the miRNA to the 3' untranslated region of a particular gene. The mechanism of OTEs of siRNA indicate that it can mimic miRNA molecules, which results in a widespread alteration of gene expression<sup>360,361</sup>. Some chemical modifications, such as 2'-O-methyl, can be incorporated into the siRNA molecule to reduce OTEs. However, most of these modifications result in a reduced efficacy of the siRNA<sup>309,316</sup>. Researchers may never be able to abrogate OTE activity with RNAi completely, so design of siRNA molecules with the fewest and least deleterious OTEs needs to be considered for any siRNA translated to the clinic.

It is known that long dsRNA molecules elicit an innate immune response through TLRs. TLRs recognize pathogen-associated molecular patterns. One of the mechanisms of this immune pathway enables an organism to

defend itself against any exogenous RNA or DNA, usually from a viral infection. While this is a typical response to exogenous RNA, researchers thought that siRNA was incapable of stimulating an immune response due to its short length. Any DNA/RNA below 30 base pairs did not seem to activate the immune pathway. Early RNAi studies typically assessed one or two immune activation proteins, such as interferons and cytokines<sup>308,311,325</sup>. Just like the early attempts to deduce siRNA OTEs, attempts to find immune activation via siRNA were very narrow. Eventually, it was shown that treating a cell line that possessed immune system markers with siRNA resulted in immune activation. The activation occurred either through TLR-3 or TLR7/8. TLR-3 commonly recognizes dsRNA molecules, and TLR7/8 recognizes ssRNA molecules. TLR activation may occur through the endosomal pathway after endocytosis of the siRNA. Activation through TLR-3 or TLR7/8 increased interferon production<sup>324,344</sup>. Additionally, TLR-3 signaling leads to an increase in IL8, TNF $\alpha$ , and activation of NF- $\kappa$ B promoters. One consequence of immune activation is sequence-dependent gene suppression<sup>324</sup>. Immune activation by siRNA remained controversial for some time as the immune response was not seen in all cell lines or even animal models. Again, the animal model screens might have been too narrow or were looking at the wrong part of the immune system<sup>362</sup>. Differences in cell lines might account for the variabilities and might be attributed to genetic abnormalities or immune versus non-immune cell lines. A non-immune cell line revealed immune activation through the PKR pathway instead of the TLR pathway<sup>345</sup>. Use of transfection reagent or carrier also affects immune stimulation, as noted above with liposomes. Certain poly(U) or G/U rich sequences also contribute to an immune response, so siRNA should be designed without these sequence stretches<sup>363</sup>. Structural modifications of the siRNA, such as 2'-O-methyl and LNAs, decrease immune stimulation but modified siRNAs need to be verified that potency is not affected<sup>316,344</sup>. Like OTEs, careful design of the siRNA and carrier need to be made to reduce the amount of immune stimulation, especially in animal or human models.

## **The Blood-Brain Barrier**

### ***Structure and Function***

The BBB remains the biggest obstacle in developing pharmaceuticals for diseases that affect the CNS. In physiological conditions, the BBB maintains ion homeostasis, prevents toxic substances from entering the brain, and aids in immune surveillance. Neurons and other cells in the CNS depend on ions and nutrients for support and maintenance. However, ions and nutrients must be provided to these cells in strict concentrations, too much or too

little of these molecules results in neuronal damage. The BBB provides the transport needed for the ions/nutrients while also providing protection against fluctuations of these molecules since they vacillate wildly in the blood stream<sup>364</sup>.

There are three main layers to the BBB that support its role in limiting access of substances to neurons. The first layer, the endothelial cells, provides a physical barrier for all compounds in the blood stream. Astrocytes support the endothelial cells of the BBB and make up part of the physical barrier. Pericytes also aid in support and maintenance of the BBB by changing vascular permeability of blood vessels. The endothelial cells are connected via tight junctions with little to no movement of nutrients occurring through these junctions<sup>364,365</sup>. Therefore, the majority of compounds use transcytosis for transport across the BBB to neuronal cells. Nutrients, such as glucose and amino acids, are transported across the barrier using various membrane transporters. Larger molecules use either adsorptive mediated transcytosis or receptor mediated transcytosis. Both of these transport pathways result in compounds being endocytosed into the endothelial cells via a clathrin-dependent mechanism. It is not clearly understood how transcytosis occurs using these pathways but it is clear that there is a mechanism that releases the molecules before they are deposited into lysosomes for degradation. These transport pathways represent the transport barrier of the BBB. This layer of the BBB also includes multiple different types of efflux pumps. If a molecule is able to bypass the physical barrier, it can be pumped out of the endothelial cells by the efflux pumps<sup>365,366</sup>. The last barrier of the BBB is the enzymatic barrier, which consists of intracellular and extracellular enzymes. These enzymes are capable of digesting molecules around or in the endothelial cell layer. It is difficult for any drug to remain intact after crossing the BBB due to these three barriers. Once a drug does pass through the barrier it does not have to travel far for its site of action as most neurons sit between 8-25  $\mu\text{m}$  from a microvessel. There are a variety of ways to circumvent these layers of the BBB to deliver drugs to the CNS<sup>364,365</sup>.

The most common way to transport drugs across the BBB is by the 'Trojan horse' method. This method employs couples a therapeutic with a known molecule that is able to cross the BBB. These molecules are referred to as targeting peptides as they directly target a therapeutic to the CNS. Many of these molecules transport therapeutics across the BBB using receptor mediated endocytosis. While this method has proven effective in transporting therapeutics across the barrier, many of the therapeutics that employ this method alter the endocytic pathway in a way that a substantial portion of the therapeutic is shuttled to lysosomes for degradation. However, the argument remains that disease outcomes might be changed if even small concentrations of a therapeutic cross the BBB<sup>364-366</sup>.

Some molecules that have been utilized in the ‘Trojan horse’ method include transferrin, leptin, insulin, thiamine, and small viral peptides and bacterial toxins. Researchers have commonly used transferrin or transferrin-like molecules to transport oligonucleotides across the BBB. Early on in RNAi research it was found that phosphorothioate oligonucleotides (discussed above) utilized a specific transporter for delivery across the barrier<sup>367</sup>. That specific transporter was later identified as the transferrin receptor. Since then, multiple different groups have taken advantage of the transferrin/transferrin receptor transport system to deliver therapeutics to the brain. One example that exploits the transferrin receptor transport pathway used a monoclonal antibody, OX26, towards the transferrin receptor as a targeting peptide. The OX26 antibody was bound to polymersomes, which are vesicles made of copolymers that are stronger than lipid based vesicles, such as liposomes. The vasopressin drug NC-1900 was packaged within the polymersomes and targeted towards the brain using the OX26 antibody. OX26 allowed NC-1900 to cross the BBB and resulted in an improvement in memory deficits of a scopolamine rat model<sup>368</sup>.

Other monoclonal antibodies towards cell surface receptors are also used as targeting peptides. The human insulin receptor monoclonal antibody was fused with the tumor necrosis factor receptor, which suppresses tumor necrosis factor  $\alpha$  (TNF $\alpha$ ). TNF $\alpha$  is an inflammatory cytokine that can lead to neuronal damage in traumatic brain injuries and neurodegenerative conditions. By itself, the tumor necrosis factor receptor is not able to cross the BBB but coupled to the insulin receptor monoclonal antibody it is transported across the BBB and is selectively targeted to the brain in a rhesus monkey. A problem with utilizing certain cellular surface receptors is that they bind their ligands in a saturable manner. Both transferrin and insulin receptors have saturable binding domains. Therefore, only a certain amount of drug is allowed to bind to these receptors before all the active sites are blocked. Also, drugs that use these receptors must compete with the endogenous ligand for active binding sites. These two factors limit the amount of drug that can be transported across the BBB with these cellular receptors<sup>369</sup>. The thiamine receptor is also used to transport therapeutics to the brain but also has saturable binding and therapeutics have been shown to compete with the natural ligands for this receptor<sup>365</sup>.

Several groups have taken advantage of peptides from viruses or bacteria that can enter the CNS. As discussed above, Kumar *et al.* used the small peptide RVG-9r from the rabies virus glycoprotein to target siRNA towards the CNS<sup>327</sup>. Other groups have found that the C-terminal fragment of the tetanus toxin delivered superoxide dismutase to neurons *in vivo* by a number of routes, including intramuscular and intraperitoneal injections<sup>370</sup>. Based on this observation, the tetanus fragment was conjugated to nanoparticles, which delivered drugs to neuroblastoma

cells. One problem that remains with the use of the tetanus fragment is immunogenicity due to mass vaccination against tetanus. Therefore, several molecules identical to the tetanus fragment have been generated to overcome the immune system. One of these tetanus-like compounds, CRM197, was able to deliver polymersomes across the BBB<sup>371</sup>. More studies are needed to determine if these targeting peptides are useful in neurodegenerative disease models.

Other methods of crossing the BBB include the generation of analogs for cellular transporters, bypassing the barrier completely using either intrathecal or intranasal administration, and taking advantage of certain disease processes that make the BBB more permeable. While many of these methods have proven successful in transporting therapeutics to the brain, many obstacles of brain delivery remain before one of these methods is approved for pharmaceutical use. An ideal delivery method would not only transport therapeutics to the brain but would also be biodegradable and nontoxic, selective for neuronal cells, non-damaging to the BBB, and deliver therapeutic concentrations to the brain<sup>372</sup>.

## **Introduction to Work in this Dissertation**

The primary objectives of this research are to understand the pharmacological effects of transiently decreasing PrP<sup>C</sup>, due to a RNAi therapeutic, in prion diseases, and investigate the biodistribution and pharmacodynamics of novel *in vivo* liposomal delivery systems in the central nervous system (CNS). The overall hypothesis of this research is that the novel liposomal delivery systems will deliver PrP<sup>C</sup> siRNA to neuronal cells in the CNS, which will decrease neuronal PrP<sup>C</sup> and result in the extension of survival times of prion-infected mice. We employed various techniques such as flow cytometry, western blotting, digital drop PCR, protein misfolding cyclic amplification, and ELISA to investigate the following questions:

**Question 1: Can liposome-siRNA-peptide complexes (LSPCs) and peptide-addressed liposome-encapsulated therapeutic siRNA (PALETS) deliver PrP<sup>C</sup> siRNA to neuronal cells using systemic *in vivo* administration?**

Numerous studies have shown that many targets are decreased *in vitro* by siRNA using a mechanism that cleaves target mRNA. However, translating these studies *in vivo* remains a challenge. For efficient *in vivo* delivery of siRNA, the siRNA must be protected from serum nucleases and should be targeted to the proper cell type. Targeting siRNA to neuronal cells remains a challenge due to the blood-brain barrier (BBB). The BBB is a tightly regulated barrier that does not allow most therapeutic drugs to cross unassisted. Therefore, it is necessary to design

any drug delivery system with a CNS targeting peptide. We have developed three different liposomal drug delivery systems to the brain using both cationic and anionic liposomal formulations. These LSPCs and PALETS are directed towards the CNS using a small peptide from the rabies virus glycoprotein (RVG-9r) that targets nicotinic acetylcholine receptors. In chapter 2, we show that both LSPCs and PALETS effectively cross the BBB and deliver PrP<sup>C</sup> siRNA to mouse neuronal cells *in vivo*. Each liposomal formulation that we created, demonstrated a unique pharmacodynamics profile. We speculate that the different profiles are due to either distinctive uptake efficiencies of the liposomes into the CNS or different efficiencies of siRNA unloading.

**Question 2: What are the pharmacodynamics properties of PrP<sup>C</sup> siRNA in LSPCs delivered intravenously?**

Gene therapy either results in a permanent or a transient decrease of protein levels of the targeted gene. Specifically, for this project, the use of RNAi leads to a transient decrease in protein levels, and because no two siRNAs are alike, this temporary decline is highly variable. Therefore, pharmacodynamics profiles are needed for every siRNA to determine its efficacy and viability as a therapeutic option. Here we are using the cellular prion protein (PrP<sup>C</sup>) as a target for siRNA due to its ability to misfold and cause disease. Since PrP<sup>C</sup> is used as a template for the infectious form, a reduction in PrP<sup>C</sup> protein levels decreases the amount of substrate available for conversion to the infectious form. In chapter 3, we show that our PrP<sup>C</sup> siRNA targeted towards the 3' UTR of the *prnp* gene results in a 40-50% reduction of cell surface PrP<sup>C</sup> in two different mouse models. This decrease was seen to last as long as 21 days after siRNA treatment. The LSPCs did have some off-target effects in the kidney due to the presence of nicotinic acetylcholine receptors in that organ. We also demonstrate that PrP<sup>C</sup> mRNA levels are reduced at certain time points after siRNA treatments. However, to our surprise, some mice showed an increase in PrP<sup>C</sup> mRNA after siRNA treatment.

**Question 3: Do PrP<sup>C</sup> siRNA-containing LSPCs increase the survival time of mice with established prion infection in a scrapie mouse model?**

Many therapeutic options have been proposed for prion diseases. These options, discussed in more detail above, are effective at reducing PrP<sup>Res</sup> in prion-infected cell lines. Some of these compounds are too toxic to be tested *in vivo* or cannot readily cross the BBB. Other compounds that have been investigated for efficacy *in vivo* are either effective only at the time of inoculation or only delay onset of clinical disease signs. Early RNAi studies in prion disease revealed that a decrease in PrP<sup>C</sup> substrate for PrP<sup>Res</sup> conversion leads to a reversal of prion disease neuropathology. Therefore, we have used our PrP<sup>C</sup> siRNA-containing LSPCs to treat prion-infected mice. In chapter

4, we show that siRNA treatment every two weeks or every four weeks from the midpoint to late infection does not increase survival times of prion-infected mice. Consequently, the repeated siRNA treatments resulted in a Type III hypersensitivity response in the uninfected, treated control mice and total IgG levels increased after siRNA treatment. We also demonstrate that behavioral scores are improved with repeated LSPCs treatment, as shown with improved performance of treated mice in burrowing and nesting behavioral tests.

## References

1. Hunter, G. D. *Scrapie and Mad Cow Disease: The smallest and most lethal living thing*. (Vantage Press, 1993).
2. M'Gowan, J. P. *Investigation into the disease of sheep called 'Scrapie'*. (William Blackwood and Sons, 1914).
3. Liberski, P. P. Historical overview of prion diseases: a view from afar. *Folia Neuropathol* **50**, 1–12 (2012).
4. Besnoit, C. & Morel, C. Note sur les lésions nerveuses de la tremblante du mouton. *Rev Vet - Toulouse* **23**, 397–400 (1898).
5. Besnoit, C. La tremblante ou névrite périphérique enzootique du mouton. *Rev Vet - Toulouse* **23**, 307–343 (1899).
6. Brown, P. & Bradley, R. 1755 and all that: a historical primer of transmissible spongiform encephalopathy. *BMJ* **317**, 1688–1692 (1998).
7. Zabel, M. D. & Reid, C. A brief history of prions. *Pathog Dis* **73**, ftv087 (2015).
8. Greig, J. R. Scrapie in sheep. *J Comp Pathol* **60**, 263–266 (1950).
9. Stamp, J. T., Brotherston, J. G., Zlotnik, I., Mackay, J. M. K. & Smith, W. Further Studies on Scrapie. *J Comp Path* **69**, 268–280 (1959).
10. Creutzfeldt, H. G. Über eine eigenartige herdformige Erkrankung des Zentralnervensystems. *Gesamte Neurol* **57**, 1–8 (1920).
11. Jakob, A. Über eigenartige Erkrankungen des Zentralnervensystems mit bemerkenswertem anatomischem Befunde (spastische Pseudosklerose-Encephalomyelopathie mit disseminierten Degenerationsherden). *Dtsch Nervenheilkunde* **10**, 132–146 (1921).
12. Sternbach, G., Dibble, C. L. & Varon, J. From Creutzfeldt-Jakob disease to the mad cow epidemic. *J Emerg Med* **15**, 701–705 (1997).
13. Gajdusek, D. C. & Zigas, V. Degenerative disease of the central nervous system in New Guinea - The endemic occurrence of Kuru in the native population. *N Engl J Med* **257**, 974–978 (1957).
14. Gajdusek, D. C. & Zigas, V. Kuru: Clinical study of a new syndrome resembling Paralysis Agitans in natives of the eastern Highlands of Australian New Guinea. *Med J Aust* **2**, 745–754 (1957).
15. Gajdusek, D. C. & Zigas, V. Kuru: clinical, pathological and epidemiological study of an acute progressive degenerative disease of the central nervous system among natives of the Eastern Highlands of New Guinea. *Am J Med* **26**, 442–469 (1959).
16. Gajdusek, D. C. Unconventional viruses and the origin and disappearance of kuru. *Science* **197**, 943–960 (1977).
17. Hadlow, W. J. *Scrapie and kuru*. (The Lancet, 1959).
18. Klatzo, I., Gajdusek, D. C. & Zigas, V. Pathology of kuru. *Lab Invest* **8**, 799–847 (1959).
19. Gajdusek, D. C., Gibbs, C. J. & Alpers, M. Experimental transmission of a Kuru-like syndrome to chimpanzees. *Nature* **209**, 794–796 (1966).
20. Gibbs, C. J. *et al.* Creutzfeldt-Jakob disease (spongiform encephalopathy): transmission to the chimpanzee. *Science* **161**, 388–389 (1968).
21. Chandler, R. L. Encephalopathy in mice produced by inoculation with scrapie brain material. *The Lancet* **1**, 1378–1379 (1961).
22. Morris, J. A. & Gajdusek, D. C. Encephalopathy in mice following inoculation of scrapie sheep brain. *Nature* (1963).
23. Eklund, C. M., Kennedy, R. C. & Hadlow, W. J. Pathogenesis of scrapie virus infection in the mouse. *J Infect. Dis.* **117**, 15–22 (1967).
24. Kimberlin, R. H. & Walker, C. A. Pathogenesis of mouse scrapie: dynamics of agent replication in spleen, spinal cord and brain after infection by different routes. *J Comp Pathol* **89**, 551–562 (1979).
25. Kimberlin, R. H. Experimental scrapie in the mouse: a review of an important model disease. *Sci Prog* **63**, 461–481 (1976).
26. Kimberlin, R. H., Millson, G. C. & Hunter, G. D. An experimental examination of the scrapie agent in cell membrane mixtures: III. Studies of the operational size. *J Comp Pathol* 1–9 (2003).
27. Andrewes, C. H. Classification of viruses of vertebrates. *Adv Virus Res* **9**, 271–296 (Elsevier, 1963).

28. Cho, H. J. Is the scrapie agent a virus? *Nature* **262**, 411–412 (1976).
29. Gibbons, R. A. & Hunter, G. D. Nature of the scrapie agent. *Nature* 1–3 (1967).
30. Alper, T., Haig, D. A. & Clarke, M. C. The exceptionally small size of the scrapie agent. *Biochem Biophys Res Commun* **22**, 278–284 (1966).
31. Alper, T., Cramp, W. A., Haig, D. A. & Clarke, M. C. Does the agent of scrapie replicate without nucleic acid? *Nature* **214**, 764–766 (1967).
32. Field, E. J., Farmer, F., Caspary, E. A. & Joyce, G. Susceptibility of scrapie agent to ionizing radiation. *Nature* **222**, 90–91 (1969).
33. Alper, T., Haig, D. A. & Clarke, M. C. The scrapie agent: evidence against its dependence for replication on intrinsic nucleic acid. *J. Gen. Virol.* **41**, 503–516 (1978).
34. Pattison, I. H. & Millson, G. C. Further Observations on the Experimental Production of Scrapie in Goats and Sheep. *J Comp Pathol* **70**, 182–193 (1960).
35. Hunter, G. D. & Millson, G. C. Attempts to release the scrapie agent from tissue debris. *J Comp Pathol* **77**, 301–307 (1967).
36. Hunter, G. D. & Millson, G. C. Studies on the heat stability and chromatographic behaviour of the scrapie agent. *J. Gen. Microbiol.* **37**, 251–258 (1964).
37. Pattison, I. H. Resistance of the scrapie agent to formalin. *J Comp Pathol* **75**, 159–164 (1965).
38. Diener, T. O. Is the scrapie agent a viroid? *Nature New Biol.* **235**, 218–219 (1972).
39. Marsh, R. F., Semancik, J. S., Medappa, K. C., Hanson, R. P. & Rueckert, R. R. Scrapie and transmissible mink encephalopathy: search for infectious nucleic acid. *J Virol* **13**, 993–996 (2004).
40. Pattison, I. H. & Jones, K. M. The possible nature of the transmissible agent of scrapie. *Vet Rec* **80**, 2–9 (1967).
41. Griffith, J. S. Self-replication and scrapie. *Nature* **215**, 1043–1044 (1967).
42. Lewin, P. Scrapie: an infective peptide? *The Lancet* (1972).
43. Hunter, G. D., Kimberlin, R. H., Millson, G. C. & Gibbons, R. A. An experimental examination of the scrapie agent in cell membrane mixtures. I. Stability and physicochemical properties of the scrapie agent. *J Comp Pathol* **81**, 23–32 (1971).
44. Hunter, G. D., Gibbons, R. A., Kimberlin, R. H. & Millson, G. C. Further studies of the infectivity and stability of extracts and homogenates derived from scrapie affected mouse brains. *J Comp Pathol* **79**, 101–108 (1969).
45. Hunter, G. D., Millson, G. C. & MEEK, G. The intracellular location of the agent of mouse scrapie. *J. Gen. Microbiol.* **34**, 319–325 (1964).
46. Mould, D. L., Smith, W. & Dawson, A. Centrifugation Studies on the Infectivities of Cellular Fractions Derived from Mouse Brain Infected with Scrapie ('Suffolk strain'). *Microbiology* (1965).
47. Hunter, G. D., Kimberlin, R. H. & Gibbons, R. A. Scrapie: a modified membrane hypothesis. *J. Theor. Biol.* **20**, 355–357 (1968).
48. Millson, G. C., Hunter, G. D. & Kimberlin, R. H. An experimental examination of the scrapie agent in cell membrane mixtures. II. The association of scrapie activity with membrane fractions. *J Comp Pathol* **81**, 255–265 (1971).
49. Clarke, M. C. & Millson, G. C. The membrane location of scrapie infectivity. *J. Gen. Virol.* **31**, 441–445 (2017).
50. Haig, D. A. & Clarke, M. C. Multiplication of the scrapie agent. *Nature* **234**, 106–107 (1971).
51. Prusiner, S. B., Hadlow, W. J., Eklund, C. M. & Race, R. E. Sedimentation properties of the scrapie agent. *Proc. Natl. Acad. Sci. U.S.A.* **74**, 4656–4660 (1977).
52. Prusiner, S. B. *et al.* Partial purification and evidence for multiple molecular forms of the scrapie agent. *Biochemistry* **17**, 4993–4999 (1978).
53. Prusiner, S. B. Novel proteinaceous infectious particles cause scrapie. *Science* **216**, 136–144 (1982).
54. Prusiner, S. B. *et al.* Scrapie agent contains a hydrophobic protein. *Proc. Natl. Acad. Sci. U.S.A.* **78**, 6675–6679 (1981).
55. Prusiner, S. B. Chemistry and biology of prions. *Biochemistry* (1992).
56. McKinley, M. P., Masiarz, F. R. & Prusiner, S. B. Reversible chemical modification of the scrapie agent. *Science* **214**, 1259–1261 (1981).
57. McKinley, M. P., Bolton, D. C. & Prusiner, S. B. A protease-resistant protein is a structural component of the scrapie prion. *Cell* **35**, 57–62 (1983).
58. Bolton, D. C., McKinley, M. P. & Prusiner, S. B. Identification of a protein that purifies with the scrapie prion. *Science* **218**, 1309–1311 (1982).

59. Bendheim, P. E., Barry, R. A., DeArmond, S. J. & Stites, D. P. Antibodies to a scrapie prion protein. *Nature* (1984).
60. Brown, P. *et al.* Diagnosis of Creutzfeldt-Jakob disease by western blot identification of marker protein in human brain tissue. *N Engl J Med* **314**, 547–551 (1986).
61. Prusiner, S. B., Groth, D. F., Bolton, D. C., Kent, S. B. & Hood, L. E. Purification and structural studies of a major scrapie prion protein. *Cell* **38**, 127–134 (1984).
62. Prusiner, S. B. *et al.* Scrapie prions aggregate to form amyloid-like birefringent rods. *Cell* **35**, 349–358 (1983).
63. Bolton, D. C., Meyer, R. K. & Prusiner, S. B. Scrapie PrP 27-30 is a sialoglycoprotein. *J Virol* (1985).
64. Dickinson, A. G. & Mackay, J. M. Genetical control of the incubation period in mice of the neurological disease, scrapie. *Heredity (Edinb)* **19**, 279–288 (1964).
65. Dickinson, A. G., Meikle, V. M. & Fraser, H. Identification of a gene which controls the incubation period of some strains of scrapie agent in mice. *J Comp Pathol* **78**, 293–299 (1968).
66. Dickinson, A. G. & Fraser, H. Genetical control of the concentration of ME7 scrapie agent in mouse spleen. *J Comp Pathol* **79**, 363–366 (1969).
67. Dickinson, A. G., Meikle, V. M. & Fraser, H. Genetical control of the concentration of ME7 scrapie agent in the brain of mice. *J Comp Pathol* **79**, 15–22 (1969).
68. Outram, G. W. Changes in drinking and feeding habits of mice with experimental scrapie. *J Comp Pathol* (1972).
69. Dickinson, A. G. & Outram, G. W. Genetic aspects of unconventional virus infections: the basis of the virino hypothesis. *Wiley* 63–83 (1988).
70. Dickinson, A. G., Stamp, J. T., Renwick, C. C. & Rennie, J. C. Some factors controlling the incidence of scrapie in Cheviot sheep injected with a Cheviot-passaged scrapie agent. *J Comp Pathol* **78**, 313–321 (1968).
71. Oesch, B. *et al.* A cellular gene encodes scrapie PrP 27-30 protein. *Cell* **40**, 735–746 (1985).
72. Chesebro, B. *et al.* Identification of scrapie prion protein-specific mRNA in scrapie-infected and uninfected brain. *Nature* **315**, 331–333 (1985).
73. Locht, C., Chesebro, B. & Race, R. Molecular cloning and complete sequence of prion protein cDNA from mouse brain infected with the scrapie agent. *Proc. Natl. Acad. Sci. U.S.A.* (1986).
74. Robakis, N. K., Sawh, P. R. & Wolfe, G. C. Isolation of a cDNA clone encoding the leader peptide of prion protein and expression of the homologous gene in various tissues. *Proc. Natl. Acad. Sci. U.S.A.* (1986). doi:10.1016/j.exppara.2016.05.009
75. Basler, K. *et al.* Scrapie and cellular PrP isoforms are encoded by the same chromosomal gene. *Cell* **46**, 417–428 (1986).
76. Westaway, D. *et al.* Distinct prion proteins in short and long scrapie incubation period mice. *Cell* **51**, 651–662 (1987).
77. Carlson, G. A. *et al.* Linkage of prion protein and scrapie incubation time genes. *Cell* **46**, 503–511 (1986).
78. Carlson, G. A. *et al.* Genetics and polymorphism of the mouse prion gene complex: control of scrapie incubation time. *Mol. Cell. Biol.* **8**, 5528–5540 (2007).
79. Hunter, N., Foster, J. D., Dickinson, A. G. & Hope, J. Linkage of the gene for the scrapie-associated fibril protein (PrP) to the Sip gene in Cheviot sheep. *Vet Rec* **124**, 364–366 (1989).
80. Moore, R. C. *et al.* Mice with gene targeted prion protein alterations show that Prnp, Sinc and Prni are congruent. *Nature Genet* **18**, 118–125 (1998).
81. Mahal, S. P., Asante, E. A., Antoniou, M. & Collinge, J. Isolation and functional characterisation of the promoter region of the human prion protein gene. *Gene* (2001).
82. Puckett, C., Concannon, P., Casey, C. & Hood, L. Genomic structure of the human prion protein gene. *Am J Hum Genet* **49**, 320–329 (1991).
83. Westaway, D. *et al.* Structure and polymorphism of the mouse prion protein gene. *Proc. Natl. Acad. Sci. U.S.A.* **91**, 6418–6422 (1994).
84. Haigh, C. L., Wright, J. A. & Brown, D. R. Regulation of Prion Protein Expression by Noncoding Regions of the Prnp Gene. *J. Mol. Biol.* **368**, 915–927 (2007).
85. Inoue, S., Tanaka, M., Horiuchi, M., Ishiguro, N. & Shinagawa, M. Characterization of the bovine prion protein gene: the expression requires interaction between the promoter and intron. *J. Vet. Med. Sci.* **59**, 175–183 (1997).
86. Beringue, V. Regional heterogeneity of cellular prion protein isoforms in the mouse brain. *Brain* **126**, 2065–2073 (2003).

87. Manson, J., West, J. D., Thomson, V. & McBride, P. The prion protein gene: a role in mouse embryogenesis? *Development* **115**, 117-122 (1992).
88. Miele, G. *et al.* Embryonic activation and developmental expression of the murine prion protein gene. *Gene Exp* **11**, 1–12 (2003).
89. Lazarini, F., Deslys, J. P. & Dormont, D. Regulation of the glial fibrillary acidic protein, beta actin and prion protein mRNAs during brain development in mouse. *Brain Res. Mol. Brain Res.* **10**, 343–346 (1991).
90. McKinley, M. P., Hay, B., Lingappa, V. R., Lieberburg, I. & Prusiner, S. B. Developmental expression of prion protein gene in brain. *Dev Biol* **121**, 105–110 (1987).
91. Kretzschmar, H. A., Prusiner, S. B. & Stowring, L. E. Scrapie prion proteins are synthesized in neurons. *Am J Pathol* **122**, 1-5 (1986).
92. Lotscher, M., Recher, M., Hunziker, L. & Klein, M. A. Immunologically Induced, Complement-Dependent Up-Regulation of the Prion Protein in the Mouse Spleen: Follicular Dendritic Cells Versus Capsule and Trabeculae. *J. Immunol.* **170**, 6040–6047 (2003).
93. Martinez del Hoyo, G., Lopez-Bravo, M., Metharom, P., Ardavin, C. & Aucouturier, P. Prion Protein Expression by Mouse Dendritic Cells Is Restricted to the Nonplasmacytoid Subsets and Correlates with the Maturation State. *J. Immunol.* **177**, 6137–6142 (2006).
94. Li, R. *et al.* The Expression and Potential Function of Cellular Prion Protein in Human Lymphocytes. *Cellular Immunol* **207**, 49–58 (2001).
95. Shyu, W.-C. *et al.* Molecular modulation of expression of prion protein by heat shock. *Mol Neurobiol* **26**, 1–12 (2002).
96. Prusiner, S. B. Scrapie prions. *Annu Rev Microbiol*(1989).
97. Riek, R. *et al.* NMR structure of the mouse prion protein domain PrP(121-231). *Nature* **382**, 180–182 (1996).
98. Zahn, R., Liu, A., Lührs, T. & Riek, R. NMR solution structure of the human prion protein. in (2000).
99. Riek, R., Hornemann, S., Wider, G., Glockshuber, R. & Wüthrich, K. NMR characterization of the full-length recombinant murine prion protein, raPrP(23-231). *FEBS Letters* **413**, 282–288 (1997).
100. Stahl, N. *et al.* Structural studies of the scrapie prion protein using mass spectrometry and amino acid sequencing. *Biochemistry* **32**, 1991–2002 (1993).
101. Pan, K. M. *et al.* Conversion of alpha-helices into beta-sheets features in the formation of the scrapie prion proteins. *Proc. Natl. Acad. Sci. U.S.A.* **90**, 10962–10966 (1993).
102. Haraguchi, T. *et al.* Asparagine-linked glycosylation of the scrapie and cellular prion proteins. *Arch Biochem Biophys* **274**, 1–13 (2003).
103. Lawson, V. A., Collins, S. J., Masters, C. L. & Hill, A. F. Prion protein glycosylation. *J Neurochem* **93**, 793–801 (2005).
104. Bruce, M. E. *et al.* Transmissions to mice indicate that ‘new variant’ CJD is caused by the BSE agent. *Nature* **389**, 498–501 (1997).
105. Sarnataro, D. *et al.* PrP(C) association with lipid rafts in the early secretory pathway stabilizes its cellular conformation. *Mol. Biol. Cell* **15**, 4031–4042 (2004).
106. Hegde, R. S. *et al.* A transmembrane form of the prion protein in neurodegenerative disease. *Science* **279**, 827–834 (1998).
107. Hegde, R. S., Voigt, S. & Lingappa, V. R. Regulation of protein topology by trans-acting factors at the endoplasmic reticulum. *Mol. Cell* **2**, 85–91 (1998).
108. Stewart, R. S. Neurodegenerative Illness in Transgenic Mice Expressing a Transmembrane Form of the Prion Protein. *J Neurosci* **25**, 3469–3477 (2005).
109. Taraboulos, A., Raeber, A. J., Borchelt, D. R., Serban, D. & Prusiner, S. B. Synthesis and trafficking of prion proteins in cultured cells.
110. Brown, D. A. & Rose, J. K. Sorting of GPI-anchored proteins to glycolipid-enriched membrane subdomains during transport to the apical cell surface. *Cell* **68**, 533–544 (1992).
111. Morris, R., Cox, H., Mombelli, E. & Quinn, P. J. Rafts, little caves and large potholes: how lipid structure interacts with membrane proteins to create functionally diverse membrane environments. *Subcell. Biochem.* **37**, 35–118 (2004).
112. Sunyach, C., Jen, A., Deng, J. & Fitzgerald, K. T. The mechanism of internalization of glycosylphosphatidylinositol-anchored prion protein. *EMBO J* **22**, 3591-3601 (2003).
113. Taylor, D. R. & Hooper, N. M. The prion protein and lipid rafts (Review). *Mol Membr Biol* **23**, 89–99 (2009).

114. Naslavsky, N., Stein, R., Yanai, A., Friedlander, G. & Taraboulos, A. Characterization of detergent-insoluble complexes containing the cellular prion protein and its scrapie isoform. *J. Biol. Chem.* **272**, 6324–6331 (1997).
115. Taraboulos, A., Scott, M. & Semenov, A. Cholesterol depletion and modification of COOH-terminal targeting sequence of the prion protein inhibit formation of the scrapie isoform. *J Cell Biol* **129**, 121-132 (1995).
116. Caughey, B. & Raymond, G. J. The scrapie-associated form of PrP is made from a cell surface precursor that is both protease- and phospholipase-sensitive. *J. Biol. Chem.* **266**, 18217–18223 (1991).
117. Brown, L. R. & Harris, D. A. Copper and zinc cause delivery of the prion protein from the plasma membrane to a subset of early endosomes and the Golgi. *J Neurochem* **87**, 353–363 (2003).
118. Taylor, D. R. Assigning functions to distinct regions of the N-terminus of the prion protein that are involved in its copper-stimulated, clathrin-dependent endocytosis. *J. Cell. Sci.* **118**, 5141–5153 (2005).
119. Nunziante, M., Gilch, S. & Schätzl, H. M. Essential Role of the Prion Protein N Terminus in Subcellular Trafficking and Half-life of Cellular Prion Protein. *J Biol Chem* **278**, 3726–3734 (2003).
120. Shyng, S. L., Heuser, J. E. & Harris, D. A. A glycolipid-anchored prion protein is endocytosed via clathrin-coated pits. *J Cell Biol* **125**, 1239–1250 (1994).
121. Gilch, S., Winklhofer, K. F. & Groschup, M. H. Intracellular re-routing of prion protein prevents propagation of PrP Sc and delays onset of prion disease. *EMBO J* **20**, 3957-3966 (2001).
122. Borchelt, D. R., Taraboulos, A. & Prusiner, S. B. Evidence for synthesis of scrapie prion proteins in the endocytic pathway. *J Biol Chem* **267**, 16188-16199 (1992).
123. Caughey, B., Race, R. E., Ernst, D., Buchmeier, M. J. & Chesebro, B. Prion protein biosynthesis in scrapie-infected and uninfected neuroblastoma cells. *J Virol* **63**, 175–181 (1989).
124. Parizek, P. *et al.* Similar Turnover and Shedding of the Cellular Prion Protein in Primary Lymphoid and Neuronal Cells. *J Biol Chem* **276**, 44627–44632 (2001).
125. Büeler, H. *et al.* Normal development and behaviour of mice lacking the neuronal cell-surface PrP protein. *Nature* **356**, 577–582 (1992).
126. Manson, J. C. *et al.* 129/Ola mice carrying a null mutation in PrP that abolishes mRNA production are developmentally normal. *Mol Neurobiol* **8**, 121–127 (1994).
127. Büeler, H. *et al.* Mice devoid of PrP are resistant to scrapie. *Cell* **73**, 1339–1347 (1993).
128. Prusiner, S. B. *et al.* Ablation of the prion protein (PrP) gene in mice prevents scrapie and facilitates production of anti-PrP antibodies. *Proc. Natl. Acad. Sci. U.S.A.* **90**, 10608–10612 (1993).
129. Tobler, I., Gaus, S. E., Deboer, T., Achermann, P. & Fischer, M. Altered circadian activity rhythms and sleep in mice devoid of prion protein. *Nature* **380**, 639-642 (1996).
130. Roesler, R. *et al.* Normal inhibitory avoidance learning and anxiety, but increased locomotor activity in mice devoid of PrP(C). *Brain Res. Mol. Brain Res.* **71**, 349–353 (1999).
131. Nico, P. B. C. *et al.* Altered behavioural response to acute stress in mice lacking cellular prion protein. *Behav Brain Res* **162**, 173–181 (2005).
132. Colling, S. B., Khana, M., Collinge, J. & Jefferys, J. G. R. Mossy fibre reorganization in the hippocampus of prion protein null mice. *Behav Brain Res* **755**, 28–35 (2011).
133. Coitinho, A. S., Roesler, R., Martins, V. R., Brentani, R. R. & Izquierdo, I. Cellular prion protein ablation impairs behavior as a function of age. *NeuroReport* **14**, 1375–1379 (2003).
134. Criado, J. R. *et al.* Mice devoid of prion protein have cognitive deficits that are rescued by reconstitution of PrP in neurons. *Neurobiol Dis* **19**, 255–265 (2005).
135. Hundt, C., Peyrin, J. M., Haïk, S. & Gauczynski, S. Identification of interaction domains of the prion protein with its 37-kDa/67-kDa laminin receptor. *EMBO J* **20**, 5876-5886 (2001).
136. Gauczynski, S., Peyrin, J. M., Haïk, S. & Leucht, C. The 37-kDa/67-kDa laminin receptor acts as the cell-surface receptor for the cellular prion protein. *EMBO J* **20**, 5863-5875 (2001).
137. Graner, E. *et al.* Cellular prion protein binds laminin and mediates neuritegenesis. *Brain Res. Mol. Brain Res.* **76**, 85–92 (2000).
138. Coitinho, A. S. *et al.* The interaction between prion protein and laminin modulates memory consolidation. *Eur J Neurosci* **24**, 3255–3264 (2006).
139. Kaneko, K. *et al.* Evidence for protein X binding to a discontinuous epitope on the cellular prion protein during scrapie prion propagation. *Proc. Natl. Acad. Sci. U.S.A.* **94**, 10069–10074 (1997).
140. Telling, G. C. *et al.* Prion propagation in mice expressing human and chimeric PrP transgenes implicates the interaction of cellular PrP with another protein. *Cell* **83**, 79–90 (1995).
141. Martins, V. R. *et al.* Complementary hydrophathy identifies a cellular prion protein receptor. *Nat. Med.* **3**,

- 1376–1382 (1997).
142. Lopes, M. H. Interaction of Cellular Prion and Stress-Inducible Protein 1 Promotes Neuritogenesis and Neuroprotection by Distinct Signaling Pathways. *J Neurosci* **25**, 11330–11339 (2005).
  143. Zanata, S. M., Lopes, M. H. & Mercadante, A. F. Stress-inducible protein 1 is a cell surface ligand for cellular prion that triggers neuroprotection. *EMBO J* **21**, 3307–3316 (2002).
  144. Stöckel, J., Safar, J., Wallace, A. C., Cohen, F. E. & Prusiner, S. B. Prion protein selectively binds copper(II) ions. *Biochemistry* **37**, 7185–7193 (1998).
  145. Hornshaw, M. P., McDermott, J. R. & Candy, J. M. Copper binding to the N-terminal tandem repeat regions of mammalian and avian prion protein. *Biochem Biophys Res Commun* **2**, 621–629(1995).
  146. Brown, D. R., Qin, K., Herms, J. W., Madlung, A. & Manson, J. The cellular prion protein binds copper in vivo. *Nature* 1–4 (1997).
  147. Jones, C. E., Abdelraheim, S. R., Brown, D. R. & Viles, J. H. Preferential Cu<sup>2+</sup> Coordination by His 96 and His 111 Induces  $\beta$ -Sheet Formation in the Unstructured Amyloidogenic Region of the Prion Protein. *J Biol Chem* **279**, 32018–32027 (2004).
  148. Vassallo, N. & Herms, J. Cellular prion protein function in copper homeostasis and redox signalling at the synapse. *J Neurochem* **86**, 538–544 (2003).
  149. Brown, D. R., Boon-Seng, W., Hafiz, F. & Clive, C. Normal prion protein has an activity like that of superoxide dismutase. *Biochem J* **344**, 1–5 (1999).
  150. Brown, D. R., Clive, C. & Haswell, S. J. Antioxidant activity related to copper binding of native prion protein. *J Neurochem* **76**, 69–76 (2001).
  151. McMahan, H. E. M. *et al.* Cleavage of the Amino Terminus of the Prion Protein by Reactive Oxygen Species. *J Biol Chem* **276**, 2286–2291 (2001).
  152. Kurschner, C. & Morgan, J. I. The cellular prion protein (PrP) selectively binds to Bcl-2 in the yeast two-hybrid system. *Brain Res. Mol. Brain Res.* **30**, 165–168 (1995).
  153. Kurschner, C. & Morgan, J. I. Analysis of interaction sites in homo- and heteromeric complexes containing Bcl-2 family members and the cellular prion protein. *Brain Res. Mol. Brain Res.* **37**, 249–258 (1996).
  154. Kuwahara, C. *et al.* Prions prevent neuronal cell-line death. *Nature* **400**, 225–226 (1999).
  155. McLennan, N. F. *et al.* Prion Protein Accumulation and Neuroprotection in Hypoxic Brain Damage. *The Am J Pathol* **165**, 227–235 (2010).
  156. Weise, J. *et al.* Upregulation of cellular prion protein (PrP<sup>c</sup>) after focal cerebral ischemia and influence of lesion severity. *Neurosci Lett* **372**, 146–150 (2004).
  157. Spudich, A. *et al.* Aggravation of ischemic brain injury by prion protein deficiency: Role of ERK-1/-2 and STAT-1. *Neurobiol Dis* **20**, 442–449 (2005).
  158. Bounhar, Y., Zhang, Y., Goodyer, C. G. & LeBlanc, A. Prion Protein Protects Human Neurons against Bax-mediated Apoptosis. *J Biol Chem* **276**, 39145–39149 (2001).
  159. Roucou, X. *et al.* Cellular prion protein inhibits proapoptotic Bax conformational change in human neurons and in breast carcinoma MCF-7 cells. *Cell Death Differ* **12**, 783–795 (2005).
  160. Paitel, E. *et al.* Primary Cultured Neurons Devoid of Cellular Prion Display Lower Responsiveness to Staurosporine through the Control of p53 at Both Transcriptional and Post-transcriptional Levels. *J Biol Chem* **279**, 612–618 (2003).
  161. Westaway, D., DeArmond, S. J. & Cayetano-Canlas, J. Degeneration of skeletal muscle, peripheral nerves, and the central nervous system in transgenic mice overexpressing wild-type prion proteins. *Cell* (1994).
  162. Büeler, H., Fischer, M., Lang, Y., Bluethmann, H. & Lipp, H. P. Normal development and behaviour of mice lacking the neuronal cell-surface PrP protein. *Nature* **356**, 577–582 (1992).
  163. Mallucci, G. R., Ratte, S., Asante, E. A. & Linehan, J. Post-natal knockout of prion protein alters hippocampal CA1 properties, but does not result in neurodegeneration. *EMBO J* **21**, 202–210 (2002).
  164. Linden, R. *et al.* Physiology of the Prion Protein. *Physiol Rev* **88**, 673–728 (2008).
  165. Chiarini, L. B. *et al.* Cellular prion protein transduces neuroprotective signals. *EMBO J.* **21**, 3317–3326 (2002).
  166. Chen, S., Mangé, A., Dong, L., Lehmann, S. & Schachner, M. Prion protein as trans-interacting partner for neurons is involved in neurite outgrowth and neuronal survival. *Mol Cell Neurosci* **22**, 227–233 (2003).
  167. Monnet, C., Gavard, J., Mège, R.-M. & Sobel, A. Clustering of cellular prion protein induces ERK1/2 and stathmin phosphorylation in GT1-7 neuronal cells. *FEBS Letters* **576**, 114–118 (2004).
  168. Solfrosi, L. *et al.* Cross-linking cellular prion protein triggers neuronal apoptosis in vivo. *Science* **303**,

- 1514–1516 (2004).
169. Mouillet-Richard, S. *et al.* Signal transduction through prion protein. *Science* **289**, 1925–1928 (2000).
170. Herms, J. W. *et al.* Altered intracellular calcium homeostasis in cerebellar granule cells of prion protein-deficient mice. *J Neurochem* **75**, 1487–1492 (2000).
171. Kim, B.-H. *et al.* The cellular prion protein (PrP<sup>C</sup>) prevents apoptotic neuronal cell death and mitochondrial dysfunction induced by serum deprivation. *Mol Brain Res* **124**, 40–50 (2004).
172. Brini, M., Miuzzo, M., Pierobon, N., Negro, A. & Sorgato, M. C. The prion protein and its paralogue Doppel affect calcium signaling in Chinese hamster ovary cells. *Mol. Biol. Cell* **16**, 2799–2808 (2005).
173. Vassallo, N. *et al.* Activation of phosphatidylinositol 3-kinase by cellular prion protein and its role in cell survival. *Biochem Biophys Res Commun* **332**, 75–82 (2005).
174. Mazzoni, I. E., Ledebur, H. C., Jr, Paramithiotis, E. & Cashman, N. Lymphoid signal transduction mechanisms linked to cellular prion protein. *Biochem. Cell Biol.* **83**, 644–653 (2005).
175. Mattei, V. *et al.* Prion protein is a component of the multimolecular signaling complex involved in T cell activation. *FEBS Letters* **560**, 14–18 (2004).
176. Hugel, B. *et al.* Modulation of signal transduction through the cellular prion protein is linked to its incorporation in lipid rafts. *Cell. Mol. Life Sci.* **61**, 2998–3007 (2004).
177. Zhang, C. C., Steele, A. D. & Lindquist, S. Prion protein is expressed on long-term repopulating hematopoietic stem cells and is important for their self-renewal. *Proc. Natl. Acad. Sci. U.S.A.* **103**, 2184–2189 (2006).
178. Barclay, G. R., Hope, J., Birkett, C. R. & Turner, M. L. Distribution of cell-associated prion protein in normal adult blood determined by flow cytometry. *Br. J. Haematol.* **107**, 804–814 (1999).
179. Politopoulou, G., Seebach, J. D., Schmugge, M., Schwarz, H. P. & Aguzzi, A. Age-related expression of the cellular prion protein in human peripheral blood leukocytes. *Haematologica* **85**, 580–587 (2000).
180. Dodelet, V. C. & Cashman, N. R. Prion protein expression in human leukocyte differentiation. *Blood* **91**, 1556–1561 (1998).
181. Mabbott, N. A., Brown, K. L., Manson, J. & Bruce, M. E. T-lymphocyte activation and the cellular form of the prion protein. *Immunology* **92**, 161–165 (1997).
182. Ballerini, C. *et al.* Functional Implication of Cellular Prion Protein in Antigen-Driven Interactions between T Cells and Dendritic Cells. *J. Immunol.* **176**, 7254–7262 (2006).
183. Liu, T. *et al.* Normal Cellular Prion Protein Is Preferentially Expressed on Subpopulations of Murine Hemopoietic Cells. *J. Immunol.* **166**, 3733–3742 (2001).
184. Cashman, N. R. *et al.* Cellular isoform of the scrapie agent protein participates in lymphocyte activation. *Cell* **61**, 185–192 (2003).
185. Stuermer, C. A. O. PrP<sup>C</sup> capping in T cells promotes its association with the lipid raft proteins reggie-1 and reggie-2 and leads to signal transduction. *FASEB J* **18**, 1731–1733 (2004). doi:10.1096/fj.04-2150fje
186. Aguzzi, A., Heppner, F. L. & Heikenwalder, M. Immune system and peripheral nerves in propagation of prions to CNS. *Br Med Bull* **66**, 141–159 (2003). doi:10.1093/bmb/dg66.141
187. Mabbott, N. A. & MacPherson, G. G. Prions and their lethal journey to the brain. *Nat Rev Micro* **4**, 201–211 (2006).
188. Brandner, S. *et al.* Normal host prion protein necessary for scrapie-induced neurotoxicity. *Nature* **379**, 339–343 (1996).
189. Borchelt, D. R. & Sisodia, S. S. Loss of functional prion protein: a role in prion disorders? *Chem. Biol.* **3**, 619–621 (1996).
190. Mallucci, G. Depleting Neuronal PrP in Prion Infection Prevents Disease and Reverses Spongiosis. *Science* **302**, 871–874 (2003).
191. Mallucci, G. & Collinge, J. Update on Creutzfeldt-Jakob Disease. *Curr Opin Neurobiol* **17**, 641–647 (2004).
192. Gray, F., Chrétien, F. & Adle-Biassette, H. Neuronal apoptosis in Creutzfeldt-Jakob disease. *J Neuropathol Exp Neurol* **58**, 321–328 (1999).
193. Dorandeu, A. *et al.* Neuronal apoptosis in fatal familial insomnia. *Brain Pathol.* **8**, 531–537 (1998).
194. Chrétien, F. *et al.* A process of programmed cell death as a mechanisms of neuronal death in prion diseases. *Int J Clin Exp Pathol* **47**, 181–191 (1999).
195. Imran, M. & Mahmood, S. An overview of animal prion diseases. *Viol. J.* **8**, 493 (2011).
196. Fast, C. & Groschup, M. H. in *Prions and Diseases* 15–44 (Springer New York, 2012). doi:10.1007/978-1-4614-5338-3\_2
197. Wilesmith, J. W., Wells, G. A., Cranwell, M. P. & Ryan, J. B. Bovine Spongiform Encephalopathy:

- epidemiological studies. *Vet Rec* **128**, 199–203 (1991).
198. Brown, P. Bovine spongiform encephalopathy and variant Creutzfeldt-Jakob disease. *British Medical Journal* **322**, 841–844 (2001).
199. Brown, P., Will, R. G., Bradley, R. & Asher, D. M. Bovine spongiform encephalopathy and variant Creutzfeldt-Jakob disease: background, evolution, and current concerns. *Emerging infectious ...* (2001).
200. Williams, E. S. & Young, S. Chronic wasting disease of captive mule deer: a spongiform encephalopathy. *J. Wildl. Dis.* (1980).
201. Williams, E. S., Miller, M. W., Kreeger, T. J. & Kahn, R. H. Chronic wasting disease of deer and elk: a review with recommendations for management. *The Journal of wildlife ...* (2002).
202. Meyerett-Reid, C. *et al.* De Novo Generation of a Unique Cervid Prion Strain Using Protein Misfolding Cyclic Amplification. *mSphere* **2**, (2017).
203. Benestad, S. L., Mitchell, G., Simmons, M., Ytrehus, B. & Vikøren, T. First case of chronic wasting disease in Europe in a Norwegian free-ranging reindeer. *Vet. Res.* 1–7 (2016). doi:10.1186/s13567-016-0375-4
204. Sigurdson, C. J. A prion disease of cervids: Chronic wasting disease. *Vet. Res.* **39**, 41 (2008).
205. Imran, M. & Mahmood, S. An overview of human prion diseases. *Virol. J.* **8**, 559 (2011).
206. Alperovitch, A., Poser, S., Pocchiari, M. & Hofman, A. A new variant of Creutzfeldt-Jakob disease in the UK. *The Lancet* (1996).
207. Zarranz, J. J., Pomar, J. M. R. & Salisachs, P. Kuru plaques in the brain of two cases with Creutzfeldt-Jakob disease. A common origin for the two diseases? *J Neurol Sci* **43**, 291–300 (1979).
208. Wadsworth, J. D. F. *et al.* The origin of the prion agent of kuru: molecular and biological strain typing. *Philosophical Transactions of the Royal Society B: Biological Sciences* **363**, 3747–3753 (2008).
209. Alpers, M. P. The epidemiology of kuru: monitoring the epidemic from its peak to its end. *Philosophical Transactions of the Royal Society B: Biological Sciences* **363**, 3707–3713 (2008).
210. Collinge, J. *et al.* A clinical study of kuru patients with long incubation periods at the end of the epidemic in Papua New Guinea. *Philosophical Transactions of the Royal Society B: Biological Sciences* **363**, 3725–3739 (2008).
211. Liberski, P. P. *et al.* Kuru: genes, cannibals and neuropathology. *J. Neuropathol. Exp. Neurol.* **71**, 92–103 (2012).
212. Soto, C. Unfolding the role of protein misfolding in neurodegenerative diseases. *Nat Rev Neurosci* **4**, 49–60 (2003).
213. Ovádi, J. & Orosz, F. *Protein folding and misfolding: neurodegenerative diseases.* (2008).
214. Yehiely, F. *et al.* Identification of candidate proteins binding to prion protein. *Neurobiology of Disease* **3**, 339–355 (1997).
215. Laurén, J., Gimbel, D. A., Nygaard, H. B., Gilbert, J. W. & Strittmatter, S. M. Cellular prion protein mediates impairment of synaptic plasticity by amyloid- $\beta$  oligomers. *Nature* **457**, 1128–1132 (2009).
216. Voigtländer, T., Klöppel, S., Birner, P. & Jarius, C. Marked increase of neuronal prion protein immunoreactivity in Alzheimer's disease and human prion diseases. *Acta ...* (2001). doi:10.1007/s004010100405
217. Ferrer, I., Blanco, R., Carmona, M., Puig, B. & Ribera, R. Prion protein expression in senile plaques in Alzheimer's disease. *Acta ...* (2001). doi:10.1007/s004010000271
218. Parkin, E. T., Watt, N. T. & Hussain, I. Cellular prion protein regulates  $\beta$ -secretase cleavage of the Alzheimer's amyloid precursor protein. in (2007).
219. Haig, D. A. & Clarke, M. C. The effect of beta-propiolactone on the scrapie agent. *J. Gen. Virol.* **3**, 281–283 (1968).
220. Cochran, K. W. Failure of adenine arabinoside to modify scrapie in mice. *J. Gen. Virol.* **13**, 353–354 (1971).
221. Tateishi, J. Antibiotics and antivirals do not modify experimentally-induced Creutzfeldt-Jakob disease in mice. *J. Neurol. Neurosurg. Psychiatr.* **44**, 723–724 (1981).
222. Stewart, L. A., Rydzewska, L. H., Keogh, G. F. & Knight, R. Systematic review of therapeutic interventions in human prion disease. *Neurology* **70**, 1272–1281 (2008).
223. Pocchiari, M., Casaccia, P. & Ladogana, A. Amphotericin B: a novel class of antiscrapie drugs. *J. Infect. Dis.* **160**, 795–802 (1989).
224. Pocchiari, M., Schmittinger, S. & Masullo, C. Amphotericin B delays the incubation period of scrapie in intracerebrally inoculated hamsters. *J. Gen. Virol.* **68 (Pt 1)**, 219–223 (1987).
225. Demaimay, R. *et al.* Pharmacological studies of a new derivative of amphotericin B, MS-8209, in mouse

- and hamster scrapie. *J. Gen. Virol.* **75 ( Pt 9)**, 2499–2503 (1994).
226. McKenzie, D., Kaczkowski, J., Marsh, R. & Aiken, J. Amphotericin B delays both scrapie agent replication and PrP-res accumulation early in infection. *J Virol* **68**, 7534–7536 (1994).
227. Demaimay, R. *et al.* Late treatment with polyene antibiotics can prolong the survival time of scrapie-infected animals. *J Virol* **71**, 9685–9689 (1997).
228. Beringue, V. *et al.* Inhibiting scrapie neuroinvasion by polyene antibiotic treatment of SCID mice. *J. Gen. Virol.* **80 ( Pt 7)**, 1873–1877 (1999).
229. Mangé, A., Milhavel, O., McMahon, H. E., Casanova, D. & Lehmann, S. Effect of amphotericin B on wild-type and mutated prion proteins in cultured cells: putative mechanism of action in transmissible spongiform encephalopathies. *J Neurochem* **74**, 754–762 (2000).
230. Mangé, A. *et al.* Amphotericin B inhibits the generation of the scrapie isoform of the prion protein in infected cultures. *J Virol* **74**, 3135–3140 (2000).
231. Doh-ura, K., Iwaki, T. & Caughey, B. Lysosomotropic agents and cysteine protease inhibitors inhibit scrapie-associated prion protein accumulation. *J Virol* **74**, 4894–4897 (2000).
232. Ryou, C. *et al.* Differential Inhibition of Prion Propagation by Enantiomers of Quinacrine. *Lab Invest* **83**, 837–843 (2003).
233. Doh-ura, K. *et al.* Treatment of Transmissible Spongiform Encephalopathy by Intraventricular Drug Infusion in Animal Models. *J Virol* **78**, 4999–5006 (2004).
234. Collins, S. J. *et al.* Quinacrine does not prolong survival in a murine Creutzfeldt-Jakob disease model. *Ann. Neurol.* **52**, 503–506 (2002).
235. Kocisko, D. A. & Caughey, B. Mefloquine, an Antimalaria Drug with Antiprion Activity In Vitro, Lacks Activity In Vivo. *J Virol* **80**, 1044–1046 (2005).
236. Martínez-Lage, J. F. *et al.* Creutzfeldt-Jakob disease acquired via a dural graft: failure of therapy with quinacrine and chlorpromazine. *Surg Neurol Int* **64**, 542–545 (2005).
237. Haik, S., Brandel, J. P., Salomon, D. & Sazdovitch, V. Compassionate use of quinacrine in Creutzfeldt–Jakob disease fails to show significant effects. *Neurology* (2004).
238. Collinge, J. *et al.* Safety and efficacy of quinacrine in human prion disease (PRION-1 study): a patient-preference trial. *Lancet Neurol* **8**, 334–344 (2009).
239. Ghaemmaghami, S. *et al.* Continuous Quinacrine Treatment Results in the Formation of Drug-Resistant Prions. *PLoS Pathog* **5**, e1000673 (2009).
240. Bian, J., Kang, H. E. & Telling, G. C. Quinacrine promotes replication and conformational mutation of chronic wasting disease prions. *Proc. Natl. Acad. Sci. U.S.A.* **111**, 6028–6033 (2014).
241. Supattapone, S., Nguyen, H. O., Cohen, F. E., Prusiner, S. B. & Scott, M. R. Elimination of prions by branched polyamines and implications for therapeutics. *Proc. Natl. Acad. Sci. U.S.A.* **96**, 14529–14534 (1999).
242. Supattapone, S. *et al.* Branched Polyamines Cure Prion-Infected Neuroblastoma Cells. *J Virol* **75**, 3453–3461 (2001).
243. Supattapone, S., Piro, J. & Rees, J. Complex polyamines: unique prion disaggregating compounds. *CNS Neurol Disord Drug Targets* **8**, 323–328 (2009).
244. Kimberlin, R. H. & Walker, C. A. The antiviral compound HPA-23 can prevent scrapie when administered at the time of infection. *Arch. Virol.* **78**, 9–18 (1983).
245. Kimberlin, R. H. & Walker, C. A. Suppression of scrapie infection in mice by heteropolyanion 23, dextran sulfate, and some other polyanions. *Antimicrob. Agents Chemother.* **30**, 409–413 (1986).
246. Ehlers, B. & Diringer, H. Dextran sulphate 500 delays and prevents mouse scrapie by impairment of agent replication in spleen. *J. Gen. Virol.* **65 ( Pt 8)**, 1325–1330 (1984).
247. Caughey, B. & Raymond, G. J. Sulfated polyanion inhibition of scrapie-associated PrP accumulation in cultured cells. *J Virol* **67**, 643–650 (1993).
248. Farquhar, C., Dickinson, A. & Bruce, M. Prophylactic potential of pentosan polysulphate in transmissible spongiform encephalopathies. *Lancet* **353**, 117 (1999).
249. Shyng, S. L., Lehmann, S. & Moulder, K. L. Sulfated glycans stimulate endocytosis of the cellular isoform of the prion protein, PrPC, in cultured cells. *J Biol Chem* **270**, 30221–30229 (1995).
250. Adjou, K. T. A novel generation of heparan sulfate mimetics for the treatment of prion diseases. *J Gen Virol* **84**, 2595–2603 (2003).
251. Ingrosso, L., Ladogana, A. & Pocchiari, M. Congo red prolongs the incubation period in scrapie-infected hamsters. *J Virol* **69**, 506–508 (1995).
252. Beringue, V., Adjou, K. T., Lamoury, F. & Maignien, T. Opposite effects of dextran sulfate 500, the

- polyene antibiotic MS-8209, and Congo red on accumulation of the protease-resistant isoform of PrP in the spleens of mice inoculated intraperitoneally with the scrapie agent. *J Virol* **74**, 5432-5440 (2000).
253. Caughey, B., Brown, K. & Raymond, G. J. Binding of the protease-sensitive form of PrP (prion protein) to sulfated glycosaminoglycan and congo red. *J Virol* **68**, 2135-2141 (1994).
254. Caspi, S. *et al.* The anti-prion activity of Congo red. Putative mechanism. *J. Biol. Chem.* **273**, 3484–3489 (1998).
255. Gabizon, R., McKinley, M. P., Groth, D. & Prusiner, S. B. Immunoaffinity purification and neutralization of scrapie prion infectivity. *Proc. Natl. Acad. Sci. U.S.A.* **85**, 6617–6621 (2006).
256. Horiuchi, M. & Caughey, B. Specific binding of normal prion protein to the scrapie form via a localized domain initiates its conversion to the protease-resistant state. *EMBO J* **18**, 3193-3203 (1999).
257. Peretz, D. *et al.* Antibodies inhibit prion propagation and clear cell cultures of prion infectivity. *Nature* **412**, 739–743 (2001).
258. Beringue, V. *et al.* PrP ScBinding Antibodies Are Potent Inhibitors of Prion Replication in Cell Lines. *J Biol Chem* **279**, 39671–39676 (2004).
259. Kim, C. L. Cell-surface retention of PrPC by anti-PrP antibody prevents protease-resistant PrP formation. *J Gen Virol* **85**, 3473–3482 (2004).
260. Enari, M. & Flechsig, E. Scrapie prion protein accumulation by scrapie-infected neuroblastoma cells abrogated by exposure to a prion protein antibody. *Proc. Natl. Acad. Sci. U.S.A.* **98**, 9295-9299 (2001).
261. Perrier, V. *et al.* Anti-PrP antibodies block PrPSc replication in prion-infected cell cultures by accelerating PrPC degradation. *J Neurochem* **89**, 454–463 (2004).
262. Müller-Schiffmann, A. & Korth, C. Vaccine Approaches to Prevent and Treat Prion Infection. *BioDrugs* (2008).
263. White, A. R. *et al.* Monoclonal antibodies inhibit prion replication and delay the development of prion disease. *Nature* **422**, 80–83 (2003).
264. Sigurdsson, E. M. *et al.* Immunization delays the onset of prion disease in mice. *Am J Pathol* **161**, 13–17 (2010).
265. Goñi, F. *et al.* Mucosal vaccination delays or prevents prion infection via an oral route. *Neuroscience* **133**, 413–421 (2005).
266. Tal, Y. *et al.* Complete Freund's adjuvant immunization prolongs survival in experimental prion disease in mice. *J. Neurosci. Res.* **71**, 286–290 (2003).
267. Outram, G. W., Dickinson, A. G. & Fraser, H. Reduced susceptibility to scrapie in mice after steroid administration. *Nature* **249**, 855–856 (1974).
268. Manuelidis, L., Fritch, W. & Zaitsev, I. Dapsone to delay symptoms in Creutzfeldt-Jakob disease. *Lancet* **352**, 456 (1998).
269. Daude, N. Specific inhibition of pathological prion protein accumulation by small interfering RNAs. *J. Cell. Sci.* **116**, 2775–2779 (2003).
270. Tilly, G., Chapuis, J., Vilette, D., Laude, H. & Vilotte, J. L. Efficient and specific down-regulation of prion protein expression by RNAi. *Biochem Biophys Res Commun* **305**, 548–551 (2003).
271. Kim, Y. *et al.* Utility of RNAi-mediated prnp gene silencing in neuroblastoma cells permanently infected by prions: Potentials and limitations. *Antiviral Res* **84**, 185–193 (2009).
272. Pulford, B. *et al.* Liposome-siRNA-Peptide Complexes Cross the Blood-Brain Barrier and Significantly Decrease PrPC on Neuronal Cells and PrPRES in Infected Cell Cultures. *PLoS ONE* **5**, e11085 (2010).
273. Sutou, S. *et al.* Knockdown of the bovine prion gene PRNP by RNA interference (RNAi) technology. *BMC Biotechnol* **7**, 44 (2007).
274. Ohnishi, Y., Tamura, Y., Yoshida, M., Tokunaga, K. & Hohjoh, H. Enhancement of Allele Discrimination by Introduction of Nucleotide Mismatches into siRNA in Allele-Specific Gene Silencing by RNAi. *PLoS ONE* **3**, e2248 (2008).
275. White, M. D. *et al.* Single treatment with RNAi against prion protein rescues early neuronal dysfunction and prolongs survival in mice with prion disease. *Proc. Natl. Acad. Sci. U.S.A.* **105**, 10238–10243 (2008).
276. Pfeifer, A. *et al.* Lentivector-mediated RNAi efficiently suppresses prion protein and prolongs survival of scrapie-infected mice. *J. Clin. Invest.* **116**, 3204–3210 (2006).
277. Gallozzi, M. *et al.* Prnp knockdown in transgenic mice using RNA interference. *Transgenic Res.* **17**, 783–791 (2008).
278. Golding, M. C., Long, C. R., Carmell, M. A., Hannon, G. J. & Westhusin, M. E. Suppression of prion protein in livestock by RNA interference. *Proc. Natl. Acad. Sci. U.S.A.* **103**, 5285–5290 (2006).
279. Proske, D. *et al.* Prion-protein-specific aptamer reduces PrPSc formation. *Chembiochem* **3**, 717–725

- (2002).
280. Rhie, A. *et al.* Characterization of 2'-Fluoro-RNA Aptamers That Bind Preferentially to Disease-associated Conformations of Prion Protein and Inhibit Conversion. *J Biol Chem* **278**, 39697–39705 (2003).
281. Caughey, B. *et al.* Inhibition of Protease-Resistant Prion Protein Accumulation In Vitro by Curcumin. *J Virology* **77**, 5499–5502 (2003).
282. Kocisko, D. A. *et al.* Comparison of protease-resistant prion protein inhibitors in cell cultures infected with two strains of mouse and sheep scrapie. *Neurosci Lett* **388**, 106–111 (2005).
283. Trevitt, C. R. A systematic review of prion therapeutics in experimental models. *Brain* **129**, 2241–2265 (2006).
284. Gallardo-Godoy, A. *et al.* 2-Aminothiazoles as Therapeutic Leads for Prion Diseases. *J. Med. Chem.* **54**, 1010–1021 (2011).
285. Berry, D. B., Lu, D., Geva, M. & Watts, J. C. Drug resistance confounding prion therapeutics. *Proc. Natl. Acad. Sci. U.S.A.* **110**, E4160-9 (2013).
286. Fire, A. *et al.* Potent and specific genetic interference by double-stranded RNA in *Caenorhabditis elegans*. *Nature* **391**, 806–811 (1998).
287. Zamore, P. D., Tuschl, T., Sharp, P. A. & Bartel, D. P. RNAi: double-stranded RNA directs the ATP-dependent cleavage of mRNA at 21 to 23 nucleotide intervals. *Cell* **101**, 25–33 (2000).
288. Bernstein, E., Caudy, A. A., Hammond, S. M. & Hannon, G. J. Role for a bidentate ribonuclease in the initiation step of RNA interference. *Nature* **409**, 363–366 (2001).
289. Nykänen, A., Haley, B. & Zamore, P. D. ATP requirements and small interfering RNA structure in the RNA interference pathway. *Cell* **107**, 309–321 (2001).
290. Meister, G. *et al.* Human Argonaute2 Mediates RNA Cleavage Targeted by miRNAs and siRNAs. *Mol. Cell* **15**, 185–197 (2004).
291. Kim, D.-H. *et al.* Synthetic dsRNA Dicer substrates enhance RNAi potency and efficacy. *Nat. Biotechnol.* **23**, 222–226 (2004).
292. Hammond, S. M., Bernstein, E., Beach, D. & Hannon, G. J. An RNA-directed nuclease mediates post-transcriptional gene silencing in *Drosophila* cells. *Nature* **404**, 293–296 (2000).
293. Martinez, J. RISC is a 5' phosphomonoester-producing RNA endonuclease. *Genes Dev* **18**, 975–980 (2004).
294. Song, J. J., Smith, S. K., Hannon, G. J. & Joshua-Tor, L. Crystal structure of Argonaute and its implications for RISC slicer activity. *Science* (2004).
295. Liu, J. Argonaute2 Is the Catalytic Engine of Mammalian RNAi. *Science* **305**, 1437–1441 (2004).
296. Gregory, R. I., Chendrimada, T. P., Cooch, N. & Shiekhattar, R. Human RISC Couples MicroRNA Biogenesis and Posttranscriptional Gene Silencing. *Cell* **123**, 631–640 (2005).
297. Hutvagner, G. & Simard, M. J. Argonaute proteins: key players in RNA silencing. *Nat Rev Mol Cell Biol* **9**, 22–32 (2008).
298. Chen, P. Y. *et al.* Strand-specific 5'-O-methylation of siRNA duplexes controls guide strand selection and targeting specificity. *RNA* **14**, 263–274 (2007).
299. Elbashir, S. M., Lendeckel, W. & Tuschl, T. RNA interference is mediated by 21- and 22-nucleotide RNAs. *Genes Dev* **15**, 188–200 (2001).
300. Khvorova, A., Reynolds, A. & Jayasena, S. D. Functional siRNAs and miRNAs exhibit strand bias. *Cell* **115**, 209–216 (2003).
301. Musacchio, T. & Torchilin, V. P. siRNA delivery: from basics to therapeutic applications. *Front Biosci (Landmark Ed)* **18**, 58–79 (2013).
302. Xia, H., Mao, Q., Paulson, H. L. & Davidson, B. L. siRNA-mediated gene silencing in vitro and in vivo. *Nat. Biotechnol.* **20**, 1006–1010 (2002).
303. Tiscornia, G., Singer, O. & Ikawa, M. A general method for gene knockdown in mice by using lentiviral vectors expressing small interfering RNA. *Proc. Natl. Acad. Sci. U.S.A.* **100**, 1844–1848 (2003).
304. Stewart, S. A. Lentivirus-delivered stable gene silencing by RNAi in primary cells. *RNA* **9**, 493–501 (2003).
305. Sui, G. *et al.* A DNA vector-based RNAi technology to suppress gene expression in mammalian cells. *Proc. Natl. Acad. Sci. U.S.A.* **99**, 5515–5520 (2002).
306. Brummelkamp, T. R. A System for Stable Expression of Short Interfering RNAs in Mammalian Cells. *Science* **296**, 550–553 (2002).
307. McCaffrey, A. P. *et al.* RNA interference in adult mice. *Nature* **418**, 38–39 (2002).

308. Song, E. *et al.* RNA interference targeting Fas protects mice from fulminant hepatitis. *Nat. Med.* **9**, 347–351 (2003).
309. Behlke, M. A. Progress Towards in Vivo Use of siRNAs. *Mol. Ther.* **13**, 644–670 (2006).
310. Braasch, D. A. *et al.* Biodistribution of phosphodiester and phosphorothioate siRNA. *Bioorg Med Chem* **14**, 1139–1143 (2004).
311. Bertrand, J.-R. *et al.* Comparison of antisense oligonucleotides and siRNAs in cell culture and in vivo. *Biochem Biophys Res Commun* **296**, 1000–1004 (2002).
312. Braasch, D. A. *et al.* RNA Interference in Mammalian Cells by Chemically-Modified RNA. *Biochemistry* **42**, 7967–7975 (2003).
313. Czauderna, F. Structural variations and stabilising modifications of synthetic siRNAs in mammalian cells. *Nucleic Acids Res* **31**, 2705–2716 (2003).
314. Layzer, J. M. In vivo activity of nuclease-resistant siRNAs. *RNA* **10**, 766–771 (2004).
315. Harborth, J. *et al.* Sequence, Chemical, and Structural Variation of Small Interfering RNAs and Short Hairpin RNAs and the Effect on Mammalian Gene Silencing. *Antisense Nucleic Acid Drug Dev* **13**, 83–105 (2004).
316. Rettig, G. R. & Behlke, M. A. Progress Toward In Vivo Use of siRNAs-II. *Mol. Ther.* **20**, 483–512 (2016).
317. Lorenz, C., Hadwiger, P., John, M., Vornlocher, H.-P. & Unverzagt, C. Steroid and lipid conjugates of siRNAs to enhance cellular uptake and gene silencing in liver cells. *Bioorg Med Chem* **14**, 4975–4977 (2004).
318. Soutschek, J., Akinc, A., Bramlage, B. & Charisse, K. Therapeutic silencing of an endogenous gene by systemic administration of modified siRNAs. *Nature* **432**, 173–178 (2004).
319. Wagner, E., Plank, C., Zatloukal, K., Cotten, M. & Birnstiel, M. L. Influenza virus hemagglutinin HA-2 N-terminal fusogenic peptides augment gene transfer by transferrin-polylysine-DNA complexes: toward a synthetic virus-like gene-transfer vehicle. *Proc. Natl. Acad. Sci. U.S.A.* **89**, 7934–7938 (1992).
320. Cotten, M., Wagner, E. & Zatloukal, K. High-efficiency receptor-mediated delivery of small and large (48 kilobase gene constructs) using the endosome-disruption activity of defective or chemically inactivated adenovirus particles. *Proc. Natl. Acad. Sci. U.S.A.* **89**, 6094–6098 (1992).
321. Wagner, E. Application of membrane-active peptides for nonviral gene delivery. *Adv Drug Deliv Rev* **38**, 279–289 (1999).
322. Muratovska, A. & Eccles, M. R. Conjugate for efficient delivery of short interfering RNA (siRNA) into mammalian cells. *FEBS Letters* **558**, 63–68 (2004).
323. Chiu, Y.-L., Ali, A., Chu, C.-Y., Cao, H. & Rana, T. M. Visualizing a Correlation between siRNA Localization, Cellular Uptake, and RNAi in Living Cells. *Chem. Biol.* **11**, 1165–1175 (2004).
324. McNamara, J. O. *et al.* Small Interfering RNAs Mediate Sequence-Independent Gene Suppression and Induce Immune Activation by Signaling through Toll-Like Receptor 3. *Nat. Biotechnol.* **172**, 1005–1015 (2004).
325. Zhou, J., Li, H., Li, S., Zaia, J. & Rossi, J. J. Novel Dual Inhibitory Function Aptamer–siRNA Delivery System for HIV-1 Therapy. *Mol. Ther.* **16**, 1481–1489 (2008).
326. Uno, Y. *et al.* High-Density Lipoprotein Facilitates In Vivo Delivery of  $\alpha$ -Tocopherol–Conjugated Short-Interfering RNA to the Brain. *Hum. Gene Ther.* **22**, 711–719 (2011).
327. Kumar, P. *et al.* Transvascular delivery of small interfering RNA to the central nervous system. *Nature* **448**, 39–43 (2007).
328. Felgner, P. L. *et al.* Lipofection: a highly efficient, lipid-mediated DNA-transfection procedure. *Proc. Natl. Acad. Sci. U.S.A.* **84**, 7413–7417 (2007).
329. Pires, P., Simões, S., Nir, S., Gaspar, R. & Düzgünes, N. Interaction of cationic liposomes and their DNA complexes with monocytic leukemia cells. *Biochim Biophys Acta* **1418**, 71–84 (1999).
330. Elouahabi, A. & Ruysschaert, J.-M. Formation and Intracellular Trafficking of Lipoplexes and Polyplexes. *Mol. Ther.* **11**, 336–347 (2005).
331. Allen, T. M. & Cullis, P. R. Liposomal drug delivery systems: From concept to clinical applications. *Adv Drug Deliv Rev* **65**, 36–48 (2013).
332. Jain, P. K. V. G. N. K., Gajbhiye, V. & Jain, N. K. Biomaterials. *Biomaterials* **33**, 7138–7150 (2012).
333. Balazs, D. A. & Godbey, W. T. Liposomes for Use in Gene Delivery. *J Drug Deliv* **2011**, 1–12 (2011).
334. Zimmermann, T. S. *et al.* RNAi-mediated gene silencing in non-human primates. *Nature* **441**, 111–114 (2006).
335. Akinc, A. *et al.* Targeted Delivery of RNAi Therapeutics With Endogenous and Exogenous Ligand-Based

- Mechanisms. *Mol Ther* **18**, 1357–1364 (2009).
336. Patil, S. D., Rhodes, D. G. & Burgess, D. J. Anionic liposomal delivery system for DNA transfection. *AAPS J* **6**, e29 (2004).
337. Bennett, M. J., Nantz, M. H., Balasubramaniam, R. P., Gruenert, D. C. & Malone, R. W. Cholesterol enhances cationic liposome-mediated DNA transfection of human respiratory epithelial cells. *Biosci. Rep.* **15**, 47–53 (1995).
338. Papahadjopoulos, D. *et al.* Sterically stabilized liposomes: improvements in pharmacokinetics and antitumor therapeutic efficacy. *Proc. Natl. Acad. Sci. U.S.A.* **88**, 11460–11464 (1991).
339. Koltover, I., Salditt, T., Rädler, J. O. & Safinya, C. R. An inverted hexagonal phase of cationic liposome-DNA complexes related to DNA release and delivery. *Science* **281**, 78–81 (1998).
340. Escriou, V., Ciolina, C., Helbling-Leclerc, A., Wils, P. & Scherman, D. Cationic lipid-mediated gene transfer: analysis of cellular uptake and nuclear import of plasmid DNA. *Cell Biol. Toxicol.* **14**, 95–104 (1998).
341. Zuhorn, I. S. *et al.* Nonbilayer Phase of Lipoplex–Membrane Mixture Determines Endosomal Escape of Genetic Cargo and Transfection Efficiency. *Mol. Ther.* **11**, 801–810 (2005).
342. Tousignant, J. D., Gates, A. L. & Ingram, L. A. Comprehensive analysis of the acute toxicities induced by systemic administration of cationic lipid: plasmid DNA complexes in mice. *Hum Gene Ther* **11**, 2493–2513 (2000).
343. Lappalainen, K., Jääskeläinen, I., Syrjänen, K., Urtili, A. & Syrjänen, S. Comparison of cell proliferation and toxicity assays using two cationic liposomes. *Pharm. Res.* **11**, 1127–1131 (1994).
344. Hornung, V. *et al.* Sequence-specific potent induction of IFN- $\alpha$  by short interfering RNA in plasmacytoid dendritic cells through TLR7. *Nat. Med.* **11**, 263–270 (2005).
345. Reynolds, A. Induction of the interferon response by siRNA is cell type- and duplex length-dependent. *RNA* **12**, 988–993 (2006).
346. Sørensen, D. R., Leirdal, M. & Sioud, M. Gene Silencing by Systemic Delivery of Synthetic siRNAs in Adult Mice. *J. Mol. Biol.* **327**, 761–766 (2003).
347. Landen, C. N. *et al.* Intraperitoneal delivery of liposomal siRNA for therapy of advanced ovarian cancer. *Cancer Biol Ther* **5**, 1708–1713 (2014).
348. Huang, Y.-H. *et al.* Claudin-3 gene silencing with siRNA suppresses ovarian tumor growth and metastasis. *Proc. Natl. Acad. Sci. U.S.A.* **106**, 3426–3430 (2009).
349. Aharinejad, S. *et al.* Colony-stimulating factor-1 blockade by antisense oligonucleotides and small interfering RNAs suppresses growth of human mammary tumor xenografts in mice. *Cancer Res* **64**, 5378–5384 (2004).
350. Leng, Q. & Mixson, A. J. Small interfering RNA targeting Raf-1 inhibits tumor growth in vitro and in vivo. *Cancer Gene Ther* **12**, 682–690 (2005).
351. Singhal, S. S., Awasthi, Y. C. & Awasthi, S. Regression of Melanoma in a Murine Model by RLIP76 Depletion. *Cancer Res* **66**, 2354–2360 (2006).
352. Jonson, A. L., Rogers, L. M., Ramakrishnan, S. & Downs, L. S., Jr. Gene silencing with siRNA targeting E6/E7 as a therapeutic intervention in a mouse model of cervical cancer. *Gynecol Oncol* **111**, 356–364 (2008).
353. DiFiglia, M., Sena-Esteves, M. & Chase, K. Therapeutic silencing of mutant huntingtin with siRNA attenuates striatal and cortical neuropathology and behavioral deficits. *Proc. Natl. Acad. Sci. U.S.A.* **104**, 17204–17209 (2007).
354. McCormack, A. L. *et al.*  $\alpha$ -Synuclein Suppression by Targeted Small Interfering RNA in the Primate Substantia Nigra. *PLoS ONE* **5**, e12122 (2010).
355. Senechal, Y., Kelly, P. H., Cryan, J. F., Natt, F. & Dev, K. K. Amyloid precursor protein knockdown by siRNA impairs spontaneous alternation in adult mice. *J Neurochem* **102**, 1928–1940 (2007).
356. Turchinovich, A., Zoidl, G. & Dermietzel, R. Non-viral siRNA delivery into the mouse retina in vivo. *BMC Ophthalmol* **10**, 25 (2010).
357. Reich, S. J. *et al.* Small interfering RNA (siRNA) targeting VEGF effectively inhibits ocular neovascularization in a mouse model. *Mol. Vis.* **9**, 210–216 (2003).
358. Murata, M. *et al.* Inhibition of Ocular Angiogenesis by Diced Small Interfering RNAs (siRNAs) Specific to Vascular Endothelial Growth Factor (VEGF). *Curr Eye Res* **31**, 171–180 (2009).
359. Jackson, A. L. *et al.* Expression profiling reveals off-target gene regulation by RNAi. *Nat. Biotechnol.* **21**, 635–637 (2003).
360. Birmingham, A. *et al.* 3' UTR seed matches, but not overall identity, are associated with RNAi off-targets.

- Nat Meth* **3**, 199–204 (2006).
361. Jackson, A. L. Widespread siRNA ‘off-target’ transcript silencing mediated by seed region sequence complementarity. *RNA* **12**, 1179–1187 (2006).
362. Heidel, J. D., Hu, S., Liu, X. F., Triche, T. J. & Davis, M. E. Lack of interferon response in animals to naked siRNAs. *Nat. Biotechnol.* **22**, 1579–1582 (2004).
363. Morrissey, D. V. *et al.* Sequence-dependent stimulation of the mammalian innate immune response by synthetic siRNA. *Pharm. Res.* **22**, 1002–1007 (2005).
364. Abbott, N. J. Blood–brain barrier structure and function and the challenges for CNS drug delivery. *J Inherit Metab Dis* **36**, 437–449 (2013).
365. Georgieva, J., Hoekstra, D. & Zuhorn, I. Smuggling Drugs into the Brain: An Overview of Ligands Targeting Transcytosis for Drug Delivery across the Blood–Brain Barrier. *Pharmaceutics* **6**, 557–583 (2014).
366. Banks, W. A. Characteristics of compounds that cross the blood-brain barrier. *BMC Neurol* **9**, S3 (2009).
367. Banks, W. A. *et al.* Delivery across the blood-brain barrier of antisense directed against amyloid beta: reversal of learning and memory deficits in mice overexpressing amyloid precursor protein. *J. Pharmacol. Exp. Ther.* **297**, 1113–1121 (2001).
368. Pang, Z. *et al.* Preparation and brain delivery property of biodegradable polymersomes conjugated with OX26. *J Control Release* **128**, 120–127 (2008).
369. Boado, R. J., Hui, E. K.-W., Lu, J. Z., Zhou, Q.-H. & Pardridge, W. M. Journal of Biotechnology. *Journal of Biotechnol* **146**, 84–91 (2010).
370. Coen, L., Osta, R., Maury, M. & Brûlet, P. Construction of hybrid proteins that migrate retrogradely and transynaptically into the central nervous system. *Proc. Natl. Acad. Sci. U.S.A.* **94**, 9400–9405 (1997).
371. Gaillard, P. J., Brink, A. & de Boer, A. G. Diphtheria toxin receptor-targeted brain drug delivery. *Int Congr Ser* **1277**, 185–198 (2005).
372. Jain, K. K. Nanobiotechnology-based strategies for crossing the blood-brain barrier. *Nanomedicine* **7**, 1225–1233 (2012).

## Chapter 2:

### Delivery of therapeutic siRNA to the CNS using cationic and anionic liposomes<sup>1</sup>

#### Summary

The primary therapeutic challenge for any neurodegenerative disease, including prion diseases, remains delivery across the blood-brain barrier to neuronal cells. Here we generate three different delivery vehicles to the central nervous system: liposome-siRNA-peptide complexes (LSPCs) and peptide-addressed liposome-encapsulated therapeutic siRNA (PALETS) (two types). With these delivery vehicles, we can package small interfering RNA (siRNA) on the outside of the liposome or encapsulate it within the liposome. We utilize a small peptide, RVG-9r, from the rabies virus glycoprotein, to target these delivery vehicles to nicotinic acetylcholine receptors within the central nervous system. We show that the use of protamine sulfate increases the encapsulation rate of siRNA within anionic liposomes. We also show that LSPCs and PALETS protect the siRNA in the bloodstream long enough to cross the blood-brain barrier and deliver siRNA to neuronal cells resulting in a decrease of PrP<sup>C</sup>. These delivery vehicles represent a new tool for the delivery of siRNA and any small molecule drug to the central nervous system.

#### Introduction

RNA interference (RNAi) is a potential gene therapy that is capable of regulating the expression of any gene through mRNA cleavage<sup>2,3</sup>. RNAi employs the use of small interfering RNA (siRNA) to activate the RNA-induced silencing complex (RISC), which uses the Ago2 endonuclease to cleave mRNA<sup>4-7</sup>. Cleavage of mRNA is dependent on homology with the 21-23 base pair siRNA<sup>8,9</sup>. After mRNA cleavage, exo- and endonucleases degrade the mRNA, which results in a reduction of protein levels. Although siRNA has been investigated as a therapeutic for multiple diseases, complications related to its usage in animal and human models have stalled its use in therapeutic strategies<sup>10-12</sup>.

---

<sup>1</sup> <sup>1</sup> Bender, H. R., Kane, S. & Zabel, M. D. Delivery of Therapeutic siRNA to the CNS Using Cationic and Anionic Liposomes. *Journal of Visualized Experiments* e54106 (2016).

One of the difficulties of utilizing RNAi in mammalian models is nuclease sensitivity. Naked siRNA has a short half-life in circulation due to serum nucleases. RISC loading requires siRNA to have a thermodynamically unstable end, which is extremely attractive to exonucleases. Naked siRNA is also cleared from the bloodstream rapidly by the liver and kidneys, resulting in a short half-life. The half-life of siRNA can be increased by using chemical modifications that provide nuclease stability. Modifications include 2'-O-methyl and 2'-fluoro modifications on the ribose sugar, and phosphorothioate on the 3' terminal end or a methylene bridge (locked nucleic acids, LNAs) on either the 3' or 5' termini. However, these modifications can decrease the potency of the siRNA and increase the synthesizing expense<sup>13-17</sup>. Another option to achieve nuclease stability of siRNA is to link the siRNA molecules to delivery vehicles, such as liposomes.

Liposomes have been widely used as delivery vehicles for gene therapy products in *in vitro* assays. They are also being investigated for use in animal and human models as delivery vehicles for siRNA as liposomes protect against serum nucleases and can be targeted towards specific cell types. Liposomes deliver siRNA directly into cells either through fusion to the plasma membrane or through endocytosis<sup>18-20</sup>. Liposomes with cationic lipids are the most commonly utilized liposome as the negatively-charged phosphate backbone electrostatically interacts with the positively-charged lipid. Cationic liposomes also readily interact with the anionic head groups of cell membranes<sup>10,21,22</sup>. Anionic liposomes are not commonly used, as the anionic lipid is thought to be incapable of passing the plasma membrane. Still, anionic liposomes are less immunogenic than cationic liposomes as they bind to fewer of the negatively-charged serum proteins. A limitation of anionic lipids is that the negative charge of the lipids repels the negative charge of the siRNA backbone. However, there have been reports that anionic liposomes can efficiently package and deliver DNA by using cations to condense the DNA and shield its negative charge<sup>23-28</sup>. The mononuclear phagocyte system (MPS) of the liver and spleen clears liposomes from the bloodstream but circulation times of liposomes can be increased using PEGylated lipid groups within the liposome. These groups make the liposomes invisible to serum proteins, which reduces uptake of the liposomes by cells of the MPS<sup>29</sup>. Liposomes can also be targeted to specific cell types using peptides that either electrostatically interact with or are covalently bound to the liposomes<sup>30-33</sup>. Thus, siRNA is protected from nucleases and can be targeted to specific cells or tissues to reduce off-target effects.

Prion diseases are neurodegenerative diseases caused by the misfolding of a cellular protein called PrP<sup>C34-</sup><sup>37</sup>. The conversion of PrP<sup>C</sup> to the misfolded isomer, PrP<sup>Res</sup>, results in synaptic loss, activation of astrocytes, and

vacuolation<sup>38</sup>. Currently, no known therapeutics alleviate clinical signs of prion disease in mammalian models. Decreasing or eliminating the substrate for conversion, PrP<sup>C</sup>, is an attractive therapeutic option because it may delay or abrogate the disease. Consequences of PrP<sup>C</sup> knockdown are thought to be minimal as PrP-null mice show no abnormalities throughout their lifetimes. Several research groups investigated the role of PrP<sup>C</sup> expression levels in prion disease by creating transgenic mice with reduced levels of PrP<sup>C</sup> or by injecting lentiviral vectors expressing short hairpin RNA directly into the brains of mice. These researchers found that by reducing the amount of neuronal PrP<sup>C</sup>, the life of infected animals could be extended and the neuropathology of prion diseases reversed<sup>39-42</sup>. We have previously reported that prion replication can be ameliorated in mouse neuroblastoma cells using PrP<sup>C</sup> siRNA<sup>43</sup>. These studies suggest that the use of RNAi therapeutics, such as siRNA, to decrease PrP<sup>C</sup> expression levels, may sufficiently delay the progression of prion diseases. However, for a RNAi therapeutic to be useful in the clinical setting, it needs to be coupled to a systemic delivery system.

Here we propose to use PrP<sup>C</sup> siRNA, which is packaged into cationic and anionic liposomes, as a potential therapeutic for prion diseases. Liposome-siRNA-peptide complexes (LSPCs) are composed of liposomes with siRNA and a targeting peptide (RVG-9r) electrostatically coating the outer surface of the liposome. Peptide-addressed liposome-encapsulated therapeutic siRNA (PALETS) are composed of siRNA encapsulated within the liposome, and RVG-9r linked to lipid PEG groups on the outside of the liposome. RVG-9r is a small modified peptide from the rabies virus glycoprotein that targets nicotinic acetylcholine receptors in the central nervous system (CNS). This peptide allows the liposome complexes to be targeted directly to the CNS to reduce siRNA off-target effects. For anionic PALETS, we also use the cation protamine sulfate to condense the siRNA so that it becomes encapsulated within the anionic liposomes. We show that LSPCs decrease surface PrP<sup>C</sup> 40-50% in neuronal cells, and that, although producing minimal effects, PALETS can cross the blood-brain barrier to deliver siRNA to the CNS.

## **Materials and Methods**

### ***Mice***

FVB mice were purchased from The Jackson Laboratory (Bar Harbor, ME). Mice were euthanized using CO<sub>2</sub>. All mice were bred and maintained at Lab Animal Resources, accredited by the Association for Assessment

and Accreditation of Lab Animal Care International, in accordance with protocols approved by the Institutional Animal Care and Use Committee at Colorado State University.

### ***Generation of Liposomes***

#### *DOTAP LSPCs*

DOTAP LSPCs consist of a 1:1 DOTAP:cholesterol ratio in a 1:1 chloroform:methanol solution. Both lipids were purchased from Avanti Lipids (DOTAP - 1,2-dioleoyl-3-trimethylammonium-propane [chloride salt]). The solvents were evaporated using N<sub>2</sub> gas and the resultant dry lipid film was placed under vacuum for a total of 8 hours to remove any excess solvent. A stock solution of liposomes was made at an 8 mM (40 umole total lipid) concentration by resuspending the lipid film in 5 mL of 10% sucrose heated at 55°C. All components (lipid film and sucrose) were kept at this temperature during rehydration. The heated sucrose was added to the lipid cake 1 mL every 10 minutes. The lipid film was swirled every 3 minutes to promote lipid mixing. Resulting liposomes were stored at 4°C.

#### *DOTAP PALETS*

DOTAP PALETS consist of a 55:40:5 DOTAP:cholesterol:DSPE-PEG ratio in a 1:1 chloroform:methanol solution. All lipids were purchased from Avanti Lipids. The solvents were evaporated using N<sub>2</sub> gas and the resultant dry lipid film was placed under vacuum for a total of 8 hours to remove any excess solvent. A stock solution of liposomes was made at an 8 mM (40 umole total lipid) concentration by resuspending the lipid film in 5 mL of 10% sucrose heated at 65°C. All components (lipid film and sucrose) were kept at this temperature during rehydration. The heated sucrose was added to the lipid cake 1 mL every 10 minutes. The lipid film was swirled every 3 minutes to promote lipid mixing. Resulting liposomes were stored at 4°C.

#### *DSPE PALETS*

DSPE PALETS consist of a 55:40:5 DSPE:cholesterol:DSPE-PEG ratio in a 1:1 chloroform:methanol solution. All lipids were purchased from Avanti Lipids (DSPE - 1,2-distearoyl-sn-glycero-3-phosphoethanolamine). The solvents were evaporated using N<sub>2</sub> gas and the resultant dry lipid film was placed under vacuum for a total of 8 hours to remove any excess solvent. A stock solution of liposomes was made at an 8 mM (40 umole total lipid) concentration by resuspending the lipid film in 5 mL of 1X PBS heated at 70-75°C. All components (lipid film and 1X PBS) were kept at this temperature during rehydration. The heated PBS was added to the lipid cake 1 mL every

10 minutes. The lipid film was swirled every 3 minutes to promote lipid mixing. Resulting liposomes were stored at 4°C.

### ***Generating LSPCs or PALETS***

PrP<sup>C</sup> 1672 siRNA sequence: ACATAAACTGCGATAGCTTC (Qiagen).

RVG-9r peptide: YTIWMPENPRPGTPCDIFTNSRGKRASNGGGGrrrrrrrrr (ChemPeptide)

#### *DOTAP LSPCs*

The DOTAP LSPCs liposomes were diluted 1:100 in 1X PBS and sonicated 4X with 2-3 minute rests in between. 50 uL (4 nmole total) of diluted/sonicated liposomes was mixed with 100 uL (4 nmole total) of 1672 siRNA. The siRNA/liposome solution incubated for 10 minutes at 4°C. Then, 80uL (40 nmole total) of RVG-9r peptide was added to the solution and allowed to incubate for 10 minutes on ice.

#### *DOTAP PALETS*

The DOTAP PALETS liposomes were diluted 1:100 in 1X PBS. Single use aliquots were generated by lyophilizing 50 uL of the 1:100 liposome dilution (4 nmole total) for 15 minutes. The lipid cake was then resuspended using 100 uL (4 nmole total) of 1672 siRNA. The solution is incubated for 5 minutes, which encapsulates the siRNA. A carbodiimide reaction was used to covalently bond the RVG-9r to the COOH-terminus of the DSPE-PEG lipids. 10 µL of a 60 mM 1-ethyl-3-(3-dimethylaminopropyl)carbodiimide hydrochloride (EDC) solution and 10 µL of a 150 mM N-hydroxysulfosuccinimide (sulfo-NHS) was added to the liposome/siRNA solution. The solution incubated for 10 minutes at room temperature. 80 uL (40 nmole total) of RVG-9r was added to the solution and allowed to incubate for 2 hours at room temperature.

#### *DSPE PALETS*

The DSPE PALETS liposomes were diluted 1:100 in 1X PBS. Single use aliquots were generated by lyophilizing 50 uL of the 1:100 liposome dilution (4 nmole total) for 15 minutes. 1.4 uL of a 26.6 uM solution of protamine sulfate (Sigma Aldrich) was incubated with 100 uL of a 40 uM stock solution of the 1672 siRNA for 10 minutes at room temperature. The lipid cake was then resuspended using 100 uL (4 nmole total) of the 1672 siRNA/protamine solution and incubated for 10 minutes at 4°C to encapsulate the siRNA within the liposomes. Then, 80 uL (40 nmole total) of RVG-9r peptide was added to the solution and allowed to incubate for 10 minutes on ice.

### ***Treating Mice with LSPCs or PALETS***

Mice were placed under a heat lamp for 5 minutes and anesthetized with 1.5-2% isoflurane (VetOne). The mouse tails were disinfected using 70% EtOH. LSPCs or PALETS were injected into the tail veins of mice using a 29-gauge insulin syringe.

### ***Measuring Encapsulation Efficiency***

The encapsulation efficiency of the siRNA within DSPE PALETS using the cation protamine sulfate was determined by separating encapsulated from unencapsulated siRNA. The 1672 siRNA was encapsulated with the help of protamine within the DSPE PALETS using the above protocol to assemble DSPE PALETS. After encapsulation, the liposome/siRNA complex was incubated for 10 minutes on ice. The encapsulated siRNA was separated from the unencapsulated siRNA by its retention on a 50 kDa centrifugal filter. The concentration of siRNA was measured using a spectrophotometer (Nanodrop, ThermoFisher) at 260 nm.

### ***Flow Cytometry***

Mice treated with either LSPCs or PALETS were euthanized 4 days after treatment for protein analysis via flow cytometry. Half a hemisphere of brain and one kidney from each mouse was pressed through a 40  $\mu$ m cell strainer (Falcon, VWR) using the plunger from a 5 mL syringe and 5 mL of FACS buffer (1X PBS, 1% fetal bovine serum, 10 mM EDTA). The cell suspension was transferred to a 15 mL conical, of which 450  $\mu$ L of each cell suspension was used for flow cytometric analysis. Cells were washed 3X by centrifugation at 2000 rpm (250 x g) and resuspension of the cells with 1 mL of FACS buffer. Fc receptors were blocked using 100  $\mu$ L of a 1:100 dilution of a 0.5 mg/mL rat anti-mouse CD16/CD32 Fc block (BD Pharmingen) in FACS buffer with 7% goat serum for 20 minutes on ice. The cell pellet was washed once as above. The cells were stained with 100  $\mu$ L of a 1:100 dilution of a 20  $\mu$ g/mL solution of the PrP<sup>C</sup> antibody BAR-224 conjugated to Dylight 650 (per manufacturer's instructions) in FACS buffer for 40 minutes at room temperature. Red blood cells were lysed with 1 mL of RBC lysis buffer (1X PBS, 155 mM NH<sub>4</sub>Cl, 12 mM NaHCO<sub>3</sub>, 0.1 mM EDTA) for 3 minutes and then centrifuged at 2000 rpm for 3 minutes. Cells were washed 2X with 1 mL of FACS buffer. Cells were stained with propidium iodide (FisherSci) 10-15 minutes before analyzing a 1:2 dilution of the cells on a DakoCytomation Cyan ADP flow cytometer. Results were evaluated using FlowJo version 10.

### ***In vivo Live Imaging***

LSPCs were assembled as described above. siRNA labeled on the 5' end with Alexa Fluor 488 (Qiagen) and RVG-9r labeled with Dylight 650 (per manufacturer's instructions) (ThermoFisher) were used. Mice were anesthetized with 2% isoflurane, injected intravascularly with LSPCs, and then immediately imaged for up to one hour after treatment using an IVIS Spectrum *in vivo* live imaging system. Autoexposure settings were used. siRNA signal was viewed on 500/540 nm filter and RVG-9r signal was viewed on 640/680 nm filter.

### ***Digital Droplet PCR (ddPCR)***

RNA was extracted from the cell suspensions using a RNeasy minikit (Qiagen). DNase digestion was performed off-column using RQ1 RNase-free DNase (Promega) per manufacturer's instructions. The RNA was purified from the DNase using EtOH precipitation. A 1:10 volume of 2 M NaAcetate and 2.5X volume of 100% EtOH was added to the RNA after DNase digestion. The RNA was stored at -20°C for at least 24 hours. The samples were then centrifuged at 13,000 rpm (16,060 x g) for 45 minutes. The RNA pellet was washed with 200 uL of 100% EtOH and centrifuged again at the same conditions. The RNA pellet was allowed to dry for 1 hour and was resuspended in 40 uL of molecular grade H<sub>2</sub>O. RNA concentration was assessed via spectrophotometer (Denovix) at 260 nm. Approximately 150 ng of RNA was used to generate cDNA using the High Capacity cDNA Reverse Transcription kit from ThermoFisher. A final concentration of 0.035 ng of cDNA was used for ddPCR reactions. A final concentration of 1.25 uM of the following PrP primers was used in the final ddPCR reaction: forward primer 5'-CCTTGGTGGCTACATGCTGG-3' and reverse primer 5'-GGCCTGTAGTACACTTGG-3'. A final concentration of 125 nM of the following actin primers was used in the final ddPCR reaction: forward primer 5'-GACCTGACAGACTACCTCAT-3' and reverse primer 5'-AGACAGCACTGTGTTGGCAT-3'. The cDNA/primer solution was mixed with 10 uL of Supermix (BioRad) to generate a final reaction volume of 20 uL. Droplets were generated by combining the reaction mix with 60 uL of droplet generator oil (BioRad) using a QX-100 droplet generator. The droplets were then transferred to a 96-well plate and sealed with pierceable sealing foil sheets (BioRad). The PCR amplification was performed using a C1000 Touch Thermal Cycler (BioRad) with the following cycling parameters: enzyme activation at 95°C for 5 minutes, denaturation at 95°C for 30 seconds, annealing/elongation at 57°C for 1 minute for 40 cycles, signal stabilization at 4°C for 5 minutes and 95°C for 5 minutes, and hold at 4°C. Following amplification, the droplets were transferred to a QX100 droplet reader and analyzed using QuantaSoft (BioRad) software. PrP<sup>C</sup> was normalized to actin. Fold change was determined by

dividing the treated sample by the untreated control (set as 1) and by the mRNA upregulation seen in control experiments that is caused by the LSPC treatment.

### *Statistical Analysis*

Statistical analysis was performed using a combination of Excel and GraphPad Prism. All error bars represent standard error of the mean (SEM) to show how closely the data resembles the population mean

## **Results**

The experimental setup is shown in Figure 2.1. The thin lipid film hydration method was used to generate the liposomes as described (Figure 2.2). Figure 2.3 shows an artistic rendition of the differences between LSPCs and PALETS. For LSPCs, the siRNA is bound to the outside of the liposome with RVG-9r. For PALETS, the siRNA is encapsulated within the liposome, with RVG-9r attached to the outside either through a covalent modification or electrostatic interaction. Protamine is utilized in DSPE PALETS to condense the siRNA and give it an overall positive charge so it can be encapsulated within the liposome.

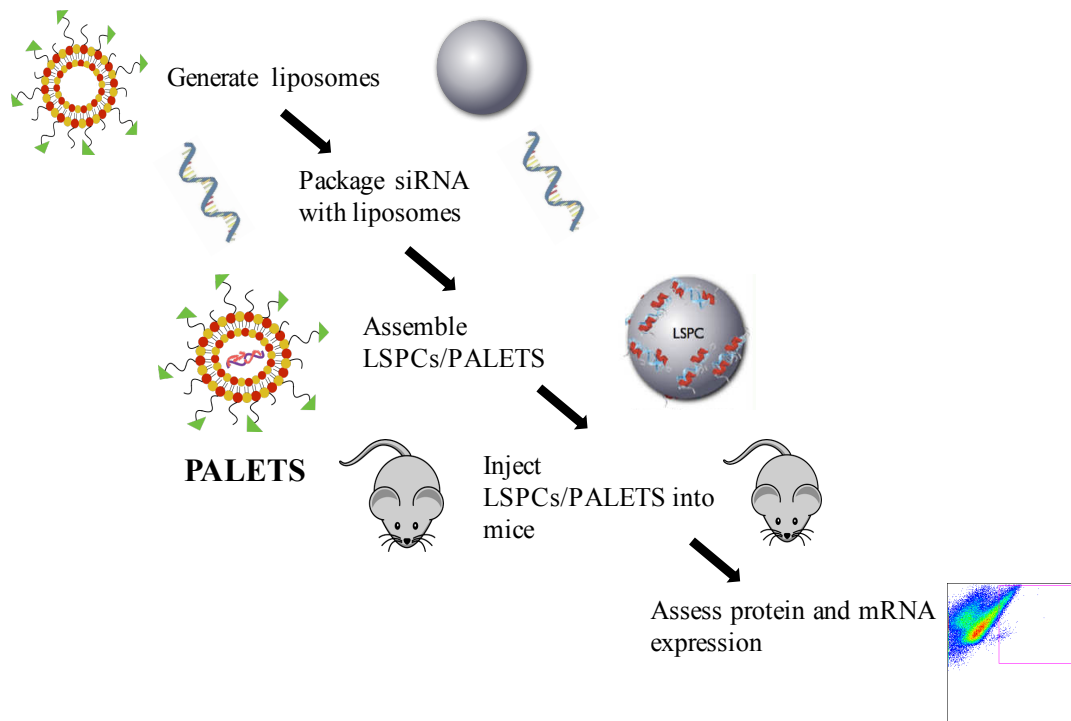


**Figure 2.1. Experimental setup of LSPCs and PALETS experiments.**

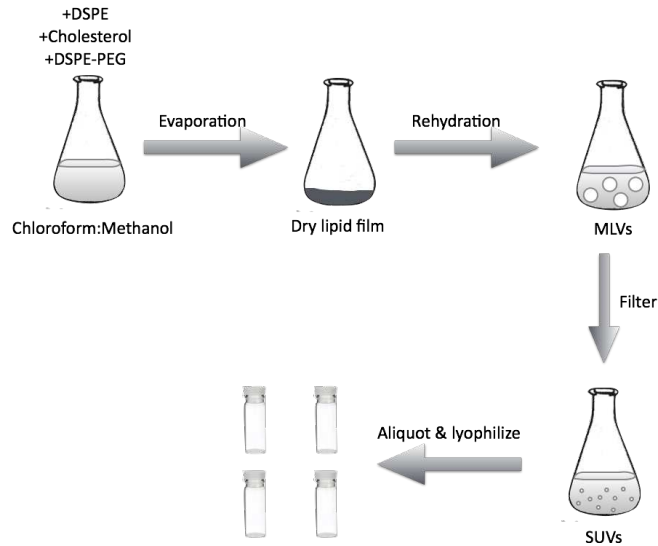


**Figure 2.3. Protocol of the thin lipid film hydration method.**

Solvents are used to thoroughly mix the lipids. The solution is then dried into a thin lipid cake using  $N_2$  gas. The resultant thin lipid film is rehydrated using either 10% sucrose or 1X PBS depending on the lipid composition of the liposomes.

### LSPCs



### PALETS

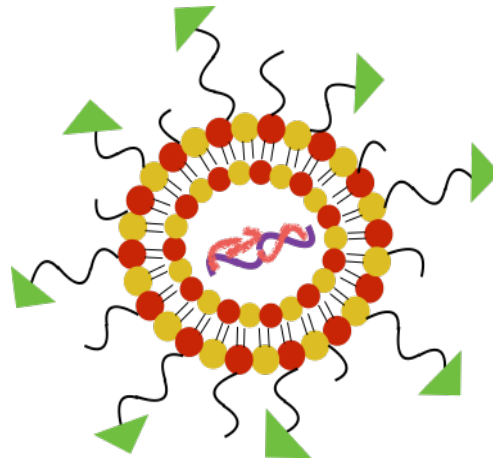


**Figure 2.2. Schematic representation of LSPCs and PALETS.**

For LSPCs, PrP<sup>C</sup> siRNA electrostatically interacts with the cationic liposome. The RVG-9r also electrostatically interacts with the PrP<sup>C</sup> siRNA due to the nine arginine residues. For PALETS (both formulations), the PrP<sup>C</sup> siRNA is encapsulated in the liposome. DSPE PALETS utilize protamine sulfate to aid in siRNA encapsulation. PALETS also contain PEGylated lipids to increase circulation time and to allow the covalent modification of the RVG-9r.

### ***Protamine sulfate efficiently encapsulates siRNA within DSPE PALETS***

The siRNA was mixed with varying concentrations of protamine, 0.7:1 to 2:1 protamine:siRNA molar ratio, to determine the optimal protamine concentration for siRNA encapsulation within DSPE PALETS. PALETS were formed as described in the methods section. The concentration of siRNA was measured before and after DSPE PALETS formation. Molar ratios 1.5:1 (29.26 nM protamine concentration) and above resulted in precipitation of protamine:siRNA complexes, which could not be encapsulated in the anionic liposomes (Figure 2.4A). Protamine:siRNA molar ratios from 0.7:1 to 1.3:1 (13.3 nM to 26.6 nM protamine concentration) encapsulated 80-90% of the siRNA. There was a 60-65% encapsulation efficiency of siRNA in DSPE PALETS without the use of protamine (Figure 2.4A and C). A protamine concentration of 18.6 nM (0.9:1 protamine:siRNA ratio) was chosen to be used throughout the rest of the experiments as it is the mean concentration that gives an 80-90% encapsulation efficiency of siRNA (Figure 2.4C).

Similarly, the concentration of the siRNA was measured during each step of PALETS formation to assess the effect of protamine on siRNA concentration and the amount of siRNA that became encapsulated. After the addition of protamine to the siRNA there is a decrease in the concentration of the siRNA; however, the level remains stable afterward (Figure 2.4B). PALETS were then filtered through 50 kDa centrifugal filters. Any encapsulated siRNA is found within the retentate with the liposome complexes, while any unencapsulated siRNA is located in the filtrate. After filtering, 90-95% of the siRNA is associated with the liposome retentate, while 5-10% of the siRNA is 'free' in the filtrate (Figure 2.4B). No siRNA is detected in protamine or liposome only samples (Figure 2.4C).

### ***Neuronal PrP<sup>C</sup> is decreased in mice treated with LSPCs***

To assess the efficacy of LSPCs, one FVB mouse was injected with 1X PBS (untreated control) and three mice were injected with LSPCs. Four days after treatment, mice were euthanized, and brain and kidney samples were removed for protein and mRNA analysis. Protein analysis was determined via flow cytometry using BAR-224 conjugated to Dylight 650. All treated mice are compared to untreated controls for statistical analysis. Treatment with LSPCs resulted in a significant decrease in neuronal PrP<sup>C</sup>. The amount of PrP<sup>C</sup> positive cells stayed the same, but cell surface PrP<sup>C</sup> dropped 40-50% (Figure 2.5A and 2.6A and B). Results in the kidney suggest there is substantial binding of RVG-9r to kidney nicotinic acetylcholine receptors. Cell surface PrP<sup>C</sup> and the number of PrP<sup>C</sup> positive cells are decreased in the kidney, although not statistically significant (Figure 2.5B and 2.6 C and D). Live

animal imaging was performed to determine the biodistribution of the siRNA and the peptide. Again, one mouse was injected with PBS (untreated control) and four mice were injected with LSPCs containing siRNA labeled with Alexa 488. Mice were imaged over a one-hour period after injection. Flow cytometric analysis was performed on both the brain and kidneys of all mice to determine the number of cells with siRNA. This experiment was repeated three times. In half of all mice treated across the three experiments, one hour after injection the PrP<sup>C</sup> siRNA is concentrated in the brain (data not shown), but in the other half of treated mice, the siRNA and peptide are pooled

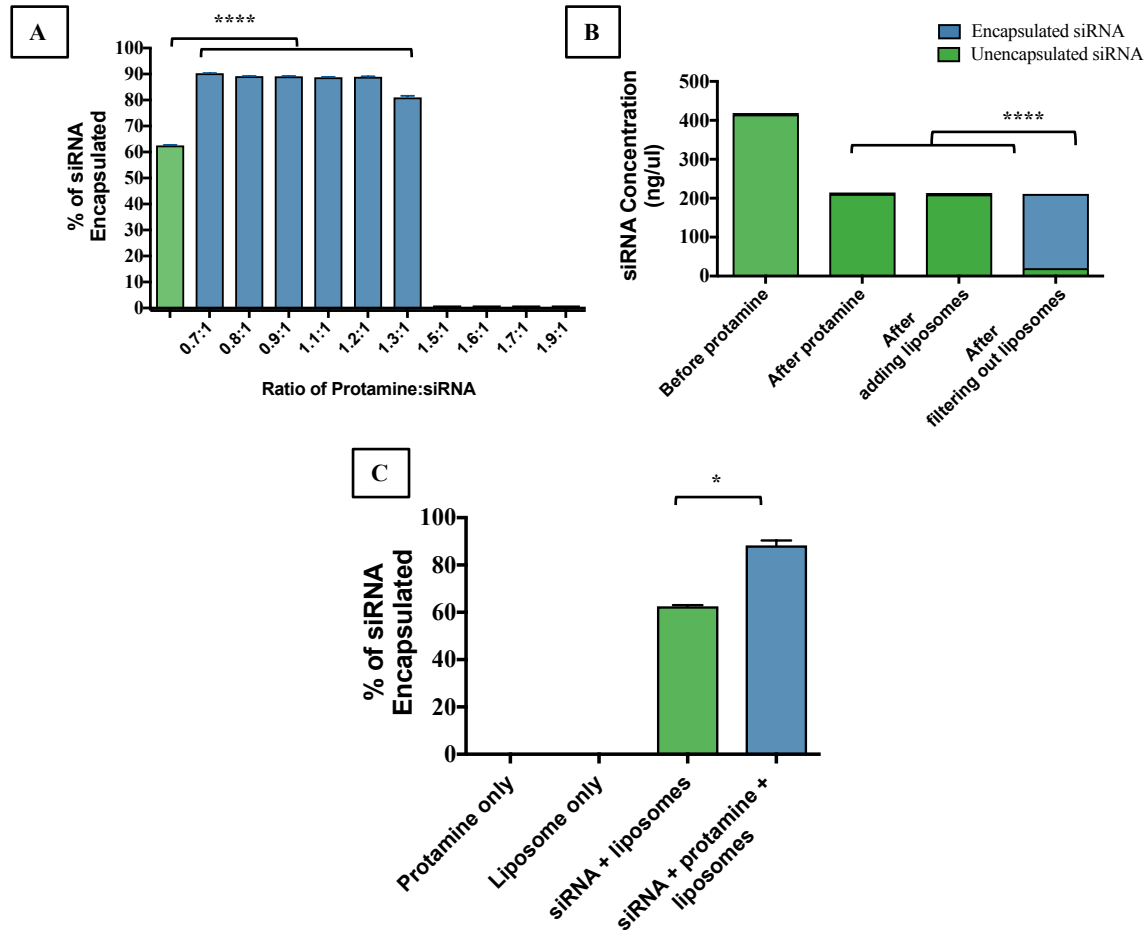


**Figure 2.4. Encapsulation of siRNA within DSPE PALETS using the cation protamine sulfate.**

A) After assembly of DSPE PALETS, protamine:siRNA ratios of 0.7:1 to 1.3:1 resulted in 80-90% encapsulation of the siRNA within DSPE PALETS. B) siRNA concentration was measured at all steps during DSPE PALETS assembly. There was a slight decrease in siRNA concentration after the addition to protamine, possibly due to masking of the siRNA. After separating free siRNA from siRNA associated with liposomes with a 50 kDa filter, 90-95% of the siRNA was associated with the liposomes while 5-10% was free siRNA in the filtrate. C) Protamine and liposome only controls do not contain any measurable amounts of RNA. 60-65% of the siRNA is encapsulated without the use of protamine and 80-90% of the siRNA is encapsulated within DSPE PALETS with protamine. Error bars indicate standard error of the mean (SEM). \* $p < 0.05$  and \*\*\* $p < 0.001$  One-way ANOVA with multiple comparisons and two-way ANOVA.

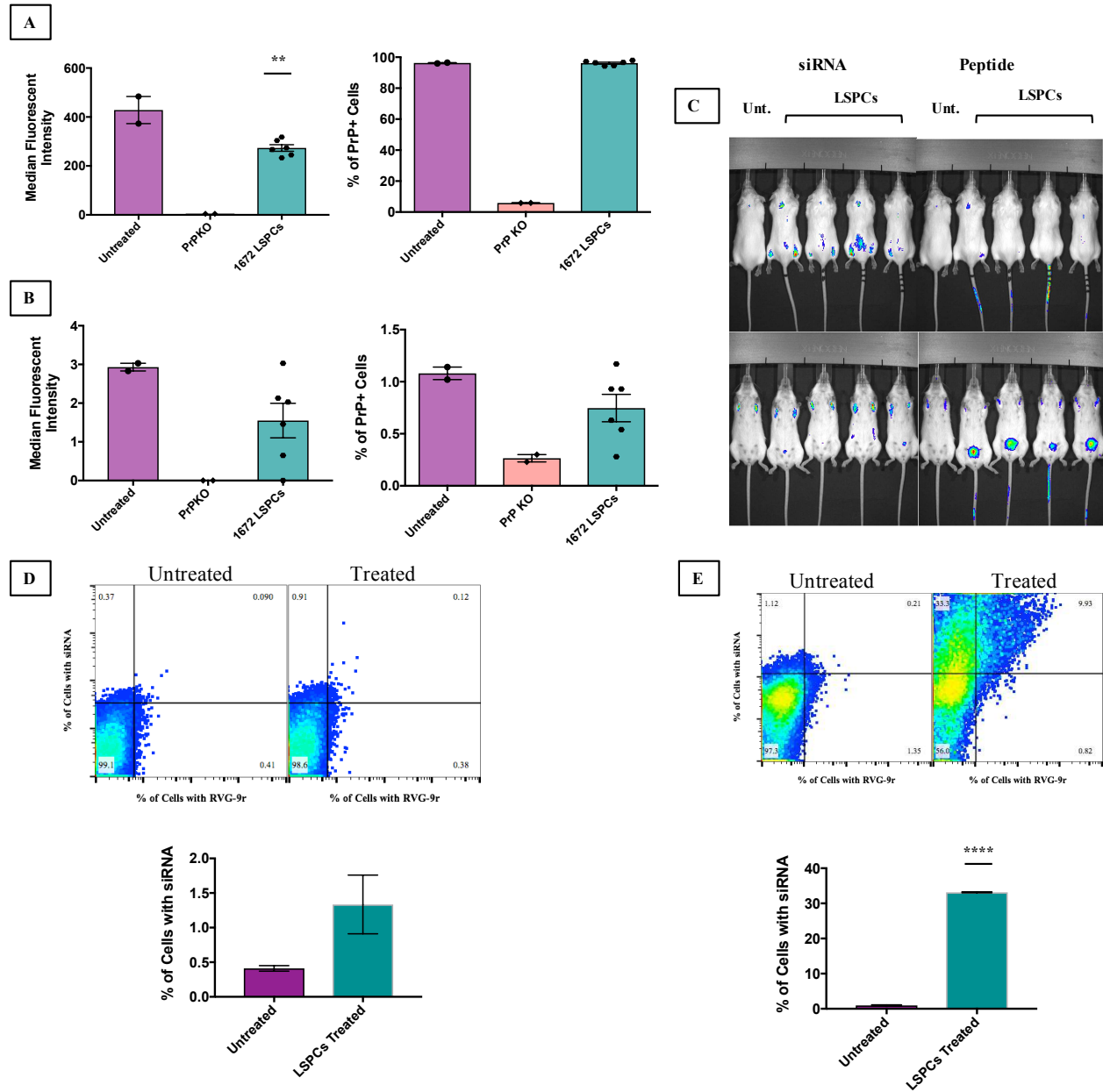


**Figure 2.5. Protein analysis and biodistribution of LSPCs treatment in vivo.**

A) Median fluorescent intensity (MFI) of PrP<sup>C</sup> is decreased 40-50% in the brains of all three LSPCs-treated mice four days after treatment during one experiment. The amount of neuronal PrP<sup>C</sup>+ cells remains unchanged at this time point B) PrP<sup>C</sup> MFI and amount of PrP<sup>C</sup>+ cells are slightly decreased in the kidney four days after LSPCs treatment, although not statistically significant. C) The four day LSPCs treatment was repeated three times. In a subset of the treated animals in those three repeated experiments, *In vivo* live imaging one hour after LSPCs treatment revealed a substantial portion of peptide around the bladder. D) Flow cytometric analysis of the brains of the treated mice in panel C showed very little siRNA in neuronal cells compared to the untreated control. E) Flow cytometric analysis of the kidneys of the mice shown in panel C revealed a large portion of the siRNA within the kidneys. Error bars indicate SEM. \*\* p<0.01 \*\*\*\* p<0.0001. t test.

within the area of the bladder with minimal amounts present in the brain (Figure 2.5C, D and E). PrP<sup>C</sup> mRNA levels in the brains of mice treated with DOTAP LSPCs were not statistically different than the untreated mouse (Figure 2.7A). However, mice treated with DOTAP LSPCs have a significant decrease in PrP<sup>C</sup> mRNA levels in the kidney (Figure 2.7B)

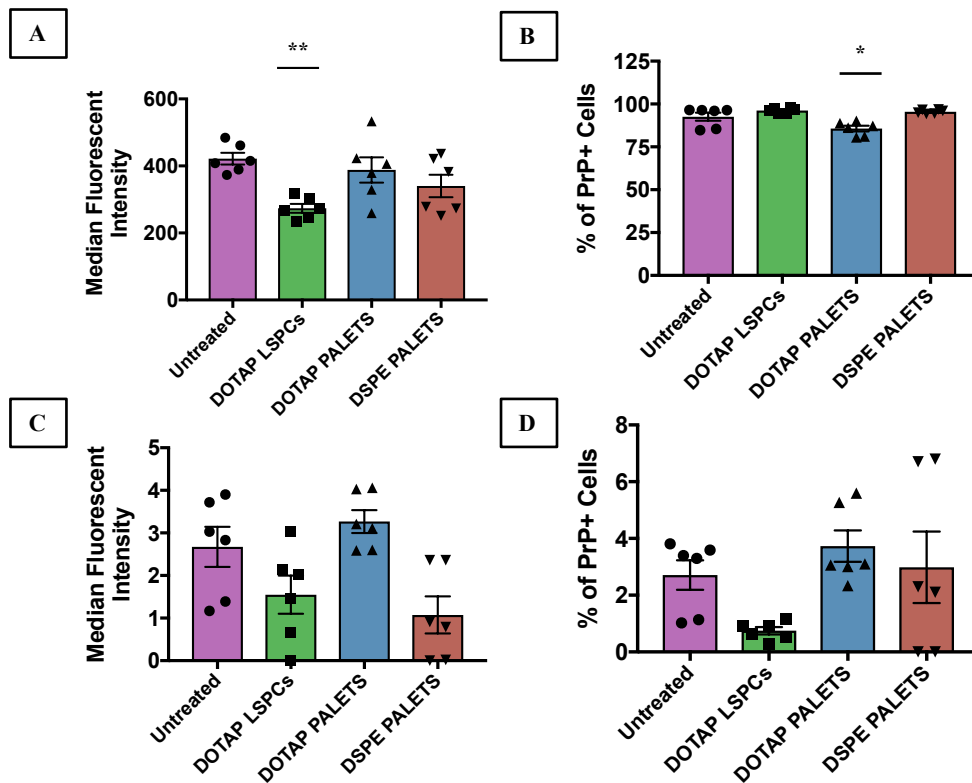


**Figure 2.6. Comparison of PrP<sup>C</sup> protein levels between LSPCs and PALETS treated mice.**

Three mice were used as untreated controls and injected with 1X PBS. Each treatment group has a total of three treated mice injected with one of the three liposomal PrP<sup>C</sup> siRNA formulations. The brains and kidneys of all mice were harvested four days after treatment and flow cytometry was performed to assess PrP<sup>C</sup> protein levels. A) Surface PrP<sup>C</sup> is decreased 40-50% in the brains of mice treated with DOTAP LSPCs. Grouped together there is no statistical difference of either of the PALETS formulations compared to untreated control but at least one mouse in each of the PALETS formulations had decreases in surface PrP<sup>C</sup>. B) Neither the DOTAP LSPCs or the DSPE PALETS resulted in a decrease of PrP<sup>C</sup> positive cells but the DOTAP PALETS did result in a slight decrease. C. Surface PrP<sup>C</sup> is decreased in mice treated with DOTAP LSPCs and DSPE PALETS, although it's not statistically significant. D) No statistical difference is seen in the number of PrP<sup>C</sup>+ cells in the treated mice compared to the untreated mice but mice treated with DOTAP LSPCs do have a decrease in PrP<sup>C</sup>+ cells. Error bars represent SEM. \*p<0.05 \*\*p<0.01. One-way ANOVA with Dunnet's multiple comparisons.

### ***PALETS delivers PrP<sup>C</sup> siRNA to the brain***

PALETS and LSPCs were assembled as described and injected intravenously into the tail veins of mice to determine if treatment with PALETS and/or LSPCs results in a significant decrease in PrP<sup>C</sup> protein and mRNA levels. Three mice were treated for each delivery vehicle group, and three mice were given PBS as an untreated control. Mice were euthanized four days after treatment, and brain and kidney samples were taken to assess PrP<sup>C</sup> mRNA and protein levels. Protein levels were determined using flow cytometry staining with the anti-PrP<sup>C</sup> antibody BAR-224, and mRNA levels were measured using ddPCR. Treated mice were compared to untreated controls for statistical analysis. While DOTAP LSPCs treatment showed the greatest reduction in the amount of PrP<sup>C</sup> on the surface of neuronal cells as shown by median fluorescent intensity, DOTAP PALETS showed the most significant decrease of PrP<sup>C</sup>-positive neuronal cells (Figure 2.6A and B). At least one mouse treated with either DOTAP PALETS or DSPE PALETS had decreased surface PrP<sup>C</sup>, but no significant difference was found between the untreated and all three-treated combined (Figure 2.6A). There were no statistically significant results seen in the kidney, but trends are present. Both DOTAP LSPCs and DSPE PALETS reduced the amount of cell surface PrP<sup>C</sup>, with DSPE PALETS having the greatest reduction (Figure 2.6C). Only DOTAP LSPCs decreased the number of PrP<sup>C</sup>-positive cells in the kidney (Figure 2.6D). Digital drop PCR was optimized to detect PrP<sup>C</sup> mRNA in wildtype mice with PrP<sup>C</sup> mRNA levels of PrP-null mice measured below the limit of detection for the assay (Figure 2.7A). Analysis of mRNA levels in the brain shows no difference between the mRNA levels of the untreated mice versus the treated mice (Figure 2.7B). In the kidney, DSPE PALETS showed an almost 2-fold increase in mRNA levels. DOTAP LSPCs and DOTAP PALETS showed a 2-fold decrease in PrP<sup>C</sup> mRNA levels in the kidney compared to the untreated control (Figure 2.7C).

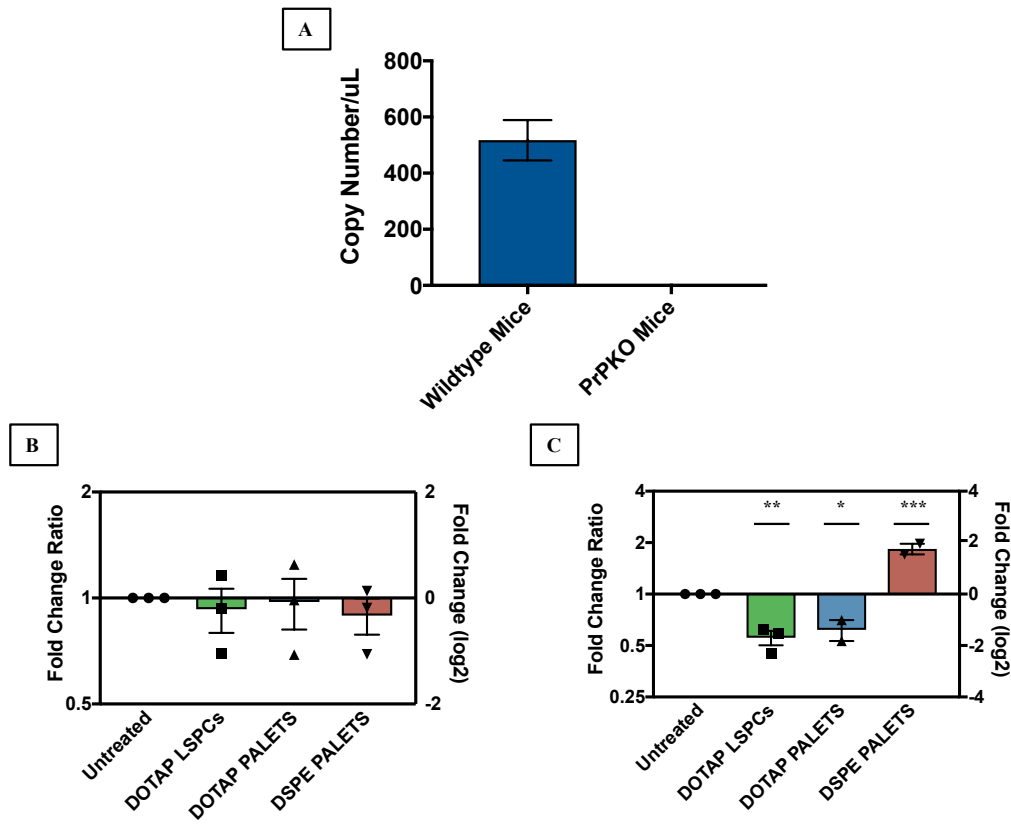


**Figure 2.7. mRNA analysis of LSPCs and PALETs treated four days after treatment.**

A) Optimization of ddPCR for PrP<sup>C</sup> mRNA levels revealed mRNA levels below the limit of detection in PrP-null mice compared to PrP-expressing mice. B) PrP<sup>C</sup> mRNA levels remained unchanged in the brain four days after treatment with any of the LSPCs or PALETs formulations containing PrP<sup>C</sup> siRNA. C) DOTAP LSPCs and DOTAP PALETs showed a two-fold decrease in mRNA levels in the kidneys four days after treatment. Mice treated with DSPE PALETs had a two-fold increase in PrP<sup>C</sup> mRNA levels at this time point. Error bars indicate SEM. \* p<0.05, \*\* p<0.01, and \*\*\* p<0.001. One-way ANOVA with Tukey's multiple comparisons

## Discussion

At the beginning of the 21<sup>st</sup> century, small interfering RNA (siRNA) was considered to be the biggest breakthrough in gene therapy in a generation<sup>2</sup>. Scientists worked quickly to discover its mechanism of action so that they could use siRNA as a therapeutic for ailments, such as liver disease<sup>44,45</sup>, cancers<sup>46-48</sup>, neurodegenerative diseases<sup>43,49</sup>, and chronic viral infections<sup>50-52</sup>. However, it quickly became apparent, that even though the mechanism was fully elucidated, there were several enormous obstacles to overcome before siRNA could be used as a therapeutic option. The two biggest challenges included how to evade the immune system and how to target naked siRNA towards distinct cell populations to reduce off-target effects.

Escaping the immune system and targeted delivery, while separate concepts, remain intimately entwined in utilizing siRNA as a therapeutic. A targeted delivery system will only be effective if it can successfully hide the siRNA from the double-stranded RNA (dsRNA) response of the immune system, and similarly, one of the only ways to bypass the immune system is to use a delivery system that conceals the siRNA from immune cells. Thus, these two challenges could be overcome by using the right form of a delivery system. An effective delivery system becomes especially important when trying to utilize siRNA as a therapeutic for neurodegenerative diseases, such as prion diseases, as the blood-brain barrier remains the most challenging obstacle to overcome in therapeutic delivery. Direct injection of siRNA into the central nervous system (CNS) remains an option, but should not be used as a first choice in the clinical setting as the damage caused by an injection could be worse than the disease trying to be cured.

Liposomes are widely used as delivery vehicles for gene therapy, including siRNA, for a number of reasons. First, they protect the siRNA from degradation by efficiently hiding the siRNA from the various nucleases within the bloodstream<sup>21</sup>. Similarly, liposomes also conceal siRNA from serum proteins and cells that might result in a triggering of the dsRNA immune response. The lipid composition of the liposome determines the circulation time of the siRNA, which is controlled by the amount of serum proteins the liposome binds to. Some lipids, such as sterols, decrease the circulation half-life of siRNA by making the liposomes more attractive to the Kupffer cells of the liver<sup>53,54</sup>. While other lipids, such as pegylated (PEG) lipids increase circulation time by making the liposomes invisible to serum proteins<sup>29</sup>. Liposomes can also be easily targeted to any cell population with the addition of a targeting molecule, whether it's a small peptide, antibody, or cellular protein<sup>55</sup>. So, liposomes represent a versatile delivery system that, when optimized, has the potential to overcome the challenges of siRNA therapeutics. Liposome-siRNA-peptide complexes (LSPCs) and peptide-addressed liposome-encapsulated therapeutic siRNA

(PALETS) were generated to determine the capability of siRNA to treat a neurodegenerative disease model and to evaluate the efficiency of a liposomal drug delivery system to the CNS.

LSPCs were described previously<sup>43</sup>. LSPCs decreased PrP<sup>C</sup> protein levels in neuroblastoma cells by more than 70%, and the liposome component delivered PrP<sup>C</sup> siRNA to these cells without the use of transfection reagents. The neuro-targeting peptide, RVG-9r, was shown to be specific in cell lines that possessed nicotinic acetylcholine receptors, which included neuroblastoma cells. Any cell line that did not possess these receptors did not have a notable decrease in PrP<sup>C</sup> protein levels. Due to the reduction of PrP<sup>C</sup>, the treatment of prion-infected neuroblastoma cells by LSPCs resulted in a reduction of PrP<sup>Res</sup> within the cells. This decrease was so dramatic that the cells were eventually 'cured' of prion infection. Since the LSPCs worked *in vitro*, the next step became characterizing their *in vivo* activity.

Treatment of mice with LSPCs resulted in a 40-50% reduction in the amount of cell surface PrP<sup>C</sup> four days after treatment. There was not a concomitant decrease in the number of PrP<sup>C</sup>-positive cells at this time. It is not known whether reducing total cellular surface PrP<sup>C</sup> or decreasing the number of cells that express PrP<sup>C</sup> is more important. Regardless, a reduction of PrP<sup>C</sup> across all cells, even with no difference in cell number, should also decrease the amount of PrP<sup>Res</sup> being converted during prion disease. These data demonstrate that LSPCs deliver PrP<sup>C</sup> siRNA across the blood-brain barrier to neuronal cells. However, it was noted that some mice did not respond to the LSPCs in the CNS but rather had a decrease of PrP<sup>C</sup> within the kidneys. While all mice were shown to have some off-target effects in the kidney, some mice did not have any response to the siRNA within the brain and had an even more dramatic reduction of PrP<sup>C</sup> within the kidney. Also, *in vivo* live imaging showed that in some mice the siRNA would immediately end up within the bladder one hour after injection. Therefore, two other delivery vehicles were designed to assess whether the circulation time and CNS targeting could be improved upon *in vivo*.

The short circulation half-life in some mice treated with DOTAP LSPCs could indicate several things: the LSPCs are being targeted towards the kidney, serum proteins are disassembling the LSPCs (such as the siRNA and RVG-9r), or binding of serum proteins is increasing the clearance of LSPCs. DOTAP PALETS were generated to address these concerns. DOTAP PALETS differ from DOTAP LSPCs by encapsulating the siRNA and incorporating PEG lipids. Serum proteins should not be able to remove the LSPCs elements so easily by encapsulating the siRNA and covalently linking the RVG-9r to the terminal PEG groups. Also, the addition of PEG

lipids to any liposome formulation increases the circulation time of the liposomes, which helps with circulation half-life.

Four days after treatment with DOTAP PALETS, treated mice showed a reduction in the number of PrP<sup>C</sup>-positive cells in the CNS by 7%, but not a decrease in cell surface PrP<sup>C</sup>. More studies are required to determine if this reduction is biologically significant. There were no changes in PrP<sup>C</sup> mRNA levels within the brains of mice treated with DOTAP PALETS, but there was a 2-fold decrease in mRNA levels in the kidney. It was expected that DOTAP PALETS would reduce cell surface PrP<sup>C</sup> as there are only minor differences between DOTAP PALETS and DOTAP LSPCs. However, only one time point was assessed in this report. Due to the PEG groups, it is possible that the circulation half-life increased and that this time point is not the optimal time to be assessing this particular vehicle. But it is just as likely that the addition of a chemical reaction resulted in an alteration of the activity of RVG-9r. If the carbodiimide reaction altered the RVG-9r peptide, it could have led to a malformed peptide with reduced activity. Thus, the LSPCs would not be efficiently targeted to the CNS. More experiments assessing the pharmacodynamics of DOTAP PALETS treatment with or without the covalent modification of the RVG-9r need to be performed to tease out whether the DOTAP PALETS require more optimization to target the CNS or if this is their optimal activity. It should be noted that DOTAP PALETS did not affect the kidneys. One of the reasons for generating a new vehicle was to increase circulation half-life so that the siRNA was not going directly to the kidneys. It seems that DOTAP PALETS have that effect as no reduction in either cell surface PrP<sup>C</sup> or number of PrP<sup>C</sup>-positive cells was seen in treated mice.

One concern on the clearance of LSPCs was that immune cells were increasing the clearance of the delivery vehicle. It is well known that cationic lipids attract more serum proteins than anionic lipids, and are more toxic due to the activation of the immune system<sup>56,57</sup>. On the other hand, anionic lipids are derived from natural lipids, which shields them from the immune system. Therefore, the last delivery vehicle iteration employed an anionic lipid as its core lipid to reduce toxicity and clearance by serum proteins. DSPE PALETS also encapsulates the siRNA on the inside of the liposome to further protect it from serum proteins/nucleases.

Anionic lipids are not typically used as delivery vehicles for gene therapy as it is harder to encapsulate the negatively-charged siRNA within the negatively-charged lipid, and toxicity profiles of anionic liposomes are lacking. Encapsulation of siRNA can be achieved with anionic liposomes by mixing small cations with the siRNA to condense it and give it an overall positive charge<sup>23-25</sup>. DSPE PALETS employ the use of the cation protamine

sulfate, which is a safe, non-toxic chemical that is routinely used in clinical settings to reverse the effects of heparin treatments. The protamine sulfate effectively condensed the PrP<sup>C</sup> siRNA and encapsulated it within the DSPE PALETS. The small decrease in siRNA concentration after the addition of protamine sulfate is most likely due to the condensation and masking of the siRNA, rather than an actual loss of siRNA. One concern using protamine sulfate is that it will bind too tightly to the anionic lipids of the liposome so that the siRNA would never be released. If this is the case, then the protamine sulfate can be excluded from the DSPE PALETS as without protamine sulfate 60-65% of the siRNA is still encapsulated.

Anionic liposomes, especially DSPE liposomes, are harder to generate than their cationic liposome counterparts. Anionic lipids can produce insoluble lipid masses upon rehydration because they are extremely attracted to other anionic lipids. Therefore, careful consideration is needed when selecting rehydrating conditions of anionic lipids. The rehydrating temperature should always be above the phase transition temperature ( $T_m$ ) of the lipids so that there is constant mixing and reorganizing of the liposomes during rehydration. In this protocol, a rehydration temperature of 70-75°C was used as it is around the phase transition temperature of DSPE, which is 74°C. Also, the rehydration buffer was changed from 10% sucrose to 1X PBS for DSPE PALETS, as anionic lipids are more soluble in salt-containing buffers. Rehydration using either 10% sucrose or water resulted in insoluble lipid masses. The main lipid component of DSPE, phosphatidylethanolamine, hydrates poorly when used at a 60% molar concentration or higher. Salt rehydration buffers aid with the hydration at this molar concentration, but the buffer doesn't solubilize all the lipid when used at greater than 60% molar concentration. Since anionic lipids like to aggregate, a significant loss is seen when sizing these liposomes through either syringe or extruder filters. Therefore, this protocol employed the use of sonication to size the DSPE liposomes to 200 nm.

Treatment of mice with DSPE PALETS did not result in a statistically significant decrease in PrP<sup>C</sup> when all three treated mice are compared to the untreated mouse. However, one mouse had a 50% reduction in cell surface PrP<sup>C</sup>, while another had a 15-20% decrease in surface PrP<sup>C</sup> levels. Therefore, DSPE PALETS did effectively deliver the PrP<sup>C</sup> siRNA to neuronal cells in a subset of treated mice. Similar to DOTAP PALETS, the use of PEG lipids in DSPE PALETS could have increased the circulation half-life of the vehicle such that the four-day time point is not the optimal time to assess protein levels using this delivery vehicle. More pharmacodynamics experiments are needed to determine the activity of DSPE PALETS. There wasn't a concomitant decrease in mRNA levels in the brain in DSPE PALETS treated mice; however, none of the treatments using any of the delivery vehicles resulted in

a reduction in mRNA levels in this organ. One explanation for the lack of a decrease in PrP<sup>C</sup> mRNA concentrations in the brains of any of the treated mice is that there is a compensation mechanism for decreases in PrP<sup>C</sup> mRNA levels. When there is a reduction in PrP<sup>C</sup>, perhaps transcription factors increase transcription of PrP<sup>C</sup> mRNA to normal or even greater than average values. Transcription regulation might explain why the treatment of DSPE PALETS resulted in a 2-fold increase of PrP<sup>C</sup> mRNA levels in the kidney. There are instances of PrP<sup>C</sup> mRNA and protein upregulation in the literature. Nerve growth factor was shown to increase PrP<sup>C</sup> mRNA levels when injected intraventricularly<sup>58</sup>. PrP<sup>C</sup> mRNA and protein levels also increase in response to heat shock or activation of Toll-like receptor ligands by lipopolysaccharide or CpG oligodeoxynucleotides<sup>59-61</sup>. Thus, regulation of PrP<sup>C</sup> mRNA and protein levels seems to be tightly controlled. Protamine sulfate, when complexed with oligoribonucleotides, also results in activation of the immune system by Toll-like receptors 7 and 8<sup>62</sup>. It is possible that the use of protamine in the DSPE PALETS activated the Toll-like receptors and indirectly resulted in an increase of PrP<sup>C</sup> mRNA in the kidney. Lastly, treatment with DSPE PALETS decreased the amount of cell surface PrP<sup>C</sup> in the kidney, indicating that there is targeting and/or clearance of this delivery vehicle to the kidney.

These three siRNA delivery vehicles represent new tools for the delivery of siRNA to the CNS for the treatment of neurodegenerative diseases. More studies are needed to determine the pharmacodynamics and pharmacokinetics of the PALETS systems. Depending on the results of future experiments, modifications and optimization might be necessary for them to deliver siRNA to the CNS effectively. The results shown here indicate that, using the current formulations, DOTAP LSPCs are the best choice as they result in a 40-50% decrease in PrP<sup>C</sup> compared to untreated controls. LSPCs may be further optimized by utilizing a different targeting peptide that is specific to the CNS. A CNS-specific targeting peptide would reduce the off-target effects seen, and could result in an even larger decrease in PrP<sup>C</sup> if 100% of the siRNA is directed towards the CNS.

## References

1. Bender, H. R., Kane, S. & Zabel, M. D. Delivery of Therapeutic siRNA to the CNS Using Cationic and Anionic Liposomes. *J Vis Exp* e54106 (2016).
2. Fire, A. *et al.* Potent and specific genetic interference by double-stranded RNA in *Caenorhabditis elegans*. *Nature* **391**, 806–811 (1998).
3. Hamilton, A. J. & Baulcombe, D. C. A species of small antisense RNA in posttranscriptional gene silencing in plants. *Science* **286**, 950–952 (1999).
4. Hammond, S. M., Bernstein, E., Beach, D. & Hannon, G. J. An RNA-directed nuclease mediates post-transcriptional gene silencing in *Drosophila* cells. *Nature* **404**, 293–296 (2000).
5. Martinez, J. RISC is a 5' phosphomonoester-producing RNA endonuclease. *Genes Dev* **18**, 975–980 (2004).
6. Meister, G. *et al.* Human Argonaute2 Mediates RNA Cleavage Targeted by miRNAs and siRNAs. *Mol. Cell* **15**, 185–197 (2004).
7. Liu, J. Argonaute2 Is the Catalytic Engine of Mammalian RNAi. *Science* **305**, 1437–1441 (2004).
8. Elbashir, S. M., Lendeckel, W. & Tuschl, T. RNA interference is mediated by 21- and 22-nucleotide RNAs. *Genes Dev* (2001).
9. Elbashir, S. M. *et al.* Duplexes of 21-nucleotide RNAs mediate RNA interference in cultured mammalian cells. *Nature* **411**, 494–498 (2001).
10. Malone, R. W., Felgner, P. L. & Verma, I. M. Cationic liposome-mediated RNA transfection. *Proc. Natl. Acad. Sci. U.S.A.* **86**, 6077–6081 (1989).
11. Liu, Y. *et al.* Factors influencing the efficiency of cationic liposome-mediated intravenous gene delivery. *Nat. Biotechnol.* **15**, 167–173 (1997).
12. Freimark, B. D. *et al.* Cationic lipids enhance cytokine and cell influx levels in the lung following administration of plasmid: cationic lipid complexes. *J Immunol* **160**, 4580–4586 (1998).
13. Rettig, G. R. & Behlke, M. A. Progress Toward In Vivo Use of siRNAs-II. *Mol. Ther.* **20**, 483–512 (2016).
14. Braasch, D. A. *et al.* RNA Interference in Mammalian Cells by Chemically-Modified RNA †. *Biochemistry* **42**, 7967–7975 (2003).
15. Braasch, D. A. *et al.* Biodistribution of phosphodiester and phosphorothioate siRNA. *Bioorg Med Chem Letters* **14**, 1139–1143 (2004).
16. Layzer, J. M. In vivo activity of nuclease-resistant siRNAs. *RNA* **10**, 766–771 (2004).
17. Soutschek, J., Akinc, A., Bramlage, B. & Charisse, K. Therapeutic silencing of an endogenous gene by systemic administration of modified siRNAs. *Nature* **432**, 173–178 (2004).
18. Escriou, V., Ciolina, C., Helbling-Leclerc, A., Wils, P. & Scherman, D. Cationic lipid-mediated gene transfer: analysis of cellular uptake and nuclear import of plasmid DNA. *Cell Biol. Toxicol.* **14**, 95–104 (1998).
19. Elouahabi, A. & Ruyschaert, J.-M. Formation and Intracellular Trafficking of Lipoplexes and Polyplexes. *Mol. Ther.* **11**, 336–347 (2005).
20. Zuhorn, I. S. *et al.* Nonbilayer Phase of Lipoplex–Membrane Mixture Determines Endosomal Escape of Genetic Cargo and Transfection Efficiency. *Mol. Ther.* **11**, 801–810 (2005).
21. Felgner, P. L. *et al.* Lipofection: a highly efficient, lipid-mediated DNA-transfection procedure. *Proc. Natl. Acad. Sci. U.S.A.* **84**, 7413–7417 (2007).
22. Balazs, D. A. & Godbey, W. T. Liposomes for Use in Gene Delivery. *J Drug Deliv* **2011**, 1–12 (2011).
23. Srinivasan, C. & Burgess, D. J. Gene delivery. *J Control Release* **136**, 62–70 (2009).
24. Lakkaraju, A. Neurons Are Protected from Excitotoxic Death by p53 Antisense Oligonucleotides Delivered in Anionic Liposomes. *J Biol Chem* **276**, 32000–32007 (2001).
25. Patil, S. D., Rhodes, D. G. & Burgess, D. J. Anionic liposomal delivery system for DNA transfection. *AAPS J* **6**, e29 (2004).
26. Sorgi, F. L., Bhattacharya, S. & Huang, L. Protamine sulfate enhances lipid-mediated gene transfer. *Gene Ther* **4**, 961–968 (1997).
27. Li, S., Rizzo, M. A., Bhattacharya, S. & Huang, L. Characterization of cationic lipid-protamine-DNA (LPD) complexes for intravenous gene delivery. *Gene Ther* **5**, 930–937 (1998).
28. Li, S. & Huang, L. In vivo gene transfer via intravenous administration of cationic lipid-protamine-DNA (LPD) complexes. *Gene Ther* **4**, 891–900 (1997).

29. Papahadjopoulos, D. *et al.* Sterically stabilized liposomes: improvements in pharmacokinetics and antitumor therapeutic efficacy. *Proc. Natl. Acad. Sci. U.S.A.* **88**, 11460–11464 (1991).
30. Chiu, Y.-L., Ali, A., Chu, C.-Y., Cao, H. & Rana, T. M. Visualizing a Correlation between siRNA Localization, Cellular Uptake, and RNAi in Living Cells. *Chem. Biol.* **11**, 1165–1175 (2004).
31. McNamara, J. O. *et al.* Small Interfering RNAs Mediate Sequence-Independent Gene Suppression and Induce Immune Activation by Signaling through Toll-Like Receptor 3. *Nat. Biotechnol.* **172**, 1005–1015 (2004).
32. Kumar, P. *et al.* Transvascular delivery of small interfering RNA to the central nervous system. *Nature* **448**, 39–43 (2007).
33. Uno, Y. *et al.* High-Density Lipoprotein Facilitates In Vivo Delivery of  $\alpha$ -Tocopherol–Conjugated Short-Interfering RNA to the Brain. *Hum. Gene Ther.* **22**, 711–719 (2011).
34. Bolton, D. C., McKinley, M. P. & Prusiner, S. B. Identification of a protein that purifies with the scrapie prion. *Science* **218**, 1309–1311 (1982).
35. McKinley, M. P., Bolton, D. C. & Prusiner, S. B. A protease-resistant protein is a structural component of the scrapie prion. *Cell* **35**, 57–62 (1983).
36. Prusiner, S. B. *et al.* Scrapie agent contains a hydrophobic protein. *Proc. Natl. Acad. Sci. U.S.A.* **78**, 6675–6679 (1981).
37. Prusiner, S. B. Novel proteinaceous infectious particles cause scrapie. *Science* **216**, 136–144 (1982).
38. Jeffrey, M., McGovern, G., Sisó, S. & González, L. Cellular and sub-cellular pathology of animal prion diseases: relationship between morphological changes, accumulation of abnormal prion protein and clinical disease. *Acta Neuropathol* **121**, 113–134 (2010).
39. Pfeifer, A. *et al.* Lentivector-mediated RNAi efficiently suppresses prion protein and prolongs survival of scrapie-infected mice. *J. Clin. Invest.* **116**, 3204–3210 (2006).
40. White, M. D. *et al.* Single treatment with RNAi against prion protein rescues early neuronal dysfunction and prolongs survival in mice with prion disease. *Proc. Natl. Acad. Sci. U.S.A.* **105**, 10238–10243 (2008).
41. Gallozzi, M. *et al.* Prnp knockdown in transgenic mice using RNA interference. *Transgenic Res.* **17**, 783–791 (2008).
42. Mallucci, G. Depleting Neuronal PrP in Prion Infection Prevents Disease and Reverses Spongiosis. *Science* **302**, 871–874 (2003).
43. Pulford, B. *et al.* Liposome-siRNA-Peptide Complexes Cross the Blood-Brain Barrier and Significantly Decrease PrPC on Neuronal Cells and PrPRES in Infected Cell Cultures. *PLoS ONE* **5**, e11085 (2010).
44. McCaffrey, A. P. *et al.* RNA interference in adult mice. *Nature* **418**, 38–39 (2002).
45. Song, E. *et al.* RNA interference targeting Fas protects mice from fulminant hepatitis. *Nat. Med.* **9**, 347–351 (2003).
46. Huang, Y.-H. *et al.* Claudin-3 gene silencing with siRNA suppresses ovarian tumor growth and metastasis. *Proc. Natl. Acad. Sci. U.S.A.* **106**, 3426–3430 (2009).
47. Aharinejad, S. *et al.* Colony-stimulating factor-1 blockade by antisense oligonucleotides and small interfering RNAs suppresses growth of human mammary tumor xenografts in mice. *Cancer Res* **64**, 5378–5384 (2004).
48. Jonson, A. L., Rogers, L. M., Ramakrishnan, S. & Downs, L. S., Jr. Gene silencing with siRNA targeting E6/E7 as a therapeutic intervention in a mouse model of cervical cancer. *Gynecol Oncol* **111**, 356–364 (2008).
49. DiFiglia, M., Sena-Esteves, M. & Chase, K. Therapeutic silencing of mutant huntingtin with siRNA attenuates striatal and cortical neuropathology and behavioral deficits. *Proc. Natl. Acad. Sci. U.S.A.* **104**, 17204–17209 (2007).
50. McCaffrey, A. P. *et al.* RNA interference in adult mice. *Nature* **418**, 38–39 (2002).
51. McCaffrey, A. P. *et al.* Inhibition of hepatitis B virus in mice by RNA interference. *Nat. Biotechnol.* **21**, 639–644 (2003).
52. Ge, Q. *et al.* Inhibition of influenza virus production in virus-infected mice by RNA interference. *Proc. Natl. Acad. Sci. U.S.A.* **101**, 8676–8681 (2004).
53. Lorenz, C., Hadwiger, P., John, M., Vornlocher, H.-P. & Unverzagt, C. Steroid and lipid conjugates of siRNAs to enhance cellular uptake and gene silencing in liver cells. *Bioorg Med Chem* **14**, 4975–4977 (2004).
54. Bennett, M. J., Nantz, M. H., Balasubramaniam, R. P., Gruenert, D. C. & Malone, R. W. Cholesterol enhances cationic liposome-mediated DNA transfection of human respiratory epithelial cells. *Biosci. Rep.* **15**, 47–53 (1995).

55. Akinc, A. *et al.* Targeted Delivery of RNAi Therapeutics With Endogenous and Exogenous Ligand-Based Mechanisms. *Mol Ther* **18**, 1357–1364 (2009).
56. Fillion, M. C. & Phillips, N. C. Toxicity and immunomodulatory activity of liposomal vectors formulated with cationic lipids toward immune effector cells. *Biochim. Biophys. Acta* **1329**, 345–356 (1997).
57. Nguyen, L. T., Atobe, K., Barichello, J. M., Ishida, T. & Kiwada, H. Complex formation with plasmid DNA increases the cytotoxicity of cationic liposomes. *Biol. Pharm. Bull.* **30**, 751–757 (2007).
58. Mobley, W. C., Neve, R. L., Prusiner, S. B. & McKinley, M. P. Nerve growth factor increases mRNA levels for the prion protein and the beta-amyloid protein precursor in developing hamster brain. *Proc. Natl. Acad. Sci. U.S.A.* **85**, 9811–9815 (1988).
59. Lotscher, M., Recher, M., Hunziker, L. & Klein, M. A. Immunologically Induced, Complement-Dependent Up-Regulation of the Prion Protein in the Mouse Spleen: Follicular Dendritic Cells Versus Capsule and Trabeculae. *J. Immunol.* **170**, 6040–6047 (2003).
60. Martinez del Hoyo, G., Lopez-Bravo, M., Metharom, P., Ardavin, C. & Aucouturier, P. Prion Protein Expression by Mouse Dendritic Cells Is Restricted to the Nonplasmacytoid Subsets and Correlates with the Maturation State. *J. Immunol.* **177**, 6137–6142 (2006).
61. Shyu, W.-C. *et al.* Molecular modulation of expression of prion protein by heat shock. *Mol Neurobiol* **26**, 1–12 (2002).
62. Scheel, B. *et al.* Toll-like receptor-dependent activation of several human blood cell types by protamine-condensed mRNA. *Eur. J. Immunol.* **35**, 1557–1566 (2005).

## Chapter 3:

# Intravenous injection of LSPCs delivers PrP<sup>C</sup> siRNA to the brain *in vivo* and reduce neuronal PrP<sup>C</sup>

## Summary

The prion protein, PrP<sup>C</sup>, is a normal host cellular protein that becomes misfolded into an infectious isomer during prion disease. Early drug compounds targeting the infectious isomer have proven unreliable in treating prion disease *in vivo*. Therefore, PrP<sup>C</sup> has become an attractive target for anti-prion therapeutics, as decreasing or eliminating PrP<sup>C</sup> has no known detrimental effects and has the potential to reduce the amount of infectious isomer in prion-infected tissues. This report describes using siRNA as a therapeutic to target neuronal PrP<sup>C</sup>. We have packaged this PrP<sup>C</sup> siRNA into our liposome-siRNA-peptide complexes (LSPCs) to improve serum stability and to target the siRNA towards neuronal cells using a small peptide from the rabies virus glycoprotein (RVG-9r). We show that LSPCs can cross the blood-brain barrier and decrease the amount of neuronal surface PrP<sup>C</sup> by 40-50% within the central nervous system, while total PrP<sup>C</sup> protein levels remain mostly unchanged. We demonstrate PrP<sup>C</sup> knockdown in two mouse models, with each model responding slightly differently to the PrP<sup>C</sup> siRNA. Neuronal surface PrP<sup>C</sup> and mRNA levels are decreased up to 21 days after LSPC treatment. Surprisingly, mRNA levels increased in some LSPC-treated mice. We observed off-target effects in the kidney, which resulted in a decrease of PrP<sup>C</sup> protein and some mRNA levels. Treatment of mice with either LSPCs with control peptide or LSPCs with scrambled siRNA had minimal effect on neuronal PrP<sup>C</sup> protein levels. We also show that repetitive two-week treatments of our siRNA results in a 70% decrease in PrP<sup>C</sup> protein levels by the 3<sup>rd</sup> treatment in prion-infected mice. mRNA analysis of these mice also shows a reduction in mRNA levels at the 3<sup>rd</sup> time point. These LSPCs represent a new delivery method for siRNA to the central nervous system that could affect the outcome of prion disease.

## Introduction

Prion diseases are neurodegenerative diseases that have an impact on a broad range of species from sheep (scrapie) and cattle (bovine spongiform encephalopathy [BSE]) to humans (Creutzfeldt-Jakob disease among

others). Plaque deposits, neuronal vacuolation, glial activation, and neuronal cell death characterize these diseases. Prion diseases result when a normal host cellular protein, PrP<sup>C</sup>, misfolds into an infectious isomer, PrP<sup>Res</sup><sup>1-4</sup>. Currently, there are no known clinical therapeutic interventions that lead to an elongation of survival periods in individuals or animals infected with prions. However, the literature discusses many compounds with anti-prion activity.

Most of the early therapeutic compounds that were investigated for anti-prion activity targeted the conversion of PrP<sup>C</sup> into PrP<sup>Res</sup>. Antivirals were the first group of therapeutics investigated for prion diseases when the agent of scrapie was still considered to be a virus<sup>5-7</sup>. Antibacterials (amphotericin B)<sup>7-12</sup>, antimalarials (quinacrine)<sup>13-17</sup> and an anti-cancer drug (IDX)<sup>18</sup> have also shown anti-prion activity. Other compounds with anti-prion activity include drugs within the polycationic and polyanionic categories. Polycationic drugs include polyamine compounds that contain positively-charged amino groups on their terminal ends, which are the active groups that confer anti-prion activity<sup>19-23</sup>. On the other hand, some polyanionic compounds, which contain a negatively-charged terminal group, have anti-prion activity such as HPA-23<sup>24,25</sup>, dextran sulfate 500<sup>25-28</sup>, pentosan polysulphate<sup>27-30</sup>, and congo red<sup>31-33</sup>. In recent years, anti-PrP antibodies administered as either active or passive immunization have also shown promise<sup>34-37</sup>.

These compounds can ‘cure’ prion-infected cells, and some are even able to prolong the survival times of animal models infected with prion disease. However, many challenges remain before large-scale clinical trials are considered. Most of the drugs do not cross the blood-brain barrier and do not specifically target neuronal cells. Therefore, delivery vehicles would need to be employed to target these molecules. Quite a few of the polyanionic and polycationic compounds are toxic and cannot be given in large doses or over an extended period. Some drugs only have anti-prion activity for specific prion strains. Most of the above compounds have a pronounced effect on survival times with early-stage treatment either before or directly after prion inoculation, but few have shown any promise when given at late or clinical stages. Because of these limitations, researchers are now focusing on targeting PrP<sup>C</sup> to affect clinical stages of prion disease.

Mallucci’s group demonstrated the usefulness of targeting PrP<sup>C</sup> when they used a Cre/loxP system to eliminate PrP<sup>C</sup> after the establishment of prion neuropathology in a mouse model. After PrP<sup>C</sup> was removed in mice with prion disease, the neuropathology was reversed, and the mice did not succumb to clinical stages of prion disease<sup>38,39</sup>. Another benefit of targeting PrP<sup>C</sup> is that PrP-null mice live relatively healthy lives<sup>40</sup>. PrP-null mice show

some long-term potentiation changes,<sup>41-43</sup> circadian rhythm alterations<sup>44</sup>, and reorganization of neuronal circuits<sup>43,45,46</sup>, but do not display an overt phenotype due to the loss of PrP<sup>C</sup>. It is thought that either the function is non-essential or that, more likely, there is a redundant protein or pathway that performs the function in the absence of PrP<sup>C</sup>. Thus, gene therapies targeting PrP<sup>C</sup> are being investigated for their use in treating prion disease.

RNA interference is a pathway that utilizes RNA molecules to decrease mRNA levels of a particular protein. These RNA molecules, short hairpin RNA (shRNA) or small interfering RNA (siRNA), activate the RNA-induced silencing complex that cleaves mRNA. The cleavage enables endo- and exonucleases to degrade the targeted mRNA resulting in a decrease in protein levels<sup>47-52</sup>. Both shRNA and siRNA treatment targeted towards PrP<sup>C</sup> can reduce the level of PrP<sup>Res</sup> in cultured and primary cells by decreasing the amount of PrP<sup>C</sup> available for conversion<sup>53-55</sup>. Treatment of mice into the brain with either shRNA or siRNA is typically achieved through a stereotactic injection. A single injection of shRNA into the hippocampus of prion-infected mice resulted in an increase in survival times and a reversal of prion neuropathology<sup>56</sup>. Chimeric mice that expressed 50% less PrP<sup>C</sup>, due to the expression of shRNA in their cells, also have prolonged survival periods when infected with prions<sup>57</sup>. However, these methods are unrealistic as therapeutic options because stereotactic injections cause damage to the brain and generating chimeric humans is unethical. Still, these molecules are considered relatively safe as toxicity is achieved at much higher levels than is needed to decrease protein levels, and these molecules are relatively small so they can easily be packaged within delivery vehicles for targeting to the central nervous system. One report has demonstrated the usefulness of using liposomes as delivery vehicles for siRNA, as they protect the RNA and can be targeted towards neuronal cells<sup>58</sup>.

Here we show that a single intravascular injection of siRNA results in a 40-50% decrease in neuronal PrP<sup>C</sup> levels in two different mouse lines. We have packaged our PrP<sup>C</sup> siRNA into liposome-siRNA-peptide complexes (LSPCs) that are targeted towards nicotinic acetylcholine receptors (nAChRs) using a small peptide from the rabies virus glycoprotein (RVG-9r). We also show that our LSPCs can effectively cross the blood-brain barrier and deliver siRNA to neuronal cells resulting in a decrease of PrP<sup>C</sup>. The response of the mice to the siRNA lasts up to 21 days after injection. Also, repeated doses of our LSPCs every two weeks results in an even larger decrease in neuronal PrP<sup>C</sup> levels. Our LSPCs represent a new method of delivering PrP<sup>C</sup> siRNA *in vivo* to the central nervous system.

## Materials and Methods

### *Mice*

CR1 KO and CR2 KO were kindly provided by Dr. John Weis at the University of Utah<sup>59,60</sup>. CR1/2 hemizygous mice were generated by crossing CR1 KO and CR2 KO mice. The CR1/2 hemizygous mice contain one allele of CR1 and one allele of CR2. FVB mice were purchased from The Jackson Laboratory (Bar Harbor, ME). Mice were euthanized using CO<sub>2</sub>. All mice were bred and maintained at Lab Animal Resources, accredited by the Association for Assessment and Accreditation of Lab Animal Care International, in accordance with protocols approved by the Institutional Animal Care and Use Committee at Colorado State University.

### *Generation of Liposomes*

#### *DOTAP LSPCs*

DOTAP LSPCs consist of a 1:1 DOTAP:cholesterol ratio in a 1:1 chloroform:methanol solution. Both lipids were purchased from Avanti Lipids. The solvents were evaporated using N<sub>2</sub> gas and the resultant dry lipid film was placed under vacuum for a total of 8 hours to remove any excess solvent. A stock solution of liposomes was made at an 8 mM (40 umole total) concentration, by resuspending the lipid film in 5 mL of 10% sucrose heated at 55°C. All components (lipid film and sucrose) were kept at this temperature during rehydration. The lipid film was swirled every 3 minutes to promote lipid mixing. The heated sucrose was added to the lipid cake 1 mL every 10 minutes. Resulting liposomes were stored at 4°C.

#### *Generating LSPCs and Treating Mice with LSPCs*

PrP<sup>C</sup> 1672 siRNA sequence: ACATAAACTGCGATAGCTTC (Qiagen).

RVG-9r peptide: YTIWMPENPRPGTPCDIFTNSRGKCRASNGGGGrrrrrrrrr (ChemPeptide)

#### *LSPCs*

The DOTAP LSPCs liposomes were diluted 1:100 in 1X PBS and sonicated 4X with 2-3 minute rests in between. 50 uL (4 nmole total) of diluted/sonicated liposomes was mixed with 100 uL (4 nmole total) of 1672 siRNA. The siRNA/liposome solution was incubated for 10 minutes at 4°C. Then, 80 uL (40 nmole total) of RVG-9r peptide was added to the solution and allowed to incubate for 10 minutes on ice. Mice were placed under a heat lamp for 5 minutes and anesthetized with 1.5-2% isoflurane (VetOne). The mouse tails were disinfected using 70% EtOH. LSPCs were injected into the tail veins of mice using a 29-gauge insulin syringe.

### ***Flow Cytometry***

Mice treated with LSPCs were euthanized after certain time points and assayed for protein levels using flow cytometry. Half a hemisphere of brain and one kidney was pressed through a 40  $\mu$ m cell strainer (Falcon, VWR) using the plunger from a 5 mL syringe and 5 mL of FACS buffer (1X PBS, 1% fetal bovine serum, 10 mM EDTA). The cell suspension was transferred to a 15 mL conical, of which 450  $\mu$ L of each cell suspension was used for flow cytometric analysis. Cells were washed 3X by centrifugation at 2000 rpm (250 x g) and resuspension of the cells with 1 mL of FACS buffer. Fc receptors were blocked using 100  $\mu$ L of a 1:100 dilution of a 0.5 mg/mL rat anti-mouse CD16/CD32 Fc block (BD Pharmingen) in FACS buffer with 7% goat serum for 20 minutes on ice. The cell pellet was washed once as above. The cells were stained with 100  $\mu$ L of a 1:100 dilution of 20  $\mu$ g/mL solution of the PrP<sup>C</sup> antibody BAR-224 conjugated to Dylight 650 (per manufacturer's instructions) in FACS buffer for 40 minutes at room temperature. Red blood cells were lysed with 1 mL of RBC lysis buffer (1X PBS, 155 mM NH<sub>4</sub>Cl, 12 mM NaHCO<sub>3</sub>, 0.1 mM EDTA) for 3 minutes and then centrifuged at 2000 rpm for 3 minutes. Cells were washed 2X with 1 mL of FACS buffer. Cells were stained with propidium iodide (FisherSci) 10-15 minutes before analyzing a 1:2 dilution of the cells on a DakoCytomation Cyan ADP flow cytometer. Results were evaluated using FlowJo version 10.

### ***Western Blots***

Mice treated with LSPCs were euthanized after certain time points and assayed for protein levels using western blot. After dissection, brains were kept at -20°C until processed. Brains were thawed on ice for 1 hour, weighed and transferred to new tubes containing 2.5mm glass beads. 1X PBS was added to each brain to obtain a 20% weight/volume (w/v) homogenate. Brains were homogenized using a Bead Blaster 24 (Benchmark). The brain homogenates were further diluted to 10% w/v with the addition of an equal volume of 1X PBS with 1% Triton X. Samples were immediately prepared for PrP<sup>C</sup> western blot by further diluting the brain homogenates to 1% with 1X PBS and 3X sample loading buffer (Invitrogen). 1% samples were heated at 95°C for 10 minutes and frozen at -20°C until western blots were performed. Samples were prepared in triplicate for two repeated experiments. Before starting western blots, samples were thawed on ice for 30 minutes and reheated at 95°C for 3 minutes. Proteins were electrophoretically separated using 12% sodium dodecyl sulfate polyacrylamide gels (Invitrogen). Proteins were then transferred to a polyvinylidene difluoride membrane (Millipore). Membranes were blocked using 5% non-fat dry milk for 1 hour. Membranes were washed 2X for 10 minutes each using 1X PBS with 0.2% Tween. Membranes

were incubated with horseradish peroxidase-conjugated BAR-224 (SPI Bio) anti-PrP<sup>C</sup> antibody diluted 1:20,000 for overnight at 4°C. Membranes were washed again 6X for 10 minutes each, and incubated with enhanced chemiluminescent substrate (Millipore) for 5 minutes. Membranes were photographed using an ImageQuant LAS 4000 (GE). The membranes were then stripped with restore stripping buffer (ThermoFisher) for 10 minutes at room temperature. Membranes were again blocked as above, but this time incubated with 1:10,000 anti-actin antibody (Santa Cruz) overnight at 4°C. Protocol proceeded as above for washing and imaging. Densitometric analysis was performed using ImageJ.

### ***In vivo Live Imaging***

LSPCs were assembled as described above. siRNA labeled on the 5' end with Alexa Fluor 488 (Qiagen) and RVG-9r labeled with Dylight 650 (per manufacturer's instructions) (ThermoFisher) were used. Mice were anesthetized with 2% isoflurane, injected intravascularly with LSPCs, and then immediately imaged for up to one hour after treatment using an IVIS Spectrum *in vivo* live imaging system. Autoexposure settings were used. siRNA signal was viewed with a 500/540 nm filter and RVG-9r signal was viewed with a 640/680 nm filter.

### ***Digital Droplet PCR (ddPCR)***

RNA was extracted from brain and kidney cell suspensions using a RNeasy minikit (Qiagen). DNase digestion was performed off-column using RQ1 RNase-free DNase (Promega) per manufacturer's instructions. The RNA was purified from the DNase using EtOH precipitation. A 1:10 volume of 2 M NaAcetate and 2.5X volume of 100% EtOH was added to the RNA after DNase digestion. The RNA was stored at -20°C for at least 24 hours. The samples were then centrifuged at 13,000 rpm (16,060 x g) for 45 minutes. The RNA pellet was washed with 200 uL of 100% EtOH and centrifuged again at the same conditions. The RNA pellet was allowed to dry for 1 hour, and was resuspended in 40 uL of molecular grade H<sub>2</sub>O. RNA concentration was assessed via spectrophotometer (Denovix) at 260 nm. Approximately 150 ng of RNA was used to generate cDNA using the High Capacity cDNA Reverse Transcription kit from ThermoFisher. A final concentration of 0.035 ng of cDNA was used for ddPCR reactions. A final concentration of 1.25 uM of the following PrP primers was used in the final ddPCR reaction: forward primer 5'-CCTGGTGGCTACATGCTGG-3' and reverse primer 5'-GGCCTGTAGTACACTTGG-3'. A final concentration of 125 nM of the following actin primers was used in the final ddPCR reaction: forward primer 5'-GACCTGACAGACTACCTCAT-3' and reverse primer 5'-AGACAGCACTGTGTTGGCAT-3'. The cDNA/primer solution was mixed with 10 uL of Supermix (BioRad) to generate a final reaction volume of 20 uL. Droplets were

generated by combining the reaction mix with 60  $\mu$ L of droplet generator oil (BioRad) using a QX-100 droplet generator. The droplets were then transferred to a 96-well plate and sealed with pierceable sealing foil sheets (BioRad). The PCR amplification was performed using a C1000 Touch Thermal Cycler (BioRad) with the following cycling parameters: enzyme activation at 95°C for 5 minutes, denaturation at 95°C for 30 seconds, annealing/elongation at 57°C for 1 minute for 40 cycles, signal stabilization at 4°C for 5 minutes and 95°C for 5 minutes, and hold at 4°C. Following amplification, the droplets were transferred to a QX100 droplet reader and analyzed using Quantasoft (BioRad) software. ddPCR results are presented as copy number/ $\mu$ L and fold change. PrP<sup>C</sup> was normalized to actin. Fold change was determined by dividing the treated sample by the untreated control (set as 1) and by the mRNA upregulation seen in control experiments that is caused by the LSPC treatment.

### ***Intraperitoneal Inoculations***

RML-5 prions were prepared as previously described<sup>61</sup>. 10% brain homogenates were diluted 1:100 in 1X PBS supplemented with 100 units/mL of Penicillin and 100  $\mu$ g/mL of Streptomycin (Gibco) immediately before inoculation. Mice were scruffed and flipped upside down for inoculation. 100  $\mu$ L inoculum was injected in the left or right bottom quadrant of the intraperitoneal cavity with a 29-gauge insulin syringe (BD).

### ***Statistical Analysis***

Statistical analysis was performed using GraphPad Prism. Standard deviation (SD) error bars are used to show the variability between technical replicates of individual treated mice. When mice are grouped together, standard error of the mean (SEM) is used to show how closely the mean of the treated mice represents the population mean of all treated mice.

## **Results**

### ***LSPCs deliver PrP<sup>C</sup> siRNA to the brain***

Mice were injected with LSPCs and monitored via *in vivo* live imaging. Mice were monitored up to 48 hours after injection of LSPCs with Alexa 488-labeled siRNA and Dylight 650-labeled RVG-9r LSPCs. While RVG-9r was not visible under these conditions (data not shown), labeled siRNA was visible directly after injection into the tail veins of mice. The untreated control (PBS) showed no signal for PrP<sup>C</sup> siRNA, while the LSPCs and the liposome+siRNA (L+S) only control showed a signal for PrP<sup>C</sup> siRNA using a 500/540 nm filter one hour after injection (Figure 3.1). The LSPCs treated mouse has most of the siRNA signal concentrated towards the area of the

brain on the dorsal side, while the L+S control shows minimal amounts of siRNA signal concentrated in the area around the brain one hour after injection. Both LSPCs treated and L+S control mice show siRNA signal distributed throughout the entire ventral side (Figure 3.1A). Nearly two hours after injection, more PrP<sup>C</sup> siRNA signal is present in the area surrounding the brains of both the LSPCs and L+S treated mice. Flow cytometric analysis was performed on these same mice to determine if the siRNA signal in the area of the brain corresponded to siRNA in neuronal cells. This analysis revealed that a significant amount of PrP<sup>C</sup> siRNA is found in neuronal cells in LSPCs-treated mice (Figure 3.1B). No siRNA signal was detected in the brains of any treated mice 24 hours after LSPCs treatment (Figure A.1).

***Injection of LSPCs containing control peptide or scrambled siRNA results in an increase in neuronal PrP<sup>C</sup> mRNA levels and a slight reduction of cellular PrP<sup>C</sup>***

To determine if scrambled siRNA or the RVM control peptide changes PrP<sup>C</sup> protein or mRNA levels, FVB mice were treated with either no LSPCs, 1672 LSPCs, LSPCs with scrambled 1672 siRNA or LSPCs with the RVM control peptide. One FVB mouse was injected with one treatment in each experiment, with the experiment being repeated for a total of two mice in each treatment group. The scrambled siRNA has no homology with the *prnp* gene and the RVM peptide does not specifically target any cellular receptors. Protein and mRNA levels were assessed in the brain and kidney four days after treatment using flow cytometry and ddPCR, respectively. Normalized median fluorescent intensity (MFI), calculated as treated/untreated, is reported for flow cytometry to evaluate surface PrP<sup>C</sup>. Fold change of ddPCR results was calculated by dividing copy number/ $\mu$ L of treated mice with copy number/ $\mu$ L of untreated mice. All treated mice were compared to untreated mice for statistical analysis. Flow cytometry analysis of the brain revealed that surface PrP<sup>C</sup> levels are slightly but significantly decreased relative to the untreated control in mice treated with scrambled LSPCs (Figure 3.2A). However, the 14% reduction of PrP<sup>C</sup> using scrambled LSPCs did not equal the 40-50% reduction in PrP<sup>C</sup> using 1672 LSPCs. The opposite is true for mice treated with RVM peptide LSPCs as they have a slight increase in MFI in the brain (Figure 3.2A). Protein analysis in the kidney revealed that scrambled LSPCs decrease surface PrP<sup>C</sup> levels as much as 1672 LSPCs, indicating that the treatment alone without a specific siRNA or peptide causes a decrease in surface PrP<sup>C</sup> (Figure 3.2C). Scrambled LSPCs also reduce the number of PrP<sup>C</sup>-positive kidney cells (Figure A.2). mRNA analysis of both brain (Figure 3.2B) and kidney (Figure 3.2D) cells revealed that both the scrambled LSPCs and RVM peptide LSPCs increased the amount of PrP<sup>C</sup> mRNA transcripts within these tissues four days after treatment.

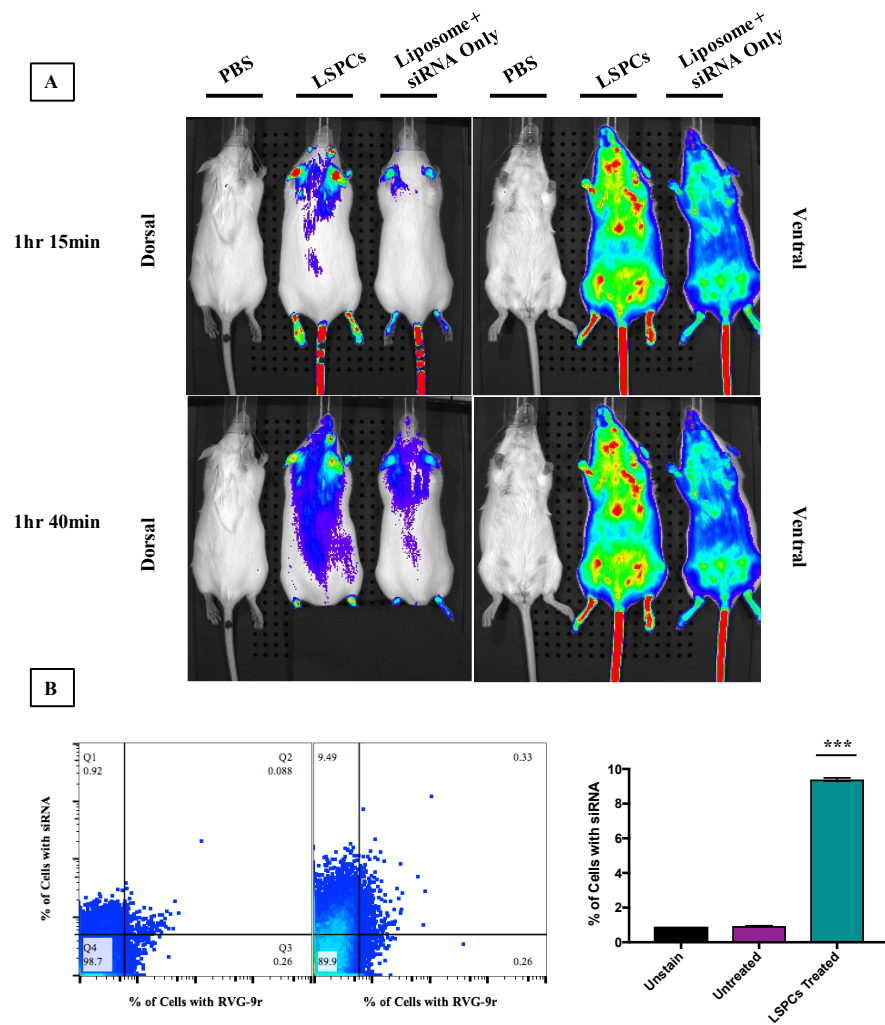


**Figure 3.1. LSPCs injected intravenously deliver PrP<sup>C</sup> siRNA to the brain.**

One mouse was used as an untreated control and injected with 1X PBS. Two mice were injected with either full LSPCs or liposome+siRNA only (no peptide). *In vivo* live imaging was performed one to two hours after injection to determine biodistribution and flow cytometry was performed on all mice 24 hours after injection to determine if PrP<sup>C</sup> siRNA was delivered to neuronal cells. A) *in vivo* live imaging shows that the LSPCs are delivered to the area around the brain one to two hours after injection. More PrP<sup>C</sup> siRNA is observed in the area around the brain using the RVG-9r neuro-targeting peptide than is without (liposome+siRNA only) B) Flow cytometry analysis revealed that PrP<sup>C</sup> siRNA is found in neuronal cell 24 hours after injection in these treated mice compared to the untreated.

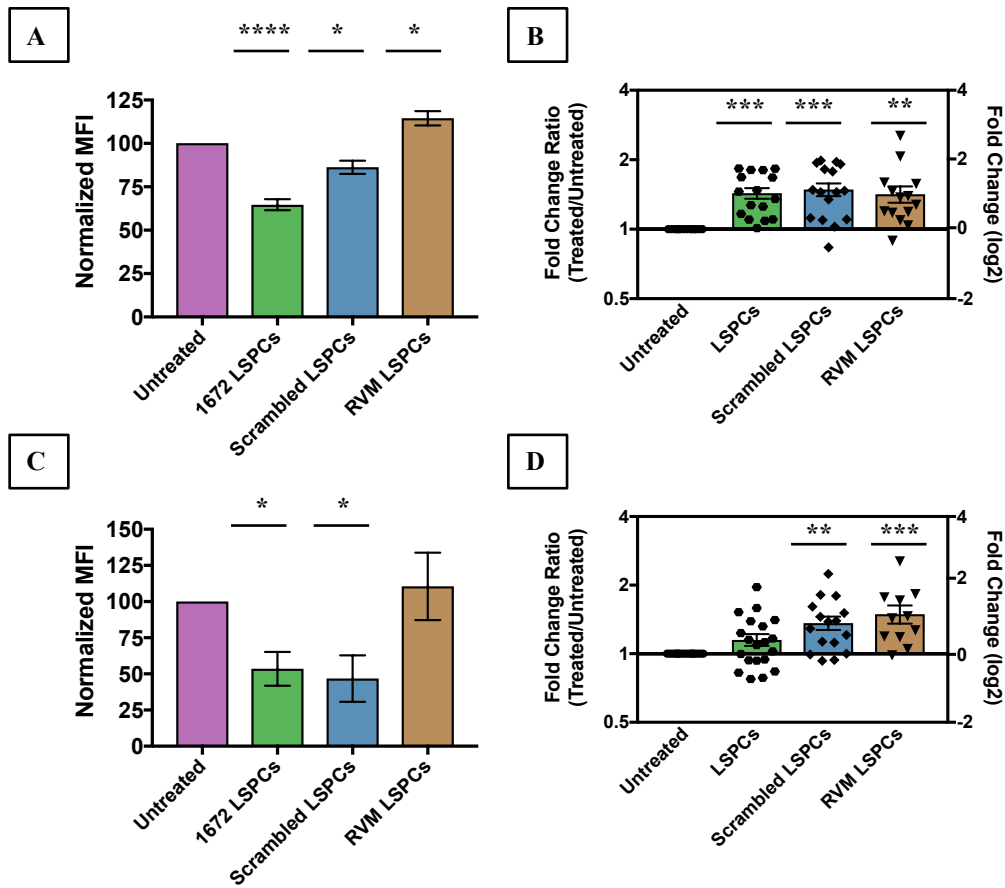


**Figure 3.2. Scrambled LSPCs and control peptide LSPCs cause an increase in PrP<sup>C</sup> mRNA levels.**

One mouse was injected with one treatment group for each experiment. The experiment was repeated for a total of two mice for each treatment group. All mice across the experiments were treated with either PBS or LSPCs for four days. A) Flow cytometry analysis of PrP<sup>C</sup> protein levels in the brains of treated mice revealed a 10-15% decrease in protein levels with the use of scrambled siRNA LSPCs and an increase in protein levels using RVM LSPCs. Normalized median fluorescent intensity (MFI) of PrP<sup>C</sup> levels in the brain of treated mice to untreated control. B) Neuronal PrP<sup>C</sup> mRNA analysis of treated mice showed an increase in PrP<sup>C</sup> mRNA levels in all LSPCs-treated mice compared to untreated control. C) Surface PrP<sup>C</sup> levels in the kidney were significantly decreased using scrambled siRNA LSPCs. D) mRNA analysis of PrP<sup>C</sup> levels in the kidney of treated mice also revealed a 1- to 2-fold increase in PrP<sup>C</sup> mRNA levels in this organ. Error bars indicate SEM. \* p<0.05, \*\* p<0.01, \*\*\* p<0.001, \*\*\*\* p<0.0001. One-way ANOVA with Dunnett's multiple comparisons.

***Analysis of cells that bind RVG-9r within the brain and kidney of wild-type mice***

To assess the number of cells that contain nAChRs and that the LSPCs target, both in the brain and kidney, primary cells were incubated with anti-PrP antibody BAR-224 and RVG-9r labeled with Dylight 650. Flow cytometry analysis was performed. In this experiment, BAR-224 bound to 96.4% of neuronal cells, while RVG-9r bound to on average about 87% of neuronal cells (Figure 3.3A). Within neurons that bound RVG-9r, 51% express PrP<sup>C</sup>. In the kidney, BAR-224 recognizes less than 5% of the cells as PrP-positive (Figure 3.3B). RVG-9r, on the other hand, binds to 95% of kidney cells. Within the 95% RVG-9r positive cells, 52% are positive for BAR-224 staining (Figure 3.3B). The discrepancy between the BAR-224 binding alone and BAR-224 binding RVG-9r positive cells in the kidney is not understood.

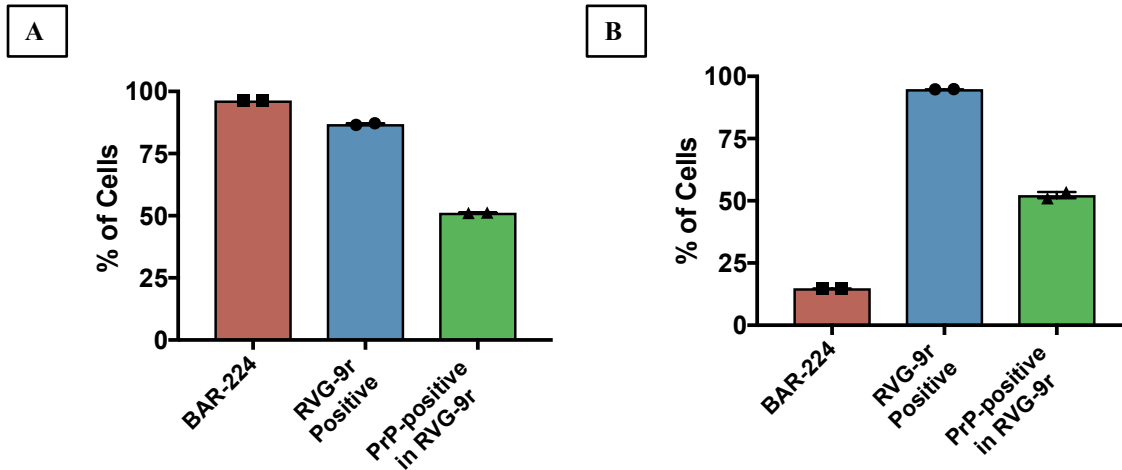


***Figure 3.3. RVG-9r binds to the majority of neuronal and kidney cells.***

A) About 90% of cells in the brain have surface PrP<sup>C</sup> as shown by binding of the anti-PrP<sup>C</sup> antibody BAR-224. A slightly smaller portion (80%) of cells bind RVG-9r, indicating that these cells have nAChRs. Within the cells that bind RVG-9r, about 50% express PrP<sup>C</sup>. B) Only about 5-10% of cells within the kidney have PrP<sup>C</sup> on the surface, whereas almost 90% of kidney cells bind to RVG-9r.

**Study design of LSPCs treatments with CR1/2 hemi mice and CD1 wild-type mice**

Two mouse lines, CR1/2 hemizygous (hemi) and CD1 wild-type, were utilized to assess the pharmacodynamics of LSPCs over time (Figure 3.4). CR1/2 hemi mice, on a C57Bl/6 background, were used to ensure that the results we obtained using the CD1 mice were not due solely to the background genetics of that mouse line. The transgenic nature of the CR1/2 hemi mice does not affect neuronal PrP<sup>C</sup> levels (Figure A.3). Both CR1/2 hemi mice and CD1 mice were intravenously treated once through the tail vein with LSPCs. At each time point for each mouse line, there was one untreated mouse injected with 1X PBS and three treated mice injected with LSPCs. Protein and mRNA levels were assessed at varying time points after treatment using flow cytometry, western blots, and ddPCR. PrP<sup>C</sup> protein and mRNA levels of CR1/2 hemi mice were measured 24 hours, 48 hours, and 4 days after a single treatment, whereas levels of CD1 mice were measured at 48 hours, 4, 15, and 21 days after treatment. Total protein was calculated using western blots with an anti-PrP<sup>C</sup> antibody conjugated to horseradish peroxidase and surface protein was measured using flow cytometry using the same anti-PrP<sup>C</sup> antibody conjugated to Dylight 650. Analysis of PrP<sup>C</sup> mRNA levels employed ddPCR. Flow cytometry results are presented as median fluorescent intensity (MFI), as a measure of surface PrP<sup>C</sup>, amount of PrP<sup>C</sup> positive cells, and fold change of treated MFI divided by untreated MFI. ddPCR analysis is presented as copy number/ $\mu$ L, fold change and grouped fold change. Copy number/ $\mu$ L is shown to illustrate the true physiological conditions at time of sampling. Fold change was calculated as treated divided by untreated, and divided again by the increase observed in control LSPCs experiments using scrambled and control

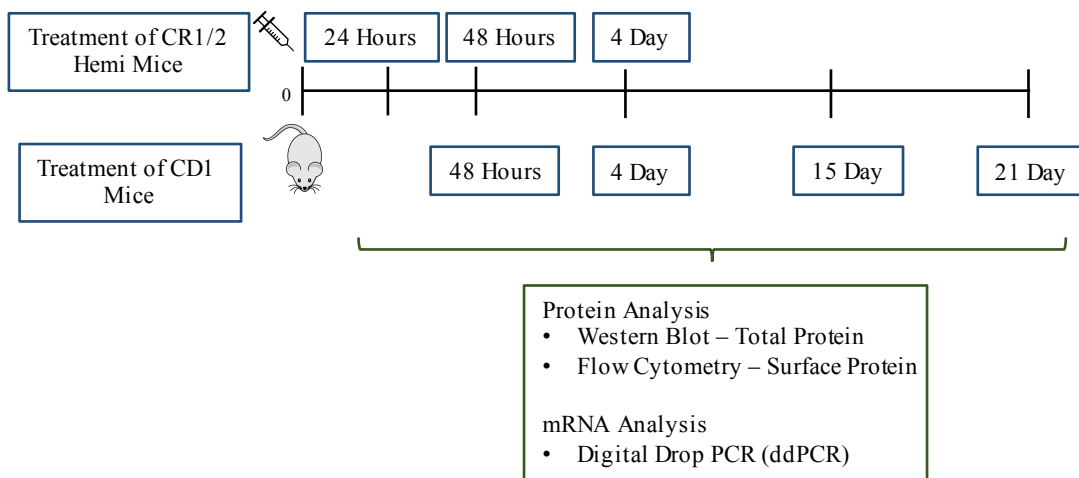


**Figure 3.4. Study design of pharmacodynamics experiments of CR1/2 hemi and CD1 mice.**

peptide LSPCs. Fold change was calculated this way to show the effect of only the PrP<sup>C</sup> siRNA. Grouped fold change is presented to show biological significance. For all statistical analyses, all treated mice were compared to untreated controls.

***Total protein analysis reveals a decrease in total protein at various time points in both CR1/2 hemi and CD1 mice***

After CR1/2 hemi or CD1 mice were treated, brain and kidneys were collected at different time points. Total protein analysis of PrP<sup>C</sup> was conducted on ½ a hemisphere of the brain at these time points. The hemispheres were homogenized at 20% w/v and electrophoretically separated using a western blot at a 1% w/v. Actin and total protein were used as loading controls to ensure that the same amount of protein was loaded in each sample and to normalize PrP<sup>C</sup> levels. Densitometry was performed using ImageJ software provided by the NIH. The Y-axis on each fold change graph was log transformed to guarantee that a 2-fold increase was viewed aesthetically like a 2-fold decrease. The right Y-axis shows the actual fold change values.

Unfortunately, the western blots reveal little statistical significance of either CR1/2 hemi or CD1 mice. Figure 3.5A shows representative western blots of the PrP<sup>C</sup> and actin samples for each sample. At 48 hours after treatment in CR1/2 hemi mice, total neuronal PrP<sup>C</sup> protein levels are reduced in two out of the three treated mice (Figure 3.5C). The reduction equates to a 1- or 2-fold decrease in PrP<sup>C</sup> levels compared to untreated control. No statistical significance was found between untreated and treated mice in CR1/2 hemi mice at 24 hours (Figure 3.5B) or 4 days after treatment (Figure 3.5D). For the CD1 mice, there is a statistical difference in total neuronal PrP<sup>C</sup> levels at 21 days after LSPCs treatment in two out of the three mice. PrP<sup>C</sup> is decreased 5-fold in two of the treated mice compared to the untreated control (Figure 3.6D). No statistical significance is seen in PrP<sup>C</sup> levels in CD1 treated mice at any other time points compared to the untreated control (Figure 3.6A-C).

***CR1/2 hemi mice treated with LSPCs have decreased surface PrP<sup>C</sup> with variable mRNA levels at 24, 48 hours, and 4 days after treatment***

To determine the pharmacodynamics of the PrP<sup>C</sup> siRNA and LSPC treatment in C57Bl/6 mice, CR1/2 hemi mice were anesthetized and injected with either 1X PBS (one mouse) or 1672 LSPCs (three mice) at various time points. Surface PrP<sup>C</sup> and total mRNA levels in the brain and kidney were assessed using flow cytometry and ddPCR analysis, respectively. Expression in the kidney was assessed due to some off-target effects observed in previous *in vitro* experiments, so kidney levels were measured to evaluate any potential adverse effects of the LSPCs treatment.

mRNA levels are shown for each treated mouse as copy number/ $\mu\text{L}$  and fold change. Fold change was calculated as discussed in the study design section. The time points were not repeated.

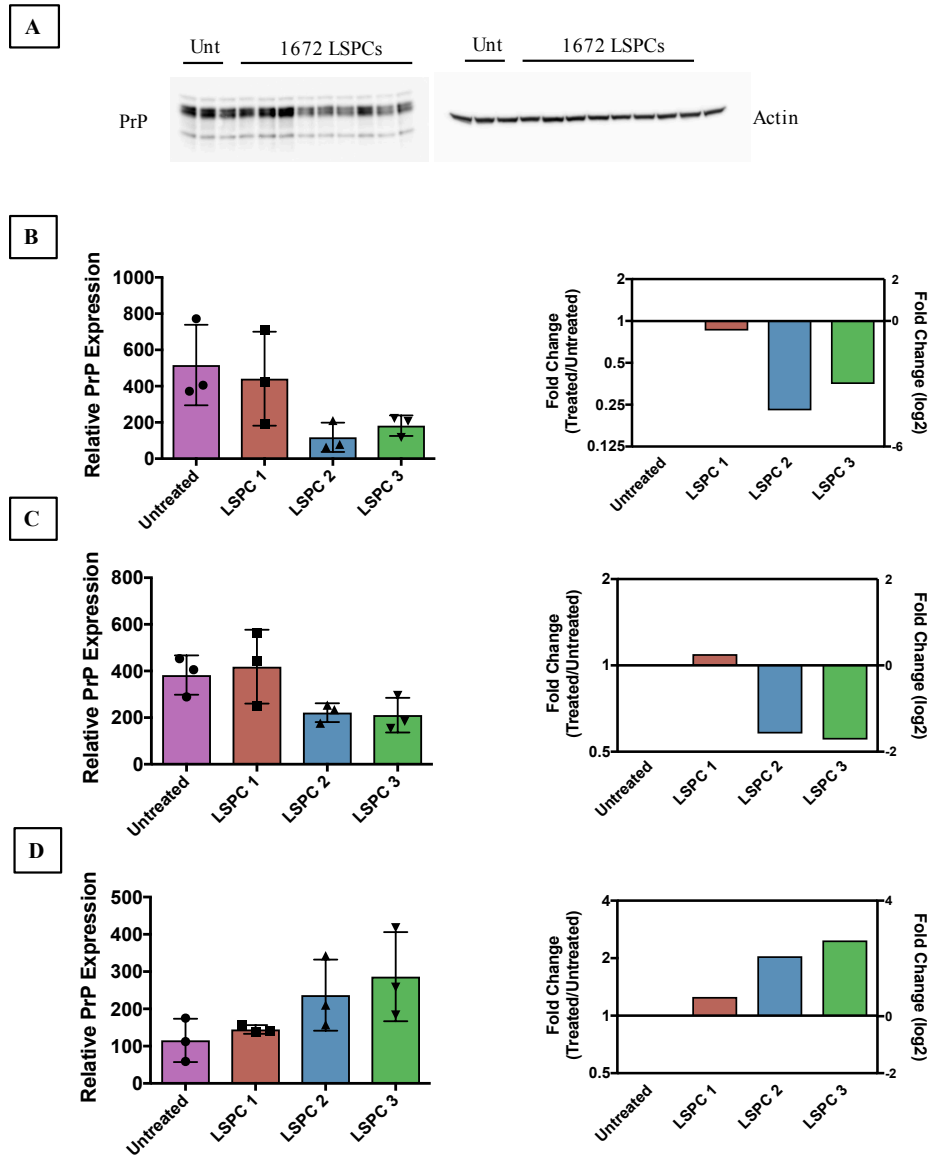


**Figure 3.5. Western blot analysis of PrP<sup>C</sup> levels in the brains of CR1/2 treated mice.**

A) Representative western blot analysis of PrP<sup>C</sup> and Actin blots of LSPCs-treated mice. Unt = Untreated control  
 B) At 24 hours after treatment, two out of the three treated mice have decreases in total PrP<sup>C</sup> levels (not statistically significant). C) Two out of the three LSPCs-treated mice at 48 hours after treatment had decreases in the amount of total PrP<sup>C</sup> in the brain, although it was not statistically different than untreated. D) All CR1/2 treated mice had increased levels of total PrP<sup>C</sup> four days after LSPCs treatment. Error bars represent SD. The fold change graphs do not contain error bars as each technical replicate was averaged into one mean before fold change calculation. The fold change graph is only a visual representation of the changes in total PrP<sup>C</sup> protein in the brains of treated mice so no statistical analyses were performed on the fold change graphs. One-way ANOVA with Dunnett's multiple comparisons

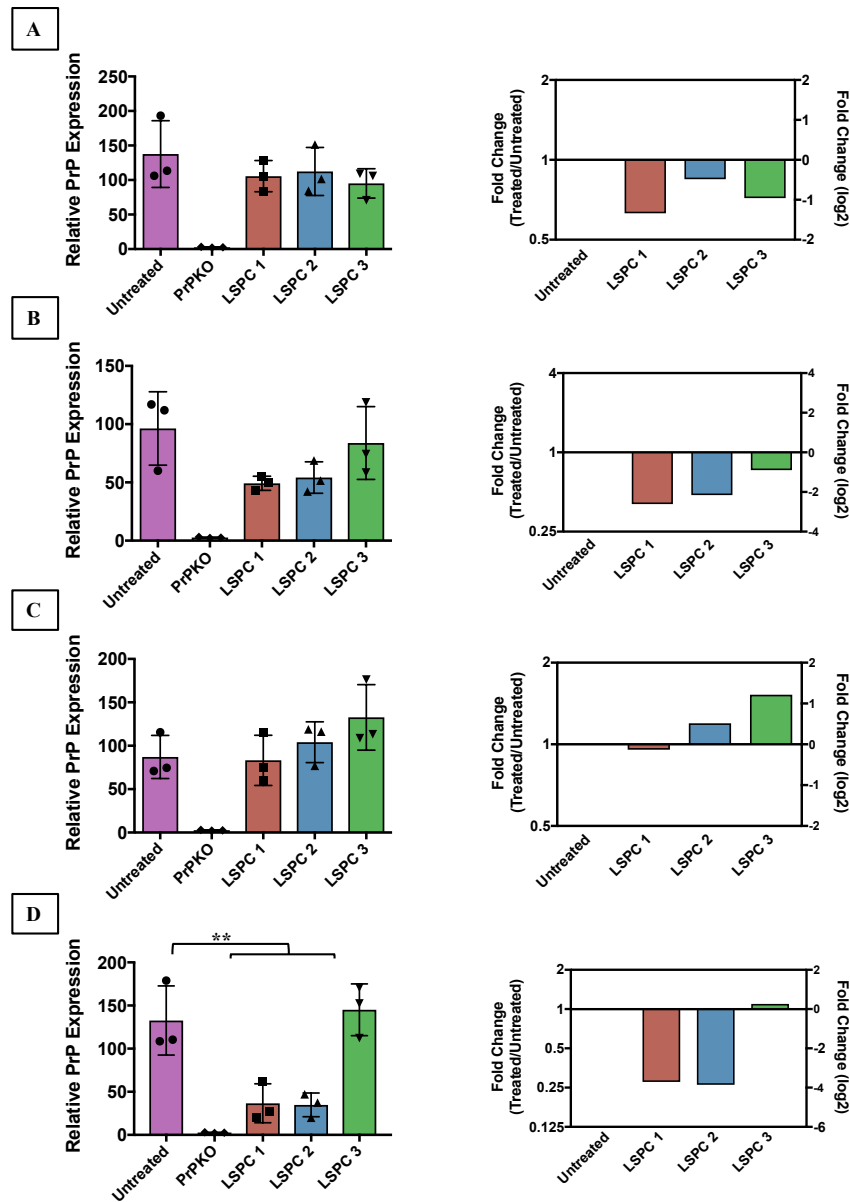


**Figure 3.6. Western blot analysis of PrP<sup>C</sup> levels in the brains of CD1 treated mice.**

A) Total PrP<sup>C</sup> analysis of the brain 48 hours after LSPCs-treatment in CD1 mice revealed no statistical difference between untreated controls, with perhaps a 1-fold decrease in all LSPCs-treated mice. B) Two out of the three LSPCs-treated mice at 4 days after treatment showed a 2-fold decrease in total PrP<sup>C</sup> levels in the brain. C) No statistical difference is observed 15 days after LSPCs treatment with one mouse having a 1-fold or less increase in total PrP<sup>C</sup> levels. D) Total neuronal PrP<sup>C</sup> levels are significantly decreased in two out of the three mice 21 days after LSPCs treatment of CD1 mice. Error bars represent SD. The fold change graphs do not contain error bars as each technical replicate was averaged into one mean before fold change calculation. The fold change graph is only a visual representation of the changes in total PrP<sup>C</sup> protein in the brains of treated mice so no statistical analyses were performed on the fold change graphs. \*\* p<0.01. One-way ANOVA with Dunnett's multiple comparisons.

All mice treated with LSPCs had a decrease in surface PrP<sup>C</sup> levels in the brain at 24 hours after treatment (Figure 3.7A). There was no effect on the number of PrP<sup>C</sup>-positive cells, but the median fluorescent intensity (MFI) of the brain samples was reduced in all treated mice compared to the untreated control. The 35-40% decrease in brain MFI was more significant than the 14% reduction observed with scrambled LSPCs. The opposite was true in the kidney where the MFI was not decreased compared to the untreated controls (Figure 3.7C). When the MFI of the treated mice is normalized to the MFI of the untreated control, one out of the three mice does have a decrease in surface PrP<sup>C</sup>. The reduction in the kidney might be due to the siRNA treatment in general as the scrambled siRNA LSPCs resulted in a decline of MFI in the kidney. The number of PrP<sup>C</sup>-positive cells in the kidney was also significantly reduced; however, again, this could be due to an effect of just the treatment and not the PrP<sup>C</sup> siRNA as this effect was seen using scrambled siRNA (Figure 3.7C). PrP<sup>C</sup> mRNA levels in the brain in two out of the three mice were also significantly decreased when analyzed individually but there is no difference when grouped (Figure 3.7B). Interestingly, the mouse with the lowest surface PrP<sup>C</sup> MFI had the highest copy number/ $\mu$ L of PrP<sup>C</sup> mRNA. mRNA levels were also increased 2-fold in the kidney across all treated mice. When grouped, the treated mice had significantly higher PrP<sup>C</sup> mRNA levels in the kidney compared to the untreated control (Figure 3.7D).

At 48 hours post-treatment, flow cytometry data is only available for the brain due to a staining error in the kidney. Surface neuronal PrP<sup>C</sup> levels are decreased significantly in all three treated mice (Figure 3.8A). The number of PrP<sup>C</sup>-positive cells also decreased in the brain at this time point. When normalized to the untreated mouse, the three treated mice have a 20-25% reduction in surface PrP<sup>C</sup> levels (MFI) (Figure 3.8A). mRNA analysis shows that all three treated mice have a 1- to 2-fold decrease in fold change of PrP<sup>C</sup> mRNA levels in the brain compared to the untreated mouse (Figure 3.8B). When grouped, PrP<sup>C</sup> mRNA levels in the brain of treated mice is statistically different than the untreated control (Figure 3.8B). Two out of the three treated mice have decreased PrP<sup>C</sup> mRNA levels in the kidney, while one mouse is increased, but there is no statistical significance in the grouped cohort (Figure 3.8C).

Surface PrP<sup>C</sup> levels are decreased in both the brain and the kidney four days post-treatment in all three treated CR1/2 hemi mice. The MFI in the brain is decreased 25-50% (Figure 3.9A), and the MFI in the kidney is reduced 10-50% (Figure 3.9C) in the treated mice compared to the untreated control. The number of PrP<sup>C</sup>-positive cells is not statistically different for either the brain or the kidney at this time point (Figure 3.9A and C). While the group fold change of PrP<sup>C</sup> mRNA levels of all treated mice is not statistically different from the untreated control

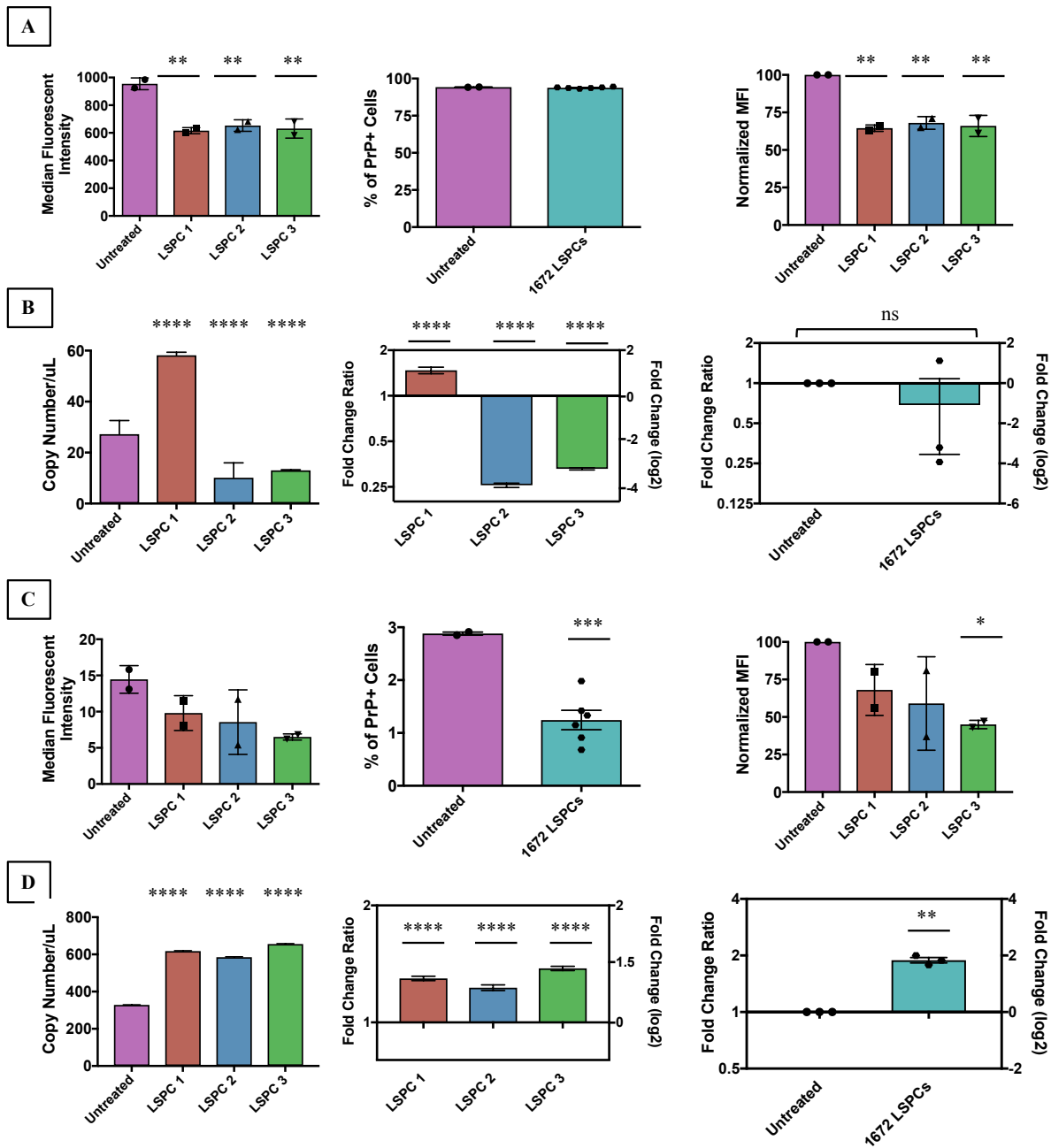


**Figure 3.7. Flow cytometric and ddPCR analysis of CR1/2 hemi mice 24 hours after LSPCs treatment.**

A) Surface PrP<sup>C</sup> but not the amount of PrP<sup>C</sup>+ cells decreased in the brains of CR1/2 mice treated with LSPCs 24 hours after treatment. The decrease equated to a 25% decrease in surface PrP<sup>C</sup> levels. B) One LSPCs treated mouse had an increase in neuronal PrP<sup>C</sup> mRNA levels 24 hours after treatment, while the other two treated mice had a 2-fold decrease in PrP<sup>C</sup> mRNA. C) Only one mouse had a decrease in surface PrP<sup>C</sup> levels in the kidney at this time point. All mice had a significant decrease in the number of PrP<sup>C</sup>+ cells in the kidney. D) All mice had an increase in PrP<sup>C</sup> mRNA in the kidney 24 hours after LSPCs treatment. Error bars for graphs with individual treated mice indicate SD. Error bars for graphs with grouped treated mice indicate SEM. \* p<0.05, \*\* p<0.01, \*\*\* p<0.001, \*\*\*\* p<0.0001. One-way ANOVA with Dunnett's multiple comparisons and t test.

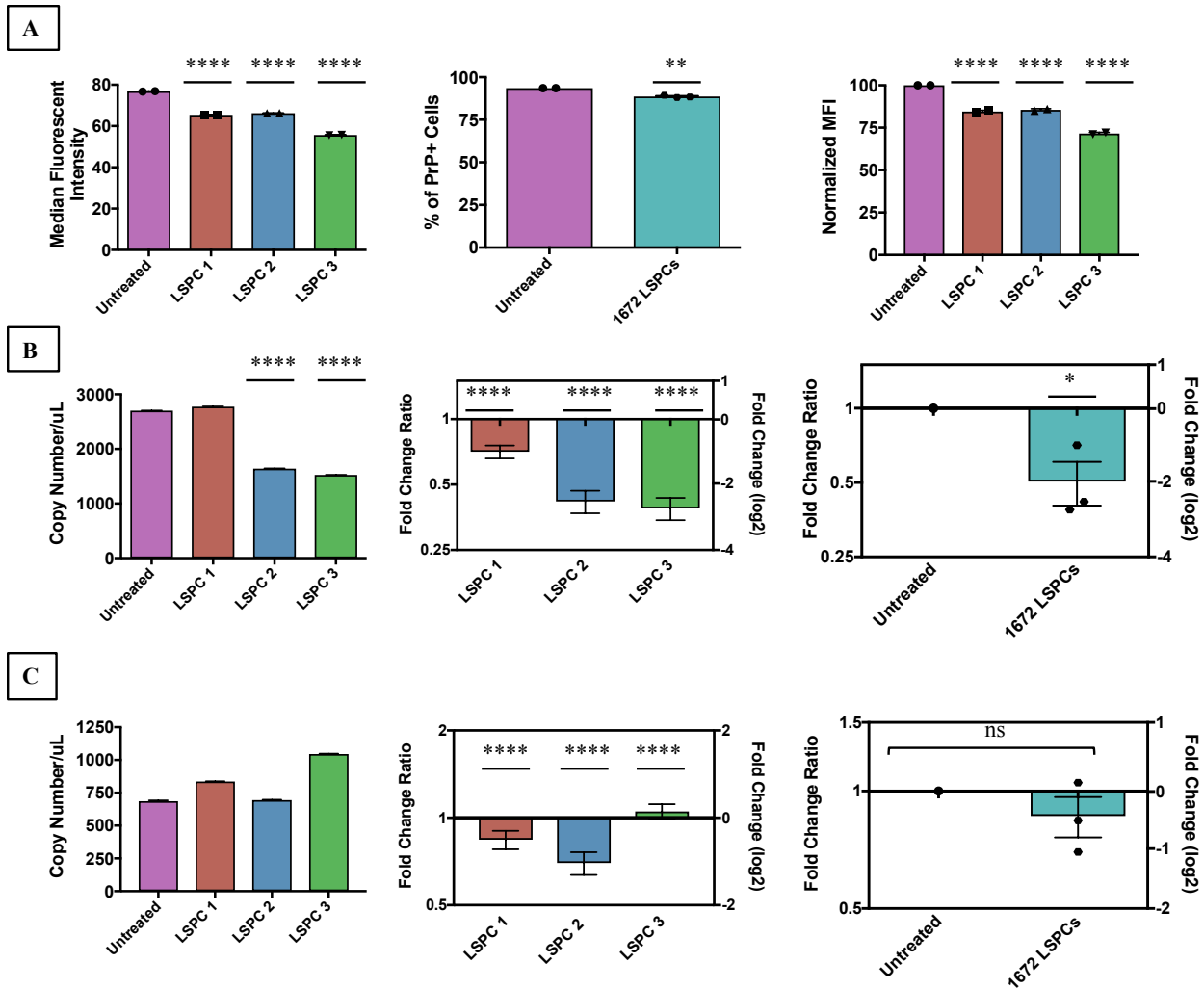


**Figure 3.8. Flow cytometric and ddPCR analysis of CR1/2 hemi mice 48 hours after LSPCs treatment.**

A) All three CR1/2 hemi LSPCs-treated mice had a decrease in surface PrP<sup>C</sup> in the brain 48 hours after treatment, with a slight but statistically significant decrease in the number of PrP<sup>C</sup>+ cells. B) Two out of the three treated mice had significant decreases in PrP<sup>C</sup> mRNA, 1- to 2-fold, in the brain at this time point. C) mRNA analysis of CR1/2 LSPCs-treated mice showed slight changes in PrP<sup>C</sup> mRNA in the kidney 48 hours after LSPCs treatment but no statistical significance is seen when the mice are grouped. Error bars for graphs with individual treated mice indicate SD. Error bars for graphs with grouped treated mice indicate SEM. \* p<0.05, \*\* p<0.01, \*\*\*\* p<0.0001. One-way ANOVA with Dunnett's multiple comparisons and t test.

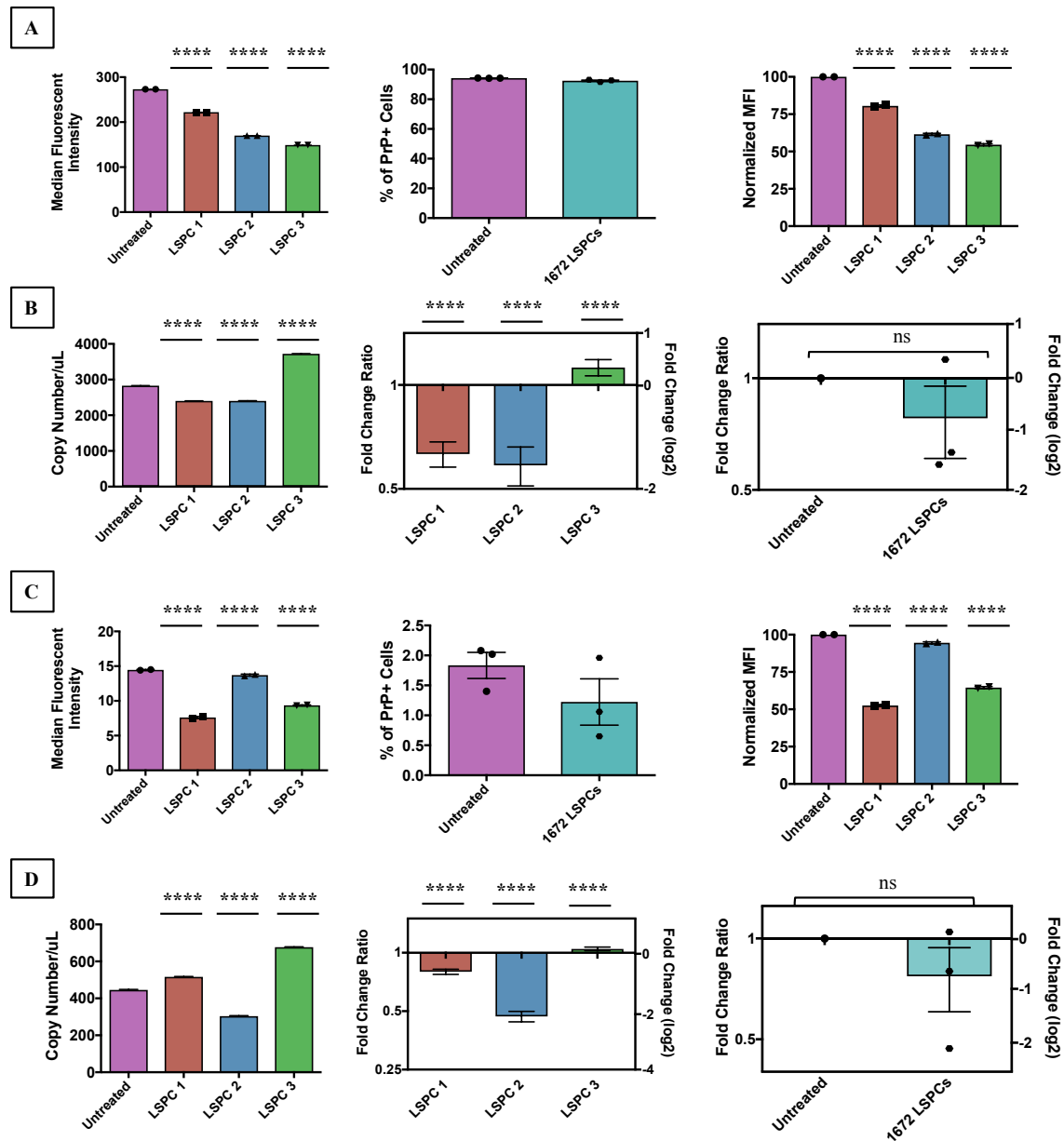


**Figure 3.9. Flow cytometric and ddPCR analysis of CR1/2 hemi mice four days after LSPCs treatment.**

A) At 4 days after treatment, all three CR1/2 LSPC-treated mice had a decrease in surface PrP<sup>C</sup> levels in the brain. This was a 25-50% decrease across all three treated mice. There was no decrease in the number of PrP<sup>C</sup>+ cells in the brain at this time point. B) Two out of the three LSPCs treated mice had decreased levels of neuronal PrP<sup>C</sup> mRNA 4 days after treatment. This decrease was 1.5- to 2-fold lower than controls. C) All three LSPCs-treated mice also had a decrease (10-50%) in surface PrP<sup>C</sup> in the kidney 4 days after treatment. D) Kidney PrP<sup>C</sup> mRNA levels varied in the three CR1/2 treated mice. One LSPCs-treated mouse had a 2-fold decrease but grouped the mice do not have a significant decrease in kidney PrP<sup>C</sup> mRNA levels. Error bars for graphs with individual treated mice indicate SD. Error bars for graphs with grouped treated mice indicate SEM. \*\*\*\* p<0.0001. One-way ANOVA with Dunnett's multiple comparisons and t test.

in either organ, there are some mRNA expression differences between the individual treated mice. In the brain, two out of the three treated mice have decreased levels of PrP<sup>C</sup> mRNA, while the third treated mouse has an increase in PrP<sup>C</sup> mRNA levels (Figure 3.9B). Again, the mouse with the lowest PrP<sup>C</sup> MFI also has the highest PrP<sup>C</sup> copy number/ $\mu$ L levels in the brain. In the kidney, two out of the three treated mice have a decrease in PrP<sup>C</sup> mRNA levels, a <1- to 2-fold reduction. The other mouse has a < 1-fold increase in PrP<sup>C</sup> mRNA levels (Figure 3.9D).

***LSPCs treatment results in a reduction of surface PrP<sup>C</sup> protein levels and PrP<sup>C</sup> mRNA levels in CD1 wild-type mice***

CD1 mice were also treated with LSPCs intravenously to assess whether the LSPCs are efficacious in mice on different backgrounds. For each time point, one mouse was treated with 1X PBS as an untreated control and three mice were treated with LSPCs. Brain and kidney samples were collected at 48 hours, 4, 15, and 21 days post-treatment. Protein analysis was performed using flow cytometry, and mRNA levels were analyzed using ddPCR. Fold change of ddPCR analysis was calculated as explained in the study design section. The time points were not repeated.

CD1 mice responded differently than the CR1/2 hemi mice at 48 hours post-treatment. Unlike the CR1/2 hemi mice, CD1 mice did not have a decrease in surface PrP<sup>C</sup> levels in the brain at this time point. There was also no reduction in the number of PrP<sup>C</sup>-positive cells in this organ (Figure 3.10A). Even though the MFI was not decreased in the brain, mRNA analysis revealed that all three treated mice had reduced levels of PrP<sup>C</sup> mRNA (Figure 3.10B). This decrease was between a 1- and a 2-fold decrease in mRNA levels. Grouped the 1672 siRNA-treated mice had a statistically significant reduction in fold change of PrP<sup>C</sup> mRNA levels in the brain compared to the untreated control (Figure 3.10B). The kidney at 48 hours post-treatment in CD1 mice had a different response than the brain by flow cytometry. Two out of the three treated mice have a decrease in MFI, and the number of PrP<sup>C</sup>-positive cells is reduced to numbers seen in PrP-null mice. The reduction in surface PrP<sup>C</sup> of these two mice is greater than 50% in one mouse and around 75% in the other (Figure 3.10C). The decline of PrP<sup>C</sup> in the kidney could be due to LSPCs treatment in general; however, this reduction is more than what was observed with scrambled siRNA. mRNA analysis of the kidney revealed that PrP<sup>C</sup> mRNA copy number was increased in two out of the three treated mice. Grouped all three treated mice had no statistical difference to the untreated control (Figure 3.10D).

At four days post-treatment in CD1 mice, the MFI is not significantly decreased in the brain nor the number of PrP<sup>C</sup>-positive cells. However, when the treated mice are normalized to the untreated control, there is a statistically

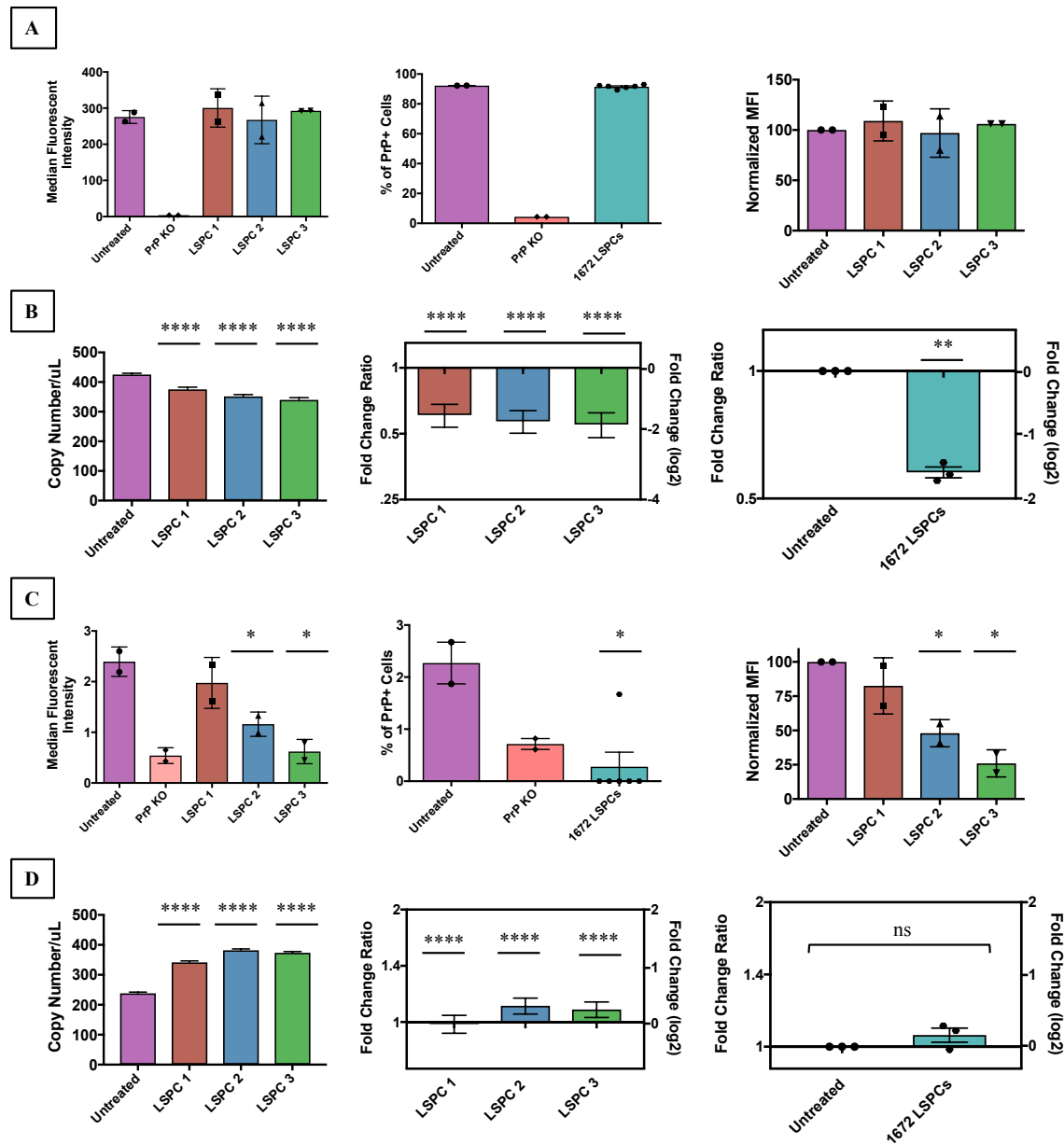


**Figure 3.10. Flow cytometric and ddPCR analysis of CD1 mice 48 hours after LSPCs treatment.**

A) None of the CD1 LSPCs-treated mice had a significant decrease in either neuronal surface PrP<sup>C</sup> levels or the number of PrP<sup>C</sup>+ cells in the brain at 48 hours after treatment B) All three LSPCs-treated mice had ~2-fold decreases in PrP<sup>C</sup> mRNA levels at this time point, with statistical significance when grouped. C) Two out of the three treated mice had decreased surface PrP<sup>C</sup> in the kidney, while all three mice had significant decreases in the number of PrP<sup>C</sup>+ cells in this organ. D) PrP<sup>C</sup> mRNA varies with LSPCs treatment 48 hours after treatment in CD1 mice, with two out of the three mice showing extremely slight increases in PrP<sup>C</sup> mRNA levels. No difference in mRNA levels observed when mice are grouped. Error bars for graphs with individual treated mice indicate SD. Error bars for graphs with grouped treated mice indicate SEM. \* p<0.05, \*\* p<0.01, \*\*\*\* p<0.0001. One-way ANOVA with Dunnett's multiple comparisons and t test.

significant drop in surface PrP<sup>C</sup> in the brain in all three treated mice (Figure 3.11A). PrP<sup>C</sup> mRNA levels in the brain in two out of the three mice are slightly decreased compared to controls (Figure 3.11B). The third treated mouse has slightly increased PrP<sup>C</sup> mRNA levels than the untreated control. Grouping the treated mice show no statistical significance. The mouse with the lowest neuronal MFI also has the highest PrP<sup>C</sup> mRNA copy number and fold change (Figure 3.11A and B). In the kidney, again there is not an appreciable difference in MFI of PrP<sup>C</sup> between the untreated control and the treated mice. However, when the MFI of the treated mice is normalized to the untreated control, all three treated mice have a decrease in kidney surface PrP<sup>C</sup> (Figure 3.11C). Analysis of mRNA levels concurs with flow cytometry data in that all three treated mice have about a 2-fold or less decrease in PrP<sup>C</sup> mRNA in the kidney at this time point (Figure 3.11D). Grouping the treated mice is statistically significant (Figure 3.11D) The number of PrP<sup>C</sup>-positive cells in the kidney is not statistically different from untreated control (Figure 3.11C).

PrP<sup>C</sup> protein and mRNA levels were analyzed at 15 days to try to determine when the LSPCs treatment stops affecting CD1 mice. To our surprise, neuronal surface PrP<sup>C</sup> was decreased in two out of three mice at 15 days post-treatment (Figure 3.12A). Neuronal PrP<sup>C</sup> was reduced by 25%. There was no effect on the number of PrP<sup>C</sup>-positive cells in the brain at this time point. One treated mouse had an increase in PrP<sup>C</sup> mRNA levels in the brain, and two treated mice had a very slight decrease in mRNA levels, but when grouped the treated group was not statistically significant from the untreated control (Figure 3.12B). Again, the mouse with the greatest increase in PrP<sup>C</sup> copy number/ $\mu$ L levels had the most significant decrease in PrP<sup>C</sup> protein levels in the brain. Flow cytometry of surface PrP<sup>C</sup> in the kidney revealed that all three treated mice had decreased levels of PrP<sup>C</sup> (Figure 3.12C). MFI was reduced between 30% and 75% compared to the control. There was also a significant decline in the number of PrP<sup>C</sup>-positive cells in the kidney. The LSPC treatment alone, without PrP<sup>C</sup> siRNA, could have produced these results in the kidney. All treated mice had decreases in the fold change of PrP<sup>C</sup> mRNA levels in the kidney, with statistical significance when grouped (Figure 3.12D).

Since 15 days post-treatment showed significant decreases in PrP<sup>C</sup> levels, CD1 mice were treated out till 21 days to determine an endpoint of the treatment. Protein levels of neuronal PrP<sup>C</sup> are unchanged from the untreated control at this time point (Figure 3.13A), but, interestingly, the mRNA copy number is decreased in all three mice at 21 days post-treatment (Figure 3.13B). Fold change analysis shows that one treated mouse had a 3-fold decrease in PrP<sup>C</sup> mRNA levels in the brain, while the other two treated mice had less than a 2-fold decrease in mRNA. Grouped

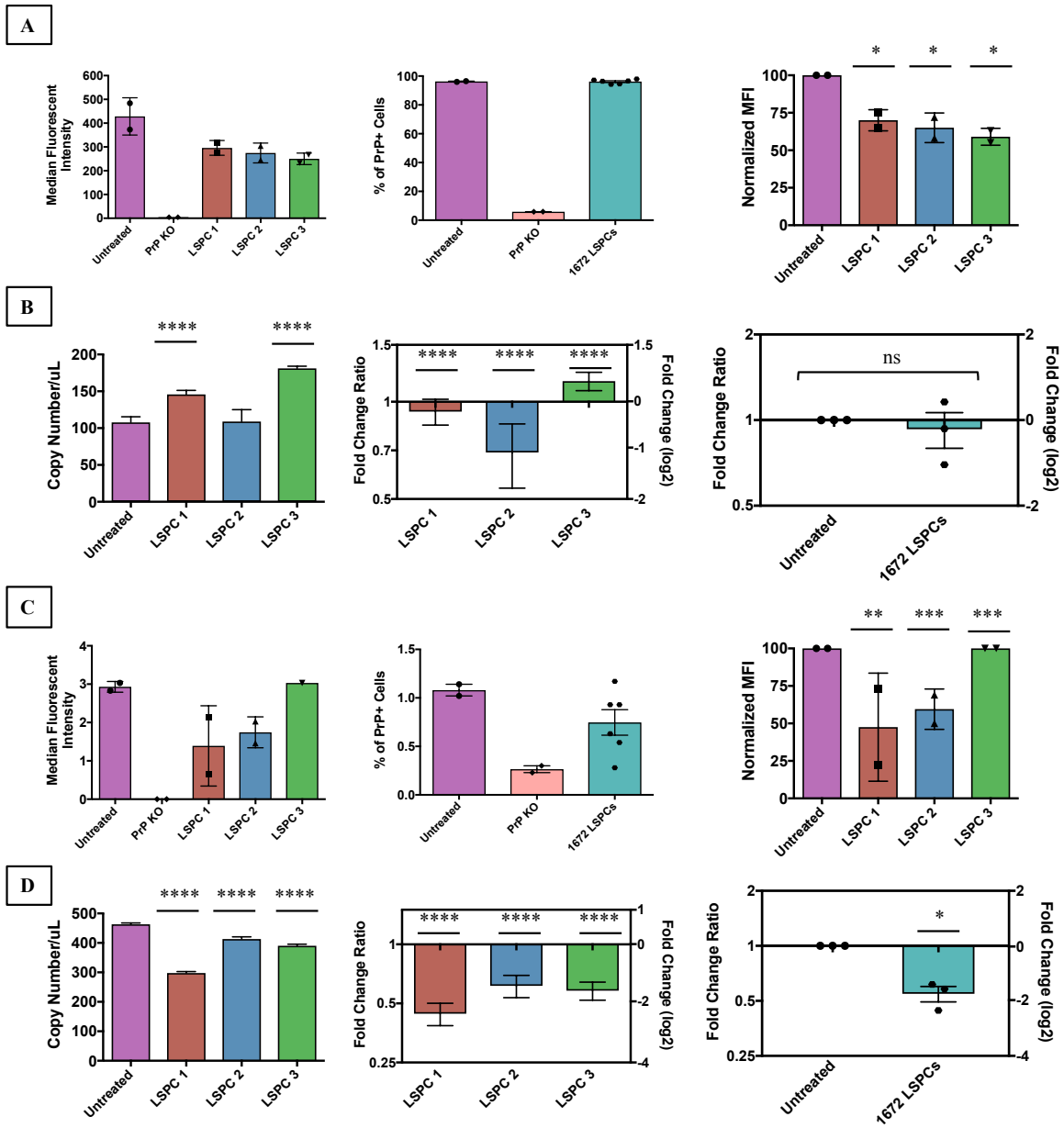


**Figure 3.11. Flow cytometric and ddPCR analysis of CD1 mice 4 days after LSPCs treatment.**

A) There is no statistical difference between PrP<sup>C</sup> MFI in the brains of untreated and treated mice at four days after LSPCs treatment but when the data is normalized to the untreated control all three treated mice have between 25-40% decrease in surface PrP<sup>C</sup>. B) Two LSPCs-treated mice have increased copy number compared to the untreated control. When the treated mice are normalized to treatment controls one LSPCs-treated mouse has a 1-fold decrease and one has a 1-fold increase in PrP<sup>C</sup> mRNA levels. Grouped the treated mice have no statistical difference in PrP<sup>C</sup> mRNA levels C) When PrP<sup>C</sup> MFI in the kidney of the treated mice is normalized to untreated controls, all three LSPCs treated mice have a decrease in surface PrP<sup>C</sup> levels in this organ at four days after treatment. D) All three LSPCs-treated mice have a decrease in PrP<sup>C</sup> mRNA levels, 2-fold or more, at four days after LSPCs treatment. Grouped there is a significant difference between the untreated and treated mice. Error bars for graphs with individual treated mice indicate SD. Error bars for graphs with grouped treated mice indicate SEM. \* p<0.05, \*\* p<0.01, \*\*\* p<0.001, \*\*\*\* p<0.0001. One-way ANOVA with Dunnett's multiple comparisons and t test.

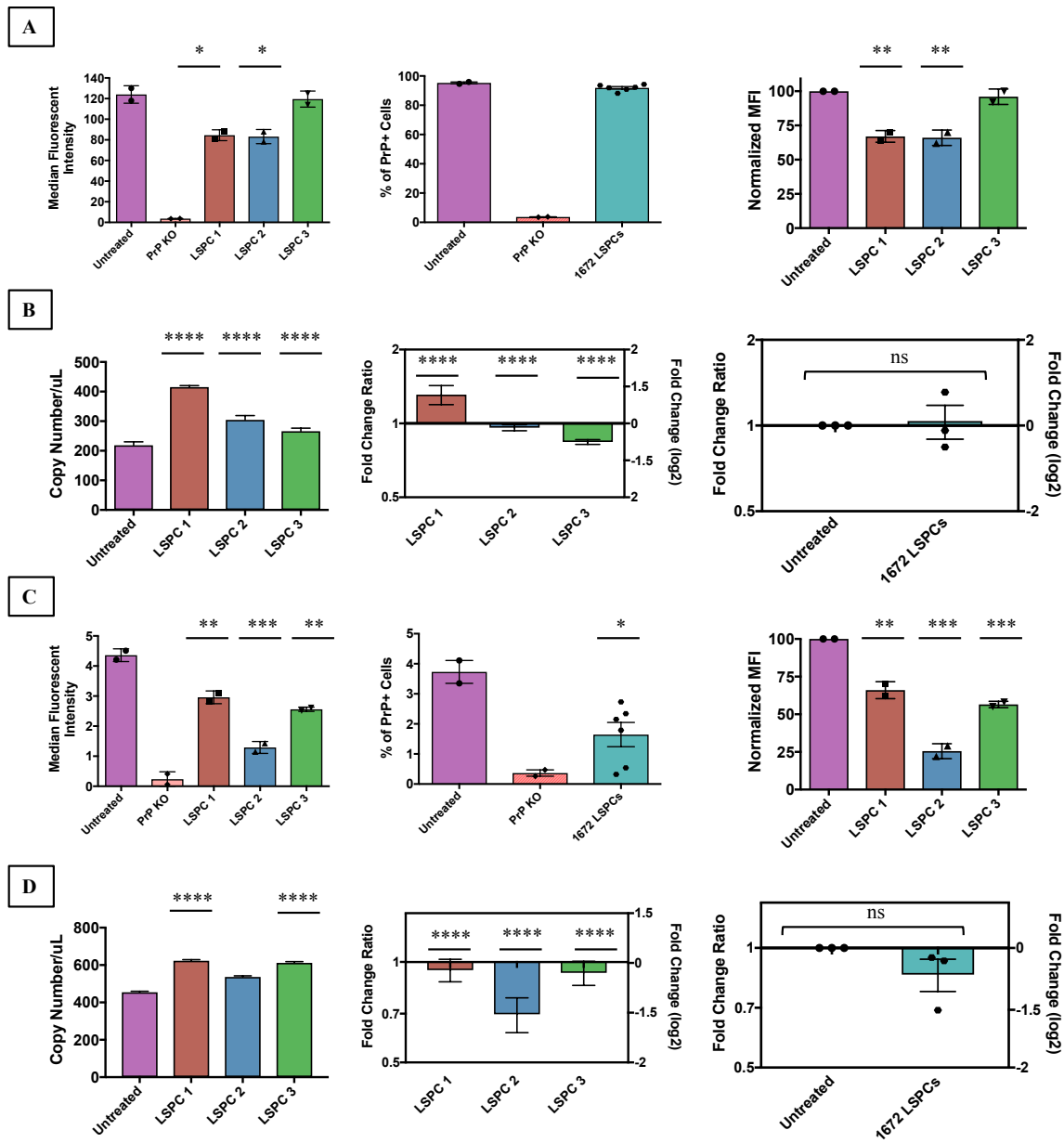


**Figure 3.12. Flow cytometric and ddPCR analysis of CD1 mice 15 days after LSPCs treatment.**

A) Two of the LSPCs-treated had had a 25% decrease in neuronal surface PrP<sup>C</sup> levels 15 days after LSPCs treatment. B) Corresponding to the flow cytometry data, two of the three LSPCs-treated mice had a decrease in PrP<sup>C</sup> mRNA levels in the brain when normalized to the untreated and treatment controls. Copy number analysis of PrP<sup>C</sup> mRNA revealed that all three LSPCs-treated mice had an increase in PrP<sup>C</sup> mRNA levels, which could be due to the treatment alone and not the PrP<sup>C</sup> siRNA. C) All three LSPCs-treated mice also had a decrease (30-75%) in surface PrP<sup>C</sup> in the kidney at this time point and a decrease in the number of PrP<sup>C</sup>+ cells in this organ. D) Two of the three LSPCs-treated mice had elevated PrP<sup>C</sup> copy number but when normalized to the untreated and treatment controls each treated mouse had a slight decrease in PrP<sup>C</sup> mRNA levels up to 1.5-fold lower. Error bars for graphs with individual treated mice indicate SD. Error bars for graphs with grouped treated mice indicate SEM. \* p<0.05, \*\* p<0.01, \*\*\* p<0.001, \*\*\*\* p<0.0001. One-way ANOVA with Dunnett's multiple comparisons and t test.

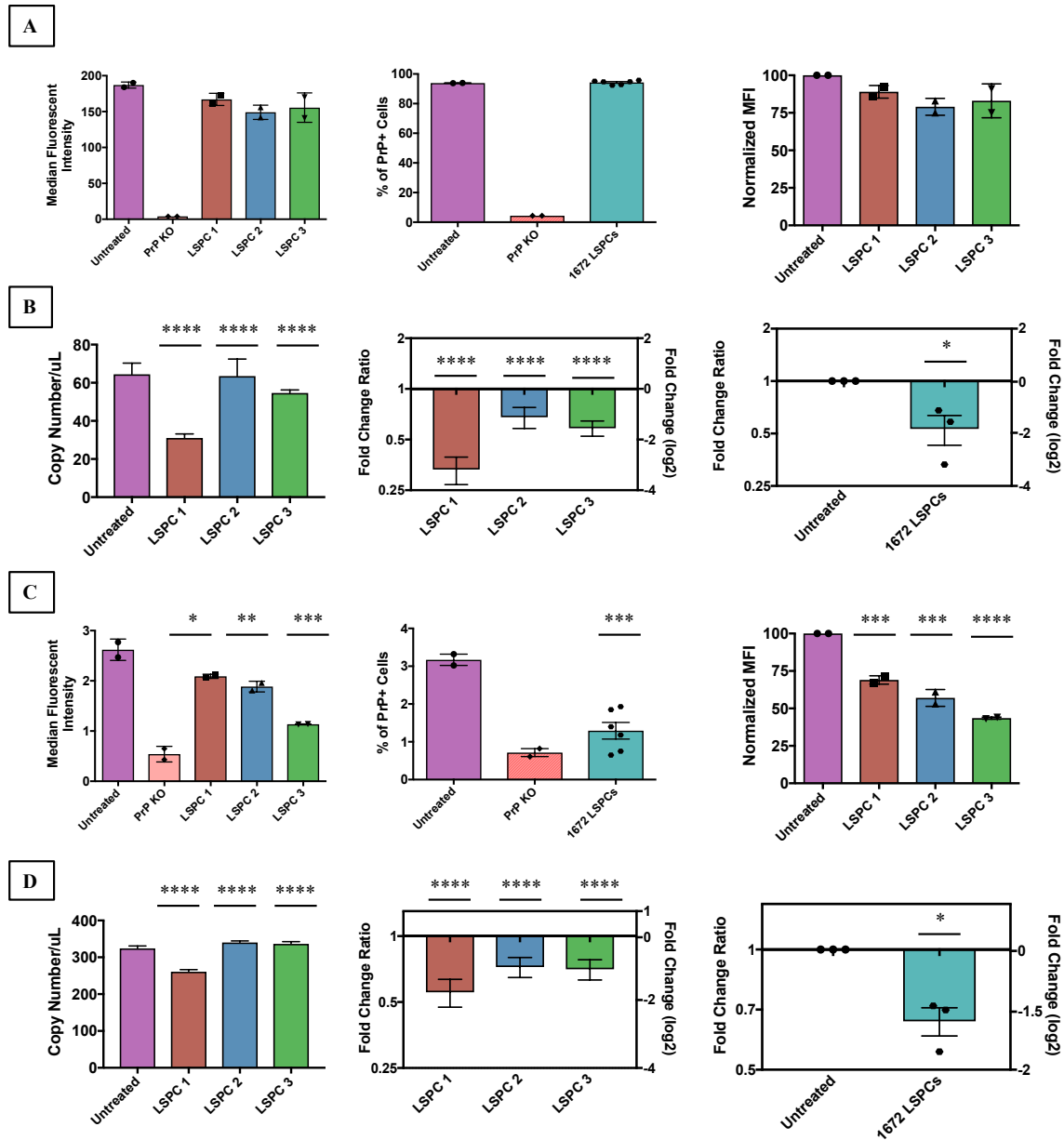


**Figure 3.13. Flow cytometric and ddPCR analysis of CD1 mice 21 days after LSPCs treatment.**

A) None of the LSPCs-treated mice had either a decrease in neuronal surface PrP<sup>C</sup> or a decrease in the number of PrP<sup>C</sup>+ cells in the brain 21 days after treatment. B) All three LSPCs-treated mice had a decrease in copy number and fold change (~2-fold decrease) to untreated and treatment controls at 21 days after LSPCs treatment in the brain. C) Surface PrP<sup>C</sup> levels in the kidney are decreased (25-55%) in all the LSPCs treated mice, as well as the number of PrP<sup>C</sup>+ cells. D) PrP<sup>C</sup> mRNA analysis in the kidney also revealed a decrease in PrP<sup>C</sup> mRNA levels in the kidney 21 days after LSPCs treatment. Error bars for graphs with individual treated mice indicate SD. Error bars for graphs with grouped treated mice indicate SEM. \* p<0.05, \*\* p<0.01, \*\*\* p<0.001, \*\*\*\* p<0.0001. One-way ANOVA with Dunnett's multiple comparisons and t test.

Other treated mice have a statistically significant reduction in PrP<sup>C</sup> mRNA levels in the brain (Figure 3.13B). Both protein levels and mRNA copy number are decreased in the kidney 21 days post-treatment, with protein levels being reduced in one mouse about 50% (Figure 3.13C). The number of PrP<sup>C</sup>-positive cells is also still decreased in the kidney but could be due to non-specific reduction by LSPCs treatment. Fold change analysis revealed a less than 2-fold change in one treated mouse and less than 1-fold change in the other two treated mice of PrP<sup>C</sup> mRNA levels in the kidney (Figure 3.13D). Grouped the treated mice are statistically different than the untreated control.

### ***Repeated siRNA treatments in prion-infected mice result in ever decreasing levels of PrP<sup>C</sup>***

FVB mice were treated with LSPCs every two weeks, for a total of twelve weeks, to determine the effect of a repetitive two-week dosing regimen on PrP<sup>C</sup> protein and mRNA levels. The mice were inoculated with 0.1% RML-5 prions. One PBS and one LSPCs-treated mouse were sacrificed every week after treatment. The '1 treatment' mice received one LSPCs treatment, the '2 treatment' received two LSPCs treatments, and so on until the last group which received a total of six LSPCs treatments. Brains and kidneys were harvested at each time point. Protein analysis was performed using flow cytometry and western blot. mRNA analysis was performed using ddPCR.

Flow cytometry data revealed that three repetitive siRNA treatments result in a decrease in PrP<sup>C</sup> MFI in the brain, indicating that surface PrP<sup>C</sup> is consistently dropping till this time point (Figure 3.14A). Subsequent treatments after the 3<sup>rd</sup> treatment result in a steady increase in MFI, indicating that PrP<sup>C</sup> levels are rebounding even in the presence of PrP<sup>C</sup> siRNA. PrP<sup>C</sup> levels in the kidney increase after the 1<sup>st</sup> and 4<sup>th</sup> treatments and then steadily decrease in subsequent treatments (Figure 3.14B). Analysis of relative PrP<sup>C</sup> expression and fold change in the brain using the western blot technique did not reveal any statistical difference between the untreated and treated mice at each time point (Figure 3.14C and D). mRNA analysis of the brain concurs with flow cytometry in that PrP<sup>C</sup> mRNA levels are consistently decreased till the 3<sup>rd</sup> siRNA treatment (Figure 3.14E). Three repetitive siRNA treatments result in a 3-fold reduction in PrP<sup>C</sup> mRNA levels in the brain. The 4<sup>th</sup> siRNA treatment results in a 2-fold increase in neuronal PrP<sup>C</sup> mRNA levels, which would explain the increase in surface PrP<sup>C</sup> as shown by flow cytometry. Interestingly the 6<sup>th</sup> treatment, while not statistically significant from the untreated, resulted in neuronal PrP<sup>C</sup> mRNA levels that are significantly decreased from the mRNA levels measured after the 4<sup>th</sup> treatment (Figure 3.14E). This significance suggests that while the mRNA levels did rebound after the 3<sup>rd</sup> treatment, they started to decrease again due to the repetitive LSPC treatments. Analysis of PrP<sup>C</sup> mRNA levels in the kidney showed a statistically significant increase

in mRNA after the 1<sup>st</sup> treatment and a decrease in mRNA levels after the 2<sup>nd</sup> treatment (Figure 3.14F). After the 2<sup>nd</sup> treatment, PrP<sup>C</sup> mRNA levels are not statistically different from the untreated control but seem to waver slightly up and down after LSPCs treatments.

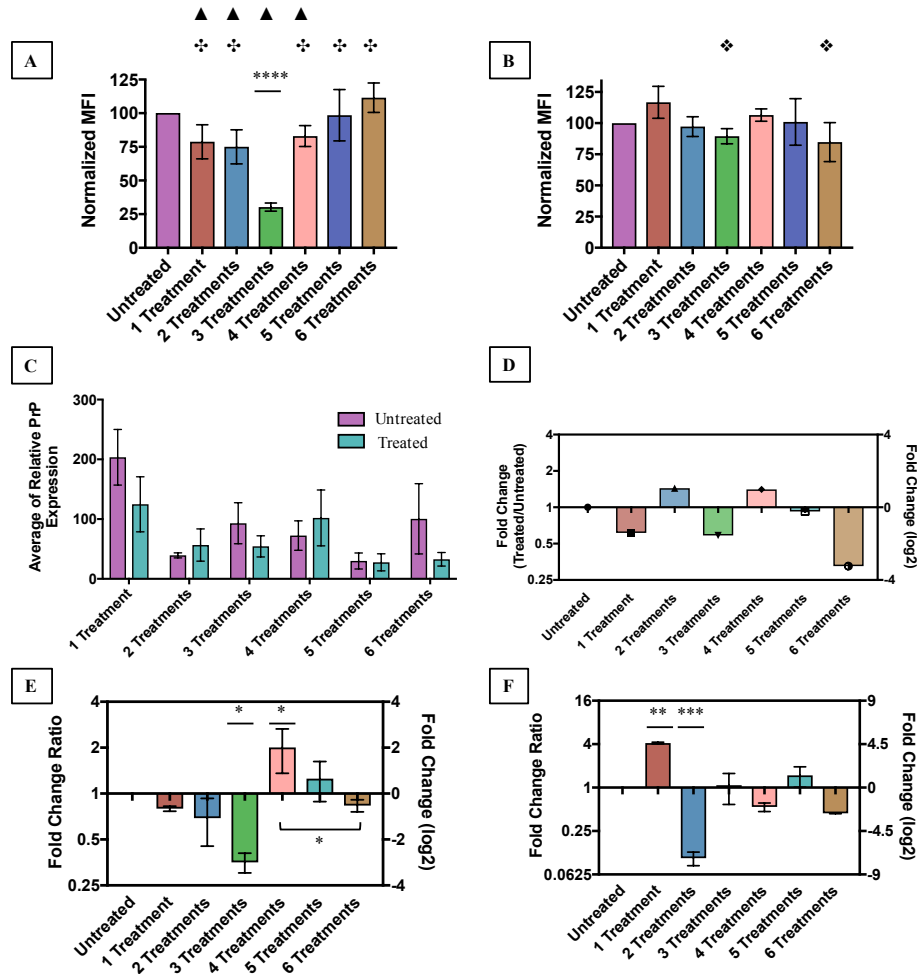


**Figure 3.14. Flow cytometric and ddPCR analysis of a repeating two-week dosing regimen in FVB mice.**

A) Mice who received one to three LSPCs treatments every two weeks had lowered surface PrP<sup>C</sup> levels in the brain, with three LSPCs treatments resulting in a 75% decrease of neuronal surface PrP<sup>C</sup> levels. PrP<sup>C</sup> protein levels start to rebound after three LPSCs treatments. B) None of the treatments resulted in a significant change in PrP<sup>C</sup> protein levels in the kidney but three and six treatments are significantly different from one and four treatments, respectively. C) Western blot analysis of the brain did not reveal any significant difference between any of the untreated and LSPCs-treated mice. However, a trend of PrP<sup>C</sup> protein levels being decreased and then increased at every other time point is observed. D) Fold change of western blot analysis more clearly shows the trend observed in PrP<sup>C</sup> protein levels after one to six LSPCs treatments E) mRNA analysis of neuronal cells revealed a decrease in PrP<sup>C</sup> mRNA after three LSPCs treatments and an increase in PrP<sup>C</sup> mRNA levels after four LSPCs treatments. The PrP<sup>C</sup> mRNA levels start to decrease again after four LSPCs treatments. F) mRNA analysis of kidney cells reveals a back and forth increase/decrease after subsequent LSPCs treatments. Error bars indicate SEM. \* p<0.05, \*\* p<0.01, \*\*\* p<0.001, \*\*\*\* p<0.0001. ▲ = statistically significant from 6 treatments. ◆ = statistically significant from 3 treatments. ◆ = statistically significant from 1 treatment. One-way ANOVA with Dunnett's or Tukeys multiple comparisons.

## Discussion

The blood-brain barrier (BBB) is the rate-limiting step for delivery of therapeutics to the brain and remains the biggest challenge in producing effective therapeutics for neurodegenerative disorders. In physiological conditions, the BBB is meant to protect neurons, glia, and other neuronal cell types from serum proteins or toxins. The BBB produces its protective effect in a number of ways. The first is the organization of the endothelial layer that provides a physical barrier to the central nervous system (CNS). This physical barrier is composed of endothelial cells, pericytes, and foot processes of astrocytes. Tight junctions between endothelial cells do not permit most solutes from crossing between cells. In fact, transport through tight junctions, in physiological conditions, is negligible meaning that the only meaningful way to transport therapeutics across the BBB is by transport through the endothelial cells. Pericytes are the primary regulators of the vascular permeability, and certain permeabilizing receptors on these cells can be upregulated in disease processes. The second protective effect comes in the form of efflux pumps, which immediately transports out any molecule lucky enough to make it into the endothelial cells of the BBB. A third protective effect is the enzymatic BBB, which uses enzymes on the surface of the plasma membrane of endothelial cells to digest any unwanted proteins<sup>62-64</sup>.

While the structure of the BBB makes it sound like an impenetrable fortress, therapeutic drugs can still cross this membrane if designed smartly. Once across the membrane, the drug doesn't have to traverse long distances as most neurons sit within 8-25  $\mu\text{m}$  from a microvessel<sup>64</sup>. Countless strategies have been employed to transport drugs across the membrane, but perhaps the best-known approach is the 'Trojan Horse' method. The 'Trojan Horse' method utilizes a targeting ligand bound to a drug or delivery system that binds to a cell-surface receptor on the endothelial cells of the BBB. The result of this binding is usually an internalization of the drug/delivery system. Care must be taken to avoid the endocytotic pathway of the endothelial cells in favor of the transcytotic pathway for transport<sup>62,63</sup>. Multiple ligands and their receptors have been used to transport drugs and delivery systems across the BBB with varying successes. These include transferrin<sup>65</sup>, insulin<sup>66</sup>, low-density lipoprotein<sup>67</sup>, low-density lipoprotein receptor ligands<sup>68</sup>, leptin<sup>69</sup>, and brain-derived neurotrophic factor<sup>63</sup>. All of these ligands/receptors have shown success but still need optimization to become a part of the 'next generation' of delivery vehicles.

We have chosen to use the neuro-targeting peptide RVG-9r to guide our PrP<sup>C</sup> siRNA therapeutic across the BBB. RVG-9r is a small peptide of the rabies virus glycoprotein that binds to the  $\alpha 7$  subunit of nicotinic

acetylcholine receptors (nAChRs). These receptors are present in other tissues besides the CNS but neuronal cells within the CNS also highly express nAChRs. Kumar et al. showed that using RVG-9r bound to siRNA dramatically increased its delivery to the CNS. SiRNA bound to RVG-9r was able to decrease exogenous GFP by 40%, and antiviral siRNA against Japanese encephalitis virus increased survival times in mice infected with the virus<sup>70</sup>. Both the PrP<sup>C</sup> siRNA and the RVG-9r, in our formulation, are protected by a liposomal delivery system to increase serum half-life and decrease nuclease attack by serum proteins. We have previously characterized the ability of our liposome-siRNA-peptide complexes (LSPCs) to deliver PrP<sup>C</sup> siRNA to neuronal cells *in vitro*. LSPCs delivered PrP<sup>C</sup> siRNA directly to mouse neuroblastoma cells without the need for lipofection reagents and decreased PrP<sup>C</sup> levels by 50-75% in these cells. The liposomes were able to protect the siRNA in increasing concentrations of serum, while the RVG-9r peptide delivered PrP<sup>C</sup> siRNA specifically to cells that expressed nAChRs<sup>58</sup>. The next steps in characterizing these LSPCs was to determine their ability to deliver PrP<sup>C</sup> siRNA to the brain *in vivo*, with the goal being, if successful, to determine an optimum dosing regimen of LSPCs in prion-infected mice.

The LSPCs delivered PrP<sup>C</sup> siRNA to the brain, as shown by *in vivo* live imaging. We were able to detect PrP<sup>C</sup> siRNA signal up to two hours after injection. Unfortunately, we did not detect any signal in the brains of any treated mice at 24 hours after injection during this experiment. However, in another experiment, we were able to detect PrP<sup>C</sup> siRNA signal up to ten days after injection<sup>71</sup>. Several factors might explain the results seen during this experiment compared to the previous experiment, including different clearance rates, different metabolism of LSPCs, and less LSPCs being injected intravenously. At 48 hours after injection, PrP<sup>C</sup> siRNA signal is seen in the bladders of all treated mice in this study (data not shown). The pooling in the bladder indicates a difference in clearance kinetics or metabolism among mice, as both of these would result in LSPCs being transported to the kidneys. The LSPC transport to the kidneys was seen to be a problem in about half of the mice that were treated, which is why two other formulations (PALETS) were designed to increase circulation time of the PrP<sup>C</sup> siRNA<sup>72</sup>. While initial results indicate that clearance kinetics have been altered in PALETS-treated mice (unpublished results), more studies are needed to determine if this is the case.

Control experiments were undertaken to determine if the LSPC treatment alone causes any alterations to PrP<sup>C</sup> protein and mRNA levels. Mice were either treated with LSPCs with scrambled siRNA or LSPCs with the RVM control peptide. Surprisingly, the LSPCs treatment causes differences in PrP<sup>C</sup> protein and mRNA levels. The slight decrease in neuronal PrP<sup>C</sup> protein levels due to scrambled siRNA sequence might be due to the activation of

the RNAi machinery by the non-specific siRNA. The scrambled siRNA sequence does not have complementarity to the sequence of the *prnp* gene that encodes for PrP<sup>C</sup>, so theoretically it should not cause a decrease in mRNA or protein levels. However, if the scrambled siRNA is loaded into the RISC complex, it might just activate non-specific cleavage of PrP<sup>C</sup>. The reduction of PrP<sup>C</sup> MFI in the kidney could be partially attributed to apoptosis of the treated cells as the number of PrP<sup>C</sup>-positive cells is decreased in the kidney for both scrambled and RVM LSPCs treatment (Figure A1.2). In the brain, apoptosis likely does not play a factor in the decrease in MFI because the number of PrP<sup>C</sup>-positive cells does not change with either scrambled LSPCs or RVM LSPCs treatment (Figure A1.2).

mRNA analysis of scrambled siRNA and RVM LSPCs treatment revealed a 1-fold increase in mRNA levels in treated mice compared to the untreated control. While this finding was unexpected, increased expression of PrP<sup>C</sup> has been observed when certain immune cells are activated. Both T cells and follicular dendritic cells will upregulate the expression of PrP<sup>C</sup> when the cells become activated by Toll-like receptor (TLR) ligands, such as lipopolysaccharide and CpG oligodeoxynucleotides<sup>73-76</sup>. While most of these immune studies assayed protein levels, it is entirely plausible that an upregulation of protein is preceded by an upregulation of mRNA levels. One study noted that they did not observe any mRNA changes of PrP<sup>C</sup> in follicular dendritic cells. However, this observation could be due to a translational regulation of PrP<sup>C</sup> in these cells or perhaps an early enough time point was not chosen to observe the mRNA increase. These studies indicate that PrP<sup>C</sup> is upregulated during an immune response. There are several factors of the LSPCs treatment that could lead to the activation of immune cells/products, which could explain the increase in PrP<sup>C</sup> mRNA that we detected in treated mice.

Early reports of siRNA indicated that the RNA molecules did not induce an immune response. Naked siRNAs injected into mice failed to produce an IL-12 or IFN $\alpha$  response<sup>77</sup>. However, later studies revealed that siRNA can signal through TLRs to increase cytokine production. This contradiction in results might be due to particular siRNA sequences, as some naked siRNA molecules do not activate an immune response while others do<sup>77,78</sup>. TLR 7 and 8, which recognize single-stranded RNA molecules, are the TLRs most commonly activated by siRNA<sup>78-81</sup>. Certain siRNA molecules will also activate TLR3, which recognizes dsRNA<sup>82</sup>. Activation of TLR 7 and 8 occurs in the endosomal pathway, suggesting that any uptake of siRNA by endocytosis can lead to an immune response through these TLRs. While most siRNAs activate TLRs in the endocytotic pathway to produce cytokines, electroporation of siRNA directly into the cytoplasm also results in the production of inflammatory cytokines<sup>79,83</sup>. The cytokines most commonly increased during TLR activation by siRNA include IFN $\alpha$ , TNF $\alpha$ , IL-6, and IL-

12<sup>79,80,82</sup>. Duplex siRNA causes less cytokine release from TLRs than does the single strands of the siRNA.

Complexing the siRNA to delivery vehicles, such as liposomes, also increases cytokine production through TLR signaling. Though liposomes alone do not increase cytokine production<sup>78,84</sup>, siRNA and liposomes together produce a potent immune response. It is not known what component of the complex triggers the activation. Although, it is thought that perhaps the siRNA and liposome complex mimics a viral particle and thus induces a stronger immune response. Again, this immune response involves the secretion of TNF $\alpha$ , IL-6, and IL-12<sup>85</sup>.

Another factor that could be causing an immune response is the rabies virus glycoprotein (RVG-9r) peptide that is used to target the LSPCs to the brain. The RVG peptide in its native form, without the nine arginine residues added to the COOH-terminus, does not elicit an immune response. Therefore, this peptide probably does not contain a proper recognition pattern for TLRs. An immune response does occur when the arginine residues are added to the end of the peptide. RVG-9r –siRNA exosomes were shown to increase IL-6 production in the mouse brain<sup>86</sup>. Again, it seems complexing two of the delivery vehicle factors together increases non-specific cytokine production.

Due to the toxicity issues of complexing siRNA to cationic liposomes and complexing the RVG-9r peptide, it is possible that the increase in PrP<sup>C</sup> mRNA levels is due to a non-specific immune response through the activation of TLR receptors. This reaction could be coming from either immune cells interacting with the LSPCs in the systemic circulation, and/or from microglia, astroglia, or neurons, which all contain TLRs 3, 7, and 8<sup>87</sup>. The cytokines produced by this non-specific response could be providing a third signal to activate immune cells<sup>88</sup>, such as T cells, that increases PrP<sup>C</sup> mRNA levels. It is unknown whether a systemic T cell activation would affect PrP<sup>C</sup> levels in the brain. It would be prudent to treat mice with only cationic liposomes, naked siRNA, RVG-9r, liposomes + siRNA, or liposomes + RVG to assess if the complexation of the siRNA and the cationic liposomes are causing the increase in mRNA levels. It is also necessary to determine the immune system profile of LSPCs treatment by measuring cytokine production in treated mice.

We evaluated the pharmacodynamics (PD) of the LSPCs treatment in two different mouse models: CR1/2 hemi transgenic mice and CD1 wild-type mice. We felt it necessary to assess the PD in two different mouse models to account for any treatment response differences in individual mice but also among different background strains of mice. The CR1/2 hemi transgenic mice express one allele of CD21 and one allele of CD35. The transgenic aspect of this mouse strain is not important to the studies in this report but the C57Bl/6 background enables us to assess LSPCs treatment in a different mouse model. The CR1/2 hemi mice have the same amount of PrP<sup>C</sup> as their C57Bl/6

wild-type counterparts, so the transgenic nature of these mice should not have influenced the effects of the LSPCs treatment or the expression level of PrP<sup>C</sup>.

Western blot analysis was utilized as another assay to evaluate PrP<sup>C</sup> protein expression in the brains of LSPCs-treated mice treated at various time points. Samples were prepared in triplicate for each experiment, and the western blot was repeated. The densitometric analysis of the western blot showed very little statistical significance of PrP<sup>C</sup> protein levels in LSPCs-treated mice. However, at 48 hours post-treatment in CR1/2 hemi mice and 21 days post-treatment in CD1 wild-type mice, there was a decrease in PrP<sup>C</sup> protein fold change in two of the treated mice at those time points compared to the untreated control, which mimicked the flow cytometry and ddPCR results from the brain obtained at these time points. CR1/2 hemi LSPC-treated mice had a decrease in both PrP<sup>C</sup> MFI and PrP<sup>C</sup> mRNA levels at 48 hours post-treatment. CD1 LSPC-treated mice at 21 days post-treatment do not have a statistically significant reduction in PrP<sup>C</sup> MFI levels in the brain, but they do have a decrease in PrP<sup>C</sup> mRNA levels at this time point. Because these two western blot results mimic the results seen from the other assays, we believe that the reason the western blots do not show a decrease in PrP<sup>C</sup> levels at other time points is due to a low sensitivity of the western blot assay compared to the other tests. The discrepancy between the flow cytometry results and the western blot results could also be due to the difference between measuring surface PrP<sup>C</sup> versus total PrP<sup>C</sup> levels. Our flow cytometry protocol does not include a fixation and permeabilization step, which would allow the PrP<sup>C</sup> antibody to label all cellular PrP<sup>C</sup>. Therefore, the antibody can only label surface PrP<sup>C</sup> in our flow cytometry assay. The western blot protocol involves permeabilization of all cells, which would result in the measurement of total cellular PrP<sup>C</sup>. Though the reduction of total PrP<sup>C</sup> would be optimal for a siRNA therapeutic against prion disease, reducing surface PrP<sup>C</sup> might be more important and still have an impact on survival times of prion-infected mice as most PrP<sup>Res</sup> formation likely occurs at the cell surface<sup>89</sup>.

CR1/2 hemi mice responded well to the LSPCs treatment and had significant decreases in surface PrP<sup>C</sup> in the brain at all time points tested. Most of the CR1/2 hemi mice also had decreases in mRNA levels in the brain. Interestingly, a pattern that presented in the treated mice revealed that most of the mice with the lowest amount of neuronal surface PrP<sup>C</sup> had an increase in PrP<sup>C</sup> mRNA levels above the untreated mouse. This discovery is interesting as it suggests that PrP<sup>C</sup> has a tight transcriptional regulation over mRNA levels, and subsequently protein levels. PrP<sup>C</sup> mRNA levels in the kidneys of CR1/2 hemi LSPC-treated mice had variable levels of PrP<sup>C</sup> at different time points. The levels in the kidney are either increased at one time point or decreased at another time point. CD1 mice

show the same type of variability within treatment groups of PrP<sup>C</sup> levels both in the brain and the kidney. At four days and fifteen days post-treatment, surface PrP<sup>C</sup> in the brains of CD1 mice are decreased relative to the untreated control, while other time points show no difference between treated and untreated groups in neuronal surface PrP<sup>C</sup>. PrP<sup>C</sup> mRNA levels in the brains of LSPC-treated CD1 mice are also variable. Some mice with decreases in surface PrP<sup>C</sup> have an increase in PrP<sup>C</sup> mRNA levels. Again, at some time points, the mouse with the lowest MFI has the highest copy number and fold change of PrP<sup>C</sup> mRNA levels compared to the untreated control. Most of the LSPC-treated CD1 mice have decreased levels of surface PrP<sup>C</sup> in the kidney, usually accompanied by a decrease in PrP<sup>C</sup> mRNA levels.

The variability not only within the treated groups and between the two different background strains was not surprising given that siRNA response varies widely in individual mice. The striking feature of these experiments was that, in some cases, protein levels did not agree with mRNA levels. Some mice had increased protein and decreased mRNA levels, while other mice had the opposite. We can conclude from these two strains of mice that LSPCs can deliver PrP<sup>C</sup> siRNA to the brains of two different mouse lines and that in both mouse lines delivery of siRNA usually results in a decrease of PrP<sup>C</sup> levels. It is important to note that we anticipated off-target effects in the kidney due to the presence of nAChRs in that organ, but we did not expect the treatment itself (scrambled siRNA or RVM peptide) having such a dramatic effect on PrP<sup>C</sup> levels in the kidney. All ddPCR results have been normalized to the non-specific increase caused solely by the LSPCs treatment. So, the fold change results observed in the kidney take into account the increase and show the increase/decrease caused only by the PrP<sup>C</sup> siRNA. However, flow cytometry results for the kidney were not normalized towards the increase seen in control experiments. Therefore, the decrease in PrP<sup>C</sup> levels in the kidney could either be caused by the PrP<sup>C</sup> siRNA or by the presence of the LSPCs.

The fold change of ddPCR results is shown as both individual mice and as a pooled group, due to the sensitivity of the ddPCR reaction. In ddPCR, every reaction has over 10,000 replicates in the form of droplets, which makes any change statistically significant. However, statistical significance does not imply biological significance. ddPCR results of individual mice are shown because it's important to assess individual variability in mRNA levels due to the LSPC treatment. Biological significance is indicated by grouping the treated mice into a single mean. If the pooled data is statistically significant from the untreated control, we feel confident that this significant change in PrP<sup>C</sup> mRNA levels might be biologically relevant.

We assessed whether multiple siRNA treatments would cause an even larger reduction in PrP<sup>C</sup> during a two-week dosing regimen of LSPCs. Infected FVB mice were treated every two weeks starting at 2.5 months post inoculation. Again, the western blot analysis did not provide any statistical significance in neuronal PrP<sup>C</sup> levels in treated mice compared to untreated mice. Conversely, flow cytometric analysis of both brain and kidney revealed that subsequent siRNA treatments with LSPCs result in even larger decreases of surface PrP<sup>C</sup>. Analysis of both organs shows a decline in surface PrP<sup>C</sup> until the 3<sup>rd</sup> LSPC treatment. After the 4<sup>th</sup> treatment in the brain, there is a subsequent increase in PrP<sup>C</sup> protein levels till the 6<sup>th</sup> treatment even in the presence of PrP<sup>C</sup> siRNA. In the brain, the 6<sup>th</sup> treatment is statistically significant from treatments 1-4, but not from the untreated, indicating that the 6<sup>th</sup> treatment has increased PrP<sup>C</sup> levels relative to the earlier time points. The kidney shows a different trend where, again, the 4<sup>th</sup> treatment increases surface PrP<sup>C</sup>, but the 5<sup>th</sup> and 6<sup>th</sup> treatments show another decrease in PrP<sup>C</sup> levels. The 6<sup>th</sup> treatment is statistically significant from the 4<sup>th</sup>, indicating PrP<sup>C</sup> levels are dropping again. However, flow cytometry results could be due to a non-specific reduction of protein levels cause by the LSPCs treatment. The kidney mRNA levels show a back and forth trend of PrP<sup>C</sup> levels, with the first two treatments being statistically significant. It's interesting that the response of the kidney to the siRNA treatment is to upregulate both PrP<sup>C</sup> mRNA and protein levels initially. The biological significance of this is unknown. Fold change of PrP<sup>C</sup> mRNA levels in the brain decrease until the 3<sup>rd</sup> treatment, where they dramatically increase at the 4<sup>th</sup> treatment. After the 4<sup>th</sup> treatment, PrP<sup>C</sup> mRNA levels start to drop again.

The two-week regimen data, along with the CR1/2 hemi and CD1 mice pharmacodynamics data, suggest that PrP<sup>C</sup> has some form of transcriptional regulation that tries to rebalance both the mRNA and protein levels to normal. PrP<sup>C</sup> is considered to be a housekeeping gene and contains several CpG islands and transcription factor sites within non-coding regions of the *prnp* gene. Transcription factor binding sites include IL6, MyoD, and Sp1. The *prnp* gene is also very G/C rich on the 5' end, which is indicative of a promoter region. The actual mechanism of transcriptional control of PrP<sup>C</sup> is unknown. Given that the field of prion therapeutics has turned to PrP<sup>C</sup> as a target, it would be beneficial to know the transcriptional regulation of PrP<sup>C</sup> to design more effective therapeutics. Without knowledge of regulation, therapeutics that target PrP<sup>C</sup> will continue to have the same complications we did with extreme variability and unpredictability of therapeutic response due to the targeting of PrP<sup>C</sup>.

This report shows that LSPCs treatment in two different mouse models decreases surface PrP<sup>C</sup> and mRNA levels in the brain. While there are off-target effects in the kidney, no animal died of treatment either in the PD

studies or the two-week regimen studies, indicating that LSPCs treatment is not overtly harmful to naïve mice. However, toxicity profiles, including immune response assays, need to be performed to evaluate the safety of LSPCs. Optimization of the LSPCs delivery vehicle might result in a better response than what was observed here. Since siRNA generates such variable and transient responses, it may not be the best therapeutic to use for a protein whose levels are tightly regulated. Therefore, it might be beneficial to test small molecules such as shRNA or CRISPR in the LSPC delivery vehicle that might prove more effective at decreasing PrP<sup>C</sup> levels. Also, if RVG-9r generates too large of an immune response, another targeting peptide may be used with the delivery vehicle. With optimization, we feel that LSPCs still represent a viable therapeutic option for prion diseases. The next step would be to test the PrP<sup>C</sup> siRNA LSPCs in prion-infected mice to determine if repeated siRNA treatments affect survival times of prion-infected mice.

## References

1. Prusiner, S. B. Novel proteinaceous infectious particles cause scrapie. *Science* **216**, 136–144 (1982).
2. Kovacs, G. G. & Budka, H. Prion Diseases: From Protein to Cell Pathology. *Am J Pathol* **172**, 555–565 (2008).
3. Šišková, Z., Reynolds, R. A., O'Connor, V. & Perry, V. H. Brain Region Specific Pre-Synaptic and Post-Synaptic Degeneration Are Early Components of Neuropathology in Prion Disease. *PLoS ONE* **8**, e55004 (2013).
4. Jeffrey, M., McGovern, G., Sisó, S. & González, L. Cellular and sub-cellular pathology of animal prion diseases: relationship between morphological changes, accumulation of abnormal prion protein and clinical disease. *Acta Neuropathol* **121**, 113–134 (2010).
5. Haig, D. A. & Clarke, M. C. The effect of beta-propiolactone on the scrapie agent. *J. Gen. Virol.* **3**, 281–283 (1968).
6. Cochran, K. W. Failure of adenine arabinoside to modify scrapie in mice. *J. Gen. Virol.* **13**, 353–354 (1971).
7. Tateishi, J. Antibiotics and antivirals do not modify experimentally-induced Creutzfeldt-Jakob disease in mice. *J. Neurol. Neurosurg. Psychiatr.* **44**, 723–724 (1981).
8. Pocchiari, M., Casaccia, P. & Ladogana, A. Amphotericin B: a novel class of antiscrapie drugs. *J. Infect. Dis.* **160**, 795–802 (1989).
9. Pocchiari, M., Schmittinger, S. & Masullo, C. Amphotericin B delays the incubation period of scrapie in intracerebrally inoculated hamsters. *J. Gen. Virol.* **68 ( Pt 1)**, 219–223 (1987).
10. McKenzie, D., Kaczkowski, J., Marsh, R. & Aiken, J. Amphotericin B delays both scrapie agent replication and PrP-res accumulation early in infection. *J Virol* **68**, 7534–7536 (1994).
11. Mangé, A. *et al.* Amphotericin B inhibits the generation of the scrapie isoform of the prion protein in infected cultures. *J Virol* **74**, 3135–3140 (2000).
12. Mangé, A., Milhavet, O., McMahon, H. E., Casanova, D. & Lehmann, S. Effect of amphotericin B on wild-type and mutated prion proteins in cultured cells: putative mechanism of action in transmissible spongiform encephalopathies. *J Neurochem* **74**, 754–762 (2000).
13. Collins, S. J. *et al.* Quinacrine does not prolong survival in a murine Creutzfeldt-Jakob disease model. *Ann. Neurol.* **52**, 503–506 (2002).
14. Bian, J., Kang, H. E. & Telling, G. C. Quinacrine promotes replication and conformational mutation of chronic wasting disease prions. *Proc. Natl. Acad. Sci. U.S.A.* **111**, 6028–6033 (2014).
15. Ghaemmaghami, S. *et al.* Continuous Quinacrine Treatment Results in the Formation of Drug-Resistant Prions. *PLoS Pathog* **5**, e1000673 (2009).
16. Ryou, C. *et al.* Differential Inhibition of Prion Propagation by Enantiomers of Quinacrine. *Lab Invest* **83**, 837–843 (2003).
17. Collinge, J. *et al.* Safety and efficacy of quinacrine in human prion disease (PRION-1 study): a patient-preference trial. *Lancet Neurol* **8**, 334–344 (2009).
18. Tagliavini, F. *et al.* Effectiveness of anthracycline against experimental prion disease in Syrian hamsters. *Science* **276**, 1119–1122 (1997).
19. Supattapone, S., Nguyen, H. O., Cohen, F. E., Prusiner, S. B. & Scott, M. R. Elimination of prions by branched polyamines and implications for therapeutics. *Proc. Natl. Acad. Sci. U.S.A.* **96**, 14529–14534 (1999).
20. Supattapone, S. *et al.* Branched Polyamines Cure Prion-Infected Neuroblastoma Cells. *J Virol* **75**, 3453–3461 (2001).
21. Winklhofer, K. F. & Tatzelt, J. Cationic lipopolyamines induce degradation of PrPSc in scrapie-infected mouse neuroblastoma cells. *Biol Chem* (2000).
22. Solassol, J. Cationic phosphorus-containing dendrimers reduce prion replication both in cell culture and in mice infected with scrapie. *J Gen Virol* **85**, 1791–1799 (2004).
23. Yudovin-Farber, I., Azzam, T., Metzger, E., Taraboulos, A. & Domb, A. J. Cationic Polysaccharides as Antiprion Agents. *J. Med. Chem.* **48**, 1414–1420 (2005).
24. Kimberlin, R. H. & Walker, C. A. The antiviral compound HPA-23 can prevent scrapie when administered at the time of infection. *Arch. Virol.* **78**, 9–18 (1983).
25. Kimberlin, R. H. & Walker, C. A. Suppression of scrapie infection in mice by heteropolyanion 23, dextran

- sulfate, and some other polyanions. *Antimicrob. Agents Chemother.* **30**, 409–413 (1986).
26. Ehlers, B. & Diringler, H. Dextran sulphate 500 delays and prevents mouse scrapie by impairment of agent replication in spleen. *J. Gen. Virol.* **65 ( Pt 8)**, 1325–1330 (1984).
  27. Caughey, B. & Raymond, G. J. Sulfated polyanion inhibition of scrapie-associated PrP accumulation in cultured cells. *J Virol* **67**, 643–650 (1993).
  28. Shyng, S. L., Lehmann, S. & Moulder, K. L. Sulfated glycans stimulate endocytosis of the cellular isoform of the prion protein, PrP<sup>C</sup>, in cultured cells. *J Biol Chem* **270**, 30221–30229 (1995).
  29. Farquhar, C., Dickinson, A. & Bruce, M. Prophylactic potential of pentosan polysulphate in transmissible spongiform encephalopathies. *Lancet* **353**, 117 (1999).
  30. Wong, C., Xiong, L. W., Horiuchi, M. & Raymond, L. Sulfated glycans and elevated temperature stimulate PrP<sup>Sc</sup>-dependent cell-free formation of protease-resistant prion protein. *EMBO J* **20**, 377–386 (2001).
  31. Caughey, B., Brown, K. & Raymond, G. J. Binding of the protease-sensitive form of PrP (prion protein) to sulfated glycosaminoglycan and congo red. *J Virol* **68**, 2135–2141 (1994).
  32. Ingrosso, L., Ladogana, A. & Pocchiari, M. Congo red prolongs the incubation period in scrapie-infected hamsters. *J Virol* **69**, 506–508 (1995).
  33. Caspi, S. *et al.* The anti-prion activity of Congo red. Putative mechanism. *J. Biol. Chem.* **273**, 3484–3489 (1998).
  34. Enari, M. & Flechsig, E. Scrapie prion protein accumulation by scrapie-infected neuroblastoma cells abrogated by exposure to a prion protein antibody. *Proc. Natl. Acad. Sci. U.S.A.* **98**, 9295–9299 (2001).
  35. Peretz, D. *et al.* Antibodies inhibit prion propagation and clear cell cultures of prion infectivity. *Nature* **412**, 739–743 (2001).
  36. Perrier, V. *et al.* Anti-PrP antibodies block PrP<sup>Sc</sup> replication in prion-infected cell cultures by accelerating PrP<sup>Sc</sup> degradation. *J Neurochem* **89**, 454–463 (2004).
  37. Müller-Schiffmann, A. & Korth, C. Vaccine Approaches to Prevent and Treat Prion Infection. *BioDrugs* (2008).
  38. Mallucci, G. R., Ratte, S., Asante, E. A. & Linehan, J. Post-natal knockout of prion protein alters hippocampal CA1 properties, but does not result in neurodegeneration. *EMBO J* **21**, 202–210 (2002).
  39. Mallucci, G. Depleting Neuronal PrP in Prion Infection Prevents Disease and Reverses Spongiosis. *Science* **302**, 871–874 (2003).
  40. Büeler, H. *et al.* Normal development and behaviour of mice lacking the neuronal cell-surface PrP protein. *Nature* **356**, 577–582 (1992).
  41. Coitinho, A. S., Roesler, R., Martins, V. R., Brentani, R. R. & Izquierdo, I. Cellular prion protein ablation impairs behavior as a function of age. *NeuroReport* **14**, 1375–1379 (2003).
  42. Criado, J. R. *et al.* Mice devoid of prion protein have cognitive deficits that are rescued by reconstitution of PrP in neurons. *Neurobiol Dis* **19**, 255–265 (2005).
  43. Colling, S. B., Khana, M., Collinge, J. & Jefferys, J. G. R. Mossy fibre reorganization in the hippocampus of prion protein null mice. *Brain Res* **755**, 28–35 (2011).
  44. Tobler, I., Gaus, S. E., Deboer, T., Achermann, P. & Fischer, M. Altered circadian activity rhythms and sleep in mice devoid of prion protein. *Nature* **380**, 639–642 (1996).
  45. Roesler, R. *et al.* Normal inhibitory avoidance learning and anxiety, but increased locomotor activity in mice devoid of PrP<sup>C</sup>. *Brain Res. Mol. Brain Res.* **71**, 349–353 (1999).
  46. Nico, P. B. C. *et al.* Altered behavioural response to acute stress in mice lacking cellular prion protein. *Behav Brain Res* **162**, 173–181 (2005).
  47. Fire, A. *et al.* Potent and specific genetic interference by double-stranded RNA in *Caenorhabditis elegans*. *Nature* **391**, 806–811 (1998).
  48. Elbashir, S. M. *et al.* Duplexes of 21-nucleotide RNAs mediate RNA interference in cultured mammalian cells. *Nature* **411**, 494–498 (2001).
  49. Elbashir, S. M., Lendeckel, W. & Tuschl, T. RNA interference is mediated by 21- and 22-nucleotide RNAs. *Genes Dev* **15**, 188–200 (2001).
  50. Martinez, J. RISC is a 5' phosphomonoester-producing RNA endonuclease. *Genes Dev* **18**, 975–980 (2004).
  51. Meister, G. *et al.* Human Argonaute2 Mediates RNA Cleavage Targeted by miRNAs and siRNAs. *Mol. Cell* **15**, 185–197 (2004).
  52. Liu, J. Argonaute2 Is the Catalytic Engine of Mammalian RNAi. *Science* **305**, 1437–1441 (2004).
  53. Daude, N. Specific inhibition of pathological prion protein accumulation by small interfering RNAs. *J. Cell. Sci.* **116**, 2775–2779 (2003).
  54. Tilly, G., Chapuis, J., Vilette, D., Laude, H. & Vilotte, J. L. Efficient and specific down-regulation of prion

- protein expression by RNAi. *Biochem Biophys Res Commun* **305**, 548–551 (2003).
55. Kim, Y. *et al.* Utility of RNAi-mediated prnp gene silencing in neuroblastoma cells permanently infected by prions: Potentials and limitations. *Antiviral Res* **84**, 185–193 (2009).
  56. White, M. D. *et al.* Single treatment with RNAi against prion protein rescues early neuronal dysfunction and prolongs survival in mice with prion disease. *Proc. Natl. Acad. Sci. U.S.A.* **105**, 10238–10243 (2008).
  57. Pfeifer, A. *et al.* Lentivector-mediated RNAi efficiently suppresses prion protein and prolongs survival of scrapie-infected mice. *J. Clin. Invest.* **116**, 3204–3210 (2006).
  58. Pulford, B. *et al.* Liposome-siRNA-Peptide Complexes Cross the Blood-Brain Barrier and Significantly Decrease PrPC on Neuronal Cells and PrPRES in Infected Cell Cultures. *PLoS ONE* **5**, e11085 (2010).
  59. Donius, L. R., Handy, J. M., Weis, J. J. & Weis, J. H. Optimal Germinal Center B Cell Activation and T-Dependent Antibody Responses Require Expression of the Mouse Complement Receptor Cr1. *J. Immunol.* **191**, 434–447 (2013).
  60. Donius, L. R., Orlando, C. M., Weis, J. J. & Weis, J. H. Generation of a novel Cr2 gene allele by homologous recombination that abrogates production of Cr2 but is sufficient for expression of Cr1. *Immunobiology* **219**, 53–63 (2014).
  61. Zabel, M. D. *et al.* Stromal Complement Receptor CD21/35 Facilitates Lymphoid Prion Colonization and Pathogenesis. *J. Immunol.* **179**, 6144–6152 (2007).
  62. Georgieva, J., Hoekstra, D. & Zuhorn, I. Smuggling Drugs into the Brain: An Overview of Ligands Targeting Transcytosis for Drug Delivery across the Blood–Brain Barrier. *Pharmaceutics* **6**, 557–583 (2014).
  63. Pardridge, W. M. Drug and gene delivery to the brain: the vascular route. *Neuron* (2002).
  64. Abbott, N. J. Blood–brain barrier structure and function and the challenges for CNS drug delivery. *J Inherit Metab Dis* **36**, 437–449 (2013).
  65. Pang, Z. *et al.* Preparation and brain delivery property of biodegradable polymersomes conjugated with OX26. *J Control Release* **128**, 120–127 (2008).
  66. Boado, R. J., Hui, E. K.-W., Lu, J. Z., Zhou, Q.-H. & Pardridge, W. M. Selective targeting of a TNFR decoy receptor pharmaceutical to the primate brain as a receptor-specific IgG fusion protein. *J Biotech* **146**, 84–91 (2010).
  67. Lemke, A., Kiderlen, A.F., Petri, B.P. & Kayser, O. Delivery of amphotericin B nanosuspensions to the brain and determination of activity against *Balamuthia mandrillaris* amebas. *Nanomed Nanotech Biol Med* **6**, 597–603 (2010).
  68. Ragnarsson, E. G. E. *et al.* *Yersinia pseudotuberculosis* induces transcytosis of nanoparticles across human intestinal villus epithelium via invasin-dependent macropinocytosis. *Lab Invest* **88**, 1215–1226 (2008).
  69. Régina, A. *et al.* Antitumour activity of ANG1005, a conjugate between paclitaxel and the new brain delivery vector Angiopep-2. *Br J Pharmacol* **155**, 185–197 (2009).
  70. Kumar, P. *et al.* Transvascular delivery of small interfering RNA to the central nervous system. *Nature* **448**, 39–43 (2007).
  71. Zabel, M. D. Lipopeptide delivery of siRNA to the central nervous system. *Nanotechnology for Nucleic Acid Delivery* (Humana Press, 2012)
  72. Bender, H. R., Kane, S. & Zabel, M. D. Delivery of Therapeutic siRNA to the CNS Using Cationic and Anionic Liposomes. *J Vis Exp* e54106 (2016).
  73. Lotscher, M., Recher, M., Hunziker, L. & Klein, M. A. Immunologically Induced, Complement-Dependent Up-Regulation of the Prion Protein in the Mouse Spleen: Follicular Dendritic Cells Versus Capsule and Trabeculae. *J. Immunol.* **170**, 6040–6047 (2003).
  74. Martinez del Hoyo, G., Lopez-Bravo, M., Metharom, P., Ardavin, C. & Aucouturier, P. Prion Protein Expression by Mouse Dendritic Cells Is Restricted to the Nonplasmacytoid Subsets and Correlates with the Maturation State. *J. Immunol.* **177**, 6137–6142 (2006).
  75. Li, R. *et al.* The Expression and Potential Function of Cellular Prion Protein in Human Lymphocytes. *Cell Immunol* **207**, 49–58 (2001).
  76. Mabbott, N. A., Brown, K. L., Manson, J. & Bruce, M. E. T-lymphocyte activation and the cellular form of the prion protein. *Immunology* **92**, 161–165 (1997).
  77. Heidel, J. D., Hu, S., Liu, X. F., Triche, T. J. & Davis, M. E. Lack of interferon response in animals to naked siRNAs. *Nat. Biotechnol.* **22**, 1579–1582 (2004).
  78. Morrissey, D. V. *et al.* Sequence-dependent stimulation of the mammalian innate immune response by synthetic siRNA. *Pharm. Res.* **22**, 1002–1007 (2005).
  79. Hornung, V. *et al.* Sequence-specific potent induction of IFN- $\alpha$  by short interfering RNA in plasmacytoid

- dendritic cells through TLR7. *Nat. Med.* **11**, 263–270 (2005).
80. Marques, J. T. & Williams, B. R. G. Activation of the mammalian immune system by siRNAs. *Nat. Biotechnol.* **23**, 1399–1405 (2005).
  81. Sioud, M. Induction of Inflammatory Cytokines and Interferon Responses by Double-stranded and Single-stranded siRNAs is Sequence-dependent and Requires Endosomal Localization. *J. Mol. Biol.* **348**, 1079–1090 (2005).
  82. Kariko, K., Bhuyan, P., Capodici, J. & Weissman, D. Small Interfering RNAs Mediate Sequence-Independent Gene Suppression and Induce Immune Activation by Signaling through Toll-Like Receptor 3. *J. Immunol.* **172**, 6545–6549 (2004).
  83. Robbins, M., Judge, A. & MacLachlan, I. siRNA and Innate Immunity. *Oligonucleotides* **19**, 89–102 (2009).
  84. Lappalainen, K., Jääskeläinen, I., Syrjänen, K., Urtti, A. & Syrjänen, S. Comparison of cell proliferation and toxicity assays using two cationic liposomes. *Pharm. Res.* **11**, 1127–1131 (1994).
  85. Tousignant, J. D., Gates, A. L. & Ingram, L. A. Comprehensive analysis of the acute toxicities induced by systemic administration of cationic lipid: plasmid DNA complexes in mice. *Hum Gene Ther* **11**, 2493-2513. (2000).
  86. Alvarez-Erviti, L. *et al.* Delivery Of SiRNA To Mouse Brain With Exosomes. *Nat. Biotechnol.* 1–7 (2011). doi:10.1038/nbt.1807
  87. Hanke, M. L. & Kielian, T. Toll-like receptors in health and disease in the brain: mechanisms and therapeutic potential. *Clin. Sci.* **121**, 367–387 (2011).
  88. Goral, S. The three-signal hypothesis of lymphocyte activation/targets for immunosuppression. *Dial. Transplant.* **40**, 14–16 (2011).
  89. Meier, P. *et al.* Soluble dimeric prion protein binds PrP(Sc) in vivo and antagonizes prion disease. *Cell* **113**, 49–60 (2003).

## Chapter 4:

### **LSPCs do not increase the survival periods of prion-infected mice, but do improve behavioral outcomes at specific time points**

#### **Summary**

Prion diseases are devastating neurodegenerative diseases that affect both animals and humans. Currently, there is no known therapeutic that extends the survival period or alleviates disease in prion-infected animals/individuals. Prion diseases are also similar in pathogenesis to other protein misfolding diseases, such as Alzheimer's and Parkinson's disease. There is speculation that a therapeutic effective at treating prion diseases could also be applied to the treatment of other protein misfolding disorders. Therefore, we have investigated the use of RNA interference (RNAi) as a potential therapeutic for prion diseases. Our siRNA targets the host cellular prion protein (PrP<sup>C</sup>), which becomes misfolded during prion infection. Decreasing PrP<sup>C</sup> via stereotaxic injection has proven successful in prolonging survival times and reversing prion neuropathology in prion-infected animals. Since repeated stereotaxic injections are not a feasible option for a clinical drug, we have packaged our PrP<sup>C</sup> siRNA into liposomes bound to a neuro-targeting peptide. These liposome-siRNA-peptide complexes (LSPCs) can be administered intravenously, and can cross the blood-brain barrier to decrease neuronal PrP<sup>C</sup>. The aim of this study was to determine if LSPCs treatment could prolong the survival periods of prion-infected mice and alleviate clinical signs. Unfortunately, recurring LSPCs treatment does not increase survival times in prion-infected mice. However, it does improve the performance of these mice in burrowing and nesting behavioral tests. We also observed an increase in total IgG levels against RVG-9r of LSPCs-treated mice. This immune response might explain why there was no benefit to survival times with repetitive treatments. The immune reaction will need to be addressed via different dosing regimens, targeting peptides, and/or liposomal formulations before LSPCs become a viable therapeutic for prion diseases.

## Introduction

The prion protein, PrP<sup>C</sup>, in its immature form, is a 250-amino acid protein that is expressed in all mammals experimentally tested<sup>1,2</sup>. PrP<sup>C</sup> is widely expressed throughout the body, but the highest expression levels of mRNA and protein reside in neurons within the central nervous system (CNS)<sup>3,4</sup>. PrP<sup>C</sup> matures in the endoplasmic reticulum, where it becomes a 208-amino acid protein with a glycosylphosphatidylinositol anchor. Post-translational modification of PrP<sup>C</sup> occurs in the Golgi apparatus, where glycosyl moieties are added<sup>1,5</sup>. PrP<sup>C</sup> exists mostly as an  $\alpha$ -helical protein, with three  $\alpha$ -helices and two  $\beta$ -sheets, and is contained within cholesterol-rich lipid rafts in the plasma membrane<sup>6</sup>.

PrP<sup>C</sup> can change from an  $\alpha$ -helical structure to a mostly  $\beta$ -sheet structure. When this secondary structure change occurs, PrP<sup>C</sup> becomes infectious and is known as PrP<sup>Res</sup><sup>2,7,8</sup>. The diseases that result from the conversion to PrP<sup>Res</sup> are referred to as prion diseases. A misfolded protein that encodes its replicative instructions within the structure of the protein causes prion diseases<sup>9</sup>, unlike most diseases caused by microbiological agents, which are encoded by RNA or DNA. Prion diseases affect a broad range of species, from chronic wasting disease (CWD) in cervids to Creutzfeldt-Jakob disease (CJD) in humans.

These diseases have multiple etiologies depending on the species and individuals that are afflicted. Several polymorphisms result in either susceptibility or resistance to acquiring prion disease. Individuals who possess susceptible polymorphisms have an increased likelihood of their PrP<sup>C</sup> changing secondary structure and becoming infectious. Several prion diseases that have a genetic component include scrapie in sheep, and genetic CJD and fatal familial insomnia in humans. PrP<sup>Res</sup> is also transmitted through the consumption of infected meat or exposure to infected bodily fluids. The diseases spread by these routes include bovine spongiform encephalopathy in cows, variant CJD in humans, and CWD in cervids, respectively. Incubation times of prion diseases vary between a few years to a couple of decades. However, progression of the disease, once clinical stage has been reached, is usually under six months.

Once an individual is exposed, PrP<sup>Res</sup> will first migrate to lymphoid tissues with the help from immune cells, such as B cells, follicular dendritic cells, and monocytes<sup>10</sup>. PrP<sup>Res</sup> replicates and accumulates within the spleen and lymph nodes that are part of the gut-associated lymphoid tissue. The replication eventually results in the migration of PrP<sup>Res</sup> to nerve bundles within these tissues<sup>11-13</sup>. The leading theory on how PrP<sup>Res</sup> reaches the brain is that it ascends nerve tracks originally located within these lymphoid tissues. Evidence to support this comes from

the pathology of prion diseases, which usually starts in the brain stem and migrates to the cerebellum and cerebrum, indicating that the first point-of-contact of PrP<sup>Res</sup> molecules in the CNS is the brainstem<sup>14,15</sup>. Pathology includes PrP<sup>Res</sup> plaques, neuronal degeneration, astrogliosis, and vacuolation<sup>16</sup>.

Research on PrP<sup>C</sup> began in the mid-1980s and has been ongoing for the last 30 years; however, the function of PrP<sup>C</sup> remains elusive. Evidence suggests that PrP<sup>C</sup> might be neuroprotective through antioxidant<sup>17-19</sup> and anti-apoptotic functions<sup>20,21</sup>. The regulation of Ca<sup>2+</sup> homeostasis further supports its possible neuroprotective function<sup>22-24</sup>. The management of Ca<sup>2+</sup> by PrP<sup>C</sup> is one way in which the protein can activate several cell-signaling pathways, such as MAPK/ERK, PKA, and STAT1, to modulate the response of oxidative and apoptotic damage<sup>23,25,26</sup>. The ability of PrP<sup>C</sup> to bind to Cu<sup>2+</sup> is also thought to mediate oxidative stress damage<sup>18,27,28</sup>. Another proposed function of PrP<sup>C</sup> is to activate the immune system in the presence of certain immune stimulants, such as lipopolysaccharide and CpG oligodeoxynucleotides<sup>29-31</sup>. With these potential functions, it was anticipated that PrP-null mice would show an obvious phenotypic change. However, PrP-null mice do not show any deleterious effects from the elimination of PrP<sup>C</sup><sup>32</sup>. PrP-null mice have slight circadian rhythm disruptions<sup>33</sup> and reorganization of neuronal circuits<sup>34</sup> but no overt loss-of-function phenotype. Some have argued that there is a redundant pathway that recovers the loss-of-function phenotype when PrP<sup>C</sup> is depleted<sup>35</sup>. Whatever the reason for no loss-of-function phenotype, mice with reduced or depleted PrP<sup>C</sup> live long and healthy lives.

Unfortunately, there is no known therapeutic that can improve the quality of life or the survival times of an individual afflicted with prion disease. Some therapeutics that targeted the mechanism of PrP<sup>Res</sup> conversion or its accumulation resulted in longer survival times in animal models. However, a lot of these compounds were toxic or could not breach the blood-brain barrier. Also, most of these compounds were only successful, i.e. only extended survival periods, when given before or shortly after prion inoculation<sup>36-41</sup>. Since reducing or eliminating PrP<sup>C</sup> was shown to have no deleterious effects, recent prion therapeutic research is focused on manipulating PrP<sup>C</sup> to reduce PrP<sup>Res</sup> and its pathology. Injections of short hairpin RNA directly into CNS tissue in prion-infected mice resulted in a decrease of neuronal PrP<sup>Res</sup> and a reversal of prion pathology<sup>42,43</sup>. Eliminating PrP<sup>C</sup> after established prion infection using *Cre/loxP* mice also led to a reversal of prion pathology<sup>44</sup>. However, it is not feasible to create transgenic humans or to repeatedly inject therapeutic molecules into the CNS as it causes damage to the local tissue.

We propose to use small interfering RNA (siRNA) to decrease the amount of neuronal PrP<sup>C</sup> *in vivo*. Our PrP<sup>C</sup> siRNA is packaged with cationic liposomes and a neuro-targeting peptide called RVG-9r. Together, these

complexes are referred to as liposome-siRNA-peptide complexes (LSPCs)<sup>45</sup>. We have previously shown that LSPCs, when injected intravenously, can cross the blood-brain barrier to decrease neuronal PrP<sup>C</sup> in two different mouse models (unpublished results). Therefore, we treated prion-infected mice every two weeks or every four to six weeks starting at 120 days post inoculation all the way till terminal disease. These mice were also subjected to behavioral testing via burrowing and nesting tests every two weeks. We found that repeated siRNA treatments do not extend the survival times of mice infected with prions, but repeated treatments do improve the behavior of prion-infected mice at certain time points. Treatment of mice every two weeks with LSPCs also increases total IgG levels, indicating that there is a significant immune response to our treatment. We conclude that although LSPCs are not able to extend survival times in prion-inoculated mice, behavioral scores are improved when LSPCs are administered every two weeks. Therefore, we postulate, with a little optimization, LSPCs may represent a new therapeutic option for prion diseases.

## **Materials and Methods**

### ***Mice***

FVB mice were purchased from The Jackson Laboratory (Bar Harbor, ME) and CD1 mice were purchased from Charles River Laboratories (Wilmington, MA). Mice were euthanized using CO<sub>2</sub>. All mice were bred and maintained at Lab Animal Resources, accredited by the Association for Assessment and Accreditation of Lab Animal Care International, in accordance with protocols approved by the Institutional Animal Care and Use Committee at Colorado State University.

### ***Generation of Liposomes***

#### ***DOTAP LSPCs***

DOTAP LSPCs consist of a 1:1 DOTAP:cholesterol ratio in a 1:1 chloroform:methanol solution. Both lipids were purchased from Avanti Lipids (DOTAP - 1,2-dioleoyl-3-trimethylammonium-propane [chloride salt]). The solvents were evaporated using N<sub>2</sub> gas and the resultant dry lipid film was placed under vacuum for a total of 8 hours to remove any excess solvent. A stock solution of liposomes was made at an 8 mM (40 umole total) concentration, by resuspending the lipid film in 5 mL of 10% sucrose heated at 55°C. All components (lipid film and sucrose) were kept at this temperature during rehydration. The heated sucrose was added to the lipid cake 1 mL

every 10 minutes. The lipid film was swirled every 3 minutes to promote lipid mixing. Resulting liposomes were stored at 4°C.

#### ***Generating LSPCs and treating mice with LSPCs***

PrP<sup>C</sup> 1672 siRNA sequence: ACATAAACTGCGATAGCTTC (Qiagen).

PrP<sup>C</sup> 1578 siRNA sequence: GAAGTAGGCTCCATTCCAAA (Qiagen)

RVG-9r peptide: YTIWMPENPRPGTPCDIFTNSRGKRASNGGGGrrrrrrrr (ChemPeptide)

#### ***LSPCs***

The DOTAP LSPCs liposomes were diluted 1:100 in 1X PBS and sonicated 4X with 2-3 minute rests in between. 50 uL (4 nmole total) of diluted/sonicated liposomes was mixed with 100 uL (4 nmole total) of 1672 and/or 1578 siRNA. The siRNA/liposome solution was incubated for 10 minutes at 4°C. Then, 80 uL (40 nmole total) of RVG-9r peptide was added to the solution and allowed to incubate for 10 minutes on ice. Mice were placed under a heat lamp for 5 minutes and anesthetized with isofluorane. The mouse tails were disinfected using 70% EtOH. 200-300 µl LSPCs were injected into the tail veins of mice using a 29-gauge insulin syringe. Prion-infected mice were treated every 2 weeks in the first terminal study and every 3-5 weeks in the second terminal study. A small subset of mice were treated intranasally (IN). The IN mice were laid on their dorsal side (ventral side up) and the LSPCs were dripped into the nasal cavity 1-2 µL at a time for a total of 30-50 µL.

#### ***Intraperitoneal inoculations and dissections***

RML-5 prions were prepared as previously described<sup>46</sup>. 10% RML-5 brain homogenates were diluted 1:100 (0.1%) in 1X PBS supplemented with 100 units/mL of Penicillin and 100 µg/mL of Streptomycin (Gibco) immediately before inoculation. Mice were scruffed and flipped upside down for inoculation. 100 µL of inoculum was injected in the left or right bottom quadrant of the intraperitoneal cavity with a 29-gauge insulin syringe (BD). Upon clinical stage, mice were scored based on a scoring rubric and euthanized if they reached a score of 10 or above. Brains, spleens, and serum were collected from each mouse. A hemisphere of brain and half of the spleen were frozen at -20°C for western blot analysis, and the other hemisphere of brain and spleen half were fixed in 4% paraformaldehyde.

#### ***Behavioral Testing***

Burrowing and nesting behavioral tests were performed on intraperitoneally prion-inoculated mice. Behavioral tests were started approximately 120 days post inoculation. For burrowing, mice were given

approximately 100 grams of food stuffed into a 6-inch plastic PVC pipe. Mice were allowed to burrow out the food for 30 minutes. Rate of burrowing was calculated by the number of grams of food burrowed out divided by total time burrowed. For nesting, mice were given a small cotton nestlet and allowed to build a nest overnight. Mice were scored on a scale from 0-4, with 0 being no nest built and 4 being a perfectly built nest. Average nesting scores were calculated for each treatment group.

### ***Normal brain homogenate (NBH) and Protein misfolding cyclic amplification (PMCA)***

Mice were euthanized and perfused with 30 mL of 5 mM EDTA in 1X PBS. Whole brains were removed. Brains were weighed and placed in 1.5 mL Eppendorf tubes with 2.5 mm glass beads. PMCA buffer (4 mM EDTA, 150 mM NaCl in 1X PBS) with protease inhibitor tablets (Roche) was added to make a 20% weight/volume (w/v) solution. Samples were homogenized in a BeadBug homogenizer (Sigma). All NBH samples were pooled and diluted to a 10% w/v solution using PMCA conversion buffer containing 2% Triton-X 100. NBH was aliquoted and stored at -80°C. PMCA was performed as previously described<sup>47</sup> with slight modifications. Samples were sonicated at power 20 for 40 seconds in a microplate horn sonicator (Qsonica), followed by a 30-minute incubation at 37°C repeated for 24 hours. This was equivalent to one round and a total of 6 rounds was completed on each sample. Proteinase K (PK) digestion and western blot were performed as described below. PMCA scores were calculated as previously described<sup>48</sup>. Briefly, PMCA scores were calculated based on the round that the samples first appeared, and a detection threshold based on the 99.9% confidence interval for designating NBH samples as negative was calculated from the mean PMCA score of 73 NBH samples using Student's t-table.

### ***PK digestion and western blots***

A stock solution of PK was made using 500 µg/mL of proteinase K (Roche) with a 1:10 dilution of 0.5 M EDTA in 1X PBS. The PK stock solution was added to western blot samples at a 1:10 dilution for a final concentration of 50 µg/mL. PMCA samples were incubated at 37°C for 30 minutes with a 10-minute deactivation step at 95°C. Samples were stored at -20°C before running on western blot. Before starting western blots, samples were thawed on ice for 30 minutes and denatured at 95°C for 3 minutes. Proteins were electrophoretically separated using 12% sodium dodecyl sulfate polyacrylamide gels (Invitrogen). Proteins were then transferred to a polyvinylidene difluoride membrane (Millipore). Membranes were blocked using 5% non-fat dry milk for 1 hour. Membranes were washed 2X for 10 minutes each using 1X PBS with 0.2% Tween. Membranes were incubated with horseradish peroxidase-conjugated BAR-224 (SPI Bio) anti-PrP<sup>C</sup> antibody diluted 1:20,000 overnight at 4°C.

Membranes were washed again 6X for 10 minutes each, and incubated with enhanced chemiluminescent substrate (Millipore) for 5 minutes. Membranes were photographed using an ImageQuant LAS 4000 (GE).

### ***Immunohistochemistry***

Brains from prion-infected mice from the first terminal study were sent to Colorado State University's Veterinary Diagnostic Laboratory for paraffin embedding and GFAP staining. The blank slides received from CSU's VDL were then stained for PrP<sup>Res</sup> using the following protocol. Slides were incubated at 53°C for 30 minutes before being immersed in xylene twice for 10 minutes. The slides were then rehydrated through an ethanol gradient consisting of 100%, 95% and 70% concentrations for 5 minutes each and then immersed in 88% formic acid for 10 minutes. After washing the slides in running water for 10 minutes, the slides were processed through antigen retrieval while in a citrate buffer, pH of 7.4. The slides were allowed to cool before being washed twice in a 0.1% PBS-Triton buffer for 5 minutes on a rocker. In order to extinguish exogenous peroxidase activity of the tissues, the slides were immersed in a 3% hydrogen peroxide preparation in methanol for 30 minutes before undergoing another wash cycle. The tissues were then encircled in a DAP pen and allowed to incubate with Superblock for 30 minutes. The excess block was tapped off each slide and the slides incubated overnight in 4°C with D18 antibody at a 1:1000 dilution. The next morning the slides were washed and incubated with a biotinylated anti-human Ig (1:1000) for 1 hour at room temperature. They were then washed and incubated with an avidin-biotin complex for 30 minutes at room temperature. After 3 wash cycles, the slides were incubated with DAB reagent for 5 minutes in order to develop the staining. The slides were then briefly washed and counterstained in hematoxylin for 5 minutes, and then immersed in water for 10 minutes to deactivate the hematoxylin. To complete the staining process the slides were dehydrated through the alcohol gradient and xylene before being mounted with a coverslip. All slides with either GFAP or PrP<sup>Res</sup> staining were viewed by a lab member who was blinded to the LSPCs treatment groups

### ***ELISA for Total IgG Levels***

Serum samples from terminally ill mice were collected by heart stick after euthanasia. Samples were stored at -20°C until assay was performed. 1 µg of RVG-9r was coated into 96-well Elisa plates (Nunc) using carbonate/bicarbonate buffer (Sigma) with 100 µL in each well. The plates incubated overnight at 4°C. Plates were washed 2X with 300 µL of Elisa wash buffer (1X PBS + 0.05% Tween). All wells were blocked with 100 µL SuperBlock (ThermoFisher) at room temperature for two hours. Plates were washed 2X with 300 µL of Elisa wash buffer. Plated 50 µL of the following serum dilutions from LSPCs treated mice: 1:50, 1:100, 1:250, 1:500, 1:1000,

and 1:2000. Serum incubated overnight at 4°C. All wells were washed 4X with 300 µL of Elisa wash buffer. A 1:5000 dilution of an anti-mouse IgG horseradish peroxidase secondary antibody (Cell signaling) in SuperBlock was added to each well for a total volume of 100 µL per well and incubated at room temperature for two hours. All wells were washed with 300 µL of Elisa wash buffer. 100 µL of TMB substrate (Thermo) was added to each well and allowed to incubate until a deep blue color change developed. To stop the reaction, 100 µL of a stop solution (0.5 M H<sub>2</sub>SO<sub>4</sub> in 1X PBS) was added to each well. Photometric analysis was performed at 450 nm using a Multiskan Spectrum plate reader (Thermo).

### ***Statistical Analysis***

Statistical analyses were performed using GraphPad Prism and Excel. SD error bars are used to show the variability between technical replicates of individual treated mice. When mice are grouped together, SEM is used to show how closely the mean of the treated mice represents the population mean of all treated mice.

## **Results**

### ***Repetitive LSPCs treatments do not extend the survival times of prion-infected mice***

FVB and CD1 mice were intraperitoneally inoculated with 0.1% RML-5 prions to assess whether repetitive LSPCs treatments affect survival times in prion-infected mice. Each treatment and control group contains between three and five mice. Mice were inoculated intraperitoneally with a lower dose of prions to mimic a more natural prion infection.

The 1<sup>st</sup> terminal study involved FVB mice with the treatment groups listed in Table 4.1. The LSPCs treatment groups for the 1<sup>st</sup> terminal study were treated every two weeks, starting at 119 days post-inoculation (dpi) and ending at 231 dpi (Table 4.2). Most of the treated mice received the LSPCs intravenously (IV), but a small subset of mice received the LSPCs intranasally (IN). Half of the mice in the 1<sup>st</sup> terminal study received seven LSPCs treatments, while the 8<sup>th</sup> and 9<sup>th</sup> treatments occurred after a significant number of mice were euthanized for clinical signs. Survival times of all treated mice were compared to the infected, untreated group. There was a perceived difference in development of clinical signs between male and female infected, untreated mice but the survival times calculated for each gender were not statistically significant (Figure 4.1A). The only significant difference in survival times observed in the 1<sup>st</sup> terminal study was the infected, IV and IN group (Figure 4.1C). The IV and IN group, treated both intravenously and intranasally, were euthanized earlier than the infected, untreated group due to clinical

signs. The other treatment groups had no significant differences compared to the untreated group (Figure 4.1B and C). Interestingly, three of the uninfected, treated mice died one hour after the 8<sup>th</sup> and 9<sup>th</sup> LSPCs treatments (Table 4.2 and Figure 4.1C).

The 2<sup>nd</sup> terminal study involved prion-infected CD1 mice that were treated every 3-5 weeks for a total of four treatments (Table 4.4). Table 4.3 lists the groups of the CD1 treatment study. There was a significant difference between prion-infected, untreated CD1 male and female mice (Figure 4.2A). Therefore, survival times of the male and female treated groups were analyzed separately. A couple of the male treated mice died of intercurrent death and were thus excluded from analysis. Those deaths resulted in only two male mice per each treated group. There was no statistical difference between any of the male treated groups, although more numbers are needed to make any definite conclusions (Figure 4.2C). None of the female-treated groups had a statistical difference compared to the infected, untreated control (Figure 4.2B).

**Table 4.1. Treatment groups of the 1<sup>st</sup> terminal study**

Groups of 1 <sup>st</sup> Treatment Study
Uninfected, Untreated
Uninfected, Treated
Infected, Untreated
Infected, 1578 siRNA
Infected, 1672 siRNA
Infected, 1578 + 1672
Infected, Both IV and IN
Infected, IN

**Table 4.2. Number of treatments and DPI treated in 1<sup>st</sup> terminal study**

1 <sup>st</sup> Terminal Study	DPI Treated
1 Treatment	119
2 Treatments	133
3 Treatments	147
4 Treatments	161
5 Treatments	175
6 Treatments	186
7 Treatments	203
8 Treatments	217 <sup>1,2</sup>
9 Treatments	231 <sup>1,2</sup>

<sup>1</sup> Most mice euthanized by these treatments

<sup>2</sup> Uninfected, treated controls died at these treatments

**Table 4.3. Treatment groups of the 2<sup>nd</sup> terminal study**

Groups of 2 <sup>nd</sup> Treatment Study
Uninfected, Treated
Infected, Untreated
Infected, 1578 siRNA
Infected, 1672 siRNA
Infected, 1578 + 1672

**Table 4.4. Number of treatments and DPI treated in 2<sup>nd</sup> terminal study**

2 <sup>nd</sup> Terminal Study	DPI Treated
1 Treatment	120
2 Treatment	144
3 Treatment	165
4 Treatment	198

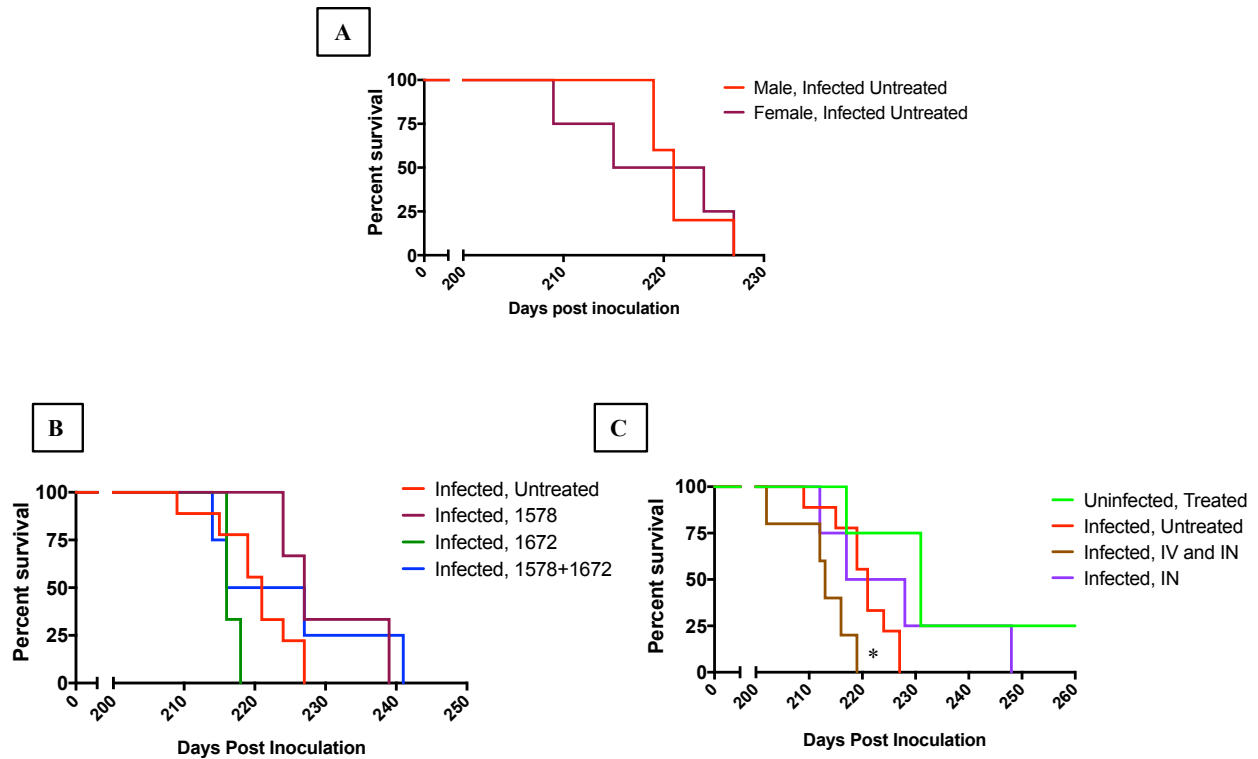


**Figure 4.1. Survival curves of LSPCs-treated FVB mice in 1<sup>st</sup> terminal study.**

FVB mice were intraperitoneally infected with RML-5 prions and treated with LSPCs every two weeks starting half way through disease progression. A) Male and female prion-infected, untreated mice did not have significantly different survival times. B) The LSPCs-treated groups 1578, 1672, and 1578+1672 did not have statistically significant survival times compared to the infected, untreated group. C) The survival times of the LSPCs-treated groups infected, IN and uninfected, treated group were not different than the infected, untreated control. The infected, IV and IN did have significantly different survival times compared to the infected, untreated control in that the IV and IN group had shorter survival periods compared to control. \*  $p < 0.05$ . Log-rank (Mantel-Cox) test with Bonferroni's correction

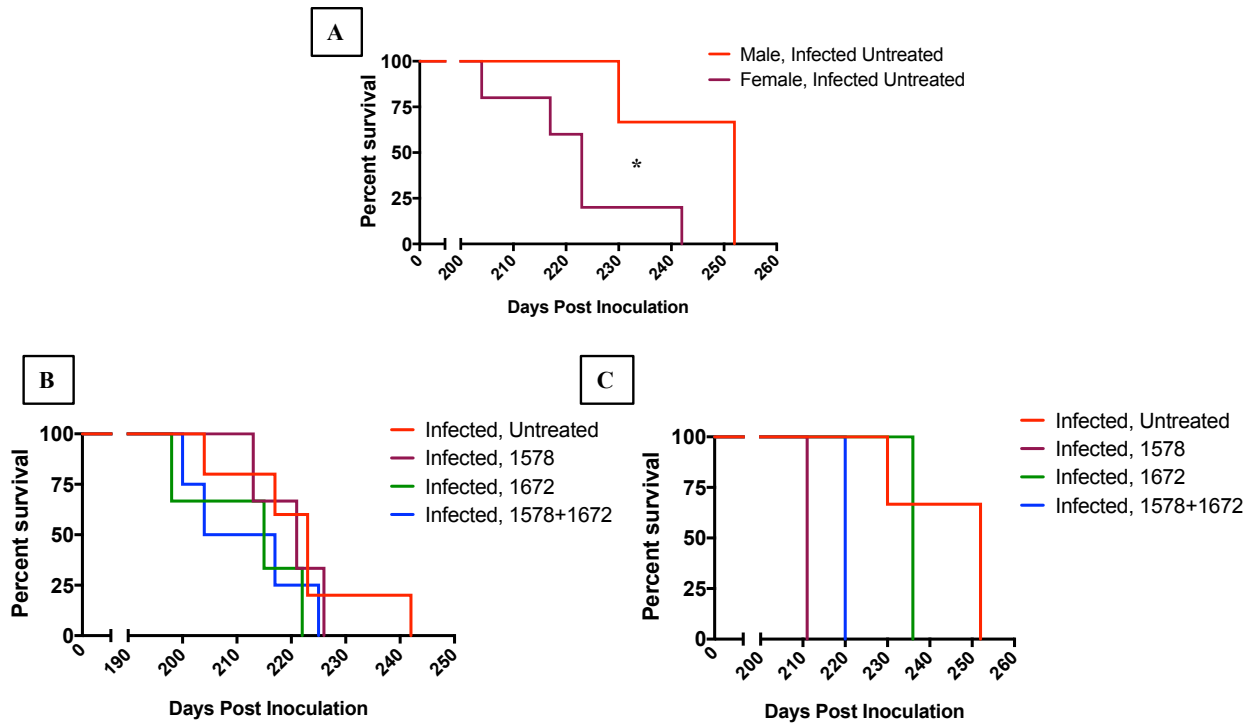


**Figure 4.2. Survival curves of LSPCs-treated CD1 mice in 2<sup>nd</sup> terminal study.**

CD1 mice were intraperitoneally infected with RML-5 prions and treated every three to five weeks with LSPCs starting half way through disease progression. A) Female CD1 prion-infected mice had shorter survival times compared to their male counterparts. B) Female mice in LSPCs-treated groups 1578, 1672, and 1578+1672 compared did not have significantly different survival times compared to the female infected, untreated control. C) Male CD1 mice in LSPCs-treated groups 1578, 1672, and 1578+1672 did not have significantly different survival times compared to the male infected, untreated control. Multiple male mice were excluded from analysis because they died of intercurrent death. \*  $p < 0.05$ . Log-rank (Mantel Cox) test with Bonferroni's correction.

***LSPCs treatment causes an increase in activated astrocytes in treated mice compared to uninfected, untreated mice***

Western blot analysis using the anti-PrP<sup>C</sup> antibody BAR-224 conjugated to horseradish peroxidase and immunohistochemistry (IHC) using an anti-glial fibrillary acidic protein (GFAP) antibody were performed to analyze prion pathology within the brains of untreated and treated mice either uninfected or infected.

Western blot analysis of the 1<sup>st</sup> and 2<sup>nd</sup> terminal study shows that all mice had prions in their brains at time of clinical disease, while uninfected mice did not (Figure 4.3A and B). IHC analysis reveals that all prion-infected mice, whether untreated or treated, have typical prion neuropathology, such as prion accumulation, vacuolation, and presence of reactive astrocytes by GFAP staining in the cerebellum and hippocampus (Figure 4.4 and 4.5).

Surprisingly, the uninfected, treated group also had the presence of reactive astrocytes in both the cerebellum and

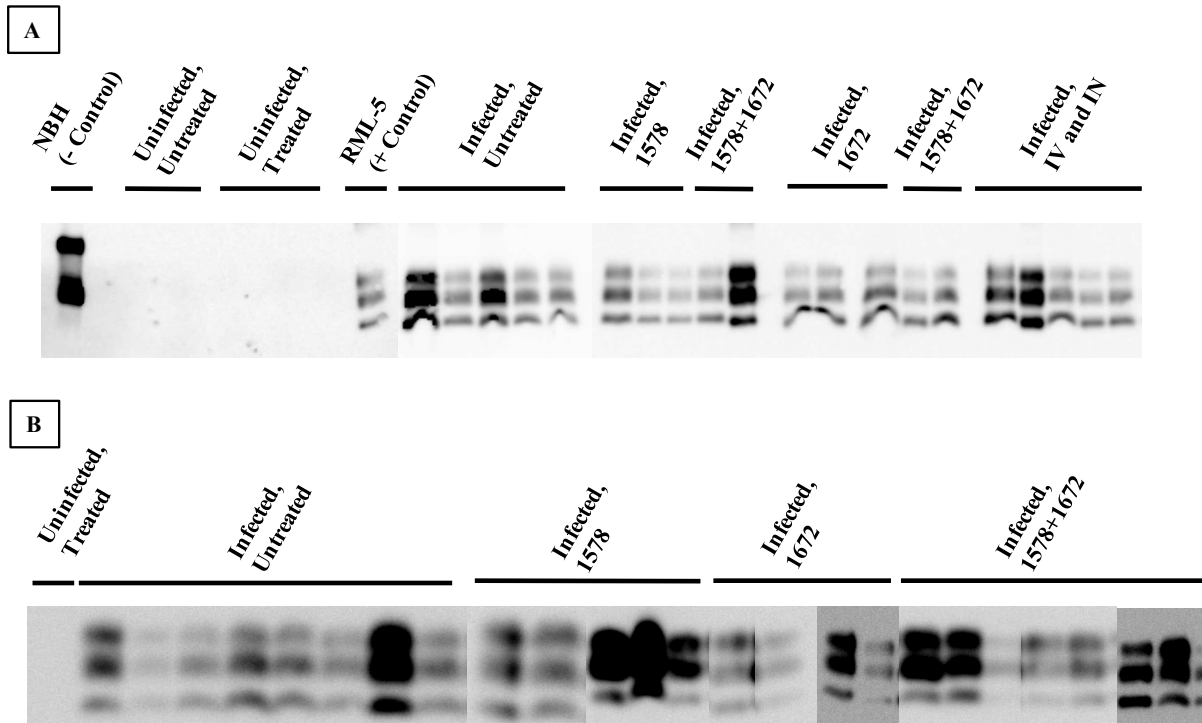


**Figure 4.3. Analyzing PrP<sup>Res</sup> deposition in prion-infected mice of the LSPCs terminal studies using western blot.**

A) All mice in the 1<sup>st</sup> terminal study that were infected with RML-5 prions had PrP<sup>Res</sup> deposition within their brains at terminal disease, regardless of treatment group. No difference in levels of PrP<sup>Res</sup> were observed between untreated and treated mice. B) All mice in the 2<sup>nd</sup> terminal study that were infected with RML-5 prions had PrP<sup>Res</sup> deposition in their brains at terminal disease, regardless of treatment groups. Again, no difference was observed in the amount of PrP<sup>Res</sup> in the brains of untreated versus treated mice.

the hippocampus compared to the age-matched uninfected, untreated group (Figure 4.5B). The uninfected, treated group did not have any prion accumulation as seen by both the western blot (Figure 4.3A) and IHC results (Figure 4.4B). Therefore, the only difference between the uninfected, untreated and the uninfected, treated group was the repetitive LSPCs treatments.

#### ***Repetitive LSPCs treatments result in a rescue of behavioral changes caused by prion infection***

All mice in the 1<sup>st</sup> and 2<sup>nd</sup> terminal studies were subjected to behavioral testing to determine if LSPCs treatment saves early behavioral deficits seen in prion-infected mice. Behavioral testing started one week before the LSPCs treatment and ended when all mice were euthanized. Both burrowing and nesting behavioral tests were chosen to assess behavioral deficits.

Since male and female mice had a difference in survival times in the 2<sup>nd</sup> terminal study, the behavior of male mice was compared to female mice to assess if the behavior was different between the genders. No difference

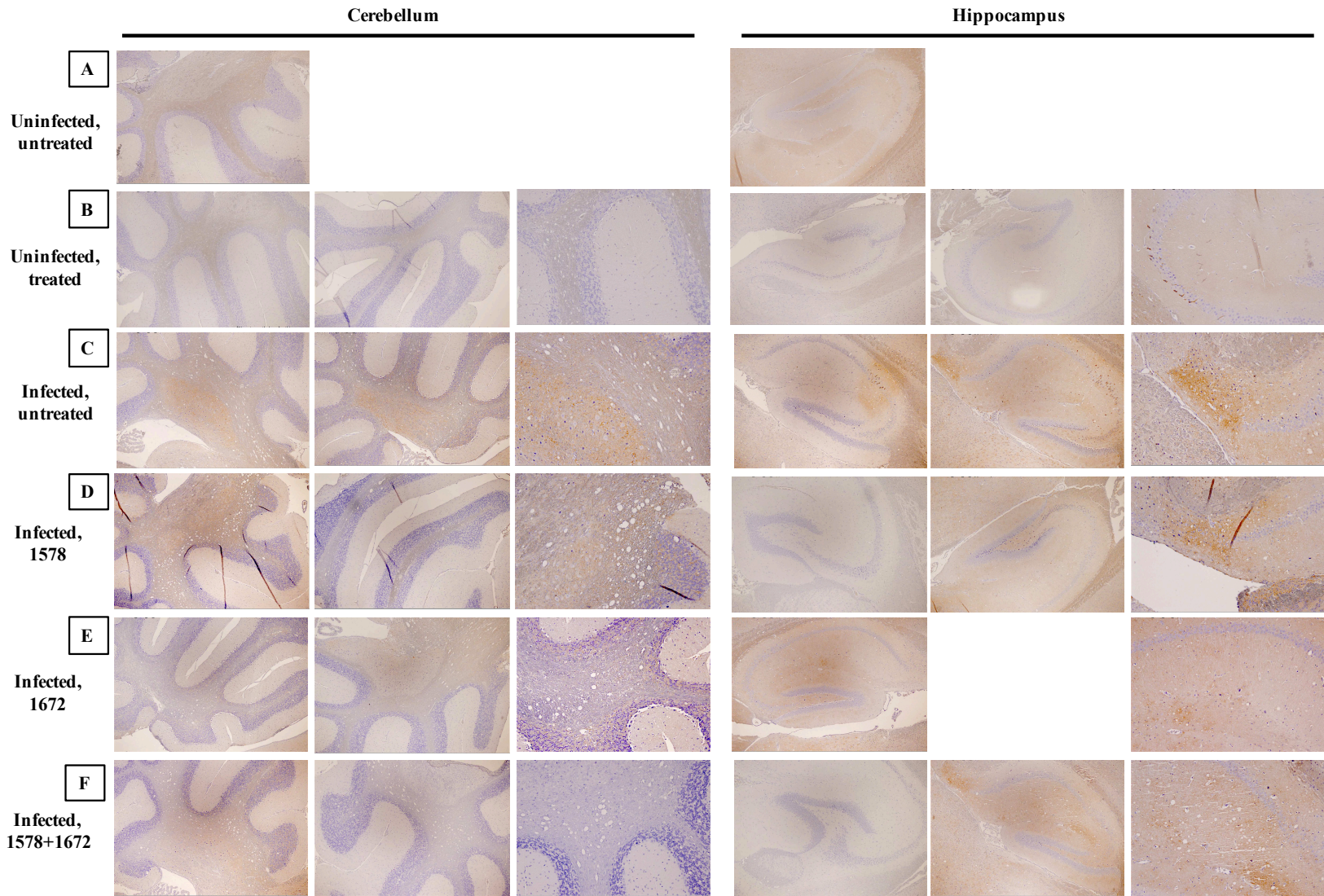


**Figure 4.4. Analysis of PrP<sup>Res</sup> deposition in the brains of mice from the 1<sup>st</sup> LSPCs treatment terminal study.**

A) Uninfected, untreated group. B) Uninfected, treated group. C) Infected, untreated group. D) Infected, 1578 group. E) Infected, 1672 group. F) Infected 1578+1672 group

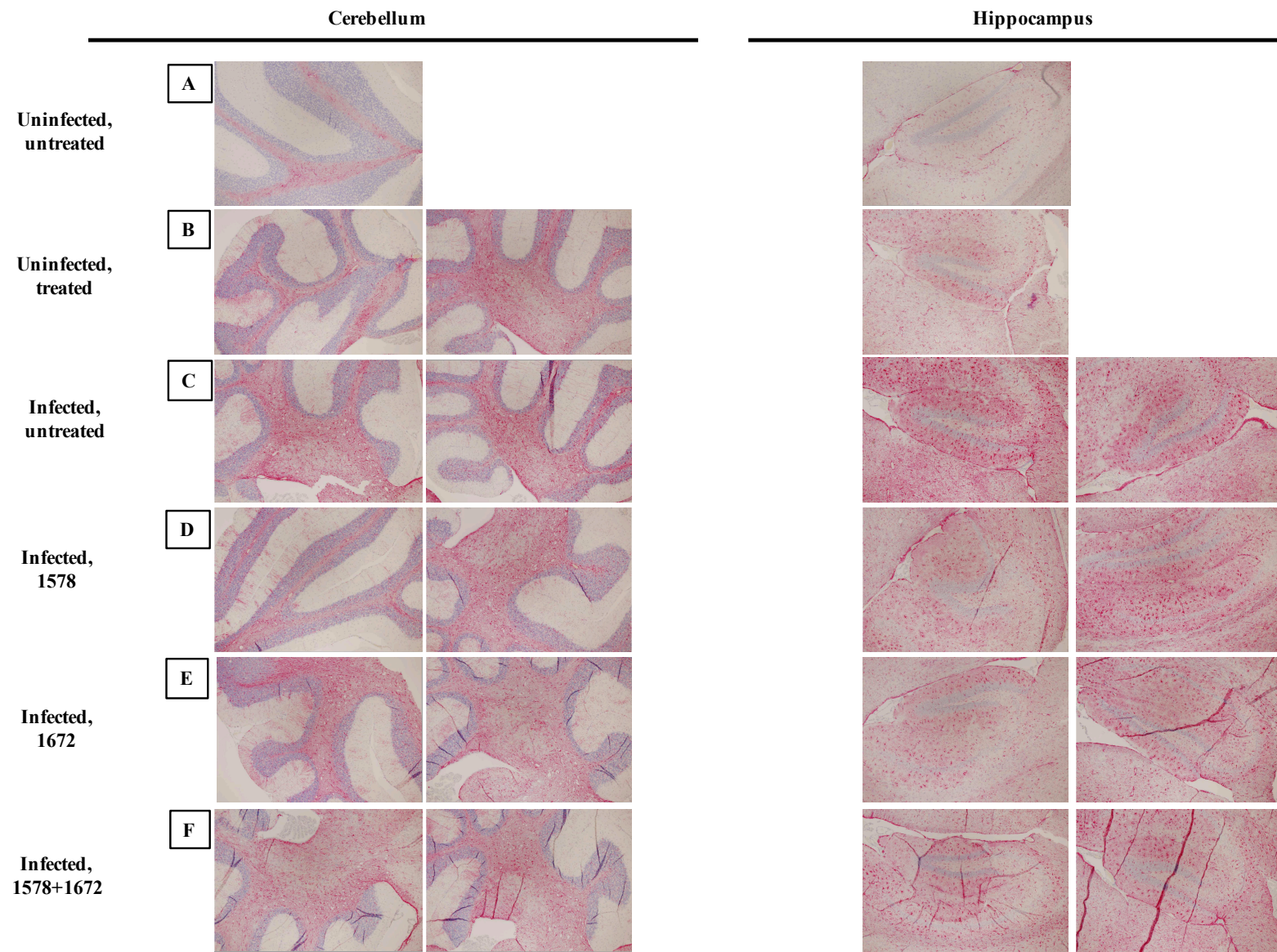


**Figure 4.5. Analysis of activated astrocytes using GFAP immunostain in the brains of mice from the 1<sup>st</sup> LSPCs treatment terminal study.**  
 A) Uninfected, untreated group. B) Uninfected, treated group. C) Infected, untreated group. D) Infected, 1578 group. E) Infected, 1672 group. F) Infected 1578+1672 group

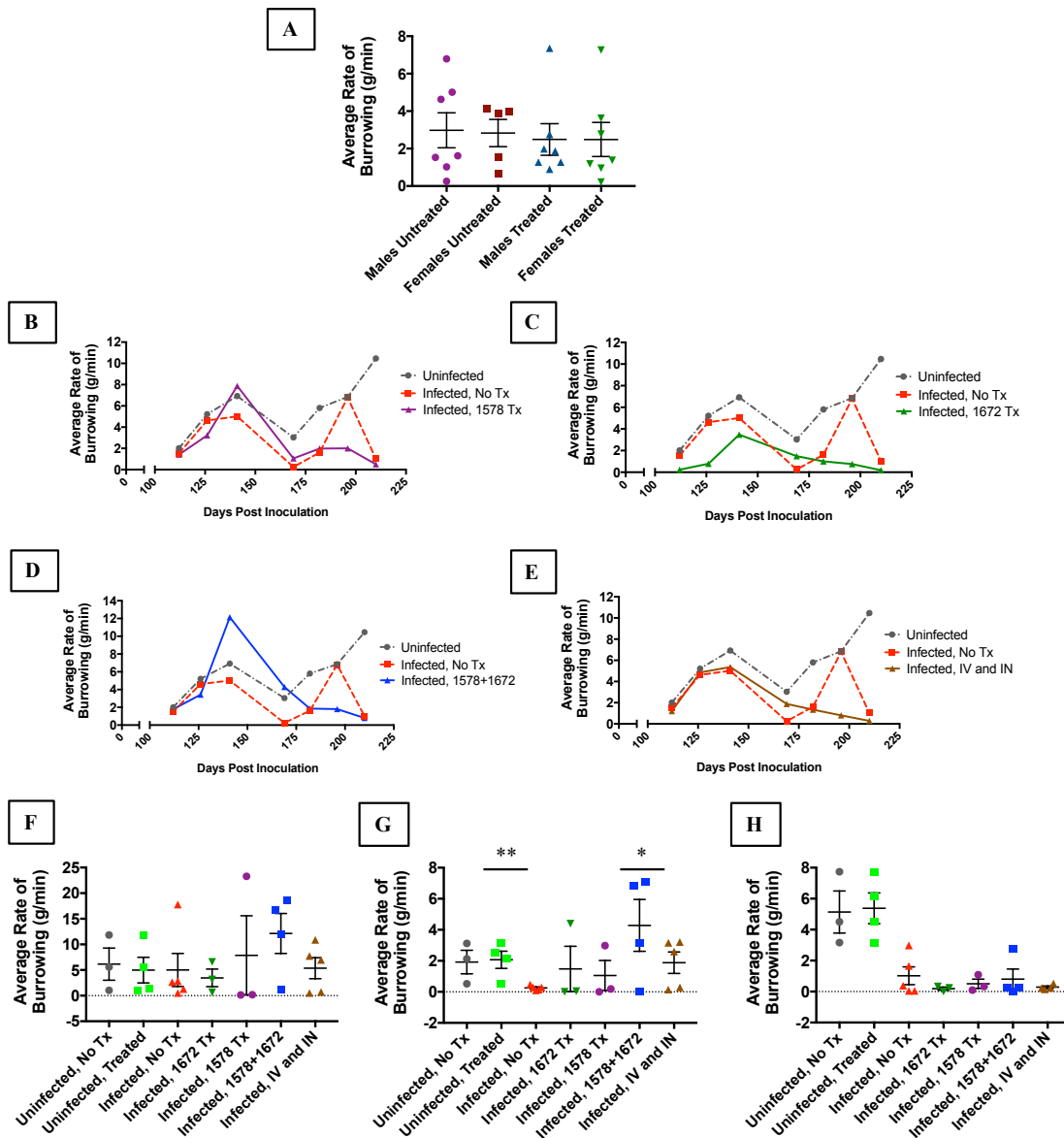


**Figure 4.6. Burrowing rates of LSPCs-treated mice from the 1<sup>st</sup> terminal study.**

A) The male and female untreated and treated groups were not statistically different from each other so male and female mice from each group were pooled and analyzed together. B) Burrowing rates of infected, 1578 treated mice were higher than the infected, untreated group at 141 dpi but not any other time point. C) Burrowing rates of infected, 1672 treated mice were lower than the infected, untreated group at most dpi. D) Burrowing rate of the infected, 1578+1672 treated mice were higher at 141 and 169 dpi compared to the infected, untreated control. The burrowing rates of the 1578+1672 mice are equal to those of the uninfected controls. E) Burrowing rates of infected, IV and IN are not any different than the infected, untreated group. F) Four out of the five mice in the infected, 1578+1672 treatment group have higher burrowing scores at 141 dpi than the infected, untreated control, although it's not a statistically significant difference. No other treatment group shows an increase in burrowing at 141 dpi. G) At 169 dpi, both the uninfected control and the 1578+1672 treatment group have significantly higher burrowing rates than the infected, untreated control. H) At clinical disease stage (210 dpi), none of the LSPCs treatment groups are significantly different than the infected, untreated control. Error bars indicate SEM. \*  $p < 0.05$ . \*\*  $p < 0.01$ . One-way ANOVA with Dunnett's multiple comparisons.

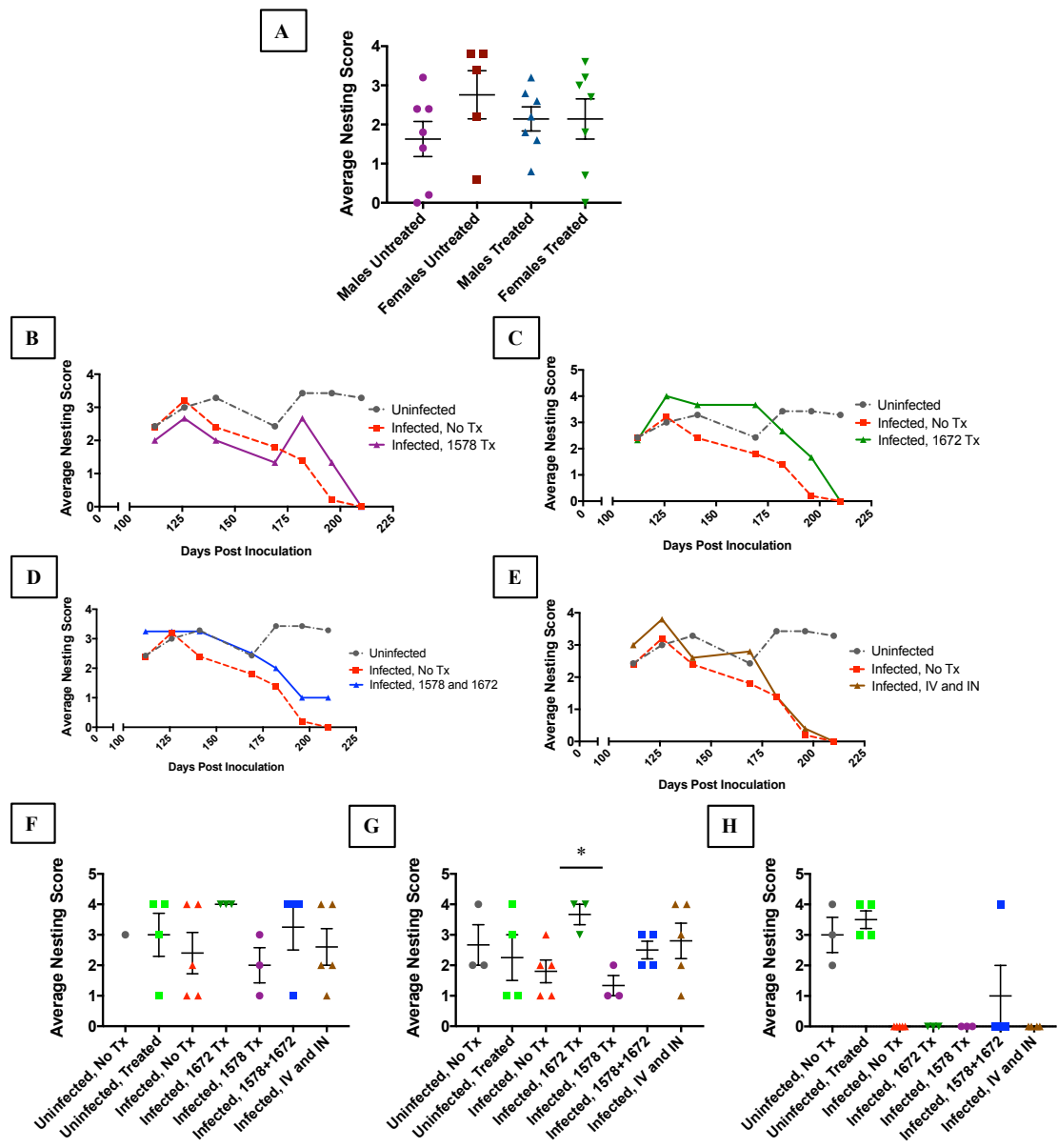


**Figure 4.7. Nesting scores of LSPCs-treated mice from the 1<sup>st</sup> terminal study.**  
 A) The male and female untreated and treated mice did not have different nesting scores, so again the male and female mice of each treatment group were pooled for further analysis. B) The infected, 1578 treatment group had lower nesting scores than the infected, untreated control. C) Higher nesting scores at 141, 169, and 180 dpi were observed in mice treated with 1672 LSPCs compared to untreated control, so much so that the scores are similar to uninfected controls. D) The 1578+1672 treatment group performed equally as well as the uninfected control at most dpi and had higher nesting scores at all dpi compared to the infected, untreated control. E) The IV and IN treatment group had higher nesting scores at 169 dpi but no other dpi than the infected, untreated control. F) The 1672 and 1578+1672 treatment groups both had higher nesting scores than the infected, untreated group at 141 dpi, although not statistically significant. G) At 169 dpi, the 1672 treatment group had significantly higher nesting scores than the infected, untreated control. The 1578+1672 group also had a higher average nesting score at this dpi but it was not statistically significant. H) At clinical disease stage (210 dpi) none of the treated mice have different nesting scores than the infected, untreated control. \* p<0.05. t test.

in either untreated or treated male and female mice was observed for either burrowing or nesting tests for the 1<sup>st</sup> terminal study (Figure 4.6A and 4.7A). Therefore, all treated mice were compared to the infected, untreated group. In the 1<sup>st</sup> terminal study, both the uninfected, treated group and the infected, 1578+1672 group have significantly higher average rate of burrowing compared to the infected, untreated group at 169 dpi (Figure 4.6D and G). The 1578+1672 group also performs higher at 141 dpi, although no statistical difference is seen (Figure 4.6F). While some mice in the other treated groups do have a higher average rate of burrowing than the untreated group, there is no other statistical difference between the infected, treated and untreated groups for burrowing (Figure 4.6B, C, E, and H).

Both the 1672 group and the 1578+1672 group perform as well as the uninfected treatment group in the nesting test, but only the 1672 group is significantly different from infected, untreated controls (Figure 4.7C, D, and G). The 1672 group has a higher average nesting score compared to the infected, untreated group at both 141 (Figure 4.7F) and 169 dpi, but is only statistically significant at 169 dpi (Figure 4.7G). No other groups perform above the infected, untreated group in nesting (Figure 4.7B, E, and H). There is no difference in performance in any treated mice in either of the behavior tests compared to infected, untreated group at 210 dpi in the 1<sup>st</sup> terminal study (Figure 4.6H and 4.7H).

There is no difference in male versus female performance in the behavior tests of the 2<sup>nd</sup> terminal study, so all treated mice were compared to the infected, untreated group (Figure 4.8A and 4.9A). No statistical difference is observed in the performance of treated mice in either the burrowing or nesting tests compared to the infected, untreated group in the 2<sup>nd</sup> terminal study (Figure 4.8 and 4.9); however, the 1672 treated group has a trend in the burrowing test. The 1672 treated group has a higher average rate of burrowing compared to the infected, untreated group at 141 and 169 dpi (Figure 4.8C and G), although, this increase in performance is not statistically significant. No differences/trends or statistical significance were observed in any other treated groups in the nesting test in the 2<sup>nd</sup> terminal study (Figure 4.9).

#### ***Total IgG levels against RVG-9r are elevated in LSPCs-treated prion-infected terminal mice***

A surprising result from the 1<sup>st</sup> terminal study was the death of the uninfected, treated controls (Figure 4.1C) as the LSPCs treatment was thought to be relatively non-toxic. Observations upon necropsy, that included enlarged and darker spleens and severe ‘clotting’ of the blood, pointed to immune activation as being the cause of

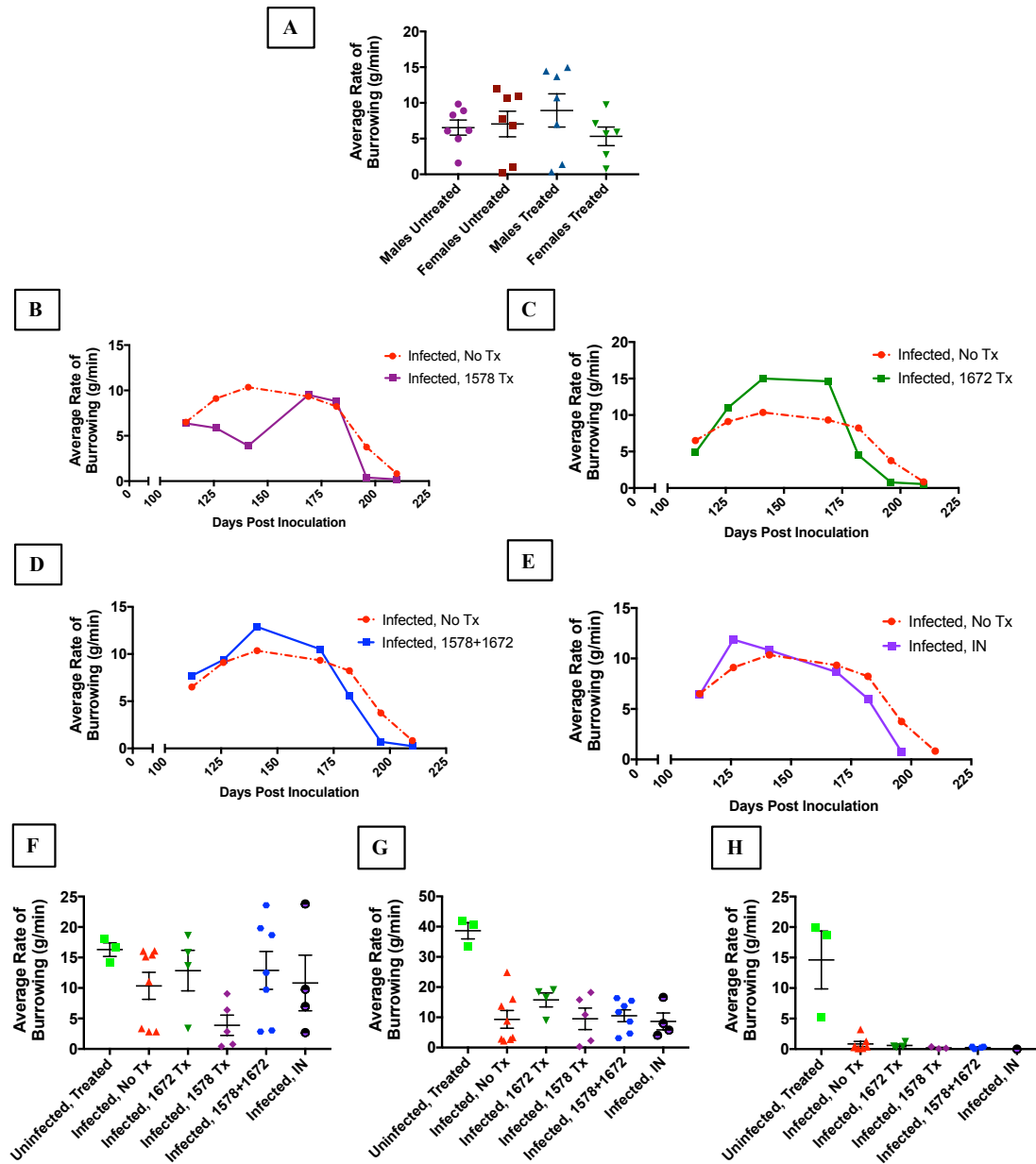


**Figure 4.8. Burrowing rates of LSPCs-treated mice from the 2<sup>nd</sup> terminal study.**

A) While the survival times of male and female CD1 mice infected with RML-5 prions were found to be statistically different, the behavior of the genders was not statistically significant in untreated or treated mice. B) The 1578 treatment group did not have improved burrowing scores compared to the infected, untreated control. C) The burrowing rate of the 1672 treated mice was improved at 141 and 169 dpi compared to the untreated control. D) The burrowing rate of the 1578+1672 was not different from the infected, untreated control at most dpi. E) There was no difference in burrowing rates of the IN treatment group to the infected, untreated group. F) At 141 dpi, none of the treated mice had significantly different burrowing rates than the infected, untreated control. G) None of the treated mice had significantly different burrowing rates than the infected, untreated control at 169 dpi, although the 1672 treatment group has a slight improvement in burrowing rates at this time. H) At clinical disease stage (210 dpi), the treated mice have the same burrowing rates as the untreated control. Error bars indicate SEM. One-way ANOVA with Dunnett's multiple comparisons.

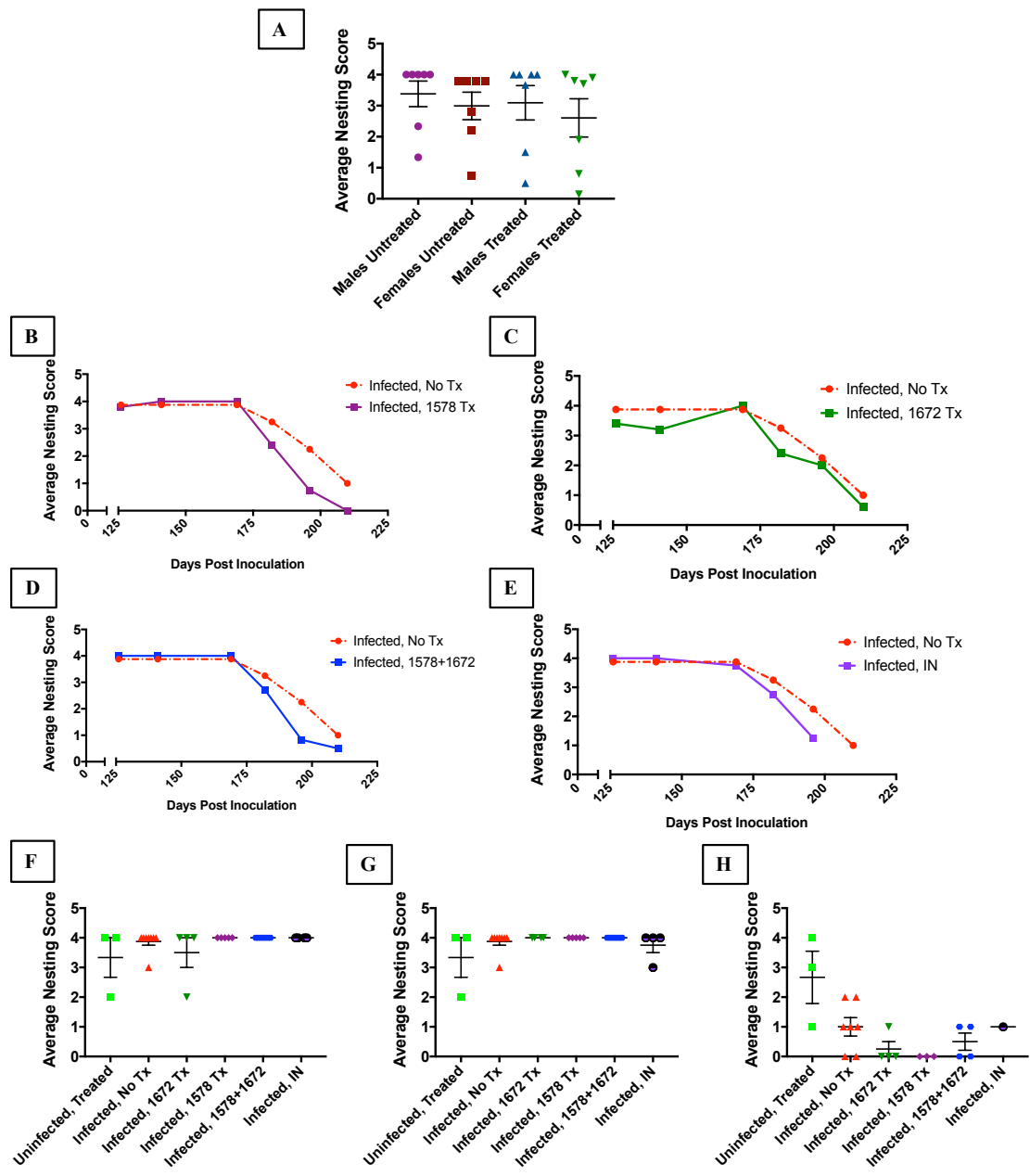


**Figure 4.9. Nesting scores of LSPCs-treated mice from the 2<sup>nd</sup> terminal study.**

A) Comparison of nesting scores of CD1 male and female mice show no difference in either untreated or treated mice, so further analysis of treatment groups pools both genders. B) The 1578 treatment group does not perform any differently in the nesting test than the infected, untreated control. C) The 1672 treatment group is not significantly different than the infected, untreated control at any dpi. D) Nesting scores of the 1578+1672 treatment group and the infected, untreated are not any different at any dpi. E) The IN treatment does not have significantly different nesting scores compared to the untreated control. F) At 141 dpi, none of the treated mice have different nesting scores compared to the infected, untreated control. G) At 169 dpi, none of the treated mice have different nesting scores compared to the untreated control. H) Nesting scores of treated mice at clinical disease stage (210 dpi) are not significantly different than the infected, untreated control. Error bars indicate SEM. One-way ANOVA with Dunnett's multiple comparisons.

death of these animals. Therefore, to determine the extent of this immune response, total IgG levels against RVG-9r were measured using an indirect ELISA. Serum samples from clinically-ill mice were collected upon euthanasia. All treated mice were compared to the total IgG levels of infected, untreated mice.

Both the uninfected, treated group and the IV and IN groups in the 1<sup>st</sup> terminal study had elevated levels of IgG against RVG-9r (Figure 4.10A). The 1578 group and the 1578+1672 group in the 2<sup>nd</sup> terminal study also had elevated IgG levels against RVG-9r (Figure 4.10B). None of the other treated groups were statistically different, although, individual mice in the other groups had elevated levels of IgG compared to the infected, untreated group.

***LSPCs treatment results in an increase in prion load levels in the brain***

To determine why survival times are not affect but behavioral scores are of LSPCs-treated mice, PrP<sup>Res</sup> levels were assessed in the brains and spleens of treated mice. FVB mice were inoculated intraperitoneally

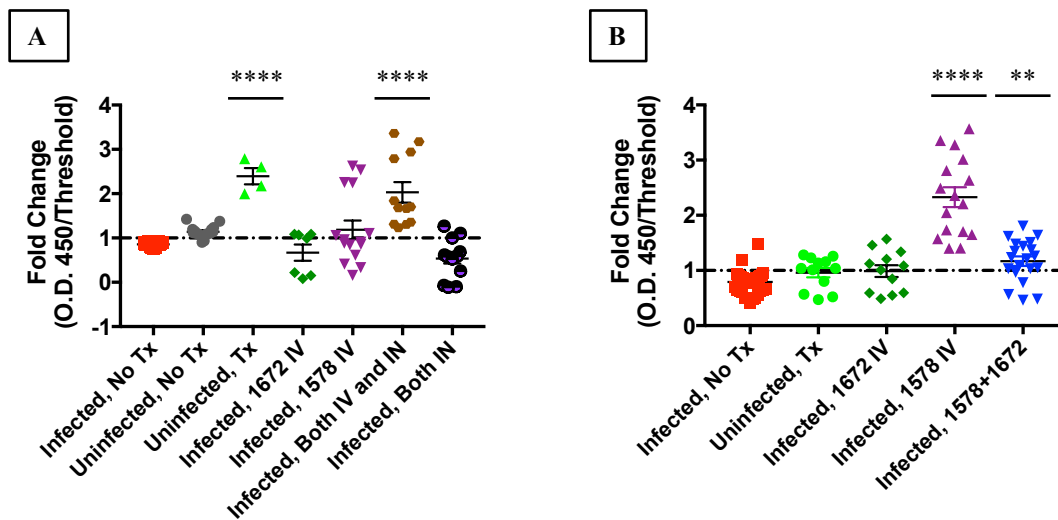


**Figure 4.10. Total IgG levels against RVG-9r in LSPCs-treated terminal mice.**

A) Total IgG levels against RVG-9r in LSPCs-treated groups were elevated in the uninfected, treated group and the IV and IN treatment group of the 1<sup>st</sup> terminal study. B) Total IgG levels against RVG-9r in the LSPCs-treated groups were elevated in the 1578 treatment group and the 1578+1672 treatment group of the 2<sup>nd</sup> terminal study. Error bars indicate SEM. \*\* p<0.01. \*\*\*\* p<0.0001. One-way ANOVA with Dunnett’s multiple comparisons.

with 0.1% RML-5 prions and treated every two weeks at early time points in disease course. Early time points were used based on the observation that spleen prion loads increase until the 3<sup>rd</sup> month after inoculation, where they peak and remain steady. At each time point (one week after LSPCs treatment), brains and spleens were collected from one untreated and one LSPCs-treated mouse after euthanasia. Mice were treated repetitively to determine if multiple siRNA treatments had a bigger effect on prion loads. The treated mouse at the ‘1 treatment’ time point only received one LSPCs treatment, whereas the treated mouse euthanized at the ‘6 treatment’ time point received a total of six LSPCs treatments. Table 4.5 lists the treatment and euthanasia dpi of early time point mice. The treatment protocol was not repeated. PMCA was performed to determine prion loads in the collected tissues by calculating a PMCA score based on when the tissue first amplified in the assay. Figure 4.11A shows a representative western blot of PrP<sup>Res</sup> amplification in the brain using PMCA. After every LSPCs treatment, prion loads are increased in the brain in treated mice compared to the untreated control (Figure 4.11B and D). Spleen prion loads at each time point are statistically significant from the untreated controls, but no trend is observed as to an increase or decrease in levels (Figure 4.11E). Prion levels are reduced after the 1<sup>st</sup> and 4<sup>th</sup> LSPCs treatments but are increased at the 2<sup>nd</sup>, 3<sup>rd</sup>, and 5<sup>th</sup> LSPCs treatments in the spleen (Figure 4.11C). The prion levels of the untreated control at the 6<sup>th</sup> LSPCs treatment could not be measured via PMCA, so no conclusions can be made at that time point.

***Table 4.5. Repetitive LSPCs treatments of early time point mice indicating the dpi that mice were treated and euthanized***

	<b>DPI Treated</b>	<b>DPI Euthanized</b>
<b>1 Treatment</b>	75	89
<b>2 Treatment</b>	89	103
<b>3 Treatment</b>	103	110
<b>4 Treatment</b>	117	125
<b>5 Treatment</b>	132	139
<b>6 Treatment</b>	161	168

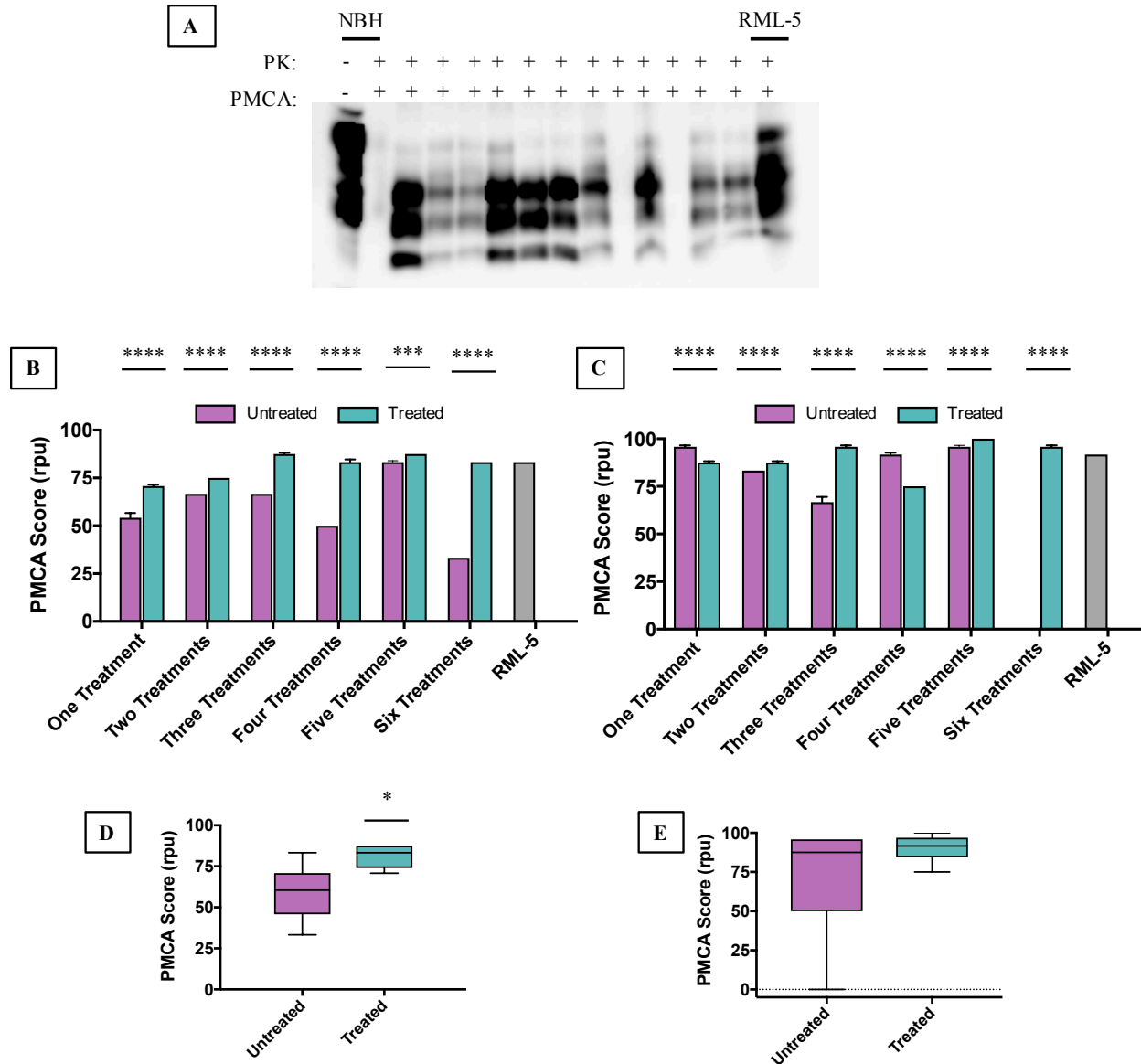


**Figure 4.11. PMCA amplification of PrP<sup>Res</sup> in LSPCs-treated early time point mice.**

A) Representative western blot of PMCA amplified PrP<sup>Res</sup> in the brain. B) At each of the time points (1 siRNA treatment or 6 siRNA treatments), there was an increase in levels of PrP<sup>Res</sup> in the brain of all treated mice compared to the untreated control. C) PrP<sup>Res</sup> levels in the spleens of treated mice are variable, with one and four siRNA treatments resulting in a decrease of PrP<sup>Res</sup> levels and an increase in PrP<sup>Res</sup> levels at all other time points. D) Cumulative PMCA scores of all untreated mice compared to all treated mice revealed a significant increase in PrP<sup>Res</sup> levels in the brains of treated mice. E) Cumulative PMCA scores of all untreated mice compared to all treated mice did not reveal a difference in PrP<sup>Res</sup> levels in the spleen. Error bars indicate SD for panels B and C and min to max for panels D and E. \* p<0.05. \*\*\* p<0.001. \*\*\*\* p<0.0001. Two-way ANOVA with Sidak's multiple comparisons or Welch's t test.

***LSPCs treatment increases total IgG levels against RVG-9r after the 3<sup>rd</sup> repetitive treatment in early time point mice***

Since total IgG levels were elevated in several treatment groups in the terminal studies, a question arose as to how many LSPCs treatments are needed to induce an IgG response towards RVG-9r. Therefore, early time point mice were euthanized one week after LSPCs treatment at which point serum was collected from each mouse. At each time point one untreated and one treated mouse were euthanized. The treated mouse euthanized at ‘one treatment’ received only one siRNA treatment, whereas the treated mouse euthanized at ‘six treatments’ received a total of six treatments given every two weeks. An ELISA was performed to determine total IgG levels compared to an untreated control. IgG levels against RVG-9r decrease compared to the untreated control in the 1<sup>st</sup> and 2<sup>nd</sup> LSPCs treatments (Figure 4.12). The decrease in IgG compared to the control could be due to either IgG being sequestered in immune complexes at these time points, or these two treated mice have lower IgG levels overall compared to the untreated mouse. IgG levels against RVG-9r are increased starting at the 3<sup>rd</sup> LSPCs treatment and continue to elevate at subsequent treatments after that (Figure 4.12), indicating that three LSPCs treatments result in an overall increase in IgG against RVG-9r.

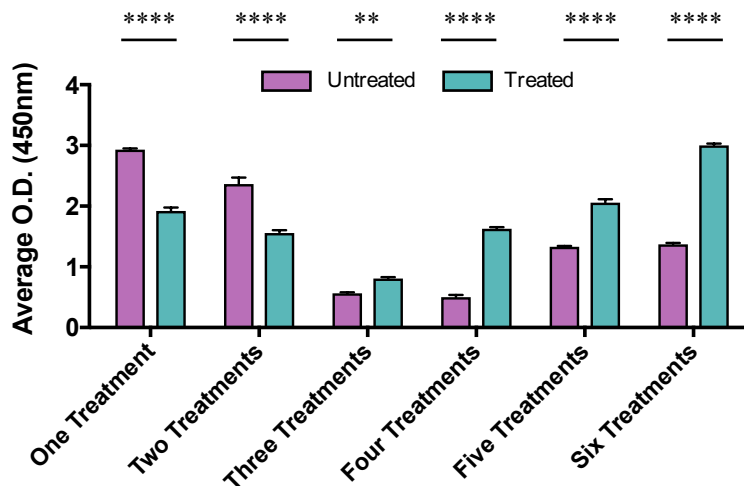


***Figure 4.12. Total IgG levels against RVG-9r in the brains of early time point mice repeatedly treated with LSPCs.***

Total IgG levels against RVG-9r increase after the third LSPCs treatment and keep increasing after subsequent treatments compared to untreated controls. Error bars indicate SD. \*\* p<0.01. \*\*\*\* p<0.0001. Two-way ANOVA with Sidak’s multiple comparisons.

## Discussion

Many compounds have been studied for their anti-prion effects, even before scientists understood the molecular basis of prion disease. These compounds are effective at decreasing prions *in vitro* but few have had success *in vivo*. Reasons for lack of *in vivo* efficacy include toxicity and an inability to cross the blood-brain barrier<sup>41,49-51</sup>. The anti-prion compounds that have worked *in vivo* extended survival times of prion-infected animals but did not alleviate clinical signs caused by prion neuropathology<sup>36,39,52,53</sup>. The one therapeutic that did both was RNA interference (RNAi) targeted towards PrP<sup>C</sup>. A single injection of short hairpin RNA resulted in an extension of survival times and a reversal of prion neuropathology<sup>54</sup>. Evidence supporting PrP<sup>C</sup> as a target for therapeutics, instead of PrP<sup>Res</sup>, was shown by the lack of negative phenotype in PrP-null mice<sup>32,33</sup>. The numerous functional studies since then indicate that there is a redundant pathway in adult animals that compensates for the functional loss of PrP<sup>C</sup>. PrP-null animals are more sensitive to damage to the central nervous system, such as hypoxia<sup>55</sup> and ischemia<sup>56</sup>, than their wild-type counterparts, but otherwise, have a normal phenotype. Several studies in the last decade have further proven that PrP<sup>C</sup> might be a better therapeutic target than PrP<sup>Res</sup>. These studies have shown that by decreasing PrP<sup>C</sup>, the amount of PrP<sup>Res</sup> declines, survival times increase, and neuropathology decreases<sup>35,43,45,57</sup>. Other advantages of targeting PrP<sup>C</sup> include independence of scrapie strain type and host cell type.

Here we have attempted to alleviate prion disease through recurring treatments of our LSPC<sup>45</sup> therapeutic that utilizes small interfering RNA (siRNA) targeted towards PrP<sup>C</sup>. We have previously shown that LSPCs can decrease the amount of neuronal PrP<sup>C</sup> protein and mRNA levels between 15 and 21 days in wild-type mice (unpublished results). In this report, we wanted to assess not only the impact of LSPCs treatment on survival times but also on behavioral outcomes of prion-infected mice. We chose to use an intraperitoneal route of inoculation with a lower dose of prions to simulate a more natural infection. We also opted to start our LSPCs therapeutic midway through the prion disease course to determine whether the treatment could reverse the early neuronal changes seen in prion-infected mice. Unfortunately, repeated LSPCs treatments either every 2 or 3-5 weeks did not extend the survival times of prion-infected mice when started midway through the prion disease course. Survival periods decreased in mice that were treated every two weeks both intravenously (IV) and intranasally (IN). IN groups were incorporated into our design study to assess whether a different administration route, other than IV would alter clinical disease outcomes in LSPCs treated mice. Multiple reports have shown that IN administration of siRNA is effective at delivering siRNA to the brain<sup>58,59</sup>.

Our behavior test results indicate that, while the LSPCs treatments may not be affecting survival times in prion-infected mice, they are improving behavioral scores in LSPCs-treated mice certain days post inoculation. Several groups of treated mice had improved behavioral scores in both burrowing and nesting at 141 and 169 dpi. This improvement was not sustained until clinical disease, but it does raise the possibility that the LSPCs treatment could still be a potential therapeutic. The results of the behavior study of the 2<sup>nd</sup> terminal study, for the most part, did not corroborate the results seen with behavior tests in the 1<sup>st</sup> terminal study. This difference in behavior is most likely due to the use of two different wild-type mouse strains. The CD1 mice tend to have better behavioral scores in burrowing and nesting tests compared to the FVB mice, and are much more consistent with their behavior across time. The CD1 mice also have better performance in the behavioral tests right up until clinical disease stage. FVB mice are perhaps more useful because of the subtle behavioral variations, indicative of prion infection, that are more noticeable in this strain of mice than the CD1 mice.

The most obvious reason that the LSPCs treatment did not affect survival times is that the treatment was not given at the proper time or dose. While ineffective dosing might be an issue with the LSPCs treatment in this study, the amount of siRNA should be carefully increased as it is at the upper limit of the concentration that can be used *in vivo* safely<sup>60</sup>. Therefore, any dosing issues should be addressed to maximize the benefit of LSPCs treatment and minimize any toxic effects. It is not known at what time a prion therapeutic would be more efficient, early stages before clinical signs or after clinical stage manifestation. Early behavioral changes indicate that initial neuronal degeneration of prion disease occurs about halfway through disease course, which is why our study started treatment at this stage. This study is the first to assess multiple siRNA treatments for prion disease, so it is not known how effective siRNA is at different stages of disease. Recent work in our laboratory indicates that the LSPCs treatment affects clinical stages of disease as it extended the survival of transgenic mice that overexpress mouse PrP<sup>C</sup> by 20% when administered three times close to the clinical disease stage (unpublished results). The results of that study do not necessarily contradict the results of this study, as it was performed in a different mouse model. It is possible that either the dosing regimen or the overexpression of mouse PrP<sup>C</sup> affected the outcome of survival with LSPCs treatment. It has been proposed that a loss-of-function phenotype for PrP<sup>C</sup> is responsible for prion neuropathology, instead of the accumulation of PrP<sup>Res</sup> within the brain. Several studies have noted that neuropathology still predominates even with little to no detectable levels of PrP<sup>Res44,61,62</sup>. If the loss-of-function hypothesis is accurate, then the loss of PrP<sup>C</sup> in wild-type mice would negate any positive effects caused by

decreasing the amount of PrP<sup>Res</sup> in the brain. The overexpressing mice might be able to compensate for this loss-of-function phenotype with the increased levels of PrP<sup>C</sup>.

The deaths of the uninfected control group in the 1<sup>st</sup> terminal study were unexpected. Three out of the four mice in this group died or was euthanized one hour after LSPCs treatment due to severe morbidity. Two of the animals died after the 8<sup>th</sup> treatment, and one was euthanized after the 9<sup>th</sup> LSPCs treatment. The unaffected mouse in this group did not receive the 7<sup>th</sup> treatment due to an inability to inject the LSPCs. This alteration in the treatment regimen probably resulted in the survival of this mouse upon subsequent treatments. Upon necropsy of the mice that died/were euthanized, it was noted that the spleens of these mice were larger than normal. Also, an attempt to collect serum from the mouse that was euthanized failed due to excessive clotting of the blood immediately after death. These observations indicate that these mice died of an acute Type III hypersensitivity. Therefore, ELISAs were performed to characterize the immune response in LSPCs-treated mice. Total IgG levels against RVG-9r were increased in several groups of treated mice, indicating that they are having an immune response to the peptide. Serum was collected at the time of euthanasia, which may be why more mice do not show an increase in IgG levels. The optimal time to collect serum for antibody measurement is seven to ten days after antigen exposure. IgG levels of the terminal mice might have already decreased by the time serum was collected since most mice were not euthanized seven to ten days after LSPC treatment. The presence of activated astrocytes in the uninfected, treated group points to an inflammatory response that could be caused by immune activation. Prion infection is known to cause activated astrocytes, and indeed infected, untreated mice have elevated levels of activated astrocytes compared to the uninfected, untreated control. Surprisingly, the uninfected, treated control mice had comparable levels of activated astrocytes to the prion-infected controls.

At this point, it is hard to determine the exact cause of the immune and inflammatory responses. The total IgG data indicates that there is, at the very minimum, an immune response to RVG-9r. The immune response towards the peptide is not too surprising as RVG-9r is known to activate levels of IL-6 when complexed with siRNA. RVG-9r is also a component of the rabies virus, so it could be recognized as an antigen by the immune system. However, native RVG alone does not stimulate the immune system, indicating that the addition of the nine arginine residues on the COOH-terminus of RVG might make the peptide more immunogenic<sup>63</sup>. Thus, removing the arginine residues and packaging the siRNA within the liposome might result in a reduction of the immune response.

Using a different targeting peptide, such as transferrin or a neuronal specific antibody, might also decrease the immune response to the LSPCs.

The RVG-9r might not be the only component generating the immune activation. Liposomes and siRNA by themselves do not elicit an immune reaction, but once complexed together they can increase cytokine production such as TNF $\alpha$  and IFN $\alpha$ <sup>60,64</sup>. The prevailing hypothesis as to why these components only elicit an immune response when complexed together is that they resemble viral particles with a membrane and nucleic acid. Cationic liposome/siRNA complexes are also known to bind to serum proteins, which generates large immune complexes that can stimulate the immune system. SiRNA is also known to activate Toll-like receptors (TLRs) in the endosomal pathway and increase production of cytokines<sup>64-66</sup>. Thus, all three components of the LSPCs treatment, when used together, could be involved in immune activation. Modifications of the LSPCs can decrease the immune response to the treatment, but there will probably always be a low level of activation by the immune system towards LSPCs. Alterations include using modified siRNA with locked nucleic acids, 2'-O-methyl, or 2'-fluoro modifications. Variations to siRNA reduce the activation of TLRs but may reduce silencing activity depending on the location and number of modifications<sup>65,67,68</sup>. Therefore, the benefit of the modified siRNA should be measured carefully to its optimal silencing activity. As noted above, different targeting peptides that are less immunogenic can be utilized instead of RVG-9r. Liposome modifications include adding PEGylated groups to the liposomes, which make them less available to bind to serum proteins and generate immune complexes<sup>69</sup>. To address some of these concerns, we have designed other liposomal delivery vehicles that package the siRNA within the liposome and use PEGylated lipid groups (PALETS)<sup>70</sup>. Thus, these PALETS, with a few modifications to increase RNAi activity, may prove to be a useful alternative to LSPCs treatment.

Nicotinic acetylcholine receptors (nAChRs) are extremely abundant in the central nervous system and are used to control the release of neurotransmitters at the synapse, such as glutamate and acetylcholine. RVG-9r specifically binds to the  $\alpha 7$  subunit of nAChRs to mediate its entry into neuronal cells<sup>71</sup>. The activation of the  $\alpha 7$  subunit of nAChRs by RVG-9r must be taken into consideration as the activation has been implicated in multiple cellular processes. Activation of this subunit results in a decrease in inflammation of neuronal cells<sup>72</sup>. This may be beneficial for LSPCs treatment, as not only would the binding of RVG-9r to neuronal cells deliver the PrP<sup>C</sup> siRNA to the brain, but it could also decrease inflammation caused by either the treatment or prion infection. Activation of  $\alpha 7$  of nAChRs does help mediate inflammation, but prolonged activation can also lead to an increase in cytosolic

Ca<sup>2+</sup> levels. Some drugs that bind to the  $\alpha 7$  subunit can cause neuronal death, autonomic dysfunction, and seizures due to the alterations in cytosolic Ca<sup>2+</sup> levels<sup>73</sup>. Therefore, while activation of nAChRs can be beneficial, too much can lead to the exact problems that the treatment is trying to solve. The increase in cytosolic Ca<sup>2+</sup> may not be an issue in the prion disease model with LSPCs treatment, as PrP<sup>C</sup> is known to modulate cytosolic Ca<sup>2+</sup> levels. PrP-null cells have been shown to have a decrease in cytosolic Ca<sup>2+</sup> levels due to an increased removal of Ca<sup>2+</sup> from the cells<sup>22-24</sup>. By decreasing PrP<sup>C</sup>, the treatment could affect Ca<sup>2+</sup> stores within the cell. However, if RVG-9r is over-activating nAChRs, then these Ca<sup>2+</sup> stores might be restored. At this point, the effect of LSPCs treatment on Ca<sup>2+</sup> is unknown.

Activation of the  $\alpha 7$  subunit of nAChRs also increases cognition and memory retention<sup>74,75</sup>. The behavioral test results observed in this study may be reflective of either a benefit of the LSPCs treatment or the activation of nAChRs. The increase in behavioral scores is most likely due to a benefit from the treatment rather than activation of nAChRs because the behavior of LSPCs-treated mice is only improved at certain time points. If the increased performance was due to the activation of nAChRs, then the behavior should be enhanced at all time points. Also, burrowing and nesting does not rely on memory or cognition skills. So, if these two processes are increased in treated mice it would not necessarily be measured using these behavioral tests. There is limited statistical significance in the behavioral studies, but an argument can be made that there is biological significance in the behavior of some of the LSPCs-treated groups. Any treatment group that performs as well or better than the uninfected, untreated group may not be statistically significant, but is biologically significant in that behavior was rescued to non-prion-infected levels.

The last point that will be made involves the observation from the pharmacodynamics study that PrP<sup>C</sup> protein and mRNA levels can increase substantially with LSPCs treatment (unpublished results). PrP<sup>C</sup> levels can increase due to an immune reaction through the activation of TLRs<sup>30,76</sup>. The immune response observed in this study could be the cause of the increase in PrP<sup>C</sup> protein levels after treatment. PrP<sup>C</sup> levels could also be tightly regulated at either the transcriptional or translational level leading to an increase in PrP<sup>C</sup> levels after LSPCs treatment. However, it is also possible that the activation of nAChRs leads to an increase in PrP<sup>C</sup> levels. Activation of nAChRs by  $\alpha$ -bungarotoxin leads to an increase in the transcription of several genes, including the proto-oncogene *c-fos* and actin<sup>77</sup>. If the activation of the nAChRs is causing an increase in PrP<sup>C</sup> levels, then another targeting peptide can be chosen to alleviate this problem.

Although the results of the present study were somewhat disappointing, all is not lost. As noted above, multiple modifications can be utilized to try to alleviate some of the effects seen due to the recurring LSPCs treatments. If it is determined that RNAi is not the best therapy for prion diseases, the LSPCs and the PALETS (without the siRNA) still represent delivery vehicles capable of delivering cargo past the blood-brain barrier. Therefore, it would be useful to test the efficacy of other small molecule drugs with the liposomal delivery vehicles.

## References

1. Oesch, B. *et al.* A cellular gene encodes scrapie PrP 27-30 protein. *Cell* **40**, 735–746 (1985).
2. Basler, K. *et al.* Scrapie and cellular PrP isoforms are encoded by the same chromosomal gene. *Cell* **46**, 417–428 (1986).
3. Manson, J., West, J. D., Thomson, V. & McBride, P. The prion protein gene: a role in mouse embryogenesis? *Development* **115**, 117–122 (1992).
4. Miele, G. *et al.* Embryonic activation and developmental expression of the murine prion protein gene. *Gene Expr* **11**, 1–12 (2003).
5. Locht, C., Chesebro, B. & Race, R. Molecular cloning and complete sequence of prion protein cDNA from mouse brain infected with the scrapie agent. *Proc. Natl. Acad. Sci. U.S.A.* **83**, 6372–6376 (1986).
6. Naslavsky, N., Stein, R., Yanai, A., Friedlander, G. & Taraboulos, A. Characterization of detergent-insoluble complexes containing the cellular prion protein and its scrapie isoform. *J. Biol. Chem.* **272**, 6324–6331 (1997).
7. McKinley, M. P., Bolton, D. C. & Prusiner, S. B. A protease-resistant protein is a structural component of the scrapie prion. *Cell* **35**, 57–62 (1983).
8. Prusiner, S. B., Groth, D. F., Bolton, D. C., Kent, S. B. & Hood, L. E. Purification and structural studies of a major scrapie prion protein. *Cell* **38**, 127–134 (1984).
9. Prusiner, S. B. Novel proteinaceous infectious particles cause scrapie. *Science* **216**, 136–144 (1982).
10. Michel, B. *et al.* Incunabular immunological events in prion trafficking. *Sci Rep* **2**, 440 (2012).
11. Eklund, C. M., Kennedy, R. C. & Hadlow, W. J. Pathogenesis of scrapie virus infection in the mouse. *J. Infect. Dis.* **117**, 15–22 (1967).
12. Kimberlin, R. H., Field, H. J. & Walker, C. A. Pathogenesis of mouse scrapie: evidence for spread of infection from central to peripheral nervous system. *J. Gen. Virol.* **64 Pt 3**, 713–716 (1983).
13. Fraser, H. & Dickinson, A. G. Pathogenesis of scrapie in the mouse: the role of the spleen. *Nature* **226**, 462–463 (1970).
14. Aguzzi, A. & Heikenwalder, M. Pathogenesis of prion diseases: current status and future outlook. *Nat Rev Micro* **4**, 765–775 (2006).
15. Aguzzi, A., Sigurdson, C. & Heikenwaelder, M. Molecular Mechanisms of Prion Pathogenesis. *Annu. Rev. Pathol. Mech. Dis.* **3**, 11–40 (2008).
16. Kovacs, G. G. & Budka, H. Prion Diseases: From Protein to Cell Pathology. *Am J Pathol* **172**, 555–565 (2008).
17. Brown, D. R., Boon-Seng, W., Hafiz, F. & Clive, C. Normal prion protein has an activity like that of superoxide dismutase. *Biochem J* **344**, 1–5 (1999).
18. Brown, D. R., Clive, C. & Haswell, S. J. Antioxidant activity related to copper binding of native prion protein. *J Neurochem* **76**, 69–76 (2001).
19. Vassallo, N. & Herms, J. Cellular prion protein function in copper homeostasis and redox signalling at the synapse. *J Neurochem* **86**, 538–544 (2003).
20. Kuwahara, C. *et al.* Prions prevent neuronal cell-line death. *Nature* **400**, 225–226 (1999).
21. Bounhar, Y., Zhang, Y., Goodyer, C. G. & LeBlanc, A. Prion Protein Protects Human Neurons against Bax-mediated Apoptosis. *J Biol Chem* **276**, 39145–39149 (2001).
22. Herms, J. W. *et al.* Altered intracellular calcium homeostasis in cerebellar granule cells of prion protein-deficient mice. *J Neurochem* **75**, 1487–1492 (2000).
23. Brini, M., Miuzzo, M., Pierobon, N., Negro, A. & Sorgato, M. C. The prion protein and its paralogue Doppel affect calcium signaling in Chinese hamster ovary cells. *Mol. Biol. Cell* **16**, 2799–2808 (2005).
24. Fuhrmann, M. *et al.* Loss of the cellular prion protein affects the Ca<sup>2+</sup> homeostasis in hippocampal CA1 neurons. *J Neurochem* **98**, 1876–1885 (2006).
25. Chiarini, L. B. *et al.* Cellular prion protein transduces neuroprotective signals. *EMBO J.* **21**, 3317–3326 (2002).
26. Chen, S., Mangé, A., Dong, L., Lehmann, S. & Schachner, M. Prion protein as trans-interacting partner for neurons is involved in neurite outgrowth and neuronal survival. *Mol Cell Neurosci* **22**, 227–233 (2003).
27. Hornshaw, M. P., McDermott, J. R. & Candy, J. M. Copper binding to the N-terminal tandem repeat regions of mammalian and avian prion protein. *Biochem Biophys Res Commun* **207**, 621–629 (1995).

28. Brown, D. R., Qin, K., Herms, J. W., Madlung, A. & Manson, J. The cellular prion protein binds copper in vivo. *Nature* **390**, 684–687 (1997).
29. Lotscher, M., Recher, M., Hunziker, L. & Klein, M. A. Immunologically Induced, Complement-Dependent Up-Regulation of the Prion Protein in the Mouse Spleen: Follicular Dendritic Cells Versus Capsule and Trabeculae. *J. Immunol.* **170**, 6040–6047 (2003).
30. Martinez del Hoyo, G., Lopez-Bravo, M., Metharom, P., Ardavin, C. & Aucouturier, P. Prion Protein Expression by Mouse Dendritic Cells Is Restricted to the Nonplasmacytoid Subsets and Correlates with the Maturation State. *J. Immunol.* **177**, 6137–6142 (2006).
31. Li, R. *et al.* The Expression and Potential Function of Cellular Prion Protein in Human Lymphocytes. *Cell Immunol* **207**, 49–58 (2001).
32. Büeler, H. *et al.* Normal development and behaviour of mice lacking the neuronal cell-surface PrP protein. *Nature* **356**, 577–582 (1992).
33. Tobler, I., Gaus, S. E., Deboer, T., Achermann, P. & Fischer, M. Altered circadian activity rhythms and sleep in mice devoid of prion protein. *Nature* **380**, 639–642 (1996).
34. Colling, S. B., Khana, M., Collinge, J. & Jefferys, J. G. R. Mossy fibre reorganization in the hippocampus of prion protein null mice. *Brain Res* **755**, 28–35 (2011).
35. Mallucci, G. R., Rante, S., Asante, E. A. & Linehan, J. Post-natal knockout of prion protein alters hippocampal CA1 properties, but does not result in neurodegeneration. *EMBO J* **21**, 202–210 (2002).
36. Pocchiari, M., Schmittinger, S. & Masullo, C. Amphotericin B delays the incubation period of scrapie in intracerebrally inoculated hamsters. *J. Gen. Virol.* **68 ( Pt 1)**, 219–223 (1987).
37. Doh-ura, K. *et al.* Treatment of Transmissible Spongiform Encephalopathy by Intraventricular Drug Infusion in Animal Models. *J Virol* **78**, 4999–5006 (2004).
38. Kocisko, D. A. & Caughey, B. Mefloquine, an Antimalaria Drug with Antiprion Activity In Vitro, Lacks Activity In Vivo. *J Virol* **80**, 1044–1046 (2005).
39. White, A. R. *et al.* Monoclonal antibodies inhibit prion replication and delay the development of prion disease. *Nature* **422**, 80–83 (2003).
40. Kimberlin, R. H. & Walker, C. A. The antiviral compound HPA-23 can prevent scrapie when administered at the time of infection. *Arch. Virol.* **78**, 9–18 (1983).
41. Ingrosso, L., Ladogana, A. & Pocchiari, M. Congo red prolongs the incubation period in scrapie-infected hamsters. *J Virol* **69**, 506–508 (1995).
42. White, M. D., Farmer, M. & Mirabile, I. Single treatment with RNAi against prion protein rescues early neuronal dysfunction and prolongs survival in mice with prion disease. *Proc. Natl. Acad. Sci. U.S.A.* **105**, 10238–10243 (2008).
43. Pfeifer, A. *et al.* Lentivector-mediated RNAi efficiently suppresses prion protein and prolongs survival of scrapie-infected mice. *J. Clin. Invest.* **116**, 3204–3210 (2006).
44. Mallucci, G. Depleting Neuronal PrP in Prion Infection Prevents Disease and Reverses Spongiosis. *Science* **302**, 871–874 (2003).
45. Pulford, B. *et al.* Liposome-siRNA-Peptide Complexes Cross the Blood-Brain Barrier and Significantly Decrease PrPC on Neuronal Cells and PrPRES in Infected Cell Cultures. *PLoS ONE* **5**, e11085 (2010).
46. Zabel, M. D. *et al.* Stromal Complement Receptor CD21/35 Facilitates Lymphoid Prion Colonization and Pathogenesis. *J. Immunol.* **179**, 6144–6152 (2007).
47. Pulford, B. *et al.* Detection of PrPCWD in feces from naturally exposed Rocky Mountain elk (*Cervus elaphus nelsoni*) using protein misfolding cyclic amplification. *J. Wildl. Dis.* **48**, 425–434 (2012).
48. Wyckoff, A. C. *et al.* Prion Amplification and Hierarchical Bayesian Modeling Refine Detection of Prion Infection. *Sci Rep* **5**, 8358 (2015).
49. Ehlers, B. & Diringer, H. Dextran sulphate 500 delays and prevents mouse scrapie by impairment of agent replication in spleen. *J. Gen. Virol.* **65 ( Pt 8)**, 1325–1330 (1984).
50. Caspi, S. *et al.* The anti-prion activity of Congo red. Putative mechanism. *J. Biol. Chem.* **273**, 3484–3489 (1998).
51. Caughey, B. & Raymond, G. J. Sulfated polyanion inhibition of scrapie-associated PrP accumulation in cultured cells. *J Virol* **67**, 643–650 (1993).
52. Demaimay, R. *et al.* Pharmacological studies of a new derivative of amphotericin B, MS-8209, in mouse and hamster scrapie. *J. Gen. Virol.* **75 ( Pt 9)**, 2499–2503 (1994).
53. Goñi, F. *et al.* Mucosal immunization with an attenuated Salmonella vaccine partially protects white-tailed deer from chronic wasting disease. *Vaccine* **33**, 726–733 (2015).
54. White, M. D. *et al.* Single treatment with RNAi against prion protein rescues early neuronal dysfunction and

- prolongs survival in mice with prion disease. *Proc. Natl. Acad. Sci. U.S.A.* **105**, 10238–10243 (2008).
55. McLennan, N. F. *et al.* Prion Protein Accumulation and Neuroprotection in Hypoxic Brain Damage. *Am J Pathol* **165**, 227–235 (2010).
  56. Spudich, A. *et al.* Aggravation of ischemic brain injury by prion protein deficiency: Role of ERK-1/-2 and STAT-1. *Neurobiol Dis* **20**, 442–449 (2005).
  57. Kim, Y. *et al.* Utility of RNAi-mediated prnp gene silencing in neuroblastoma cells permanently infected by prions: Potentials and limitations. *Antiviral Res* **84**, 185–193 (2009).
  58. Bitko, V., Musiyenko, A., Shulyayeva, O. & Barik, S. Inhibition of respiratory viruses by nasally administered siRNA. *Nat. Med.* **11**, 50–55 (2004).
  59. Zhang, W. *et al.* Inhibition of respiratory syncytial virus infection with intranasal siRNA nanoparticles targeting the viral NS1 gene. *Nat. Med.* **11**, 56–62 (2004).
  60. Tousignant, J. D., Gates, A. L. & Ingram, L. A. Comprehensive analysis of the acute toxicities induced by systemic administration of cationic lipid: plasmid DNA complexes in mice. *Hum Gene Ther* **11**, 2493–2513 (2000).
  61. Borchelt, D. R. & Sisodia, S. S. Loss of functional prion protein: a role in prion disorders? *Chem. Biol.* **3**, 619–621 (1996).
  62. Jackson, W. S. *et al.* Spontaneous Generation of Prion Infectivity in Fatal Familial Insomnia Knockin Mice. *Neuron* **63**, 438–450 (2009).
  63. Alvarez-Erviti, L. *et al.* Delivery Of siRNA To Mouse Brain With Exosomes. *Nat. Biotechnol.* 1–7 (2011). doi:10.1038/nbt.1807
  64. Hornung, V. *et al.* Sequence-specific potent induction of IFN- $\alpha$  by short interfering RNA in plasmacytoid dendritic cells through TLR7. *Nat. Med.* **11**, 263–270 (2005).
  65. Marques, J. T. & Williams, B. R. G. Activation of the mammalian immune system by siRNAs. *Nat. Biotechnol.* **23**, 1399–1405 (2005).
  66. Sioud, M. Induction of Inflammatory Cytokines and Interferon Responses by Double-stranded and Single-stranded siRNAs is Sequence-dependent and Requires Endosomal Localization. *J. Mol. Biol.* **348**, 1079–1090 (2005).
  67. Harborth, J. *et al.* Sequence, Chemical, and Structural Variation of Small Interfering RNAs and Short Hairpin RNAs and the Effect on Mammalian Gene Silencing. *Antiviral Nucleic Acid Drug Dev* **13**, 83–105 (2004).
  68. Braasch, D. A. *et al.* RNA Interference in Mammalian Cells by Chemically-Modified RNA. *Biochemistry* **42**, 7967–7975 (2003).
  69. Papahadjopoulos, D. *et al.* Sterically stabilized liposomes: improvements in pharmacokinetics and antitumor therapeutic efficacy. *Proc. Natl. Acad. Sci. U.S.A.* **88**, 11460–11464 (1991).
  70. Bender, H. R., Kane, S. & Zabel, M. D. Delivery of Therapeutic siRNA to the CNS Using Cationic and Anionic Liposomes. *J Vis Exp* e54106 (2016).
  71. Georgieva, J., Hoekstra, D. & Zuhorn, I. Smuggling Drugs into the Brain: An Overview of Ligands Targeting Transcytosis for Drug Delivery across the Blood–Brain Barrier. *Pharmaceutics* **6**, 557–583 (2014).
  72. Wang, H. *et al.* Nicotinic acetylcholine receptor  $\alpha 7$  subunit is an essential regulator of inflammation. *Nature* **421**, 384–388 (2002).
  73. Cardone, C., Szenohradszky, J., Yost, S. & Bickler, P. E. Activation of brain acetylcholine receptors by neuromuscular blocking drugs. A possible mechanism of neurotoxicity. *Anesthesiology* **80**, 1155–1161 (1994).
  74. Castner, S. A. *et al.* Immediate and Sustained Improvements in Working Memory After Selective Stimulation of 7 Nicotinic Acetylcholine Receptors. *BPS* **69**, 12–18 (2011).
  75. Albuquerque, E. X., Pereira, E. F. R., Alkondon, M. & Rogers, S. W. Mammalian Nicotinic Acetylcholine Receptors: From Structure to Function. *Physiological Reviews* **89**, 73–120 (2009).
  76. Mabbott, N. A., Brown, K. L., Manson, J. & Bruce, M. E. T-lymphocyte activation and the cellular form of the prion protein. *Immunology* **92**, 161–165 (1997).
  77. Greenberg, M. E., Ziff, E. B. & Greene, L. A. Stimulation of neuronal acetylcholine receptors induces rapid gene transcription. *Science* **234**, 80–83 (1986).

## Overall Conclusions

RNA interference, such as small interfering RNA (siRNA), has been proposed as a possible therapeutic for protein misfolding diseases. This technology has the potential to reduce the amount of misfolded protein that accumulates in the brains of affected individuals. However, crossing the blood-brain barrier remains the main challenge for delivering any small molecule drug to the central nervous system (CNS). Liposomes offer an attractive option as a small molecule delivery system. These liposomal delivery systems can protect the siRNA from serum nucleases and can be targeted directly to the brain using targeting peptides. We have previously generated liposome-siRNA-peptide complexes (LSPCs) that employ the RVG-9r peptide from the rabies virus glycoprotein to target PrP<sup>C</sup> siRNA to nicotinic acetylcholine receptors in the brain. PrP<sup>C</sup>, cellular prion protein, has been implicated to misfold into an infectious isomer, PrP<sup>Res</sup>, during prion infection. In half of the mice treated with LSPCs, the PrP<sup>C</sup> siRNA is delivered to the brain and decreases surface neuronal PrP<sup>C</sup> by 40-50%. There was no decrease in PrP<sup>C</sup> mRNA levels in the brain when assayed four days after treatment. In the other half of mice, LSPCs were cleared by the kidneys within hours after injection. To try to improve the biodistribution of PrP<sup>C</sup> siRNA in the brain, we designed two other delivery vehicles, cationic (DOTAP) and anionic (DSPE) PALETS, which can encapsulate the siRNA within the liposome and covalently modify the RVG-9r peptide to the lipid groups. To achieve encapsulation of the anionic siRNA into anionic DSPE PALETS, we utilized the cation protamine sulfate. Protamine sulfate results in encapsulation of 80-90% of the PrP<sup>C</sup> siRNA in DSPE PALETS. At least one PALETS-treated mouse had a decrease in neuronal surface PrP<sup>C</sup> out of the three treated mice for each PALETS formulation four days after injection, although grouped there was no difference between the three treated and the untreated mice. DOTAP PALETS also decreased the number of PrP<sup>C</sup>-positive cells within the brain. PrP<sup>C</sup> was also measured in the kidneys of all treated mice to assess any off-target effects and clearance kinetics. Both DOTAP LSPCs and DSPE PALETS had a significant reduction in the amount of surface PrP<sup>C</sup> in the kidney, indicating that these two delivery systems are cleared through the kidneys four days after treatment. DOTAP PALETS do not result in a decrease in surface PrP<sup>C</sup> in the kidney. DOTAP LSPCs and DOTAP PALETS have a 2-fold reduction in PrP<sup>C</sup> mRNA levels in the kidney, while DSPE PALETS have a 2-fold increase.

We have previously characterized the ability of the LSPCs treatment to deliver PrP<sup>C</sup> siRNA to mouse neuroblastoma cells and to decrease the amount of surface PrP<sup>C</sup> on these cells. The decrease in surface PrP<sup>C</sup> lead to a

'curing' of prion-infected cells. Therefore, in chapter three, we characterized the ability of LSPCs to deliver PrP<sup>C</sup> siRNA to the CNS in two different mouse models, one on a C57Bl/6 background and the other on a CD1 background. The control LSPCs using either scrambled LSPCs or the RVM control peptide that does not target nicotinic acetylcholine receptors resulted in changes in PrP<sup>C</sup> protein and mRNA levels. The scrambled LSPCs resulted in a 14% reduction in surface PrP<sup>C</sup> and a 1.5 increase in PrP<sup>C</sup> mRNA. The RVM LSPCs resulted in a slight increase of surface PrP<sup>C</sup> and a 1.5 increase in mRNA. Therefore, we normalized all the mRNA analyses by the increase caused by the non-specific LSPCs treatment. In the C57Bl/6 background mice, surface PrP<sup>C</sup> in the brain was decreased at 24, 48 hours and 4 days after LSPCs treatment. Neuronal PrP<sup>C</sup> mRNA levels were variable, with the highest mRNA levels usually occurring in the mouse with the lowest surface PrP<sup>C</sup> protein levels. CD1 mice had a decrease in surface PrP<sup>C</sup> in the brain at 4 and 15 days after LSPCs treatment but not 48 hours or 21 days after treatment. Again, PrP<sup>C</sup> mRNA levels were variable but the same trend was observed where the mouse with the highest mRNA levels had the lowest amount of PrP<sup>C</sup> protein. PrP<sup>C</sup> protein and mRNA levels were assessed in the kidney for any off-target effects and toxicity issues. Since PrP<sup>C</sup> protein levels are severely decreased with control LSPCs, no conclusions can be made regarding the decreases observed using flow cytometry. However, as stated, mRNA analyses in the brain and kidney were normalized to the effects of the control LSPCs to ascertain the effect of the PrP<sup>C</sup> siRNA only. In the kidneys of C57Bl/6 and CD1 mice, PrP<sup>C</sup> mRNA levels are variable with most mice showing a decrease in mRNA levels and a few showing an increase in mRNA levels. We hypothesize that the increases observed in both the brain and kidney of LSPCs-treated mice are caused by an immune reaction to the LSPCs, a transcriptional regulation mechanism, or both. We also assessed the ability of repetitive LSPCs treatment to reduce PrP<sup>C</sup> protein and mRNA levels. PrP<sup>C</sup> protein levels are reduced 70% and mRNA levels are reduced 3-fold in the brain by the third LSPCs treatment occurring every two weeks. Subsequent treatments result in an increase in both PrP<sup>C</sup> protein and mRNA levels in the brain.

Prion diseases are characterized by neuronal degeneration, astrogliosis, and vacuolation within the CNS. These diseases affect humans, and captive and free-ranging animals. Prion diseases result when PrP<sup>C</sup> misfolds into the infectious isomer PrP<sup>Res</sup>. The field of prion therapeutics has turned towards gene therapies that target PrP<sup>C</sup>, as molecules that target PrP<sup>Res</sup> or the mechanism of conversion have not shown any promise in clinical trials. RNAi has been postulated to be a potential therapeutic of prion diseases as it can result in the decrease of misfolded protein by targeting the mRNA of the normal cellular protein. A single treatment of RNAi injected into the hippocampus of

prion-infected mice showed that not only can RNAi increase survival times by decreasing PrP<sup>C</sup> but it can also reverse prion neuropathology. Therefore, in chapter four of this thesis, we investigated whether a repetitive PrP<sup>C</sup> siRNA therapeutic can increase the survival times of prion-infected mice when administered intravascularly or intranasally. Mice were treated every two to 3-5 weeks intravascularly/intranasally with LSPCs starting at 120 days post inoculation. These mice were also subjected to burrowing and nesting behavioral tests to determine if multiple LSPCs can affect behavioral outcomes. The repeated LSPCs treatments, either two or 3-5 weeks, did not alter survival times of prion-infected mice. The survival times of the group treated both intravascularly and intranasally actually decreased compared to the infected, untreated control. While survival times were not affected by multiple LSPCs treatment, several treated groups did perform better in the behavioral tests at 141 and 169 days post inoculation than the infected, untreated control. No treated mice had increased behavioral scores at time of terminal disease. These results show that the LSPCs treatment improved the behavioral scores for treated mice at certain time points. Since the LSPCs treatment resulted in an improvement in behavior, we assessed whether the treatment decreased the amount of PrP<sup>Res</sup> in prion-infected mice, even though survival times were not affected. Surprisingly, LSPCs treatment results in an increase of PrP<sup>Res</sup> in the brain after one to six LSPCs treatments every two weeks. We speculate that, even though LSPCs result in an initial decrease in PrP<sup>C</sup> at certain time points, the protein actually increases overall, which leads to an increase of PrP<sup>Res</sup>. The overall increase of PrP<sup>C</sup> could be due to either an immune reaction towards the LSPCs treatment or a transcriptional regulation mechanism of PrP<sup>C</sup>. Several of the uninfected, treated controls died shortly after LSPCs treatment of an apparent Type III hypersensitivity. Total IgG levels against RVG-9r were measured and found to be elevated in several of the treated groups. The increase in total IgG levels occurred after the third LSPCs treatment, when administered every two weeks. In this study, total IgG levels against RVG-9r were measured and found to be elevated but the siRNA/liposome complexes are also capable of stimulating an immune reaction (not measured in this study).

## Future Directions

In the second chapter of this dissertation, we generated three liposomal delivery vehicles capable of crossing the blood-brain barrier. More pharmacodynamics studies are needed to determine which delivery vehicle results in the greatest reduction of PrP<sup>C</sup>. Our results at four days after treatment indicate the LSPCs vehicle is more effective at reducing PrP<sup>C</sup>. However, the addition of the PEG groups to the PALETS formulations should result in an increase in circulation times so the activity of the PALETS formulations should be assessed past four days after treatment. While the non-specific response to the LSPCs treatment confounds any flow cytometry analysis in the kidney, it is still important to observe PALETS behavior in the kidney at certain time points to assess clearance kinetics. DOTAP PALETS, at four days after treatment, showed no decrease in PrP<sup>C</sup> in the kidney, indicating that clearance kinetics of this vehicle changed from the LSPCs. This finding could mean that more DOTAP PALETS are able to make it to the brain than are LSPCs.

In the fourth chapter of this dissertation, no difference was seen between prion-infected, untreated and LSPCs-treated mice. If all the LSPCs-treated mice injected intravenously are pooled together as one large treatment group with a difference of means of 3.6 from the untreated group, the power of this study is 0.1298. This power value indicates that, using the current mouse numbers, the observed effect would only be seen 12% of the time if this experiment was repeated. Thus, it is important to repeat the survival experiments using a larger number of mice. To achieve 80% power, where the data is observed 80% of the time, with a true difference of means of 3.6, and standard deviations of 5.74 for the untreated group and 11.42 for the treated group, 103 mice will be needed for the next treatment terminal study.

The formulations, targeting peptide, and therapeutic can all be altered if future studies determine that the vehicles are not optimal. If the RVG-9r peptide is causing the largest immune reaction amongst the three components of the vehicles then it can be replaced with another neuronal targeting peptide. Many different ligands/receptors have been utilized to target delivery vehicles to the central nervous system, including transferrin, leptin, low-density lipoprotein, brain-derived neurotrophic factor, and antibodies to neuronal receptors. We are currently in the process of generating camelid antibodies against PrP<sup>C</sup> that have the potential to target either the LSPCs or the PALETS to the brain. The native form of RVG-9r, RVG, might also be a better targeting ligand as, alone, it does not elicit an immune response. Multiple ligands might need to be examined to determine which one

results in the greatest amount of PrP<sup>C</sup> siRNA being delivered to the brain. The DOTAP PALETS utilized a carbodiimide reaction to covalently link the RVG-9r to the PEG lipids. This reaction catalyzes a covalent bond between an amine and a hydroxyl group. While this reaction is commonly used to link peptides to other molecules, its effect on the RVG-9r peptide is unknown. Therefore, it would be prudent to assess whether the activity of RVG-9r remains intact after the reaction. Also, it might be possible to alter the RVG-9r primary structure by changing the cysteine residue to a serine to provide a better covalent linkage between RVG-9r and the PEG groups. The lipid formulations can also be adjusted to increase circulation times. Depending on toxicity issues from using liposomes, it may be necessary to try a different vehicle altogether. Exosomes are gaining momentum as a new delivery vehicle that is less immunogenic than other vehicles. Exosome vehicles are able to encapsulate siRNA and target specific cell types with a targeting peptide. A different therapeutic, other than siRNA, might result in a more profound decrease of PrP<sup>C</sup>. An explanation for the results of the terminal studies and the PMCA experiments is that transiently decreasing PrP<sup>C</sup> allows time for the protein levels to rebound, which results in an increase in PrP<sup>Res</sup> and no increase in survival times. Therefore, a more permanent decrease of PrP<sup>C</sup> with either short hairpin RNA or CRISPR technology might affect survival times of prion-infected mice.

Perhaps the most important future direction is to characterize the immune response to the LSPCs. There will always be some immune activation towards the LSPCs, as each component is a TLR agonist, but it may be possible to alter the LSPCs so that the immune activation is lessened. Since each of the components of the LSPCs activates TLR signaling and the signaling causes cytokine and chemokine release, it would be important to measure cytokine/chemokine levels in naïve mice in response to repetitive LSPCs treatment. This would give a more complete picture as to the whole immune response towards the treatment rather than just measuring IgG levels. Cytokines can be measured using a multiplex bead assay. Naïve mice should be treated with each individual LSPCs component to assess activation due to the siRNA, peptide, or liposome. Modifications (as described above) can be made to any of the components if it is found that one component activates an immune response more than another component. Once the immune response to individual components has been measured, then naïve mice should be treated with the entire LSPCs complex both one time and multiple times to assess cytokine/chemokine release due to LSPCs treatment.

Another idea that developed in response to the data observed in this project was to understand the transcriptional control of PrP<sup>C</sup>. If researchers keep using PrP<sup>C</sup> as a therapeutic target for prion diseases, especially

with gene therapies that may result in alteration of transcription, then it would be necessary to elucidate the mechanisms of control of PrP<sup>C</sup> to optimize future therapeutics to their full potential. Otherwise, future therapeutics may have efficacy problems due to not getting around the transcriptional control. First, it should be determined whether the results seen in these studies were the result of immune activation or transcriptional regulation. The above immune assays should help tease that out but it would also be necessary to do an *in vitro* assay with a purified population of cells to assess mRNA levels at different time points. When we first assessed mRNA levels *in vitro* after LSPCs treatment, we only looked at one time point. Therefore, a purified population of neuronal cells (without any immune cells) should be treated with LSPCs and mRNA levels assessed every couple of hours to 6-12 hour increments. This experiment could also be done *in vivo*, using mice with no immune system, such as NOD SCID gamma mice. These mice can be treated with LSPCs to assess PrP<sup>C</sup> mRNA/protein levels at different time points after treatment. If the same trend is seen (with PrP<sup>C</sup> protein being low and PrP<sup>C</sup> mRNA levels being high) with the above experiments then the data observed in the present study was most likely due to a regulational mechanism of PrP<sup>C</sup>. Another drug that is known to decrease PrP<sup>C</sup> can be used as a control to determine if the response is due to the siRNA or is a general response to any drug that affects PrP<sup>C</sup>. If a regulational mechanism is responsible for the dichotomy in PrP<sup>C</sup> protein and mRNA levels, then techniques such as CHIP-seq and mobility shift assays can be performed to elucidate the mechanism of control.

## Appendix A – Additional Figures

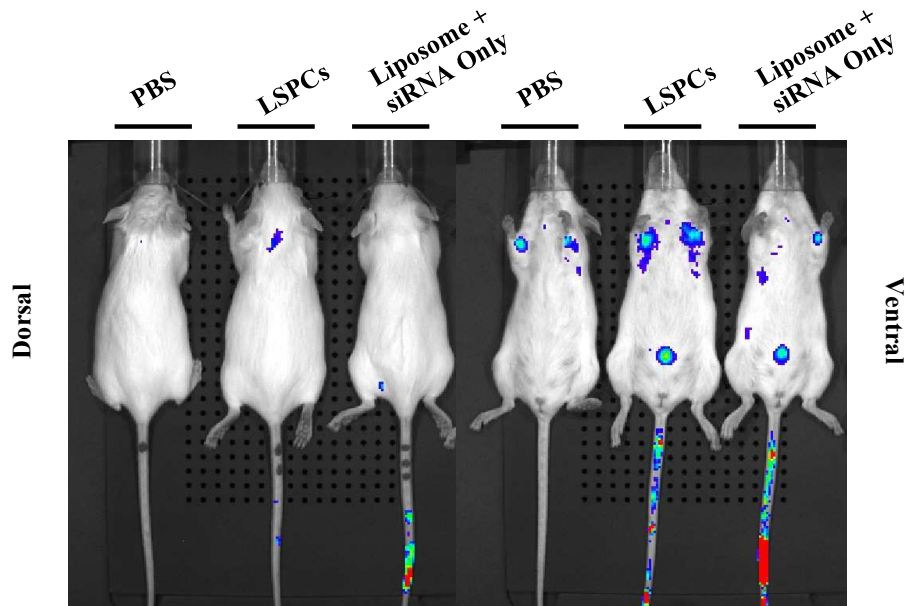


**Figure A.1. In vivo live imaging of LSPCs-treated mice 24 hours after treatment.**

Mice were injected intravenously with LSPCs and imaged for up to 24 hours after treatment. siRNA signal was imaged on 500/540 nm filter. 24 hours after treatment there is no siRNA signal in the brain. There is siRNA signal in the kidney, indicating that the siRNA was cleared from the circulation in this experiment

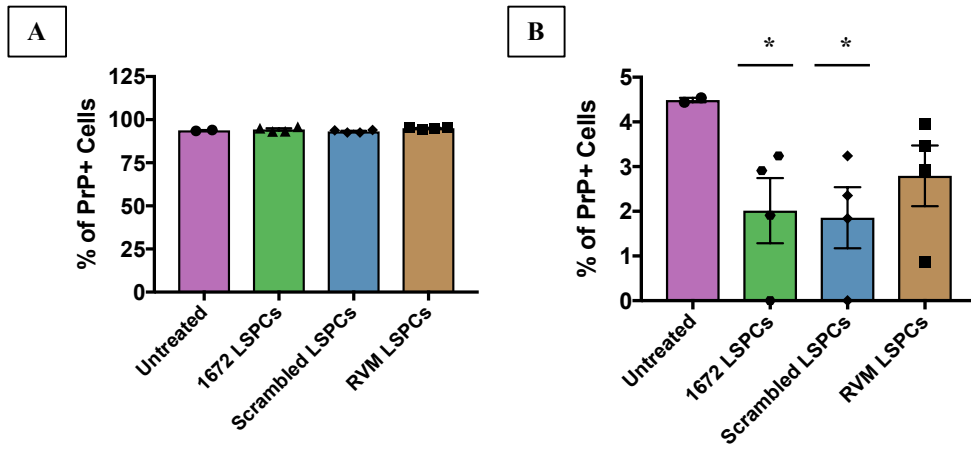


**Figure A.2. Percent of PrP<sup>C</sup>-positive cells using scrambled siRNA and RVM peptide.**

A) Percent of PrP<sup>C</sup>-positive cells in the brain. B) Percent of PrP<sup>C</sup>-positive cells in the kidney. Error bars indicate SEM. \* p<0.05. Welch's t test

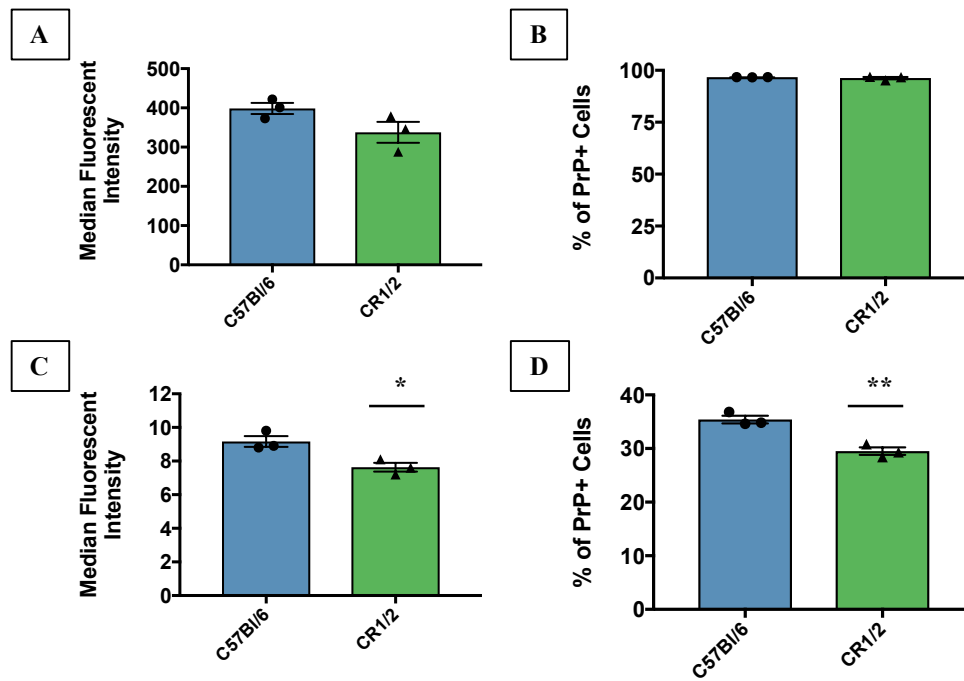


**Figure A.3. Comparison of PrP<sup>C</sup> levels in C57Bl/6 and CR1/2 hemi mice.**

A) Median fluorescent intensity (MFI) of PrP<sup>C</sup> in the brain. B) PrP<sup>+</sup> cells in the brain. C) MFI of PrP<sup>C</sup> in the kidney. D) PrP<sup>+</sup> cells in the kidney. Error bars indicate SEM. \* p<0.05, \*\* p<0.01. t test

## Appendix B – List of Abbreviations

TSE	Transmissible spongiform encephalopathy
CNS	Central nervous system
CJD	Creutzfeldt-Jakob disease
UV	Ultraviolet
GSS	Gerstmann-Sträussler-Scheinker syndrome
PrP <sup>C</sup>	Cellular prion protein (non-infectious)
PrP <sup>Res</sup>	Proteinase K resistant cellular prion protein (infectious)
ER	Endoplasmic reticulum
GPI	Glycosylphosphatidylinositol
BSE	Bovine spongiform encephalopathy
STII	Stress-inducible protein 1
Cu <sup>2+</sup>	Copper
LRP	37 kDa/67 kDa laminin receptor
K <sub>d</sub>	Dissociation constant
SOD	Superoxide dismutase
HSC	Hematopoietic stem cells
DC	Dendritic cells
GALT	Gut-associated lymphoid tissue
MBM	Meat and bone meal
CWD	Chronic wasting disease
LRS	Lymphoreticular system
TME	Transmissible mink encephalopathy
FSE	Feline spongiform encephalopathy
CJD	Creutzfeldt-Jakob disease
sCJD	Sporadic Creutzfeldt-Jakob disease
f/gCJD	Familial/genetic Creutzfeldt-Jakob disease
iCJD	Iatrogenic Creutzfeldt-Jakob disease
vCJD	Variant Creutzfeldt-Jakob disease
FFI	Fatal familial insomnia
AD	Alzheimer's disease
PD	Parkinson's disease
HD	Huntington's disease
APP	Amyloid precursor protein
A $\beta$	Amyloid $\beta$
A $\beta$ PL1	Amyloid-like precursor protein 1
AmB	Amphotericin B
PEI	Polyethyleneimine
PPI	Polypropyleneimine
N2a	Neuroblastoma cells
BBB	Blood-brain barrier
GAGs	Glycosaminoglycans
DS-500	Dextran sulfate 500
HS	Heparan sulfate
CR	Congo red
CFA	Complete Freund's adjuvant
RNAi	RNA interference
shRNA	Short hairpin RNA
siRNA	Small interfering RNA
LSPCs	Liposome-siRNA-peptide complexes
dsRNA	Double-stranded RNA
ssRNA	Single-stranded RNA

Dcr	Dicer
RISC	RNA-induced silencing complex
Ago	Argonaute
PS	Phosphorothioate
LNAs	Locked nucleic acids
CPPs	Cell-penetrating peptides
MPPs	Membrane-penetrating peptides
TLR	Toll-like receptor
RVG	Rabies virus glycoprotein
RVG-9r	Rabies virus glycoprotein with nine arginine residues
SNALP	Stable nucleic acid lipid particle
DOTAP	1,2-dioleoyl-3-trimethylammonium-propane (chloride salt)
DOTMA	1,2-di-O-octadecenyl-3-trimethylammonium propane (chloride salt)
DOPE	1,2-dioleoyl-sn-glycero-3-phosphoethanolamine
DOPC	1,2-dioleoyl-sn-glycero-3-phosphocholine
OTES	Off-target effects
miRNA	Micro RNAs
PALETS	Peptide-addressed liposome-encapsulated therapeutic siRNA
MPS	Mononuclear phagocyte system
DSPE	1,2-distearoyl-sn-glycero-3-phosphoethanolamine
ddPCR	Digital droplet polymerase chain reaction
SEM	Standard error of the mean
SD	Standard deviation
MFI	Median fluorescent intensity
PEG	Pegylated lipids
nAchRs	Nicotinic acetylcholine receptors
Hemi	Hemizygous
w/v	Weight/volume
PD	Pharmacodynamics
NBH	Normal brain homogenate
PMCA	Protein misfolding cyclic amplification
PK	Proteinase K
DPI	Days post inoculation
IV	Intravenous
IN	Intranasal
IHC	Immunohistochemistry
GFAP	Glial fibrillary acidic protein
ELISA	Enzyme-linked immunosorbent assay